Orthogonal Chemistries in the Directed Assembly of Complex Molecular Architectures

by

Megan F. Dunn

A dissertation submitted in partial fulfillment
of the requirements for the degree of
Doctor of Philosophy
(Chemical Engineering)
in The University of Michigan
2019

Doctoral Committee:

Associate Professor Timothy F. Scott, Chair
Professor Jinsang Kim
Professor Ronald Larson
Professor Michael J. Solomon

Megan F. Dunn

mdun@umich.edu

ORCID iD: 0000-0002-9038-3281

Dedication

This dissertation is dedicated to the memory of

Adeline Kathleen Hays and Darrell Shelton

Acknowledgements

I would like to thank my doctoral advisor Prof. Timothy F. Scott for his support and guidance throughout my studies at the University of Michigan. I unmistakably grew as a scientist and researcher through this relationship. I would also like to thank my dissertation committee members, Professor Ronald Larson, Professor Jinsang Kim and Professor Michael Solomon for their thoughtful advice and feedback throughout the project.

I would like to express gratitude to the people of the Ojibwe (Chippewa), Odawa (Ottawa), and Bodewadimi (Potawatomi) tribes where through the Treaty of Fort Meigs the University of Michigan came to be. The treaty stated, "believing they may wish some of their children hereafter educated, [they] do grant to the rector of the Catholic church of St. Anne of Detroit ... and to the corporation of the college at Detroit, for the use of the said college, to be retained or sold, as the said rector and corporation may judge expedient ... " This land was indeed sold and the proceeds became part of the permanent endowment of the university upon moving the campus to Ann Arbor. Chi-Miigwetch and wado udohiyu utsati for the many sacrifices made so I could attend this university.

I am fortunate to have worked with many talented and supportive individuals in my tenure in the Scott Polymer Dojo (SPD). This included Dr. Scott Zavada, Dr. Joseph Furgal, Dr. Dowon Ahn, Dr. Tao Wei, Harry van der Laan, Max Ma, Samuel Leguizamon, Abdulla Alqubati, Austin Bingham, Futianyi Wang, and Alex Commisso, Dr. Jae Hwan Jung, Dr. Junting Li, Sameer Sathe, Nathan Wood, and Dan Li. I would like to thank each of them for their friendship and constructive conversations. I would like to specifically mention co-authors that

I have been very fortunate to meet many incredible individuals throughout this time. I would like to thank Melissa, Brittany, Carla, Michon, Michelle, and Susannah for being my support system. I would like to thank Corine, Megan, Tatyana, Umar, and Franck for their support through chemical engineering courses. I would also like to thank my PoGo crew for many fun days catching monsters in the parks. I would like to thank the students in the Native American Student Association for the link to home in Michigan.

I am eternally grateful for the support of my community back home; it is my greatest ambition to make the world better for seven generations of Tsalagi people ahead of me. I would like to express my gratitude for the lifelong friends that have supported me in the past few years, namely Jaime, James, Amanda, and Oliver. I would like to thank Brian for being the best companion in stressful times. I would like to thank my extended family particularly, Skeeter and Mary, and the Silvestri family for their encouragement through the years. I would like to mom and stepdad for their unwavering love and support through challenging times. I would also like to thank my dad for always being my biggest fan and the many years of phone calls on my way home from lab. I would to thank my nieces and nephew Camryn, Jaxon, Adeline, and Charlee for always giving me a reason to smile. Lastly, I would like to thank my sisters for being my most trusted confidants, my biggest inspirations, and best friends without them none of this would have been possible.

Table of Contents

List of Tables

List of Schemes

xiv

List of Figures

Abstract

Chemical orthogonality is the ability of one or more reactions to efficiently proceed in the presence of other reactive functional groups. The concept of including orthogonal reactions to fabricate molecular structures has been applied to natural and synthetic polymers and often used as a tool to increase the level of chemical complexity. Nucleic acids (e.g., DNA and RNA), for instance, are polymers that serve as ubiquitous information-bearing species throughout biology, present the most versatile class of materials for producing diverse, specific nanostructures to date owing to their predictable, information-directed self-assembly. The information borne by nucleic acids is encoded in the sequences of orthogonal nucleobases affixed to a single (deoxy)ribophosphate strand. Thus, through careful consideration of their residue sequence, nucleic acids can be designed to predictably self-assemble *via* the hydrogen bond-based hybridization of complementary strands into arbitrary, although thermally and mechanically fragile, structures with nanometer precision.

This dissertation investigated the use of orthogonal chemistries to fabricate and functionalize different molecular architectures to overcome some of the stability issues of nucleic acid-based structures. First, we explored the formation of cyclic peptoids through the archtypical "click" reaction, a copper (I) catalyzed alkyne-azide cycloaddition reaction between terminal alkyne/azide residues. These cyclic peptoids were post-synthetically conjugated to a maleimide group through the specific spacing of furan groups on the initial oligomers that were designed to undergo a Diels-Alder reaction. This simple example of utilizing orthogonal chemistries to fabricate and decorate cyclic structures highlights the versatility of peptoids in forming more

complex molecules. The subsequent chapters in this dissertation explored the information-directed hybridization of oligomeric sequences, analogous to nucleic acid assemblies; however, instead of the hydrogen bonding observed between complementary nucleic acid strands, we employed transient or 'dynamic' covalent bonds to produce more stable and robust structures. We fabricated molecular ladders from oligopeptoids by controlling the equilibrium of three different dynamic covalent chemistries. First, a thermally-reversible reaction between a furan and maleimide mimicked the melting and annealing process of nucleic acids to form a likewise double-stranded structure as confirmed by mass spectrometry. We then explored a pH-mediated reaction forming molecular ladders with boronate ester rungs from oligomeric strands comprised of boronic acid and catechol functional groups. In addition to double-stranded structures, we introduced a method assembling "molecular grids" from precursor peptoid oligomers as a preliminary effort towards the formation of cross-linked nanosheets and ribbons. The boronate ester chemistry was ultimately combined with the final dynamic covalent chemistry of an amine and aldehyde to form Schiff base imines; we were able to confirm the formation of molecular ladders and grids bearing rungs of both boronate ester and imines in an aqueous solution by utilizing mass spectrometry. This effectively created an information system encoded in base-4 that was able to mimic the assembly process and reaction conditions for nucleic acid hybridization. The described work expands upon the foundational principles for a method that will enable a route to the facile fabrication of complex and robust assembled structures through orthogonal chemistries.

Chapter 1 Introduction

1.1 Overview of Research

This thesis defines orthogonality as the ability of two or more reactions to efficiently proceed in the presence of other functional groups. This term has referred to many chemical processes throughout time, but it was first introduced in terms of chemical reactivity in Merrifield's method of using multiple protecting groups in solid-phase synthesis of peptides.[1] The strategy invoked multiple protecting groups on adjacent amino acids that were stable to different cleavage mechanisms. This allowed for selective deprotection of desired amino acids while maintaining protection for other amino acids, a key advancement in peptide chemistry.

The term has since widened to encompass a wide range of chemical phenomena. Indeed, reactions known as "click" reactions are commonly referred to as orthogonal or bio-orthogonal reactions owing to their ability to progress in living systems without interference. The term "click chemistry" was first outlined in the early millennia by Sharpless[2] and describes reactions that have a large thermodynamic driving force that influences them to efficiently and irreversibly form a single desired product. Another class of reactions that are often described in terms of their orthogonality with one another is dynamic covalent chemistries (DCC), which refers to a set of chemical reactions where manipulating specific reaction conditions can precisely control the equilibrium.[3] This concept is most often discussed in terms of dynamic combinatorial libraries where different building blocks can combine to form more complex structures through reversible bond formation.[4]

Examples of orthogonality also exist in natural system such as DNA, where there are two sets of complementary nucleobases that will preferentially bind with their complement over other available nucleobases (i.e. cytosine binds with guanine and adenine binds with thymine).[5] The orthogonality between these sequence-specific structures has been exploited to build complex structures using only DNA as a construction material.[6]

The use of multiple chemistries to fabricate molecular structures introduces increasing levels of complexity, but it also necessitates a need to have a solid foundational understanding of how different chemistries interact in the presence of one another. This thesis will contribute to this understanding through the fabrication of sequence-specific polymers that incorporate orthogonal functional groups that are designed to assemble into different molecular architectures. It will specifically look into the orthogonal use of click and dynamic covalent chemistries in peptoids to form cyclic and ladder-based structures. This chapter will survey the field of sequence-specific polymers before discussing different orthogonal chemistries and ultimately how they are used to assemble complex structures.

1.2 Sequence-specific Polymers

Sequence-specific polymers can be found extensively in nature as nucleic acids, peptides, and proteins, and they play an essential role in biological functions. Using these materials as inspiration, there has long been a desire to control the sequence of synthetic polymers. This began with early synthesis of block copolymers (BCPs),[7] and it continues today with polymers with more complex sequences.[8] These sequence-specific polymers have recently gained interest in their potential as data storage where sequences of polymers can encode information that can then be extracted by mass spectrometry or other forms of sequencing.[9] This section will highlight some of the advances in the field of sequence-specific polymers.

1.2.1. Block copolymers

Methods of synthesizing BCPs in solution have been well researched throughout the last half-century leading to chemically diverse commercially used materials. There have been advances in the utilization of BCPs for self-assembly and nanotechnology applications reviewed recently.[10] These sequence-controlled fabrications methods lead to high molecular weight polymers, but often they lack the level of precision to produce materials with uniform dispersity. There has been some success in synthesis of well-defined multi-block copolymers through different means of mediation such as copper,[11] light,[12] and orthogonal temperature and pH reactions.[13]

1.2.2. Aperiodic Polymers

Sequence-defined polymers can refer to molecules of alternating or periodic sequences of copolymers that follow a regular pattern, but this group of polymers can also interestingly consist of structures with a precise sequence that does not follow a regular pattern. Lutz defines such sequence-defined polymers, "copolymers in which monomer sequence distribution is not regular but follows the same arrangement in all chains," as being aperiodic copolymers.[14] These polymers can be synthesized by different techniques such as iterative methods, step growth polymerizations, or chain growth polymerization.

1.2.3. Solid Phase Synthesis

Solid phase synthesis schemes have proven to be powerful iterative techniques for forming controlled polymeric sequences since Merrifield synthesized the first tetrapeptide.[15] This has become a routinely automated process of adding one monomer at a time to the end of a chain affixed to a resin, and it has provided a method of emulating natural occurring peptides as well as incorporating novel functionalities into a polyamide backbone as shown in Figure 1.1a.[16]

Peptoids, a peptidomimetic (Figure 1.1b), have been made using similar solid phase synthesis schemes that forgo the need for deprotection and can include a diverse group of monomers.[17]

(A)

Peptide Synthesis
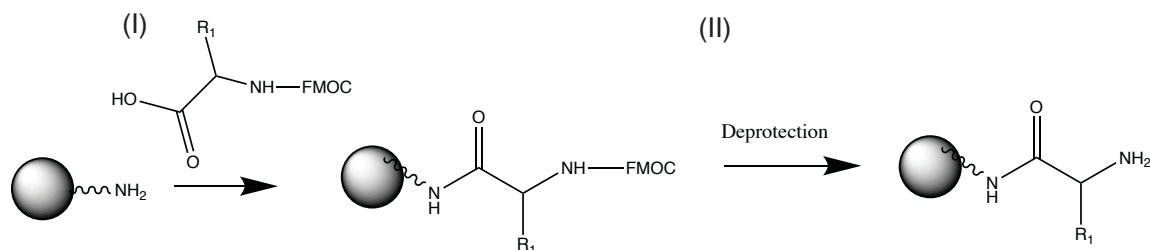
(B)

Peptoid Synthesis
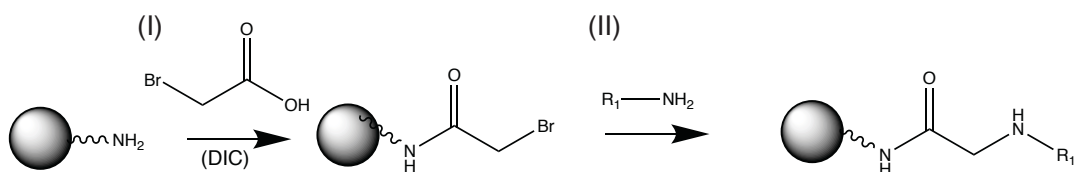
Figure 1.1. Solid phase synthesis methods (a) peptide synthesis that proceeds by first coupling the amino acid to the resin (I) and then deprotecting the FMOC protecting group from the amine (II) (b) method for preparing peptoids by first chain elongation with bromoacetic acid in the presence of an activator (I) and then displacement with any primary amine (II)

Taking inspiration from deprotection-free peptoid fabrication methods, solid phase synthesis schemes that include thiolactone chemistries were developed.[18] Martens et al. recently were able to automate a two-step iterative solid phase synthesis scheme to produce sequence-specific polymers of lengths up to a decamer by using thiolactone chemistry. The solid support has a terminal thiolactone group that can be opened by an alcohol amine exposing a thiol that undergoes a thiol-ene conjugation with an available acrylate or acrylamide. The second step of the process reintroduces the thiolactone group by a reaction between the remaining alcohol group

and α-isocyanato-γ-thiolactone. Varying the amino alcohol changes the backbone spacing and different acrylics can be used to introduce functionality into the oligomer through the side chains making this a robust method for producing a diverse library of sequenced-defined polymers.[19]

The Lutz group synthesized polyphosphates on a solid support resin using phosphoramidite chemistry classically used to form oligonucleotides of lengths up to 24 units. This method created a phosphate linkage through a two-step process where first there is a reaction of a phosphoramidite with a hydroxyl group, and then the resulting phosphite is oxidized into a phosphate. They also used copper catalyzed alkyne azide cycloaddition reaction to post-synthetically functionalize the resulting polymers by using a phosphoramidite monomer containing an alkyne group.[20] These solid phase synthesis methods lead to very controlled sequences without the need for purification between each addition; however, these approaches are not generally suitable for making longer, higher molecular weight sequences.

1.2.4. Alternative Iterative Techniques

In addition to solid phase synthesis, other iterative processes have been used to make sequenced-controlled polymers by incorporating functionality through the side-chains.[21] The Lutz group was able to create a binary system of sequence-defined poly(alkoxyamine amide)s through an iterative approach that incorporated information through 0 and 1 bits in the form of multiple dyads (00, 01, 10 and 11) that were further used to make longer coded polymers of all possible binary sequences.[22] Encoded information can be extracted from polymers using tandem mass spectrometry techniques as shown with sequence-defined poly(alkoxyamine amide)s.[23]

1.2.5. Chain Growth Polymerization

There have also been efforts to incorporate living polymerization techniques into aperiodic copolymers. Osawa et al. was able to use ROMP (ring-opening metathesis

polymerization), a chain growth polymerization technique, to produce a linear polymer with an different amide side chains on every eighth backbone carbon then further used hydrogenation to produce a polyethylene derivative.[24] Furthermore, ROMP methods have produced polymers with controlled molecular weights and defined sequences by incorporating different functionalities through the monomer placement[25] and capitalizing on the reactivity of different isomers to maintain precision.[26] The Hawker group was able to utilize so-called polymerization triggers into the macrocyclic olefins to initiate ROMP; they included both the essential enyne functional group and a hydroxyl group functioning as a handle to incorporate arbitrary groups in a sequence defined manner.[27] While ROMP methods are capable of maintaining precise control throughout polymerization, they are often limited by the availability of macrocyclic olefins with a sufficient strain to thermodynamically favor the polymerization.

An early method out of the Lutz group of utilizing controlled radical polymerization involved the conscious placement of n-substituted maleimide groups in the atom transfer radical polymerization (ATRP) of styrene.[28] They were able to further use the copolymerization of this non-stoichiometric donor (styrene) and acceptor (N-maleimides) system to create an automated method for synthesis.[29] They used this donor/acceptor relationship to incorporated functionality into chain growth polymerization through the timed control of the placement of N-maleimides.[30] They then went on to create homopolymers and copolymers with controlled compositions relying on this same relationship and the help of nitroxide-mediated polymerization (NMP); however, they used p-octadecylstyrene in place of styrene as the donor in order to affect changes in the primary structure specifically they found that adding N-maleimides had a tangible effect on the crystallization and melting temperatures.[31]

1.2.6. Template-assisted Synthesis
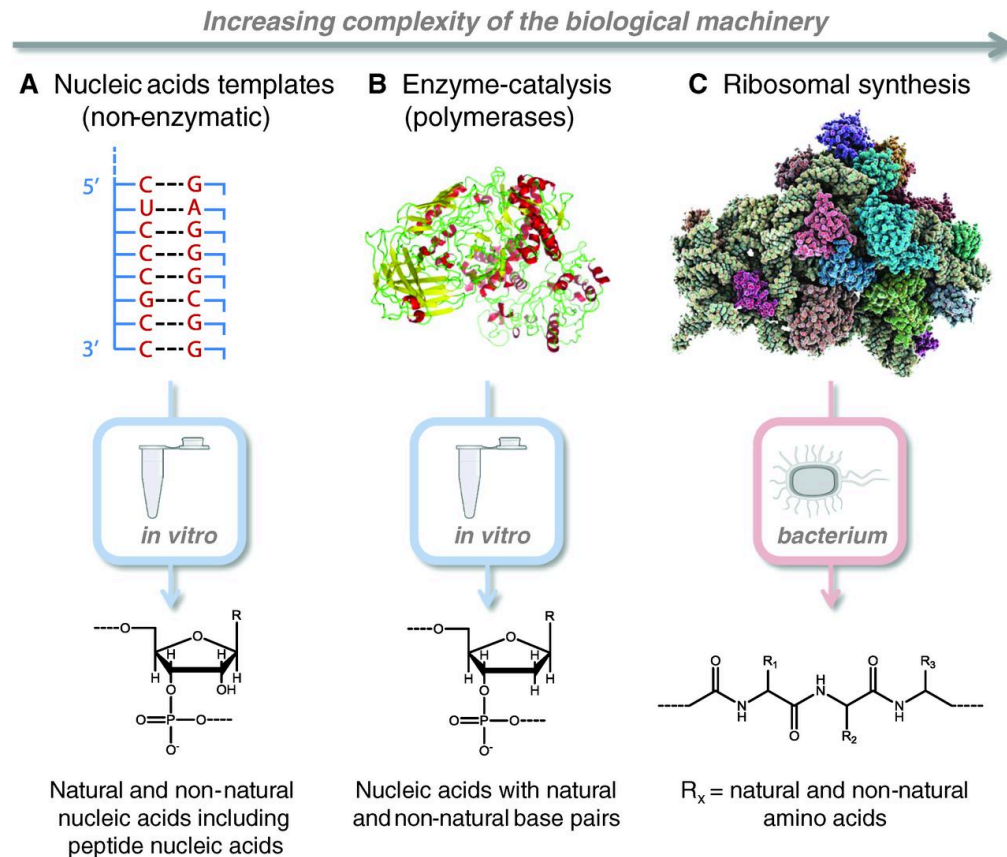
Figure 1.2. Schematic showing three methods of biological polymerizations in increasing complexity[9a]

The natural biological processes of translation, selection, replication, and mutation have been repeated in a lab setting to evolve biopolymers with desired properties. This led to a desire to apply these properties to synthetic sequenced-defined polymers. Lutz described the three methods of biological polymerization in levels of increasing complexity as shown in Figure 1.2.[9a] The first is this idea of using nucleic acid templates to create both canonical and analogous nucleic acids. The second method has relied upon enzymatic methods for synthesis. The final method relies upon the principles of ribosomal synthesis.

1.2.7. Nucleic Acid Templates

Nucleic acids (DNA and RNA) are information-bearing macromolecules that transport information through a sequence of nucleotides. Specifically, they consist of sugar-phosphate backbones attached with a sequence of complementary nucleobase residues that can self-assembly into a molecular ladder formation *via* hydrogen bonding.[32] The complementary nature of nucleic acids plays an integral role in their structure and function. There have been several different nucleic acid analogues that have been developed over the past few decades. Interestingly, several of these analogues have had the ability to not only self-pair to form duplexes but cross-pair with DNA and RNA to form stable hybridized structures using the canonical Watson-crick base pairing with a similar fidelity to DNA. Furthermore, cross pairing with natural nucleic acids has allowed for the templated synthesis of DNA from various synthetic analogues.
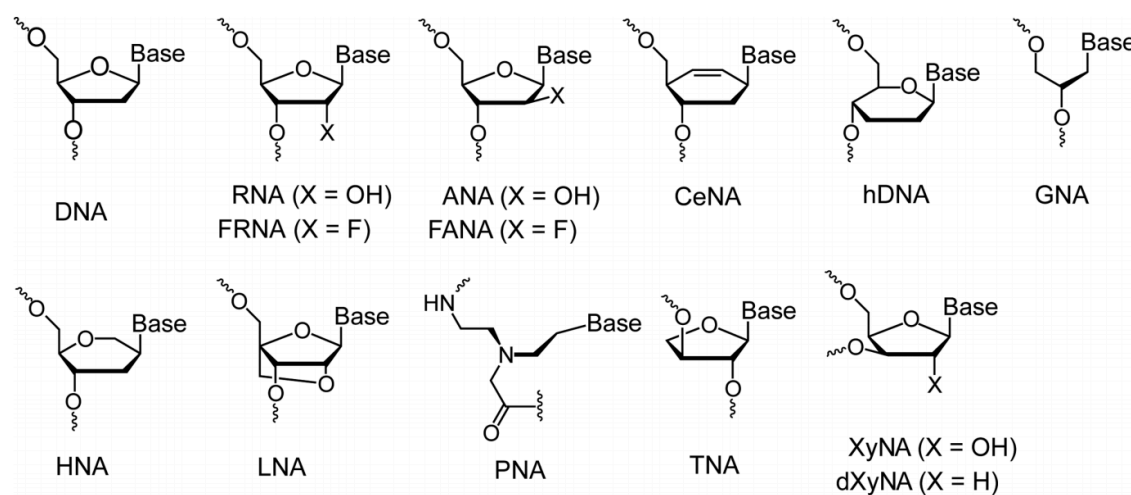
Figure 1.3. Different nucleic acid backbones[33]

Nielsen and company[34] determined that the backbone of DNA could be replaced with a polyamide backbone and maintain the sequence-specific duplex of nucleobases by first incorporating thymine groups and showcasing their ability to form stable hybrids with

complementary DNA strands. These so-called peptide nucleic acids (PNAs) are comprised of N-(2-aminoethyl)-glycine units linked by standard peptide bonds and the nucleobases attached via methylenecarbonyl linkers. They used the features of DNA as inspiration when designing the structure by mimicking the molecule spacing between nucleobases along the achiral backbone and the distance between the backbone and the nucleobases.[35] They built upon the simplistic initial design and included the remaining nucleobases into the PNA backbone showing the ability of PNAs to form stable hybrids with natural nucleic acids with an increased thermal stability owing to the decrease in electrostatic repulsion experienced by replacing the phosphate backbone of DNA with the polyamide backbone.[36] They further explored PNAs ability to form duplexes with complementary PNA strands demonstrating that nucleic acid like helices were possible without a sugar phosphate backbone. PNAs can bind their complementary strand as well as natural nucleic acids in both parallel and anti-parallel fashion.

Eschenmoser systematically explored several synthetic nucleic acids with the goal of determining the origins of DNA and RNA.[37] This strategy spurred the development of (L)- α-threofuranosyl oligonucleotides (TNA), a simplified nucleic acid, that is comprised of therose sugars connected by 2',3'-phosphodiesters bonds. TNA is able to form self-complementary duplexes and undergo cross-pairing with both DNA and RNA using the natural nucleobase interactions in a strictly anti-parallel fashion.[37] TNA has remarkable biostability under simulated physiological conditions making it a useful compound for biomedical applications; TNA monomers were combined with natural nucleic acids nucleotides to form oligonucleotides (ONs) where the TNA could protect neighboring DNA strands from nuclease degradation and shield RNA from degradation enzymes.[38]

Another alternative backbone is the glycol nucleic acids (GNAs),[39] a relatively easy to synthesize ON where the backbone consists of propylene glycol units connected by phosphodiester bonds, and the canonical Watson-Crick base pairs are used to form stable anti-parallel duplexes with complementary single GNA strand. Chirality is essential in maintaining the anti-parallel hybridization and is introduced into the backbone through enantiomer monomers that are able to pair with like enantiomers resulting in molecular ladders with superior thermal stability to natural nucleic acids. The Meggers' group has shown that S-GNA is also able to cross-pair with RNA but not with DNA to form stable duplexes.[40] Other groups have expanded on the pioneering work out of this lab to produced analogues with glycol-based backbones that have similarly been able to self-pair and selectively cross-pair to form molecular ladders.[41] The inability for GNA to cross-pair with DNA prompted Szostak and company to utilize GNA as a template for the synthesis of DNA. Enzymatic synthesis of DNA usually requires a stable duplex to be formed between the parent and daughter strand, but they were able to use a to catalyze the synthesis of DNA.

Locked nucleic acids (LNA) are ONs that contain a nucleobase where adding a methylene bond between the 2' oxygen and the 4' carbon modifies the 1,2:5,6-di-O-isopropylene-α-D-allofuranose. These oligomers are capable of forming stable duplexes with both DNA and RNA as well as forming hybrids with complementary strands also containing the LNA monomers.[42] Wengel and colleagues reported these duplexes to have increased thermal stabilities and improved nucleic acid recognitions as measured by the change in thermal stability with the incorporation of mismatched nucleobases.[43] LNAs gave rise to 2'-amino-LNA[44] nucleotides which are less synthetically challenging and provide a broadening set of applications owing to their ability to incorporate different functionalities.[45] These 2'amino-LNA are still

capable of maintaining the increased selectivity and thermal stability when incorporated into ONs. 2'amino-LNA have been used to incorporate fluorescents,[46] increase biostability,[47] thermal stability,[48] create molecular machines,[49] and explore antisense therapies.[50,51]

In addition to modifying the backbone of nucleic acids, a considerable amount of effort has been devoted to expanding the canonical nucleobases. One of the major focuses of these altered nucleobases is to include fluorescent tags. In one example, pyrimidine's at C5 were modified to include an acridone fluorescent tag. The intensity of the fluorescence decreased by one half when the DNA hybridized with its complementary strand and changed by varying amounts when mismatched making this a useful DNA probe.[52] Further modification of pyrimidine's to evaluate their reactivity and physiochemical properties, showed the versatility of thymine in modification.[53] Shirato et al. formed artificial DNA from noncanonical alkynyl C-nucleotides.[54]

Another area of interest is metal coordinated base pairs, Meggers et al.[55] was the first to incorporate metal base pairs into a oligonucleotide by replacing the hydrogen bonds with a copper-mediated base pair, pyridine-2,6-dicarboxylate nucleobase (Dipic) and pyridine nucleobase (Py) shown in Figure 1.4. They highlighted the specificity and stability of the resulting duplexes with thermal melting experiments showing mismatched oligomers had melting temperature a minimum of 10°C lower than the matched strands. Redox-active metal ions incorporated into nucleic acids could possess useful electronic properties.
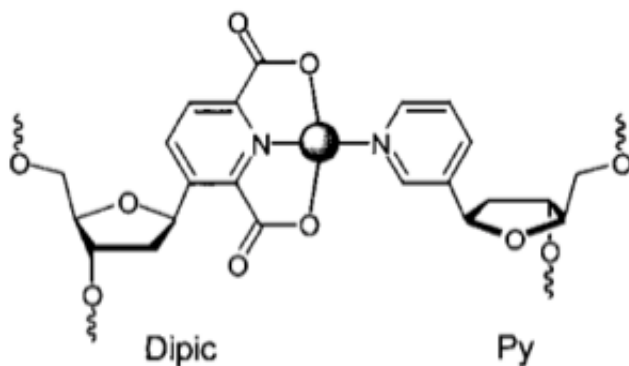
Figure 1.4. Copper-mediated base pair between Dipic and Py[55]

The Schlegel et al. was able to apply the concepts used in DNA to form duplexes that contain metal base pairs in the GNA backbone. They incorporated three different metal base pairs into the middle of the nucleic acid units: copper(II)-mediated hydroxypyridon homo-base pair, nickel(II)-mediated pyridine homo-base pair, and hydroxypyridone-pyridopurine. All three of the base pairs showed stable duplex formation with the copper base pairs showing a slightly higher stability than observed for the same pairs in DNA.[56]

The principles of metal-ion-mediated assembly of DNA has been applied to GNAs[57] to provide a model system for exploring the Pd^{2+} bridging of nucleotides. Pd had not previously been shown to be effective as a metal bridge in oliogomeric species despite its success in the monomeric pairing of nucleotides.[58] They also showed that the placement of the Pd nucleotides affected the formation of the duplex and that the stability favored the metal ions on the terminal nucelobases as opposed to intrachain placement.[57]

1.2.8. Enzyme Catalysis

The major player in enzymatic synthesis has been the development and commercialization of polymerase chain reaction, PCR.[59] The Liu group has also been particularly active in this field of enzymatic catalysis for synthesizing sequence-defined

polymers.[60] Their more recent work has developed highly functionalized nucleic acid polymers using a DNA ligase to catalyze the polymerization of consecutive functionalized oligonucleotide building blocks along a DNA template leading to a robust library of codons and side-chain diversity.[61]

1.2.9. Ribosomal Synthesis

Methods of genetic engineering have been used extensively for a wide range of applications. They have been adapted over the last several decades to include non-canonical amino acids. One method for carrying this out is to replace amino acids with synthetic analogues that encode some sort of functionality.[62] The idea of residue-specific incorporation of non-canonical amino acids shows vast potential in different applications as reviewed recently.[16]

1.3 Orthogonal Chemistries

Sequence-specific polymers are an attractive option for incorporating functionality into macromolecular structures. This led us to begin to explore different chemistries that we could utilize in sequence-specific structures to direct the assembly of different structures. We looked into two different areas: click chemistry and dynamic covalent chemistry.

1.3.1. Click Chemistry

The term "click chemistry" was coined by Sharpless and fully described to be a set of "spring-loaded" reactions that will quickly and irreversibly form a single product stemming from a high thermodynamic driving force.[2] In the prototypical click chemistry, copper-catalyzed azide-alkyne cycloaddition (CuAAC, shown in Figure 1.Xa), the addition of the copper catalyst results in preferential formation of the 1,4-isomer cycloaddition product over a wide range of reaction conditions. This was an improvement upon conventional methods that required an

excess of 100°C and several days to form a mix of cycloaddition products which led the wide spread use of this copper catalyzed chemistry in several applications.[63]

(a)

(b)
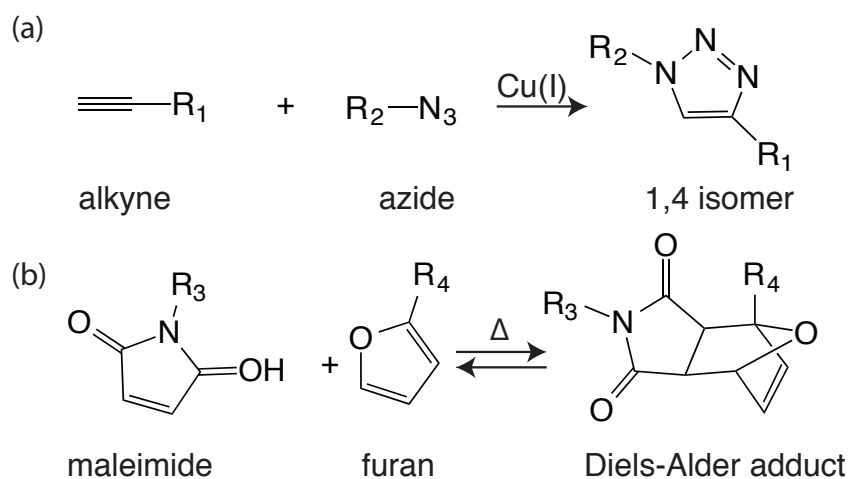
Figure 1.5. Click chemistries, including (a) copper (I) catalyzed azide-alkyne cycloaddition, and (b) Diels-Alder reaction between a maleimide and a furan

Another example of a click chemistry reaction is the thermally-mediated Diels-Alder[4+2] cycloaddition reaction that proceeds between a diene and a substituted alkene (i.e., a dienophile). At moderate temperatures, the equilibrium lies towards the Diels-Alder adduct, whereas at raised temperatures (>100°C), the adduct reverts back to the initial reactants. These materials have been used to fabricate thermoresponsive polymer networks.[64] Three common examples of Diels-Alder chemistries can be found in Figure 1.5 these reactions are attractive in different applications as they are generally stable in most reaction conditions, and they can be tuned to respond over a wide range of temperatures.[65]

One application of this chemistry was developed by Thongsomboon et al.,[66] a method for nanoprinting patterns into films that utilized a Diels-Alder reaction between a maleimide and furan as a cross-linker. They incorporated furan-protected maleimide and furanyl groups into cyclic carbonates that underwent an alcohol initiated ring-opening polymerization to form random copolymers. They spin-coated the polymer onto silicon wafers to produce a film capable

of thermal cross-linking. The cross-linking proceeded by first thermally removing the furan protection group exposing the maleimide and then lowering the temperature to allow the adduct to form. They used the reversibility of the cross-linking reaction to form patterns on the film from a master template by raising the temperature to break the cross-linking and lowering the temperature to reform the adduct in the desired shape as shown in Figure 1.6a; the subsequent images (Figure 1.6b-e) show atomic force microscopy of the imprinted patterns on the film. These biodegradable films could find utility in applications in biomedical surface coatings where the carbonate group could be functionalized for specific cellular interactions.
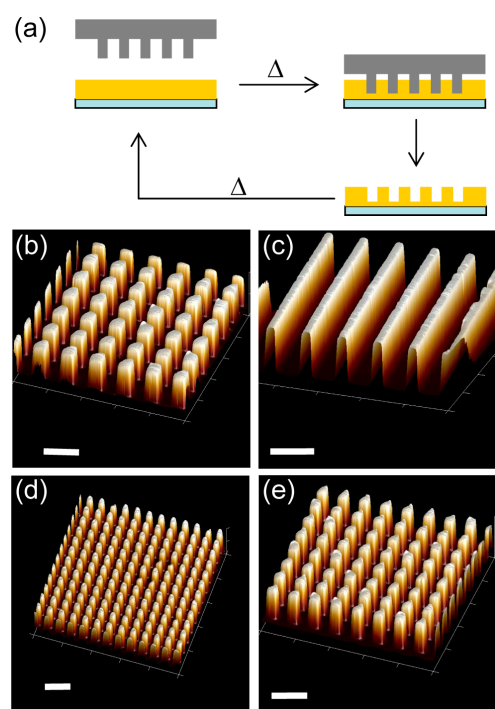
Figure 1.6. Different patterns on films a) schematic showing the fabrication of a patterned film from a template using a Diels-Alder cycloaddition reaction b-e) AFM images of the different shapes and scales made from different templates (Scale bar 1μm) [66]

1.3.2. Dynamic Covalent Chemistry

As mentioned, DCC is a class of reactions where products containing covalent bonds can be reverted back to their initial reactants under a particular set of reaction conditions. Several stimuli, such as temperaure,[67] pH, [68] and photochemical triggers,[69] can be employed to reversibly affect the equilibrium of a reaction. The reversibility of these reactions open the possibility to use them in self-assembly proeceses where they can undergo the error correction necessary to achive the most thermodynamically stable product. The Diels-Alder chemistry can also be classified as a DCC as well as a click chemistry owing to the reversible nature of the covalent bond; it has been expansively used in thermoreversible networks.[70]

(A)

Boronic acid   Diol   Boronate ester

(B)

Aldehyde   Amine   Imine
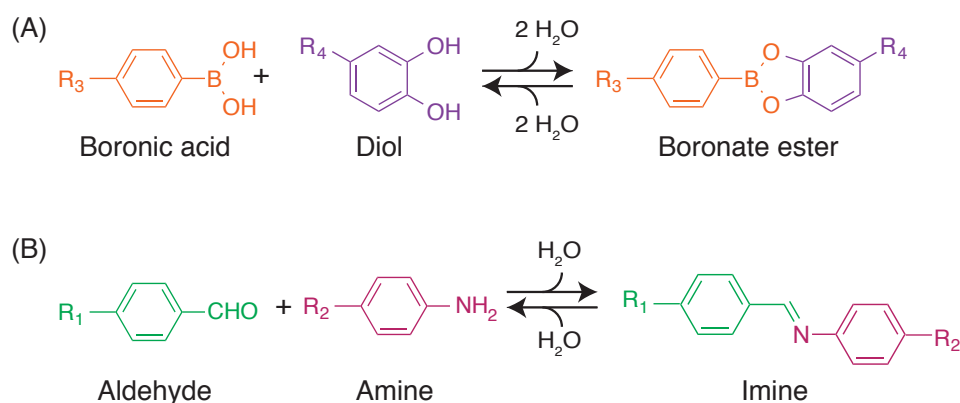
Figure 1.7. Dynamic covalent chemistries (a) esterification reaction between boronic acid and diol (b) amine aldehyde reaction to form an imine

In addition to thermally responsive pairs, there has been extensive development of pH-sensitive dynamic covalent interactions. Diols undergo a pH-reversible condensation reaction with boronic acids to form boronate esters, as shown in Figure 1.7a.[68] Boronate esterification has been used in a variety of application including nanocariers for targeted drug delivery systems,[71] assembled macro-molecular stuctures,[72] and crystal engineering.[73] The Wang group developed a detailed method for exploring the binding affinity of boronic acids with a library of diols using a competition-based assay with alazarin red s.[74] For example, they reported the binding constants

between phenylboronic acids and catechols to be 830 M^{-1} at pH of 7.5; the binding constant dramatically increases to 3300 M^{-1} at a pH of 8.5.[74a] This work was later repeated to include mutlple interactions between boronic acid and diols on polymeric strands.[75] These works have highlighted the pH-dependence of the boronate ester reactions. The strong interactions between boronic acids and diols, particularly common saccharides, have led to them being used in several different sensing applications.[76]

When looking into this esterification reactions, there tends to be stability issues with the initial reactants. For example, the Sumerlin group experienced a reduction in the self-healing ability of a hydrogel that was mediated by the condensation reaction between a catchol and boronic acid owing to the oxidation of the catechol.[77] This oxidation of the catechol to the *o-*quinones stability concern can be particular detrimental in the presence of primary amine functional groups.[78] Boronic acids have also shown to oxidize to the hydroxy groups in the presence of peroxides,[79] but also in the presence of atmospheric oxygen.[80] Boronic acids can also undergo protodeboronation, a common side product in Suzuki coupling reactions, where the boronic acid is replaced with a hydrogen in the presence of water.[81]

Another dynamic covalent condensation reaction that has been explored is that of amines and aldehydes co-reacting to form Schiff base imines (Figure 1.7b). This is an attractive dynamic covalent reactant pair owing to their ability to be incoporated into oligomeric strands and the imine can be reduced upon condensation to the corresponding secondary amine, halting the rearrangement reaction.[82] Aldehydes can also undergo DCC reactions to form C-N bonds with hydrazides and aminoxys to afford acylhydrazones and oximes, respectively.[83] Exchange of imines through transimination and imine metathesis can be accelerated by a Lewis acid such as

Sc(OTf)$_3$.[84] The C-N bond family of chemistries is the most well utilized of the DCC, the imine reaction specifically has been used extenstively.

Kovaricek et al.[85] demonstrated one application of imine chemistry with the use of salicylaldehyde (SALAL) in the reversible formation of imines with different amine compounds to understand molecular motion. They also showed motional covalent dynamics with SALAL and aliphatic diamines meaning the initial monoimines formed undergo this interchange reaction that elicits a motion that can be described as "stepping-in-place" or "single-step." They were able to control rate of the motion by changing the reaction conditions and the length of the diamines. This technology is a foundation step in the formation of molecular electronics as shown in Figure 1.8.
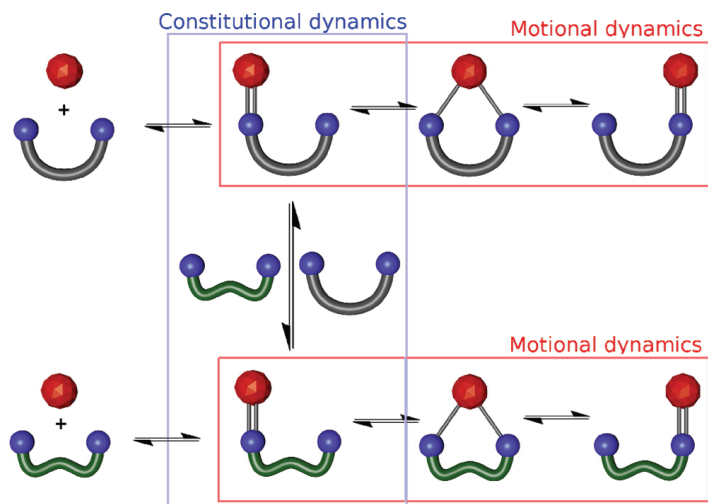
Figure 1.8. Schematic showing the motional dynamics of imine bonds from carbonyl compound (red object) and a diamine (segment) going through imine metathesis (blue box) and the "stepping-in-place" or "single-step" motions (red box)[85]

1.4 Complex Structures

The different chemistries tend to proceed specifically and efficiently making them ideal candidates for constructing different structures. This section will highlight examples and applications of assembling different molecular architectures.

1.4.1. Dynamic Covalent Micelles

Micelles have long shown to be useful molecules in drug delivery systems owing largely to their nanometer size range and their ability to encapsulate hydrophobic therapeutic agents. Micelles can be formed by the aggregation of traditional surfactants or by the self-assembly of larger block copolymers. Amphiphilic surfactants typically comprised of a hydrophilic head and hydrophobic tail self-assemble into micelles at concentrations of surfactants exceeding the so-called critical micelle concentration (CMC). Polymeric micelles are assembled from amphiphilic block copolymers where one block is a hydrophilic group that forms the outer shell of the micelle in an aqueous environment and the other block forms the hydrophobic core of the micelle. In addition to their size and ability to encapsulate water insoluble drugs, micelles can be built from a large range of block copolymers that utilize different chemistries. This allows for the fabrication of polymeric micelles that can be tailored for their intended applications.[86] Dynamic covalent chemistry has been introduced to both surfactant and polymeric micelles as a method of mediating the assembly.

Minkenberg et al.[87] converted a nonamphiphilic surfactant comprised of a polar head group with an aromatic aldehyde into an amphiphile by exposing the surfactant to an aliphatic amine that upon reversible imine bond formation between the aldehyde and amine left an apolar tail that could self-assemble into pH-controlled micelles as shown in Figure 1.9. This allowed them to control the micelle formation by switching between the assembled amphiphilic structure

19

and the disassembled nonamphiphilic state by means of reversible imine formation controlled by manipulating the pH. They also showed the potential utility of this technology to be used in drug delivery systems by controlling the uptake and release of Nile Red, a hydrophobic organic dye.
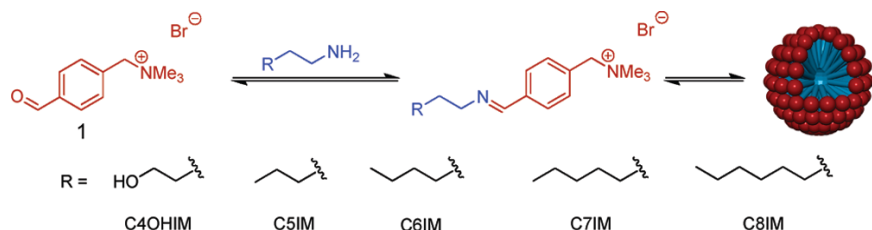
Figure 1.9 Controlled formation of micellar aggregates from (1) the aromatic aldehyde polar head group reversibly reacting with various amines to form an amphiphilic surfactant that can self-assemble into micelles[87]

Minkenberg et al.[88] further built on this work by combining two water soluble dynamic covalent surfactants containing either aldehyde or amine functional groups to generate vesicles composed of reversible imine bonds. These vesicles cluster to form vesicle networks that lead to pH-reversible gels shown in Figure 1.10, which potentially could be used as self-healing materials or as vesicles for drug delivery systems. Self-assembling hydrogels also serve as promising mimics for biological agents such as the cytoskeleton and extracellular matrix.
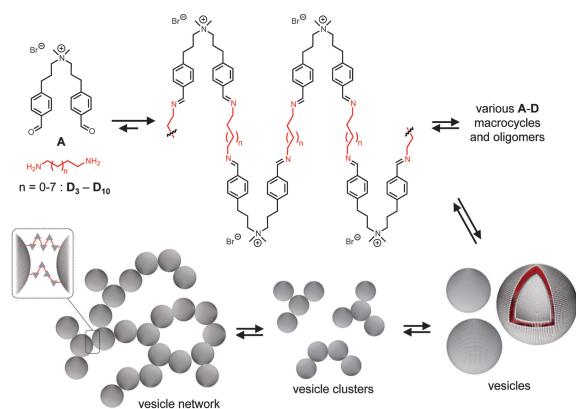
Figure 1.10. Schematic showing the formation of imine bonds from difunctionalized aldehydes and aliphatic amines to form macrocycles and oligomers leading to the vesicles, vesicle clusters, and finally vesicle networks capable of forming pH-reversible hydrogels[88]

Minkenberg et al.[89] continued this work by fabricating gemini surfactants by utilizing the same amine/aldehyde reaction then used those surfactants to make wormlike micelles as shown in Figure 1.11. Gemini surfactants are characterized by having multiple amphiphilic functional groups on each short strand. This is the first evidence of a reversible aggregation of Gemini surfactants to form wormlike micelles; these so-called Gemini surfactants have shown great potential in both biological applications such as gene transfection and industrial applications as viscoelastic additives for cosmetics. They formed the surfactants from aliphatic amines of various lengths and a bisaldehyde-functionalized quaternary ammonium head group.
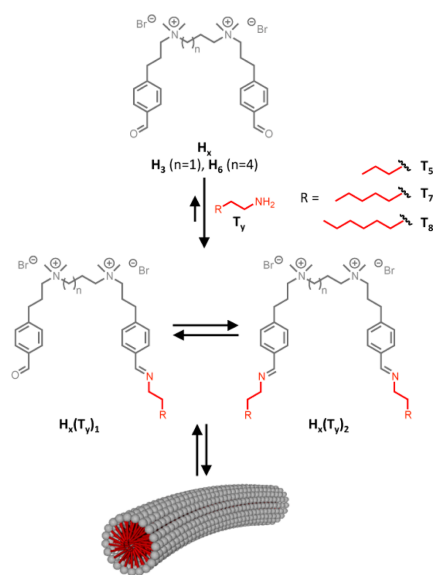
Figure 1.11. The formation of wormlike micelles from Gemini surfactants comprised of a bisaldehyde head group and amine tail groups[89]

Li et al.[90] used disulfide chemistry to fabricate responsive cross-linked micelles that were loaded with the therapeutic, paclitaxel (PTX), for controlled release on tumor sites as shown in Figure 1.12. They introduced cysteine into linear-dendritic system of polyethylene glycol(PEG) and cholic acid that was subsequently oxidized to form disulfide bonds in the core of the micelle. This cross-linked micelle had increased stability and a lower CMC than non-cross-linked

micelles; however, the cross-linked micelles had a slower release of PTX. They could control the release of the PTX by altering the amount of cellular glutathione. In animal studies, they found that the cross-linked micelles more efficiently collected and released at the tumor site of mice carrying the "SKOV-3 ovarian cancer xenograft".
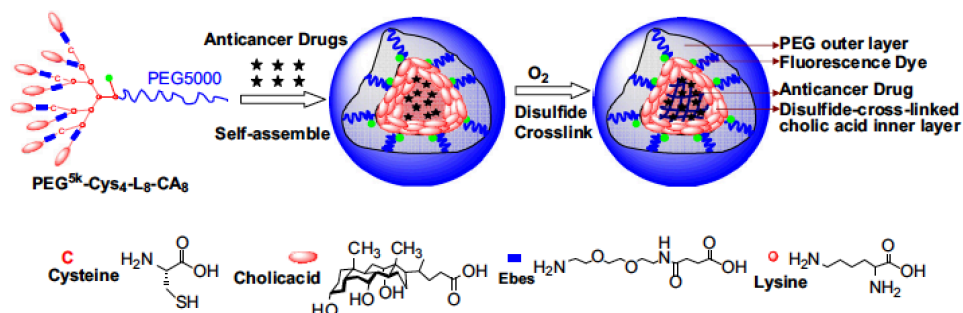
Figure 1.12. The formation of PTX loaded micelles through disulfide bond formation[90]

1.4.2. Dynamic Covalent Hydrogels[90]

Most water-soluble functionalized nanoparticles are formed by an inverse microemulsion method that is based on lipophilic solvents yielding gels that are not suitable to encapsulate hydrophobic molecules. Ryu et al.[91] developed a nonemulsion method for fabrication of these nanoparticles that are incorporated into nanogels; this method allowed for the encapsulation of hydrophobic groups as shown in Figure 8. They added a stimuli-responsive disulfide bond to form inter/intrastrand cross-linking in the gel formation making this material potentially useful in drug delivery applications where the body could reduce the disulfide bond leading to the disassembly of the nanogel and release of the encapsulated hydrophobic moiety.
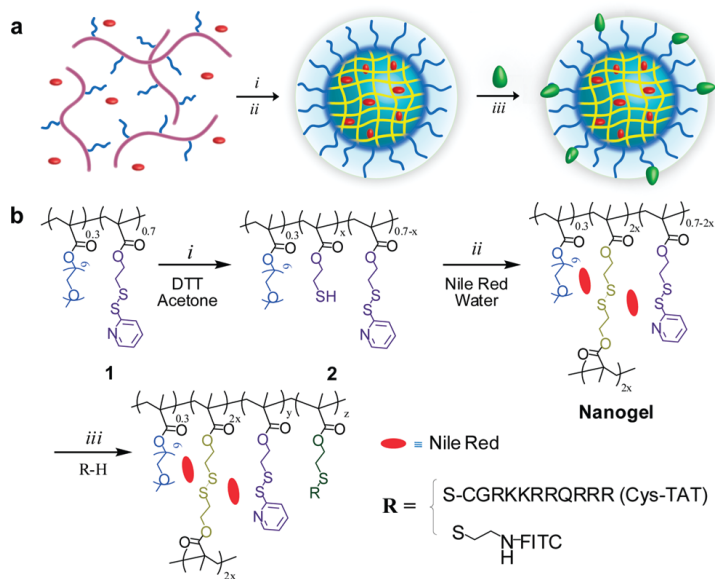
Figure 1.13. Dyanmic covalent nanogel a) schematic showing the formation of a nanogel from functionalized nanoparticles b) structures of the nanogel including the disulfide chemistry[91]

Hydrogels show potential as biological agents because of their ability to encapsulate different agents including therapeutics and cells useful for tissue engineering. Fairbanks et al.[92] were able to incorporate a lithium acylphosphinate photoinitiator (LAP) into a hydrogel formed from the oxidation of thiol-functionalized 4-armed poly(ethylene glycol) (PEG) to fabricate a photo-responsive hydrogel where LAP generated radicals could break the disulfide bonds that cross-linked the gel (Figure 1.14). They overcame the common challenges facing photoadaptable polymers of light attenuation and low quantum yield to form 2 mm thick hydrogels rapidly at light intensities of 10 mW/cm^2 at a wavelength of 365 nm. They demonstrated the self-healing abilities of the hydrogel by manipulating the photoinitiator concentration to control the number of radicals formed in the sample. Moreover, if the concentration of sulfur radicals was on the same order magnitude of the carbon- and phosphorus radicals formed from the photoinitiator, the gel would break up into PEG groups. If there were considerably more sulfur radicals in the sample, disulfide exchange would occur allowing for self-healing.
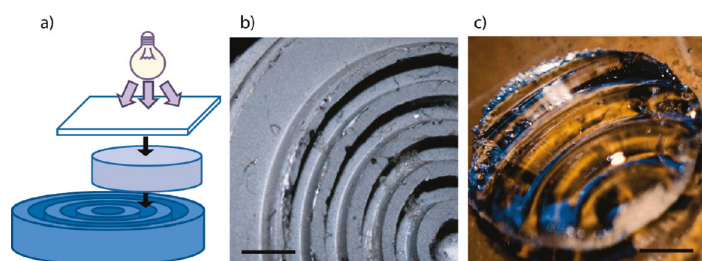
Figure 1.14. Dynamic covalent hydrogel a) Schematic showing the formation of a pattern into the photoadaptable hydrogel b) The patterned surface scale bar = 1.5mm c) The resulting patterned hydrogel scale bar = 1.5mm [92]

1.4.3. Cyclic Structures

Cyclic assemblies are found extensively in biological systems playing the role of therapeutics,[93] toxins,[94] and synthetic ion channels.[95] Several naturally occurring cyclic peptides are useful in drug discovery with many serving as therapeutic agents including antimicrobial peptides (AMPs), peptides that have been shown to kill bacteria, viruses, and fungi.[96] These characteristics have led to the development of synthetic cyclic compounds that mimic their biological potency.[97]

In addition to cyclized peptides, sequence-specific peptoids are particularly suitable for synthetic cyclic assemblies for biologically-active species owing to their proteolytic stability[98] and inherent non-immunogenicity.[99] Peptoids are easily synthesized from commercially available primary amines and have been used to prepare macrocycles that can serve as biological molecular scaffolds.[100] Cyclization of peptoids has also been suggested as a possible strategy for introducing rigidity into generally "floppy" structures to unlock specificity necessary for therapeutic design.[101]

1.4.4. Nucleic Acid Nanotechnology

Another common method of forming complex molecular structures is molecular self-assembly. Self-assembly is defined as a process in which components of a disordered system aggregate to form an organized structure or pattern based on the local interactions between the individual components.[102] The mechanism to afford these ordered structures must either be reversible or allow for the initial reactants to adjust their position after aggregate formation. This mechanism accounts for error correction during the assembly process necessary to minimize the Gibbs energy and form the most thermodynamically stable product.[102]

Examples of self-assembly are present throughout chemistry, biology, and materials science, such as surface modification through self-assembled monolayers,[103] the formation of crystals,[104] and nucleic acid hybridization.[105] These processes often rely upon weak intermolecular interactions such as hydrogen bonding, π stacking, or van der Waals interactions;[106] thus, the resultant structures are generally fragile and susceptible to thermal and mechanical degradation.

Nucleic acids (DNA and RNA) are information-bearing macromolecules that transport information through a sequence of nucleotides. Specifically, DNA consists of two single stranded sugar-phosphate backbones attached with a sequence of complementary nucleobase residues that self-assembly into a double helix formation *via* hydrogen bonding.[32] In 1982, Seeman capitalized on the hybridization selectivity of DNA to assemble non-linear structures marking the emergence of the field of nucleic acid nanotechnology.[107] By annealing oligonucleotide sequences that lack the symmetry typically found in their biological counterparts, junctions from which multiple double stranded structures originate can be fabricated (see Figure 1.15a). These junctions can be linked together directly or with linear DNA

fragments by utilizing "sticky end" unhybridized nucleotide overhangs. Seeman leveraged this technology to fabricate a cubic molecule composed exclusively of DNA (see Figure 1.15b),[108] highlighting the capacity of nucleic acids to form complex nanostructures.
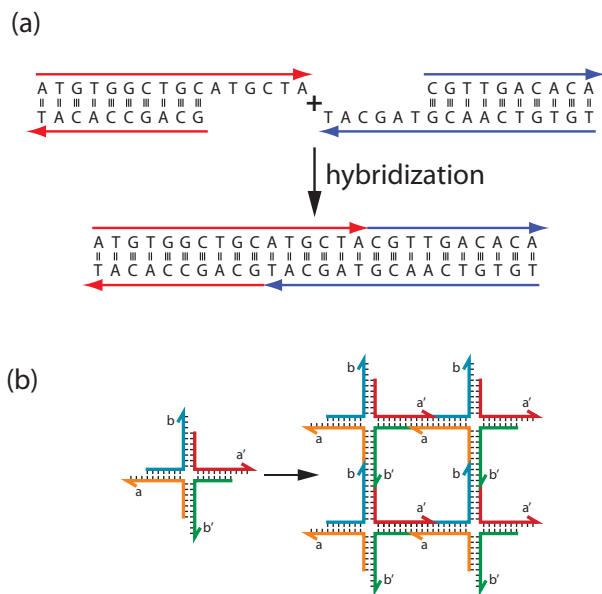
Figure 1.15. Nucleic acid nanotechnology (a) "stick end" unhybridized overhangs (b) non-linear junctions

The development of 'DNA origami',[109] a novel fabrication technique, has spurred an increased interest in nucleic acid nanotechnology in the last decade. This method involves the synthesis of pre-determined two-dimensional shapes by raster-filling with a long, viral single-stranded DNA of a known sequence held in places with several shorter oligomeric 'staple strands.' Other methods were developed that exclusively utilize shorter nucleic acid strands which can be synthetically fabricated for increased chemical diversity; these so-called 'DNA tiles' and 'DNA bricks' are able to assemble into complex 2D and 3D structures in a single annealing reaction.[110] These techniques enable the generation of arbitrary structures with unprecedented sophistication that have found utility in multiple applications such as disease diagnostics[111] and plasmonic devices.[112]

Despite nucleic acid nanotechnology making significant strides in recent years, there are still mechanical and thermal limitations in assembled structures owing to the hydrogen bonds holding the DNA together. Throughout several biological processes, it is essential that DNA be able to undergo force-induced melting;[113] however, this process is unfavorable when constructing durable nanostructures. Double stranded DNA mechanically unzips under a force of ~15 pN[114] whereas covalent bonds can withstand forces up to two orders of magnitude higher. Thus, it is anticipated that nanostructures fabricated utilizing dynamic covalent bonding will display an hundred-fold difference in mechanical stability.

1.4.6. Covalent Self-Assembly

Covalent bonds are typically irreversible, making covalent self-assembly atypical owing to the error correction mechanism necessary to form ordered structures. Although the use of this chemistry is uncommon, there are several examples of the success of dynamic covalent self-assembly. Jean-Marie Lehn (Nobel prize in Chemistry, 1987) has exploited covalent bonds for the rearrangement of dynamic, reversible nucleic acid analogues or 'DyNAs'.[115] This study showed that polymers with certain chain functionalities could be appended to nucleobases, lending to polymers that undergo constitutional changes in solution. Similarly, the Ghaderi group demonstrated the dynamic sequence modification of oligomers using side-chain-reversible functional groups.[116]

Neither of these examples specifically used dynamic covalent reactions for base pairing interactions between complementary oligomeric strands. This approach was first attempted by the Moore group, who employed scandium(III)-catalyzed imine metathesis for the dynamic covalent self-assembly of complementary *m*-phenylene ethynylene oligomers into *n*-rung molecular ladders.[117] This investigation had limited success owing to the unfavorable kinetic

trapping experienced at four or more rungs,[117b] highlighting the necessity to consider both the thermodynamic and kinetic elements in the design of oligomeric strands that are able to selectively hybridize.

Wei et al. were likewise able to form molecular ladders (Figure 1.17) through the hybridization of sequence-defined peptoid-based oligomers designed to undergo an amine/aldehyde condensation reaction with the use of a Lewis acid catalyst. The duplexes were able to overcome the kinetic limitation of the longer m-phenylene ethynylene ladders owing to the flexibility of the peptoid backbone.[118] These sequence-controlled polymers provide an alternative more mechanically robust method for encoding information than similar biological and hydrogen bonded synthetic polymers.
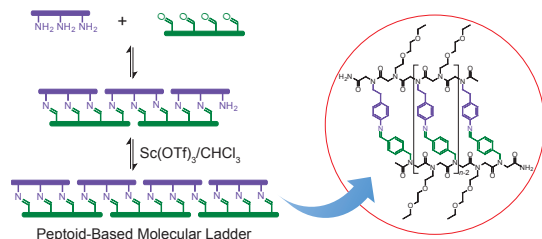
Figure 1.16. Peptoid-based covalent ladder assembly[118a]

Another example of non-ladder covalent assembly was described by Bapat et al.[72] when they use boronic acid block copolymers and various multi-function diols to form star polymers employing an arm-first synthetic approach. By capitalizing on the reversibility of the boronic acid and diol reaction, they were able to control the dissociation of the star polymers by introducing competing mono-functional diols as shown in Figure 1.17. They further developed this technology to include a method for assembling redox-responsive star polymers. By using the same arm-first method, they made disulfide-cross-linked stars from maleic anhydride and a

disulfide containing diamine. The stars underwent reductive cleavage of the disulfide bond to revert back to unimers. The resulting thiol from reduction can be readily reoxidized into a disulfide making these structures suitable for self-healing applications. This chemistry is attractive for drug delivery applications where the structure could disassemble releasing a therapeutic by utilizing the natural reducing conditions experienced in the body.[119]
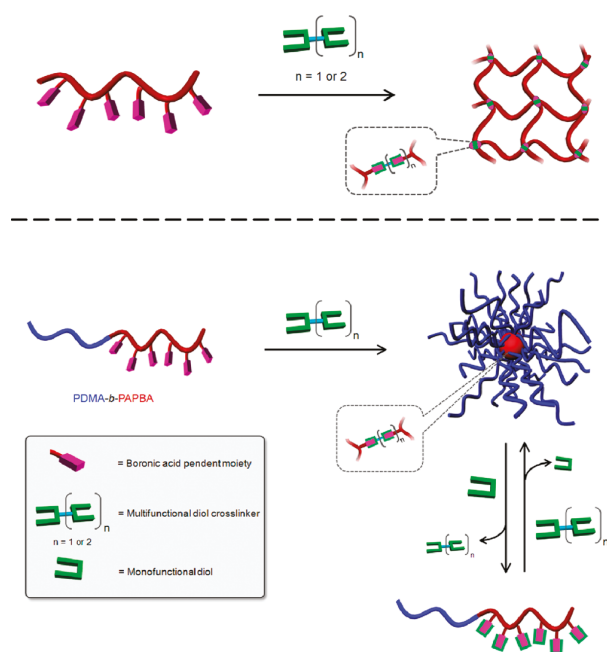
Figure 1.17. The reversible formation of star polymers from boronic acids and mono- and di-functional diols[72]

1.4.6. Orthogonal Assemblies

One of the first reports of orthogonal DCC in metal-free complex assemblies was between the boronate ester and imine reactions.[120] The Severin group soon after published worked that combined these two reactions to assemble macrocycles (Figure 1.18), molecular cages, and dendritic nanostructures.[121] These assembled structures highlight the potential of incorporating small molecules containing these two chemistries to ultimately form reversible

complex structures. More recent work has been done to incorporate different DCC into similar

molecular structures.[122]
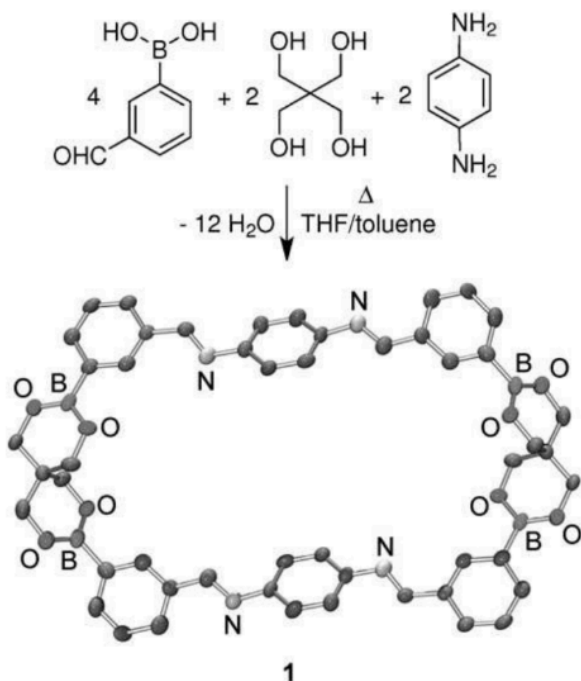
Figure 1.18. Assembly of macrocycles from orthogonal imine forming and boronate esterification reactions[145]

1.4.7. Dynamic combinatorial libraries

Dynamic combinatorial libraries (DCLs) are useful devices for discovering a wide range

of functionalities. They are a mixture of complex assemblies built from relatively simple

dynamic covalent building blocks reacting with one another to form reversible bonds. They have

proved to be an appropriate method for fabricating synthetic receptors and biological ligands.[4]

Hamieh et al.[123] use a dynamic combinatorial library to determine a receptor for nicotine, a

somewhat hydrophilic moiety, in water at a neutral pH. The building blocks of the receptor were

capable of undergoing reversible thiol-disulfide exchange and contained functional groups

capable of binding with nicotine. They used these building blocks to assemble multiple structures

to find a suitable receptor. Nicotine has shown potential as a therapeutic agent for different diseases; the receptor could act a carrier where the disulfide bond could be reduced in the body.

Bhat et al.[124] demonstrated how DCLs have been successfully applied to biological systems using disulfide/thiol exchange reactions; however, there have been limited studies showing the utility of other DCCs. They created a DCL with amine and aldehyde building blocks to show the utility of the reaction in binding proteins. In contrast to in situ reduction methods typically used in amine/aldehyde systems, this group uses aniline as a nucleophilic catalyst in the formation of stable acylhydrazones allowing the reaction to be carried out at a biologically relevant pH.

Several membrane-proteins contain glycan structures that bind to different amino acids; these saccharides are expressed differently in cancerous cells making them ideal screening targets for early detection. Bicker et al.[125] incorporated boronic acid moieties into the formation of a synthetic lectin library owing to the ability of the boronic acids to reversibly react with the diols found on the saccharides. They used this library to determine boronic acid-functionalized synthetic lectins that specifically bind with glycoproteins.

1.5 Overview of Subsequent Chapters

The remaining chapters of this dissertation will experimentally explore the ideas introduced in this chapter and are arranged as follows:

Chapter 2 will discuss the design and post-synthetic functionalization of cyclic peptoid structures through orthogonal reactions. First oligopeptoids of different lengths were cyclized by a copper (I) catalyzed alkyne-azide cycloaddition reaction between terminal alkyne/azide residues. The cyclic assemblies synthesized to include furan functional groups that were then

conjugated to a maleimide-bearing amine to highlight the potential of cyclic peptoids in the building biological scaffolds.

Chapter 3 describes the formation of molecular ladders by utilizing a thermally reversible dynamic covalent reaction between a furan and a maleimide to affect oligomer hybridization. This chapter details the reaction conditions necessary to form oligomers bearing the reversible functional groups, and the subsequent conditions necessary to mediate hybridization. It will also discuss some of the limitations of the systems and possible strategies for overcoming these challenges in the future.

Chapter 4 will detail the need for an efficient method of fabricating oligomers-bearing boronic acid functional groups. It will provide an overview of the library of methods that were explored to produce a stable oligomer. It will also highlight some key characteristics of the boronic acid oligomers before ultimately determining a strategy for a reliable and stable synthesis of the dynamic covalent oligomers.

Chapter 5 highlights the use of boronic acid and catechol moieties into peptoid-based oligomers that were designed to undergo a dynamic covalent reaction and assemble into molecular ladders with up to 6 rungs. Here we will introduce the idea of molecular grid built from dynamic covalent oligomers. We will also demonstrate the dynamic nature of the reaction through strand rearrangement with pre-assembled molecular ladders. Through the use of a competition assay with Alazarin Red S (ARS), we were also able to determine the binding constant for the formation of molecular ladders. The chapter will also discuss the importance of building molecular ladders en route to the facile fabrication of complex and robust proteomimetic nanostructures.

Chapter 6 highlights the combination of two dynamic covalent chemistries in the synthesis of a base-4 information system that has been designed to form double stranded molecular ladders and molecular grids. Herein we describe the conditions necessary to form specific molecular architectures comprised of imine and boronate ester linkages by first exploring reaction conditions for the individual systems and then combining them to form base-4 information directed assemblies.

Chapter 7 will give an overall summary of the importance of this work, and it will provide a perspective on the future of the field.

1.6. References

1.   Barany, G.; Merrifield, R. B., New Amino Protecting Group Removable By Reduction - Chemistry Of Dithiasuccinoyl (Dts) Function. *J. Am. Chem. Soc.* **1977,** *99* (22), 7363-7365.

2.   Kolb, H. C.; Finn, M. G.; Sharpless, K. B., Click chemistry: Diverse chemical function from a few good reactions. *Angew. Chem.-Int. Edit.* **2001,** *40* (11), 2004-+.

3.   Wilson, A.; Gasparini, G.; Matile, S., Functional systems with orthogonal dynamic covalent bonds. *Chemical Society Reviews* **2014,** *43* (6), 1948-1962.

4.   Li, J.; Nowak, P.; Otto, S., Dynamic Combinatorial Libraries: From Exploring Molecular Recognition to Systems Chemistry. *J. Am. Chem. Soc.* **2013,** *135* (25), 9222-9239.

5.   Schena, M.; Shalon, D.; Davis, R. W.; Brown, P. O., Quantitative Monitoring of Gene Expression Patterns with a Complementary DNA Microarray. *Science* **1995,** *270* (5235), 467-470.

6.   Endo, M.; Yang, Y.; Sugiyama, H., DNA origami technology for biomaterials applications. *Biomater. Sci.* **2013,** *1* (4), 347-360.

7.   Dunn, A. S.; Melville, H. W., Synthesis of Block Copolymers. *Nature* **1952,** *169* (4304), 699-700.

8.   Lutz, J. F., Defining the Field of Sequence-Controlled Polymers. *Macromolecular Rapid Communications* **2017,** *38* (24), 12.

9.   (a) Lutz, J. F.; Ouchi, M.; Liu, D. R.; Sawamoto, M., Sequence-Controlled Polymers. *Science* **2013,** *341* (6146), 628-+; (b) Cavallo, G.; Poyer, S.; Amalian, J. A.; Dufour, F.; Burel, A.; Carapito, C.; Charles, L.; Lutz, J. F., Cleavable Binary Dyads: Simplifying Data Extraction

and Increasing Storage Density in Digital Polymers. *Angew. Chem.-Int. Edit.* **2018,** *57* (21), 6266-6269; (c) Goela, N.; Bolot, J.; Ieee, *Encoding Movies and Data in DNA Storage*. Ieee: New York, 2016.

10.   Epps, I. I. I. T. H.; O'Reilly, R. K., Block copolymers: controlling nanostructure to generate functional materials - synthesis, characterization, and engineering. *Chemical Science* **2016,** *7* (3), 1674-1689.

11.   Alsubaie, F.; Anastasaki, A.; Wilson, P.; Haddleton, D. M., Sequence-controlled multi-block copolymerization of acrylamides via aqueous SET-LRP at 0 degrees C. *Polym. Chem.* **2015,** *6* (3), 406-417.

12.   Anastasaki, A.; Nikolaou, V.; Pappas, G. S.; Zhang, Q.; Wan, C.; Wilson, P.; Davis, T. P.; Whittaker, M. R.; Haddleton, D. M., Photoinduced sequence-control via one pot living radical polymerization of acrylates. *Chemical Science* **2014,** *5* (9), 3536-3542.

13.   Elladiou, M.; Patrickios, C. S., ABC Triblock Terpolymers with Orthogonally Deprotectable Blocks: Synthesis, Characterization, and Deprotection. *Macromolecules* **2015,** *48* (20), 7503-7512.

14.   Lutz, J.-F., Aperiodic Copolymers. *Acs Macro Letters* **2014,** *3* (10), 1020-1023.

15.   Merrifield, R. B., SOLID PHASE PEPTIDE SYNTHESIS .1. SYNTHESIS OF A TETRAPEPTIDE. *J. Am. Chem. Soc.* **1963,** *85* (14), 2149-&.

16.   Johnson, J. A.; Lu, Y. Y.; Van Deventer, J. A.; Tirrell, D. A., Residue-specific incorporation of non-canonical amino acids into proteins: recent developments and applications. *Curr. Opin. Chem. Biol.* **2010,** *14* (6), 774-780.

17.   Zuckermann, R. N.; Kerr, J. M.; Kent, S. B. H.; Moos, W. H., Efficient method for the preparation of peptoids oligo(n-substituted glycines) by submonomer solid-phase synthesis. *J. Am. Chem. Soc.* **1992,** *114* (26), 10646-10647.

18.   Espeel, P.; Carrette, L. L. G.; Bury, K.; Capenberghs, S.; Martins, J. C.; Du Prez, F. E.; Madder, A., Multifunctionalized Sequence-Defined Oligomers from a Single Building Block. *Angew. Chem.-Int. Edit.* **2013,** *52* (50), 13261-13264.

19.   Martens, S.; Van den Begin, J.; Madder, A.; Du Prez, F. E.; Espeel, P., Automated Synthesis of Monodisperse Oligomers, Featuring Sequence Control and Tailored Functionalization. *J. Am. Chem. Soc.* **2016,** *138* (43), 14182-14185.

20.   Al Ouahabi, A.; Charles, L.; Lutz, J.-F., Synthesis of Non-Natural Sequence-Encoded Polymers Using Phosphoramidite Chemistry. *J. Am. Chem. Soc.* **2015,** *137* (16), 5629-5635.

21.   Barnes, J. C.; Ehrlich, D. J. C.; Gao, A. X.; Leibfarth, F. A.; Jiang, Y.; Zhou, E.; Jamison, T. F.; Johnson, J. A., Iterative exponential growth of stereo- and sequence-controlled polymers. *Nature Chemistry* **2015,** *7* (10), 810-815.

22.   Roy, R. K.; Laure, C.; Fischer-Krauser, D.; Charles, L.; Lutz, J. F., Convergent synthesis of digitally-encoded poly(alkoxyamine amide)s. *Chem. Commun.* **2015,** *51* (86), 15677-15680.

23.   Charles, L.; Laure, C.; Lutz, J. F.; Roy, R. K., MS/MS Sequencing of Digitally Encoded Poly(alkoxyamine amide)s. *Macromolecules* **2015,** *48* (13), 4319-4328.

24.   Osawa, K.; Kobayashi, S.; Tanaka, M., Synthesis of Sequence-Specific Polymers with Amide Side Chains via Regio-/Stereoselective Ring-Opening Metathesis Polymerization of 3-Substituted cis-Cyclooctene. *Macromolecules* **2016**.

25.   Weiss, R. M.; Short, A. L.; Meyer, T. Y., Sequence-Controlled Copolymers Prepared via Entropy-Driven Ring-Opening Metathesis Polymerization. *Acs Macro Letters* **2015,** *4* (9), 1039-1043.

26.   Moatsou, D.; Hansell, C. F.; O'Reilly, R. K., Precision polymers: a kinetic approach for functional poly(norbornenes). *Chemical Science* **2014,** *5* (6), 2246-2250.

27.   Gutekunst, W. R.; Hawker, C. J., A General Approach to Sequence-Controlled Polymers Using Macrocyclic Ring Opening Metathesis Polymerization. *J. Am. Chem. Soc.* **2015,** *137* (25), 8038-8041.

28.   Pfeifer, S.; Lutz, J.-F., A facile procedure for controlling monomer sequence distribution in radical chain polymerizations. *J. Am. Chem. Soc.* **2007,** *129* (31), 9542-+.

29.   Chan-Seng, D.; Zamfir, M.; Lutz, J.-F., Polymer-Chain Encoding: Synthesis of Highly Complex Monomer Sequence Patterns by Using Automated Protocols. *Angew. Chem.-Int. Edit.* **2012,** *51* (49), 12254-12257.

30.   Zamfir, M.; Lutz, J.-F., Ultra-precise insertion of functional monomers in chain-growth polymerizations. *Nature Communications* **2012,** *3*.

31.   Srichan, S.; Kayunkid, N.; Oswald, L.; Lotz, B.; Lutz, J.-F., Synthesis and Characterization of Sequence-Controlled Semicrystalline Comb Copolymers: Influence of Primary Structure on Materials Properties. *Macromolecules* **2014,** *47* (5), 1570-1577.

32.   Watson, J. D.; Crick, F. H. C., Molecular Structure of Nucleic Acids: A Structure for Deoxyribose Nucleic Acid. *Nature* **1953,** *171* (4356), 737-738.

33.   Anosova, I.; Kowai, E. A.; Dunn, M. R.; Chaput, J. C.; Van Horn, W. D.; Egli, M., The structural diversity of artificial genetic polymers. *Nucleic Acids Res.* **2016,** *44* (3), 1007-1021.

34.   Nielsen, P. E.; Egholm, M.; Berg, R. H.; Buchardt, O., Sequence-Selective Recognition Of DNA By Strand Displacement With A Thymine-Substituted Polyamide. *Science* **1991,** *254* (5037), 1497-1500.

35.   Egholm, M.; Buchardt, O.; Nielsen, P. E.; Berg, R. H., Peptide Nucleic-Acids (Pna) - Oligonucleotide Analogs With An Achiral Peptide Backbone. *J. Am. Chem. Soc.* **1992,** *114* (5), 1895-1897.

36.   Egholm, M.; Buchardt, O.; Christensen, L.; Behrens, C.; Freier, S. M.; Driver, D. A.; Berg, R. H.; Kim, S. K.; Norden, B.; Nielsen, P. E., PNA Hybridizes To Complementary Oligonucleotides Obeying The Watson-Crick Hydrogen-Bonding Rules. *Nature* **1993,** *365* (6446), 566-568.

37.   Eschenmoser, A., Chemical etiology of nucleic acid structure. *Science* **1999,** *284* (5423), 2118-2124.

38.   Culbertson, M. C.; Temburnikar, K. W.; Sau, S. P.; Liao, J. Y.; Bala, S.; Chaput, J. C., Evaluating TNA stability under simulated physiological conditions. *Bioorg. Med. Chem. Lett.* **2016,** *26* (10), 2418-2421.

39.   Zhang, L.; Peritz, A.; Meggers, E., A Simple Glycol Nucleic Acid. *J. Am. Chem. Soc.* **2005,** *127* (12), 4174-4175.

40.   (a) Schlegel, M. K.; Essen, L.-O.; Meggers, E., Atomic resolution duplex structure of the simplified nucleic acid GNA. *Chem. Commun.* **2010,** *46* (7), 1094-1096; (b) Schlegel, M. K.; Peritz, A. E.; Kittigowittana, K.; Zhang, L.; Meggers, E., Duplex formation of the simplified nucleic acid GNA. *Chembiochem* **2007,** *8* (8), 927-932; (c) Schlegel, M. K.; Essen, L.-O.; Meggers, E., Duplex structure of a minimal nucleic acid. *J. Am. Chem. Soc.* **2008,** *130* (26), 8158-+.

41.   (a) Bose, T.; Kumar, V. A., Simple molecular engineering of glycol nucleic acid: Progression from self-pairing to cross-pairing with cDNA and RNA. *Bioorganic & Medicinal Chemistry* **2014,** *22* (21), 6227-6232; (b) Chen, J. J.; Cai, X.; Szostak, J. W., N2 '-> P3 ' Phosphoramidate Glycerol Nucleic Acid as a Potential Alternative Genetic System. *J. Am. Chem. Soc.* **2009,** *131* (6), 2119-+.

42.   Koshkin, A. A.; Singh, S. K.; Nielsen, P.; Rajwanshi, V. K.; Kumar, R.; Meldgaard, M.; Olsen, C. E.; Wengel, J., LNA (Locked Nucleic Acids): Synthesis of the adenine, cytosine, guanine, 5-methylcytosine, thymine and uracil bicyclonucleoside monomers, oligomerisation, and unprecedented nucleic acid recognition. *Tetrahedron* **1998,** *54* (14), 3607-3630.

43.   Singh, S. K.; Nielsen, P.; Koshkin, A. A.; Wengel, J., LNA (locked nucleic acids): synthesis and high-affinity nucleic acid recognition. *Chem. Commun.* **1998,** (4), 455-456.

44.   Singh, S. K.; Kumar, R.; Wengel, J., Synthesis of 2 '-amino-LNA: A novel conformationally restricted high-affinity oligonucleotide analogue with a handle. *J. Org. Chem.* **1998,** *63* (26), 10035-10039.

45.   Sorensen, M. D.; Petersen, M.; Wengel, J., Functionalized LNA (locked nucleic acid): high-affinity hybridization of oligonucleotides containing N-acylated and N-alkylated 2 '-amino-LNA monomers. *Chem. Commun.* **2003,** (17), 2130-2131.

46.   Gupta, P.; Langkjaer, N.; Wengel, J., Synthesis and Biophysical Studies of Coronene Functionalized 2 '-Amino-LNA: A Novel Class of Fluorescent Nucleic Acids. *Bioconjugate Chem.* **2010,** *21* (3), 513-520.

47.   (a) Lou, C. G.; Vester, B.; Wengel, J., Oligonucleotides containing a piperazino-modified 2 '-amino-LNA monomer exhibit very high duplex stability and remarkable nuclease resistance. *Chem. Commun.* **2015,** *51* (19), 4024-4027; (b) Astakhova, I. K.; Hansen, L. H.; Vester, B.; Wengel, J., Peptide-LNA oligonucleotide conjugates. *Organic & Biomolecular Chemistry* **2013,** *11* (25), 4240-4249; (c) Schmidt, K. S.; Borkowski, S.; Kurreck, J.; Stephens, A. W.; Bald, R.; Hecht, M.; Friebe, M.; Dinkelborg, L.; Erdmann, V. A., Application of locked nucleic acids to improve aptamer in vivo stability and targeting function. *Nucleic Acids Res.* **2004,** *32* (19), 5757-5765.

48.   (a) Andersen, N. K.; Anderson, B. A.; Wengel, J.; Hrdlicka, P. J., Synthesis and Characterization of Oligodeoxyribonucleotides Modified with 2 '-Amino-alpha-L-LNA Adenine Monomers: High-Affinity Targeting of Single-Stranded DNA. *J. Org. Chem.* **2013,** *78* (24), 12690-12702; (b) Johannsen, M. W.; Crispino, L.; Wamberg, M. C.; Kalra, N.; Wengel, J., Amino acids attached to 2 '-amino-LNA: synthesis and excellent duplex stability. *Organic & Biomolecular Chemistry* **2011,** *9* (1), 243-252.

49.   Astakhova, I. K.; Pasternak, K.; Campbell, M. A.; Gupta, P.; Wengel, J., A Locked Nucleic Acid-Based Nanocrawler: Designed and Reversible Movement Detected by Multicolor Fluorescence. *J. Am. Chem. Soc.* **2013,** *135* (7), 2423-2426.

50.   Fluiter, K.; Frieden, M.; Vreijling, J.; Rosenbohm, C.; De Wissel, M. B.; Christensen, S. M.; Koch, T.; Orum, H.; Baas, F., On the in vitro and in vivo properties of four locked nucleic acid nucleotides incorporated into an anti-H-Ras antisense oligonucleotide. *Chembiochem* **2005,** *6* (6), 1104-1109.

51.   Kumar, M.; Kumar, R.; Rana, N.; Prasad, A. K., Synthesis of 3 '-azido/-amino-xylobicyclonucleosides. *Rsc Advances* **2016,** *6* (21), 17713-17719.

52.   Hasegawa, T.; Shoji, A.; Kuwahara, M.; Ozaki, H.; Sawai, H., Synthesis and property of DNA labeled with fluorescent acridone. *Nucleic Acids Symposium Series* **2006,** *50* (1), 145-146.

53.   Plashkevych, O.; Chatterjee, S.; Honcharenko, D.; Pathmasiri, W.; Chattopadhyaya, J., Chemical and structural implications of 1 ',2 '- versus 2 ',4 '-conformational constraints in the sugar moiety of modified thymine nucleosides. *J. Org. Chem.* **2007,** *72* (13), 4716-4726.

54. Shirato, W.; Chiba, J.; Inouye, M., A firmly hybridizable, DNA-like architecture with DAD/ADA- and ADD/DAA-type nonnatural base pairs as an extracellular genetic candidate. *Chem. Commun.* **2015,** *51* (32), 7043-7046.

55. Meggers, E.; Holland, P. L.; Tolman, W. B.; Romesberg, F. E.; Schultz, P. G., A novel copper-mediated DNA base pair. *J. Am. Chem. Soc.* **2000,** *122* (43), 10714-10715.

56. Schlegel, M. K.; Zhang, L. L.; Pagano, N.; Meggers, E., Metal-mediated base pairing within the simplified nucleic acid GNA. *Organic & Biomolecular Chemistry* **2009,** *7* (3), 476-482.

57. Golubev, O.; Turc, G.; Lonnberg, T., Pd2+-mediated base pairing in oligonucleotides. *J. Inorg. Biochem.* **2016,** *155*, 36-43.

58. Tasaka, M.; Tanaka, K.; Shiro, M.; Shionoya, M., A palladium-mediated DNA base pair of a beta-C-nucleoside possessing a 2-aminophenol as the nucleobase. *Supramol. Chem.* **2001,** *13* (6), 671-675.

59. Saiki, R. K.; Gelfand, D. H.; Stoffel, S.; Scharf, S. J.; Higuchi, R.; Horn, G. T.; Mullis, K. B.; Erlich, H. A., Primer-Directed Enzymatic Amplification Of Dna With A Thermostable Dna-Polymerase. *Science* **1988,** *239* (4839), 487-491.

60. Hili, R.; Niu, J.; Liu, D. R., DNA Ligase-Mediated Translation of DNA Into Densely Functionalized Nucleic Acid Polymers. *J. Am. Chem. Soc.* **2013,** *135* (1), 98-101.

61. Chen, Z.; Lichtor, P. A.; Berliner, A. P.; Chen, J. C.; Liu, D. R., Evolution of sequence-defined highly functionalized nucleic acid polymers. *Nature Chemistry* **2018,** *10* (4), 420-427.

62. van Hest, J. C. M.; Tirrell, D. A., Protein-based materials, toward a new level of structural control. *Chem. Commun.* **2001,** (19), 1897-1904.

63. Hein, J. E.; Fokin, V. V., Copper-catalyzed azide-alkyne cycloaddition (CuAAC) and beyond: new reactivity of copper(I) acetylides. *Chemical Society Reviews* **2010,** *39* (4), 1302-1315.

64. Bergman, S. D.; Wudl, F., Mendable polymers. *Journal of Materials Chemistry* **2008,** *18* (1), 41-62.

65. Gaso-Sokac, D.; Stivojevic, M., Diels-Alder "Click" Reactions. *Curr. Org. Chem.* **2016,** *20* (21), 2211-2221.

66. Thongsomboon, W.; Sherwood, M.; Arellano, N.; Nelson, A., Thermally Induced Nanoimprinting of Biodegradable Polycarbonates Using Dynamic Covalent Cross-Links. *Acs Macro Letters* **2013,** *2* (1), 19-22.

67.   Koehler, K. C.; Durackova, A.; Kloxin, C. J.; Bowman, C. N., Kinetic and thermodynamic measurements for the facile property prediction of diels–alder-conjugated material behavior. *AIChE Journal* **2012,** *58* (11), 3545-3552.

68.   Nishiyabu, R.; Kubo, Y.; James, T. D.; Fossey, J. S., Boronic acid building blocks: tools for self assembly. *Chem. Commun.* **2011,** *47* (4), 1124-1150.

69.   Arumugam, S.; Popik, V. V., Light-Induced Hetero-Diels-Alder Cycloaddition: A Facile and Selective Photoclick Reaction. *J. Am. Chem. Soc.* **2011,** *133* (14), 5573-5579.

70.   Boul, P. J.; Reutenauer, P.; Lehn, J. M., Reversible Diels-Alder reactions for the generation of dynamic combinatorial libraries. *Organic Letters* **2005,** *7* (1), 15-18.

71.   Li, Y. P.; Xiao, W. W.; Xiao, K.; Berti, L.; Luo, J. T.; Tseng, H. P.; Fung, G.; Lam, K. S., Well-Defined, Reversible Boronate Crosslinked Nanocarriers for Targeted Drug Delivery in Response to Acidic pH Values and cis-Diols. *Angew. Chem.-Int. Edit.* **2012,** *51* (12), 2864-2869.

72.   Bapat, A. P.; Roy, D.; Ray, J. G.; Savin, D. A.; Sumerlin, B. S., Dynamic-Covalent Macromolecular Stars with Boronic Ester Linkages. *J. Am. Chem. Soc.* **2011,** *133* (49), 19832-19838.

73.   Cote, A. P.; Benin, A. I.; Ockwig, N. W.; O'Keeffe, M.; Matzger, A. J.; Yaghi, O. M., Porous, crystalline, covalent organic frameworks. *Science* **2005,** *310* (5751), 1166-1170.

74.   (a) Yan, J.; Springsteen, G.; Deeter, S.; Wang, B. H., The relationship among pKa, pH, and binding constants in the interactions between boronic acids and diols - it is not as simple as it appears. *Tetrahedron* **2004,** *60* (49), 11205-11209; (b) Springsteen, G.; Wang, B. H., A detailed examination of boronic acid-diol complexation. *Tetrahedron* **2002,** *58* (26), 5291-5300.

75.   Gennari, A.; Gujral, C.; Hohn, E.; Lallana, E.; Cellesi, F.; Tirelli, N., Revisiting Boronate/Diol Complexation as a Double Stimulus-Responsive Bioconjugation. *Bioconjugate Chem.* **2017,** *28* (5), 1391-1402.

76.   (a) Edwards, N. Y.; Sager, T. W.; McDevitt, J. T.; Anslyn, E. V., Boronic acid based peptidic receptors for pattern-based saccharide sensing in neutral aqueous media, an application in real-life samples. *J. Am. Chem. Soc.* **2007,** *129* (44), 13575-13583; (b) Wu, X.; Chen, X. X.; Zhang, M.; Li, Z.; Gale, P. A.; Jiang, Y. B., Self-assembly of a "double dynamic covalent" amphiphile featuring a glucose-responsive imine bond. *Chem. Commun.* **2016,** *52* (43), 6981-6984; (c) Zhang, X. T.; Liu, G. J.; Ning, Z. W.; Xing, G. W., Boronic acid-based chemical sensors for saccharides. *Carbohydr. Res.* **2017,** *452*, 129-148; (d) Lacina, K.; Skladal, P.; James, T. D., Boronic acids for sensing and other applications - a mini-review of papers published in 2013. *Chem. Cent. J.* **2014,** *8*, 17.

77.   Deng, C. C.; Brooks, W. L. A.; Abboud, K. A.; Sumerlin, B. S., Boronic Acid-Based Hydrogels Undergo Self-Healing at Neutral and Acidic pH. *ACS Macro Letters* **2015,** *4* (2), 220-224.

78.   Yang, J.; Saggiomo, V.; Velders, A. H.; Stuart, M. A. C.; Kamperman, M., Reaction Pathways in Catechol/Primary Amine Mixtures: A Window on Crosslinking Chemistry. *PLoS One* **2016,** *11* (12), 17.

79.   Gogoi, K.; Dewan, A.; Gogoi, A.; Borah, G.; Bora, U., Boric Acid as Highly Efficient Catalyst for the Synthesis of Phenols from Arylboronic Acids. *Heteroatom Chem.* **2014,** *25* (2), 127-130.

80.   Wu, S.; Waugh, W.; Stella, V. J., Degradation pathways of a peptide boronic acid derivative, 2-Pyz-(CO)-Phe-Leu-B(OH)2. *Journal of Pharmaceutical Sciences* **2000,** *89* (6), 758-765.

81.   Nave, S.; Sonawane, R. P.; Elford, T. G.; Aggarwal, V. K., Protodeboronation of Tertiary Boronic Esters: Asymmetric Synthesis of Tertiary Alkyl Stereogenic Centers. *J. Am. Chem. Soc.* **2010,** *132* (48), 17096-17098.

82.   AbdelMagid, A. F.; Carson, K. G.; Harris, B. D.; Maryanoff, C. A.; Shah, R. D., Reductive amination of aldehydes and ketones with sodium triacetoxyborohydride. Studies on direct and indirect reductive amination procedures. *J. Org. Chem.* **1996,** *61* (11), 3849-3862.

83.   Lehn, J. M., From supramolecular chemistry towards constitutional dynamic chemistry and adaptive chemistry. *Chemical Society Reviews* **2007,** *36* (2), 151-160.

84.   Giuseppone, N.; Schmitt, J. L.; Schwartz, E.; Lehn, J. M., Scandium(III) catalysis of transimination reactions. Independent and constitutionally coupled reversible processes. *J. Am. Chem. Soc.* **2005,** *127* (15), 5528-5539.

85.   Kovaricek, P.; Lehn, J. M., Merging Constitutional and Motional Covalent Dynamics in Reversible Imine Formation and Exchange Processes. *J. Am. Chem. Soc.* **2012,** *134* (22), 9446-9455.

86.   Miyata, K.; Christie, R. J.; Kataoka, K., Polymeric micelles for nano-scale drug delivery. *Reactive and Functional Polymers* **2011,** *71* (3), 227-234.

87.   Minkenberg, C. B.; Florusse, L.; Eelkema, R.; Koper, G. J. M.; van Esch, J. H., Triggered Self-Assembly of Simple Dynamic Covalent Surfactants. *J. Am. Chem. Soc.* **2009,** *131* (32), 11274-+.

88.   Minkenberg, C. B.; Hendriksen, W. E.; Li, F.; Mendes, E.; Eelkema, R.; van Esch, J. H., Dynamic covalent assembly of stimuli responsive vesicle gels. *Chem. Commun.* **2012,** *48* (79), 9837-9839.

89.   Minkenberg, C. B.; Homan, B.; Boekhoven, J.; Norder, B.; Koper, G. J. M.; Eelkema, R.; van Esch, J. H., Responsive Wormlike Micelles from Dynamic Covalent Surfactants. *Langmuir* **2012,** *28* (38), 13570-13576.

90.   Li, Y. P.; Xiao, K.; Luo, J. T.; Xiao, W. W.; Lee, J. S.; Gonik, A. M.; Kato, J.; Dong, T. A.; Lam, K. S., Well-defined, reversible disulfide cross-linked micelles for on-demand paclitaxel delivery. *Biomaterials* **2011,** *32* (27), 6633-6645.

91.   Ryu, J. H.; Jiwpanich, S.; Chacko, R.; Bickerton, S.; Thayumanavan, S., Surface-Functionalizable Polymer Nanogels with Facile Hydrophobic Guest Encapsulation Capabilities. *J. Am. Chem. Soc.* **2010,** *132* (24), 8246-+.

92.   Fairbanks, B. D.; Singh, S. P.; Bowman, C. N.; Anseth, K. S., Photodegradable, Photoadaptable Hydrogels via Radical-Mediated Disulfide Fragmentation Reaction. *Macromolecules* **2011,** *44* (8), 2444-2450.

93.   (a) Abdalla, M. A., Medicinal significance of naturally occurring cyclotetrapeptides. *J. Nat. Med.* **2016,** *70* (4), 708-720; (b) Newman, D. J.; Cragg, G. M., Bioactive Macrocycles from Nature. In *Macrocycles in Drug Discovery*, Levin, J. I., Ed. Royal Soc Chemistry: Cambridge, 2015; Vol. 40, pp 1-36.

94.   (a) Spangler, B. D., Structure And Function Of Cholera-Toxin And The Related Escherichia-Coli Heat-Labile Enterotoxin. *Microbiol. Rev.* **1992,** *56* (4), 622-647; (b) Branson, T. R.; McAllister, T. E.; Garcia-Hartjes, J.; Fascione, M. A.; Ross, J. F.; Warriner, S. L.; Wennekes, T.; Zuilhof, H.; Turnbull, W. B., A Protein-Based Pentavalent Inhibitor of the Cholera Toxin B-Subunit. *Angew. Chem.-Int. Edit.* **2014,** *53* (32), 8323-8327.

95.   (a) Ghadiri, M. R.; Granja, J. R.; Buehler, L. K., Artificial Transmembrane Ion Channels From Self-Assembling Peptide Nanotubes. *Nature* **1994,** *369* (6478), 301-304; (b) Montenegro, J.; Ghadiri, M. R.; Granja, J. R., Ion Channel Models Based on Self-Assembling Cyclic Peptide Nanotubes. *Accounts Chem. Res.* **2013,** *46* (12), 2955-2965.

96.   Izadpanah, A.; Gallo, R. L., Antimicrobial peptides. *Journal of the American Academy of Dermatology* **2005,** *52* (3), 381-390.

97.   (a) Fernandez-Lopez, S.; Kim, H. S.; Choi, E. C.; Delgado, M.; Granja, J. R.; Khasanov, A.; Kraehenbuehl, K.; Long, G.; Weinberger, D. A.; Wilcoxen, K. M.; Ghadiri, M. R., Antibacterial agents based on the cyclic D,L-alpha-peptide architecture. *Nature* **2001,** *412* (6845), 452-455; (b) Mallinson, J.; Collins, I., Macrocycles in new drug discovery. *Future Med. Chem.* **2012,** *4* (11), 1409-1438; (c) Collins, S.; Bartlett, S.; Nie, F. L.; Sore, H. F.; Spring, D. R., Diversity-Oriented Synthesis of Macrocycle Libraries for Drug Discovery and Chemical Biology. *Synthesis-Stuttgart* **2016,** *48* (10), 1457-1473.

98.   Miller, S. M.; Simon, R. J.; Ng, S.; Zuckermann, R. N.; Kerr, J. M.; Moos, W. H., Proteolytic Studies Of Homologous Peptide And N-Substituted Glycine Peptoid Oligomers. *Bioorg. Med. Chem. Lett.* **1994,** *4* (22), 2657-2662.

99.   Astle, J. M.; Udugamasooriya, D. G.; Smallshaw, J. E.; Kodadek, T., A VEGFR2 Antagonist and Other Peptoids Evade Immune Recognition. *International Journal of Peptide Research and Therapeutics* **2008,** *14* (3), 223-227.

100.	(a) Roy, O.; Faure, S.; Thery, V.; Didierjean, C.; Taillefumier, C., Cyclic beta-peptoids. *Organic Letters* **2008,** *10* (5), 921-924; (b) Lepage, M. L.; Schneider, J. P.; Bodlenner, A.; Meli, A.; De Riccardis, F.; Schmitt, M.; Tarnus, C.; Nguyen-Huynh, N. T.; Francois, Y. N.; Leize-Wagner, E.; Birck, C.; Cousido-Siah, A.; Podjarny, A.; Izzo, I.; Compain, P., Iminosugar-Cyclopeptoid Conjugates Raise Multivalent Effect in Glycosidase Inhibition at Unprecedented High Levels. *Chemistry-a European Journal* **2016,** *22* (15), 5151-5155; (c) Elduque, X.; Pedroso, E.; Grandas, A., Orthogonal Protection of Peptides and Peptoids for Cyclization by the Thiol-Ene Reaction and Conjugation. *J. Org. Chem.* **2014,** *79* (7), 2843-2853.

101.	Webster, A. M.; Cobb, S. L., Recent Advances in the Synthesis of Peptoid Macrocycles. *Chemistry-a European Journal* **2018,** *24* (30), 7560-+.

102.	Whitesides, G. M.; Boncheva, M., Beyond Molecules: Self-Assembly of Mesoscopic and Macroscopic Components. *Proceedings of the National Academy of Sciences of the United States of America* **2002,** *99* (8), 4769-4774.

103.	Lee, C.-Y.; Gong, P.; Harbers, G. M.; Grainger, D. W.; Castner, D. G.; Gamble, L. J., Surface Coverage and Structure of Mixed DNA/Alkylthiol Monolayers on Gold: Characterization by XPS, NEXAFS, and Fluorescence Intensity Measurements. *Analytical Chemistry* **2006,** *78* (10), 3316-3325.

104.	Blake, A. J.; Champness, N. R.; Hubberstey, P.; Li, W. S.; Withersby, M. A.; Schroder, M., Inorganic crystal engineering using self-assembly of tailored building-blocks. *Coord. Chem. Rev.* **1999,** *183*, 117-138.

105.	Zuker, M., Mfold web server for nucleic acid folding and hybridization prediction. *Nucleic Acids Res.* **2003,** *31* (13), 3406-3415.

106.	Zhang, S. G., Fabrication of novel biomaterials through molecular self-assembly. *Nat. Biotechnol.* **2003,** *21* (10), 1171-1178.

107.	Seeman, N. C., Nucleic Acid Junctions and Lattices. *J. Theor. Biol.* **1982,** *99* (2), 237-247.

108.	Chen, J. H.; Seeman, N. C., Synthesis from DNA of a molecule with the connectivity of a cube. *Nature* **1991,** *350* (6319), 631-633.

109.	Rothemund, P. W. K., Folding DNA to create nanoscale shapes and patterns. *Nature* **2006,** *440* (7082), 297-302.

110.	(a) Wei, B.; Dai, M. J.; Yin, P., Complex shapes self-assembled from single-stranded DNA tiles. *Nature* **2012,** *485* (7400), 623-626; (b) Ke, Y.; Ong, L. L.; Shih, W. M.; Yin, P., Three-Dimensional Structures Self-Assembled from DNA Bricks. *Science* **2012,** *338* (6111), 1177-1183.

111.   Elghanian, R.; Storhoff, J. J.; Mucic, R. C.; Letsinger, R. L.; Mirkin, C. A., Selective colorimetric detection of polynucleotides based on the distance-dependent optical properties of gold nanoparticles. *Science* **1997,** *277* (5329), 1078-1081.

112.   Acuna, G. P.; Bucher, M.; Stein, I. H.; Steinhauer, C.; Kuzyk, A.; Holzmeister, P.; Schreiber, R.; Moroz, A.; Stefani, F. D.; Liedl, T.; Simmel, F. C.; Tinnefeld, P., Distance Dependence of Single-Fluorophore Quenching by Gold Nanoparticles Studied on DNA Origami. *ACS Nano* **2012,** *6* (4), 3189-3195.

113.   Santosh, M.; Maiti, P. K., Force induced DNA melting. *J. Phys.-Condes. Matter* **2009,** *21* (3).

114.   (a) Bockelmann, U.; EssevazRoulet, B.; Heslot, F., Molecular stick-slip motion revealed by opening DNA with piconewton forces. *Phys. Rev. Lett.* **1997,** *79* (22), 4489-4492; (b) Bockelmann, U.; Thomen, P.; Essevaz-Roulet, B.; Viasnoff, V.; Heslot, F., Unzipping DNA with optical tweezers: high sequence sensitivity and force flips. *Biophys. J.* **2002,** *82* (3), 1537-1553.

115.   (a) Sreenivasachary, N.; Hickman, D. T.; Sarazin, D.; Lehn, J. M., DyNAs: Constitutional dynamic nucleic acid analogues. *Chem.-Eur. J.* **2006,** *12* (33), 8581-8588; (b) Hickman, D. T.; Sreenivasachary, N.; Lehn, J. M., Synthesis of components for the generation of constitutional dynamic analogues of nucleic acids. *Helv. Chim. Acta* **2008,** *91* (1), 1-20.

116.   Ura, Y.; Beierle, J. M.; Leman, L. J.; Orgel, L. E.; Ghadiri, M. R., Self-Assembling Sequence-Adaptive Peptide Nucleic Acids. *Science* **2009,** *325* (5936), 73-77.

117.   (a) Hartley, C. S.; Elliott, E. L.; Moore, J. S., Covalent assembly of molecular ladders. *J. Am. Chem. Soc.* **2007,** *129* (15), 4512-4513; (b) Elliott, E. L.; Hartley, C. S.; Moore, J. S., Covalent ladder formation becomes kinetically trapped beyond four rungs. *Chem. Commun.* **2011,** *47* (17), 5028-5030.

118.   (a) Wei, T.; Jung, J. H.; Scott, T. F., Dynamic Covalent Assembly of Peptoid-Based Ladder Oligomers by Vernier Templating. *J. Am. Chem. Soc.* **2015,** *137* (51), 16196-16202; (b) Wei, T.; Furgal, J. C.; Jung, J. H.; Scott, T. F., Long, self-assembled molecular ladders by cooperative dynamic covalent reactions. *Polym. Chem.* **2017,** *8* (3), 520-527.

119.   Bapat, A. P.; Ray, J. G.; Savin, D. A.; Sumerlin, B. S., Redox-Responsive Dynamic-Covalent Assemblies: Stars and Miktoarm Stars. *Macromolecules* **2013,** *46* (6), 2188-2198.

120.   Hutin, M.; Bernardinelli, G.; Nitschke, J. R., An iminoboronate construction set for subcomponent self-assembly. *Chemistry-a European Journal* **2008,** *14* (15), 4585-4593.

121.   (a) Christinat, N.; Scopelliti, R.; Severin, K., Multicomponent assembly of boron-based dendritic nanostructures. *J. Org. Chem.* **2007,** *72* (6), 2192-2200; (b) Christinat, N.; Scopelliti, R.; Severin, K., Multicomponent assembly of boronic acid based macrocycles and cages. *Angew. Chem.-Int. Edit.* **2008,** *47* (10), 1848-1852.

122. (a) Drozdz, W.; Bouillon, C.; Kotras, C.; Richeter, S.; Barboiu, M.; Clement, S.; Stefankiewicz, A. R.; Ulrich, S., Generation of Multicomponent Molecular Cages using Simultaneous Dynamic Covalent Reactions. *Chemistry-a European Journal* **2017,** *23* (71), 18010-18018; (b) Schmittel, M.; Saha, M. L.; Fan, J., Scaffolding a Cage-Like 3D Framework by Coordination and Constitutional Dynamic Chemistry. *Organic Letters* **2011,** *13* (15), 3916-3919.

123. Hamieh, S.; Ludlow, R. F.; Perraud, O.; West, K. R.; Mattia, E.; Otto, S., A Synthetic Receptor for Nicotine from a Dynamic Combinatorial Library. *Organic Letters* **2012,** *14* (21), 5404-5407.

124. Bhat, V. T.; Caniard, A. M.; Luksch, T.; Brenk, R.; Campopiano, D. J.; Greaney, M. F., Nucleophilic catalysis of acylhydrazone equilibration for protein-directed dynamic covalent chemistry. *Nature Chemistry* **2010,** *2* (6), 490-497.

125. Bicker, K. L.; Sun, J.; Lavigne, J. J.; Thompson, P. R., Boronic Acid Functionalized Peptidyl Synthetic Lectins: Combinatorial Library Design, Peptide Sequencing, and Selective Glycoprotein Recognition. *ACS Combinatorial Science* **2011,** *13* (3), 232-243.

Chapter 2 Synthesis and Functionalization of Peptoid Macrocycles by Orthogonal Click Reactions

2.1 Abstract

Cyclic assemblies have proved to be promising agents of biological activity which has created a need for developing new strategies for preparing and modifying cyclic structures. Here, we report the cyclization of furan-functionalized peptoid oligomers with up to 24 residues through a copper(I) catalyzed alkyne-azide cycloaddition reaction between terminal alkyne/azide residues. The cyclization was demonstrated through shifts in retention volume in reverse-phase high performance liquid chromatography and further confirmed by monitoring the azide absorbance using Fourier transfer infrared(FT-IR) spectroscopy. The furan-functionalized cyclic assemblies were conjugated to a maleimide-bearing amine to show the potential of peptoid cycles in forming biological scaffolds.

2.2 Introduction

Biologically active, cyclic assemblies are relatively common and play a wide range of roles such as therapeutics,[1] toxins,[2] and synthetic ion channels.[3] Several naturally occurring cyclic peptides are useful in drug discovery with many serving as therapeutic agents including antimicrobial peptides (AMPs), short strands of amino acids that have shown to effectively kill bacteria, viruses, and fungi.[4] These characteristics have led to the development of synthetic cyclic compounds that mimic their biological potency.[5] There is an increased interest in developing macrocyclic scaffolds to enhance their efficacy some examples include affixing

polymers to macrocycles in order to form Janus nanotubular structures[6] and pendent arms[7] as models for biological systems.

Poly-N-substituted glycines, peptoids, are a sequence-defined peptidomimetic that are particularly suitable as macrocyclic scaffolds for biologically-active species owing to their proteolytic stability[8] and inherent non-immunogenicity.[9] Peptoids are easily synthesized from commercially available primary amines and have been used to prepare macrocycles that can serve as biological molecular scaffolds.[10] Cyclization of peptoids has also been suggested as a possible strategy for introducing rigidity into generally "floppy" structures to unlock specificity necessary for therapeutic design.[11]

This chapter describes the efficient cyclization of linear peptoids by utilizing a copper (I)-catalyzed alkyne-azide cycloaddition (CuAAC)[12] This prototypical triazole forming click chemistry has been used extensively in the formation of macrocycles.[13] Upon cyclization, the furan-functionalized macrocycles are conjugated to a maleimide-bearing monomer through a thermally mediated Diels-Alder cycloaddition reaction that proceeds readily at room temperature. These two sets of click chemistries have shown chemical orthogonality in the past and have been used to make various molecular architectures.[14] Through extensive characterization, we explored the effects of peptoid length on both cyclization and functionalization. This approach highlights the synthetic versatility of peptoids in building biological scaffolds tailored to undergo site-specific modification.

2.3 Experimental

2.3.1. General Experimental Procedure

Electrospray ionization mass spectrometry (ESI-MS) mass spectra were collected using an Agilent Q-TOF 1200 series spectrometer in positive ion mode. Matrix-assisted laser

desorption/ionization (MALDI-TOF) mass spectra were recorded using a Bruker Autoflex mass spectrometer in reflectron position ion mode using 2-(4-hydroxyphenylazo)benzoic acid (HABA) as the matrix. The MALDI-TOF samples were prepared with a 3:1 ratio of matrix (100mM, 200μL acetonitrile) to sample (crude reaction mixtures). Reverse phase high performance liquid chromatography (RP-HPLC) was performed using preparative reversed phase Phenomenex Luna C18(2) columns with a linear gradient of water and acetonitrile as the eluent at 30°C. The RP-HPLC was equipped with Shimadzu LC-6AD HPLC pump, Shimadzu FRC 70A fraction collector, and monitored using Shimadzu Prominence detector at 214nm. Samples were lyophilized to a white powder to remove all residual solvents using a Labconco lyophilizer. Thermo Scientific Nicolet 6700 FT-IR spectrometer was used with and spectra were collected from 1000 to 4000 cm^{-1}. 64 spectra were collected and averaged to produce final spectra. Unless otherwise noted all reagents and materials were purchased from commercial sources Sigma Aldrich, AK Scientific, and TCI Chemical.

2.3.2. Synthesis of Furan-functionalized Oliogopeptoids
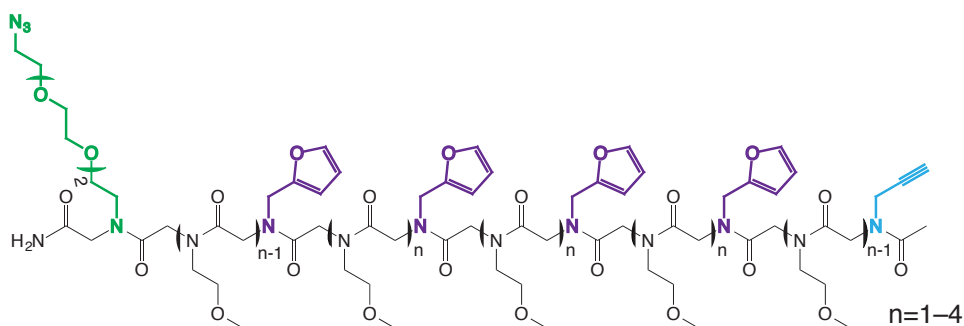
Figure 2.1. Chemical structure of CuAAC peptoids functionalized with furan

The acyclic oligomers (Figure 2.1) were formed from peptoids containing four furan functional groups affixed to a poly-N-substituted glycine backbone with azide and alkyne moieties on either end to facilitate cyclization. Each of the oligomers had a varying number of inert primary amine monomers to control the spacing between the furan functionalities within the cyclic structure. Peptoids were prepared using Zuckermann's two-step solid-phase synthesis scheme[15] using an automated microwave-assisted peptide synthesizer (Liberty Blue, CEM Corporation) on Rink Amide ProTide resin (CEM Corporation, 0.1mmol scale). The resin contains a fluorenylmethyloxycarbonyl (Fmoc)-protected amine that is initially deprotected by treatment with 4-methylpiperidine: dimethylformamide (DMF) (20:80, volume ratio) for 30 seconds at 75°C and then 90 seconds at 90°C. The synthesis then proceeds by a sequential addition reaction whereby the N-terminal amine from the solid support is acetylated with 1M bromoacetic acid using 1.2M diisopropylcarbodiimide (DIC) as an activator, to afford a terminal bromide which is subsequently displaced via nucleophilic substitution with a 0.5M primary amine in DMF bearing the desired pendant group. The acetylation and displacement steps lasted for 5 minutes at 75°C with the exception of the azide and alkyne primary amines which were displaced at 50°C for 5 minutes. The displacement reagents, bromoacetic acid and DIC, were prepared in DMF, and the primary amines (2-methoxyethylamine, furfurylamine, propargylamine, and 11-azido-3,6,9-trioxaundecan-1-amine) were prepared in N-methyl-2-pyrrolidone (NMP) and can be found in Figure 2.2. This two-step process of acetylation and displacement is repeated until the desired chain length and sequence is achieved then the N-terminal of the oligomer was capped with 1 M acetic anhydride activated with DIC to prevent further chain elongation.

Primary Amine Monomers

Nffa=furfurylamine

Nme=2-methoxyethylamine

Nppa=propargylamine

Npaz=11-azido-3,6,9-trioxaundecan-1-amine
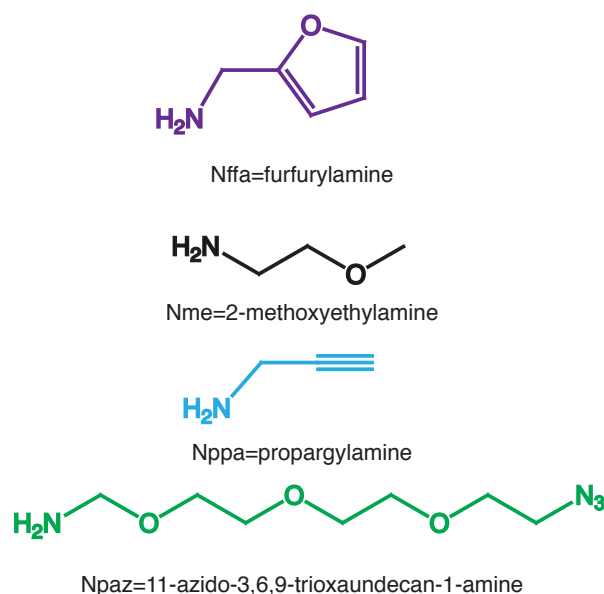
Figure 2.2. Primary amine monomers used in this study

The peptoids were cleaved by placing the solid support resin in a 25 mL solid-phase peptide synthesis vessel (CG-1866, Chemglass) and treated with 4 mL of a cleavage solution containing 95% TFA and 5% water for 5 min while bubbling with nitrogen at room temperature. The cleavage solution was then filtered through the glass frit of the reaction vessel into a round bottom flask before the resin was repeated washed with dichloromethane to wash any residual peptoid from the solid support resin. The cleavage solution and subsequent washes were combined and evaporated by blowing a gentle stream of nitrogen to yield an unbound crude peptoid with a C-terminal primary amide. The molecular weights of the crude peptoids were confirmed using ESI (Figure 2.3).
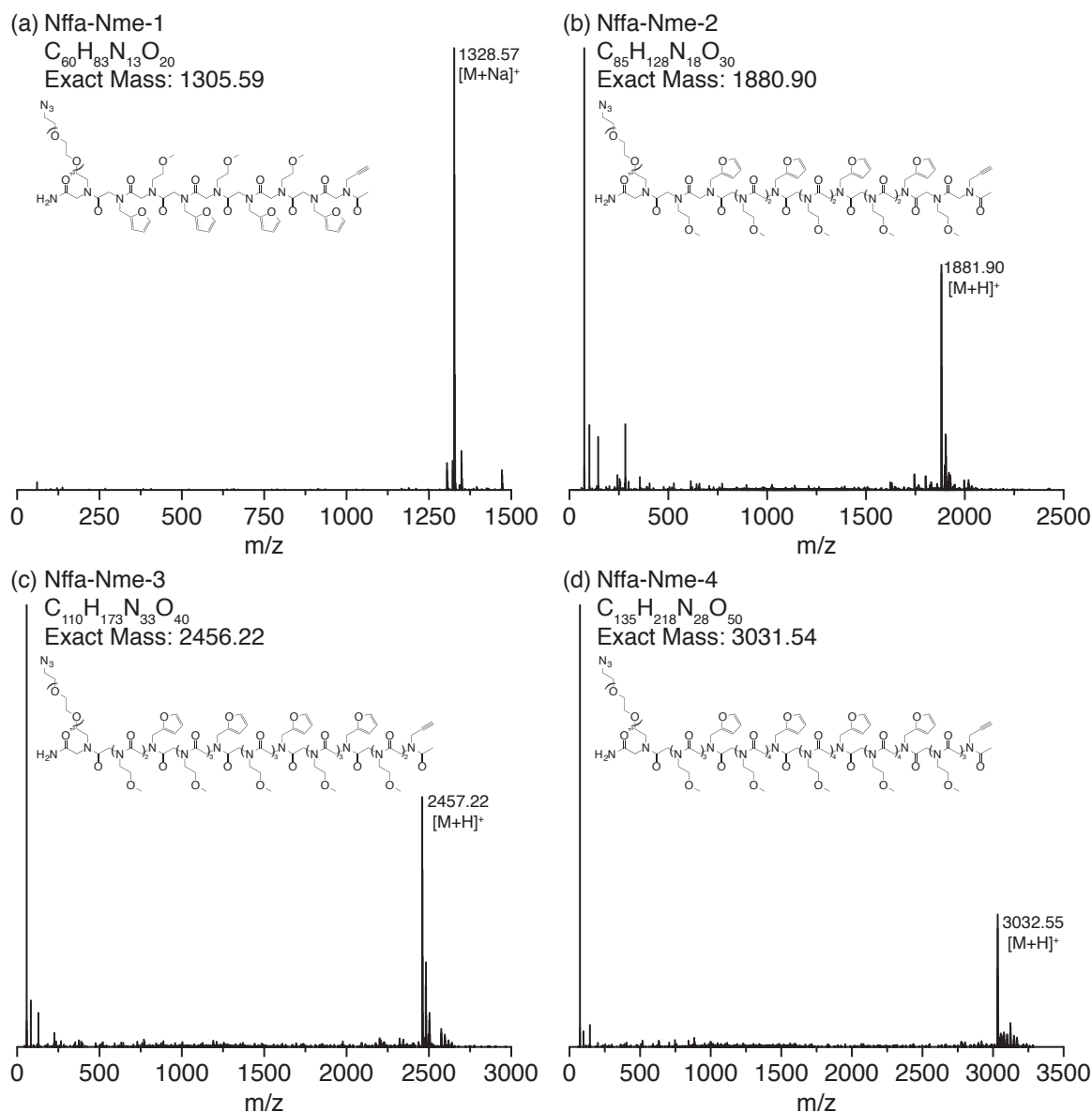
Figure 2.3. ESI-MS mass spectra of the crude furan-functionalized oligopeptoids analyzed after cleavage from the solid-support: (a) [Nffa-Nme-1+Na]$^+$ =1328.58 g/m (b) [Nffa-Nme-2+H]$^+$ =1881.90 g/mol (c) [Nffa-Nme-3+H]$^+$ = 2457.22 g/mol (d) [Nffa-Nme-4+H]$^+$ = 3032.54 g/mol

The crude peptoids were then purified by preparative RP-HPLC at a linear gradient of 10%-acetonitrile-water to 90%-acetonitrile-water over 22 minutes. Fractions corresponding to the major peaks (Figure 2.4) were collected through each subsequent run before the purified peptoid fractions were combined and lyophilized to a fine white powder. The peptoids were then

ran through the RP-HPLC system to determine the retention volume of the acyclic peptoid strands as shown in Figure 2.5. The purified fractions were also analyzed again by ESI-MS to confirm the purified peptoid was the intended structure (Figure 2.6).
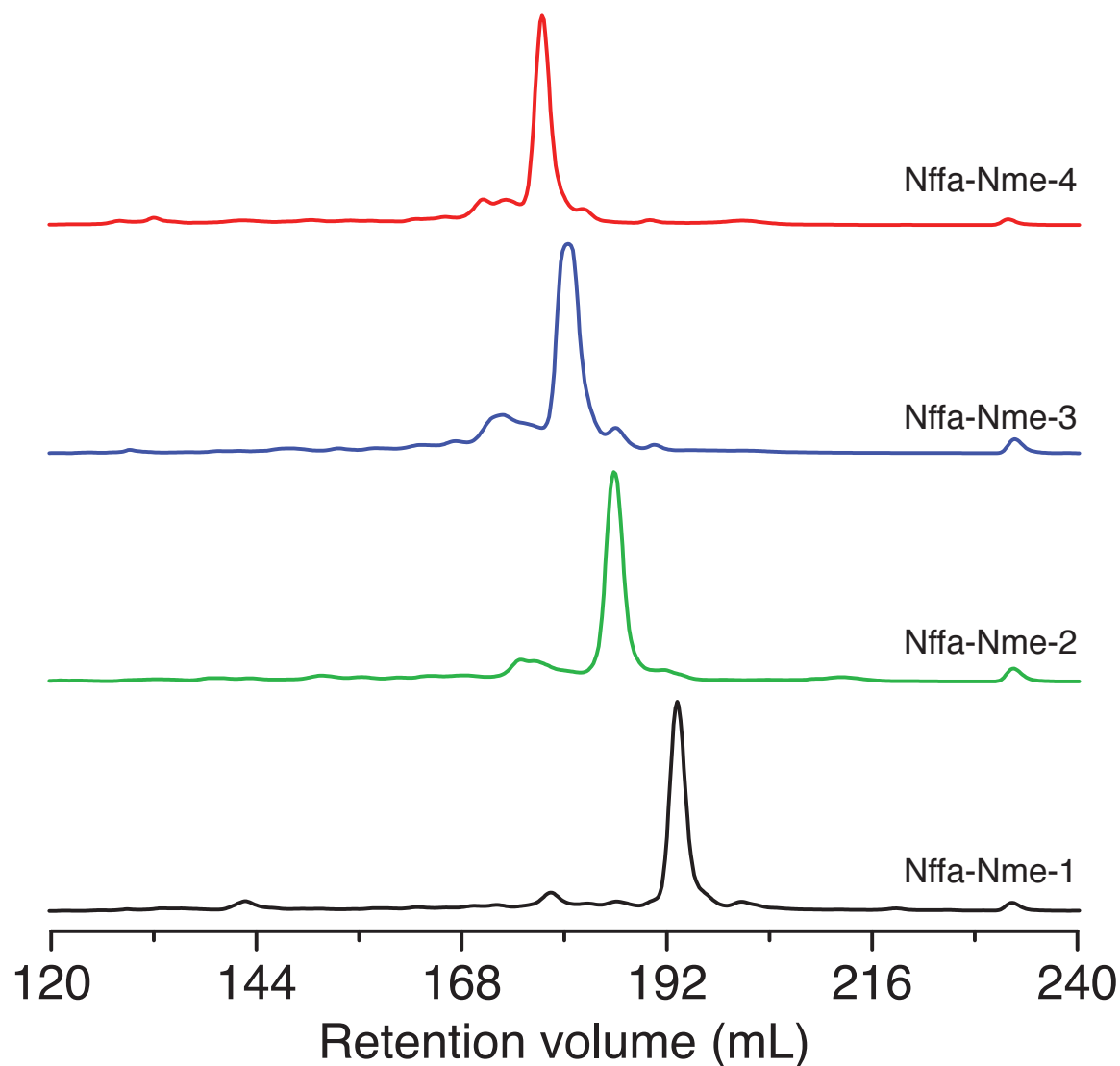
Figure 2.4. RP-HPLC (gradient of 10% MeCN to 90% MeCN over 22 minutes) of the crude furan-functionalized oligopeptoids after cleavage from the solid-support: (black) Nffa-Nme-1 (green) Nffa-Nme-2 (blue) Nffa-Nme-3 (red) Nffa-Nme-4
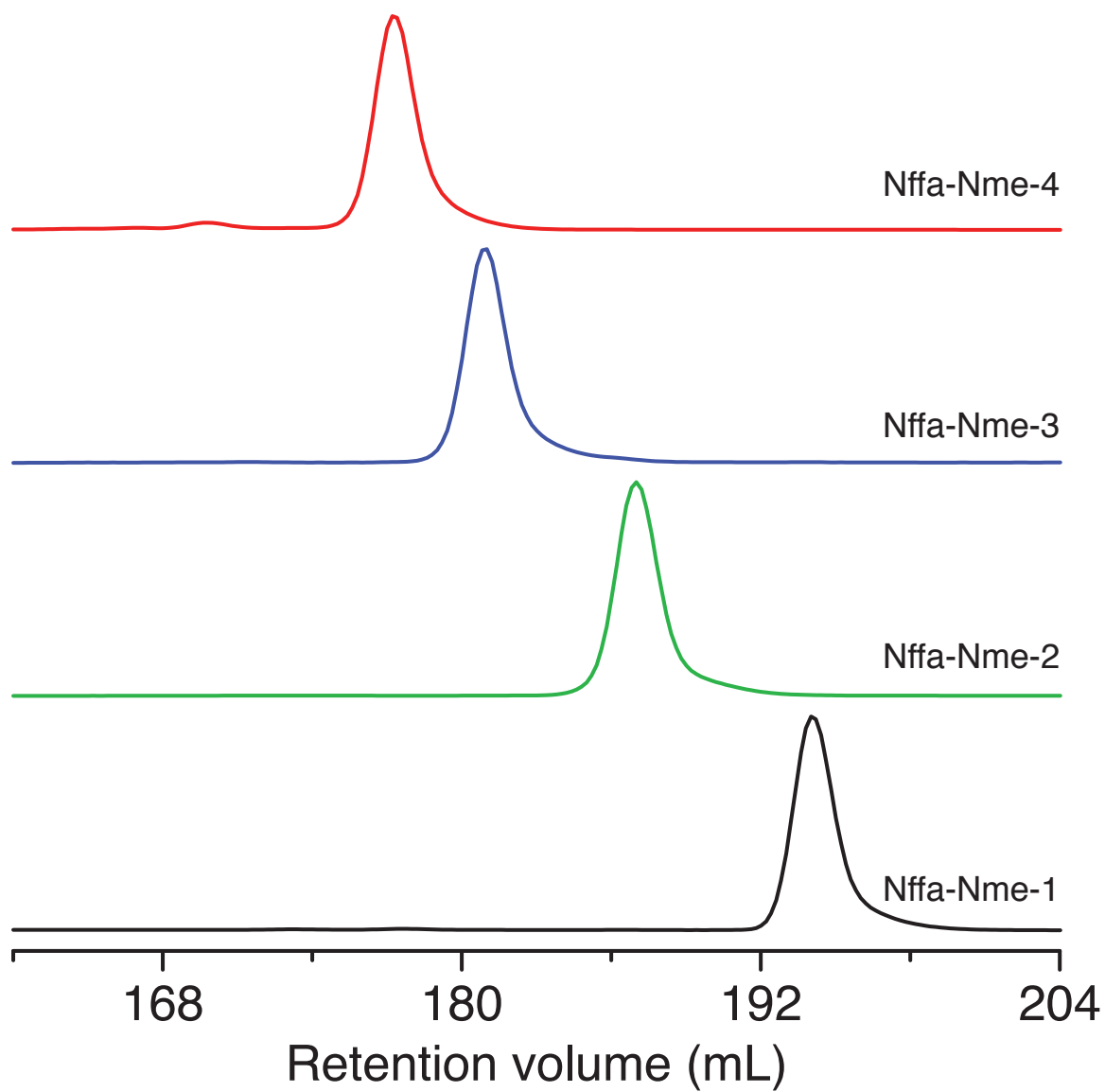
Figure 2.5. RP-HPLC (gradient of 10% MeCN to 90% MeCN over 22 minutes) spectra of purified linear furan-functionalized linear oligopeptoids analyzed after cleavage from the solid-support: (black) Nffa-Nme-p1 (green) Nffa-Nme-p2 (blue) Nffa-Nme-p3 (red) Nffa-Nme-p4

(a) Nffa-Nme-1
$C_{60}H_{83}N_{13}O_{20}$
Exact Mass: 1305.59
1328.57
[M+Na]$^+$

(b) Nffa-Nme-2
$C_{85}H_{128}N_{18}O_{30}$
Exact Mass: 1880.90
1903.89
[M+Na]$^+$
[M+H]$^+$

(c) Nffa-Nme-3
$C_{110}H_{173}N_{33}O_{40}$
Exact Mass: 2456.22
2495.2
[M+Na]$^+$

(d) Nffa-Nme-4
$C_{135}H_{218}N_{28}O_{50}$
Exact Mass: 3031.54
3076.5
[M+2Na-H]$^+$
[M+Na]$^+$
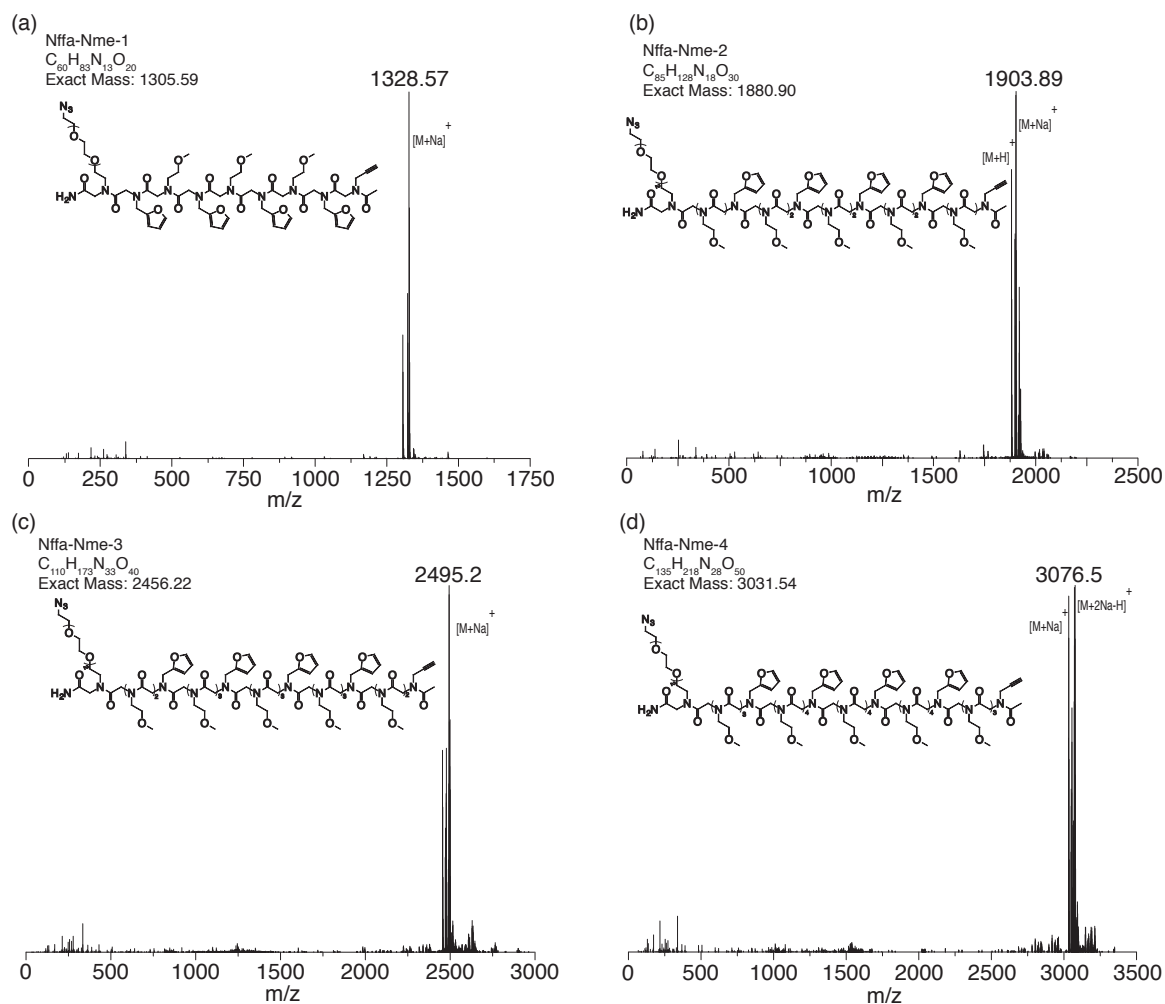
Figure 2.6. ESI-MS mass spectra of purified linear furan-functionalized linear oligopeptoids after RP-HPLC purification: (a) [Nffa-Nme-1+Na]$^+$ = 1328.58 g/m (b) [Nffa-Nme-2+Na]$^+$ = 1903.89 g/mol (c) [Nffa-Nme-3+Na]$^+$ = 2495.2g/mol (d) [Nffa-Nme-4+2Na-H-]$^+$ = 3076.5g/mol

2.3.3. Cyclization and Characterization of Oligopeptoids
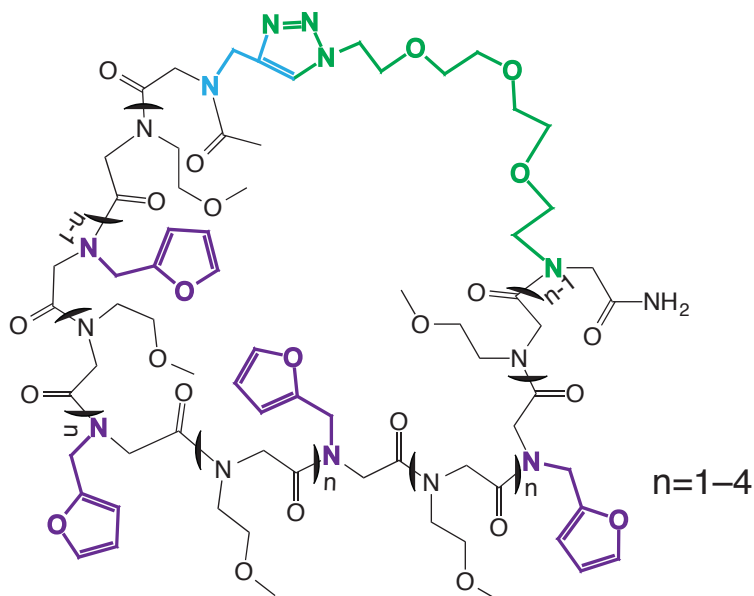
Figure 2.7. Structure of macrocycle formed through a CuAAC reaction with furan pendent groups for post synthetic functionalization

The peptoids were cyclized (Figure 2.7) at a concentration of 0.2mM in 50:50 acetonitrile: water with 0.1 equivalents of copper(I) bromide (CuBr) overnight. The cyclization was monitored by a characteristic shift in RP-HPLC with a linear gradient; both the peak attributed to the acyclic and cyclized peptoids were collected. MALDI-TOF was used to confirm the exact mass of each peak before lyophilizing the solutions to a white powder.

Each of the collected peaks for both the acyclic peptoids and macrocycles were treated with 100 equivalents of 1-azido-2-(2-(2-methoxyethoxy)ethoxy)ethane in a 0.5mM solution in 50:50 of acetonitrile: water with 0.1 equivalents of CuBr for 6 hours. MALDI-TOF was used to confirm the addition of the excess azide to the acyclic peptoid and the maintenance of molecular weight of the macrocyclic compounds. Furthermore, RP-HPLC was performed on each of the samples to show a shift in retention time for the peptoids conjugated to the excess azide. ESI-MS was used to confirm the molecular weights of the resulting RP-HPLC peaks. Additionally FT-IR

54

was used to show the presence of the characteristic azide peak at 2100cm^{-1} in the acyclic spectrum by scanning 2600 cm^{-1}-2000cm^{-1}. Approximately 5 mg of the acyclic material was dissolved in 20 μL of acetonitrile before spotting the samples on a salt plate and scanning the spectra after a blank of acetonitrile was ran. Similarly, the same process was repeated for the cyclic material.

2.3.4. Functionalization of Cyclic Peptoids

The macrocycles were treated with 50 equivalents of N-(2-aminoethyl)maleimide trifluoroacetate salt at room temperature. ESI was used to confirm conjugation after 10 days. HPLC was used to confirm the addition of the maleimide moiety for the Nffa-Nme-2 peptoid with different fractions being collected and analyzed by ESI.

2.4 Results and Discussion
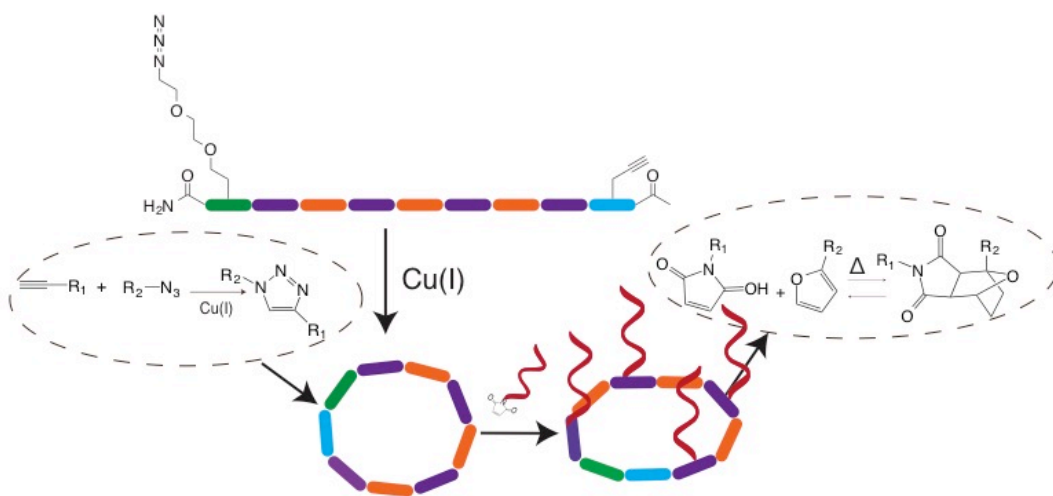
Scheme 2.1. The Cu(I) catalyzed alkyne-azide cycloaddition (CuAAC) cyclization of a furan-functionalized linear peptoid by overnight reaction in acetonitrile and water in the presence of copper(I) source

2.4.1. Synthesis of Furan Functionalized Oligopeptoids

Four different peptoid sequences each containing four furan functional groups with varying numbers of inert spacer monomers between each of the furan residues was synthesized using Zuckermann's submonomer solid-phase synthesis method.[15] The varied space between the furan moieties was to determine if any steric hindrance would prevent post-synthetic functionalization of the macrocycles. Each of the sequences had an alkyne group introduced at the C-terminus of the strand by propargylamine and an azide functional group at the N-terminus of the strand introduced by 11-azido-3,6,9-trioxaundecan-1-amine. The alkyne and azide groups were included to direct the assembly of the peptoid chains into cyclic structures, and the furan groups were for functionalization after cyclization (Scheme 2.1). The peptoids were characterized by ESI-MS a soft ionization technique used to confirmed the molecular weight of the oligomers. The mass spectrum of the crude peptoids confirmed the successful synthesis of each of the desired peptoids. The ESI-MS mass spectra showed a small amount of impurities for the varying sequences that were necessary to be removed by preparative RP-HPLC in order to minimize the formation of any undesirable by-products. The major peak in the RP-HPLC of the crude peptoids was collected, and ESI-MS and RP-HPLC were used to characterize the molecular weight and purity of the combined fractions. Each of the peptoids was >95% pure and suitable for subsequent cyclization experiments.

2.4.2. Cyclization of Oligopeptoids

(a)

(b)
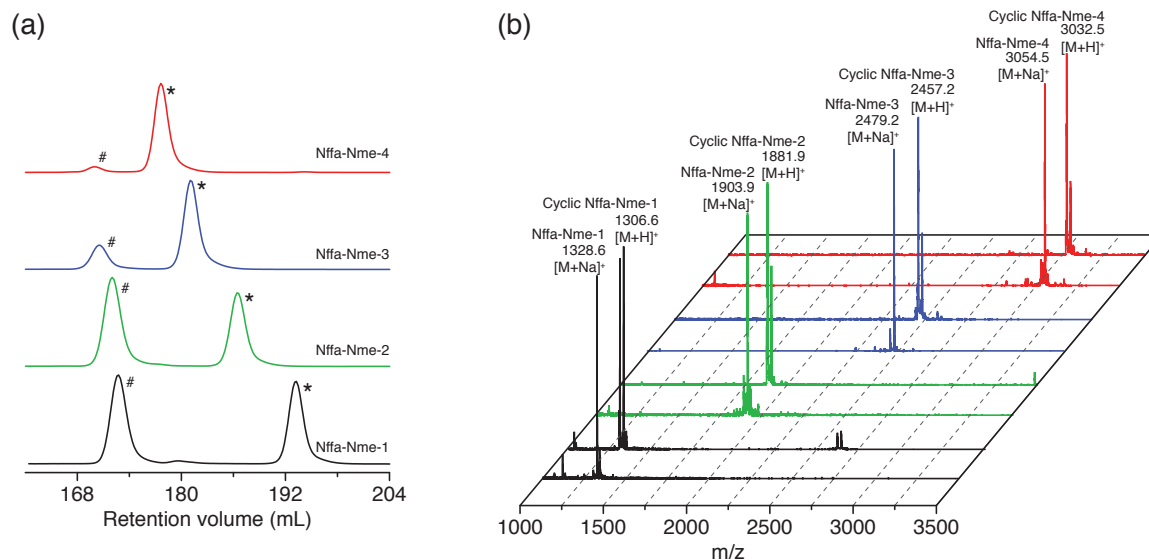
Figure 2.8. Cyclization of the oligomers for different peptoid lengths (a) The RP-HPLC spectrum of the cyclization reaction mixture. The peaks corresponding to the macrocycles are labeled with # and the linear peptoids are labeled with *. (b) MALDI-TOF mass spectra of the collected RP-HPLC peaks. Calculated molecular weights for the peptoids and cyclized structures: $[Nffa-Nme-1+H]^+$ = 1306.59 g/mol $[Nffa-Nme-1+Na]^+$ = 1328.58 g/mol; $[Nffa-Nme-2+H]^+$ = 1881.90 g/mol $[Nffa-Nme-2+Na]^+$ = 1903.89 g/mol; $[Nffa-Nme-3+H]^+$ = 2457.22 g/mol $[Nffa-Nme-3+Na]^+$ =2479.21 g/mol; $[Nffa-Nme-4+H]^+$ = 3032.54 g/mol $[Nffa-Nme-4+Na]^+$ = 3054.53 g/mol.

The cyclization of the oligopeptoids was observable by a shift in the RP-HPLC at a wavelength of 214 nm; Figure 2.8.a shows the RP-HPLC spectrum of the different reaction mixtures after an overnight reaction in the presence of a catalytic amount of Cu(I). The formation of the cyclic compounds has shifted the retention volume and is denoted by a # and the acyclic peptoids are indicated with a * and correspond to the retention volumes of the purified oligomers prior to cyclization. The MALDI-TOF, another form of mass spectrometry used for characterizing larger molecular weight structures, spectrums corresponding to each RP-HPLC peak (Figure 2.8.b) highlights the anticipated same molecular weights for the linear and cyclic peptoids. The identical observed exact mass for each of the RP-HPLC peaks confirms that the peptoids were indeed cyclizing and the retention time was attributed to an intrastrand interaction.

Alternatively, if the peptoid strands were reacting with one another forming dimers or other multi-strand assemblies there would be substantial increase in the observed molecular weight. Table 2.1 shows the conversion of the oligopeptoids to macrocycles for the varying peptoid sequences found by integrating the area under each of the RP-HPLC peaks. The efficiency of the cyclization reaction decreases with increasing number of residues affixed to the peptoid backbone. This suggests that the proximity along the backbone plays an essential role in the mechanism. Further studies would need to be done to further explain this phenomenon.

Table 2.1. Conversion of cyclic peptoids

Sequence	Conversion
Nffa-Nme-p1	53.91%
Nffa-Nme-p2	56.07%
Nffa-Nme-p3	22.67%
Nffa-Nme-p4	6.22%

2.4.3. Confirmation of Cyclic Assembly

FT-IR (Figure 2.9) was used to further verify the formation of the peptoid macrocycles, highlighting the presence of an azide peak (~2100 cm-1)[16] in acyclic Nffa-Nme-p1 that does not appear in the corresponding cyclic Nffa-Nme-p1 confirming that the azide has indeed reacted with the alkyne group to form a triazole. This experiment was performed on fractions collected from the RP-HPLC where the molecular weights were verified by MALDI-TOF to rule out the possibility of the azide reacting with another strand. The FT-IR results for the Nffa-Nme-1 sequence are demonstrative of the effectiveness of RP-HPLC and MALDI-TOF in monitoring the cyclization of the different peptoid strands.
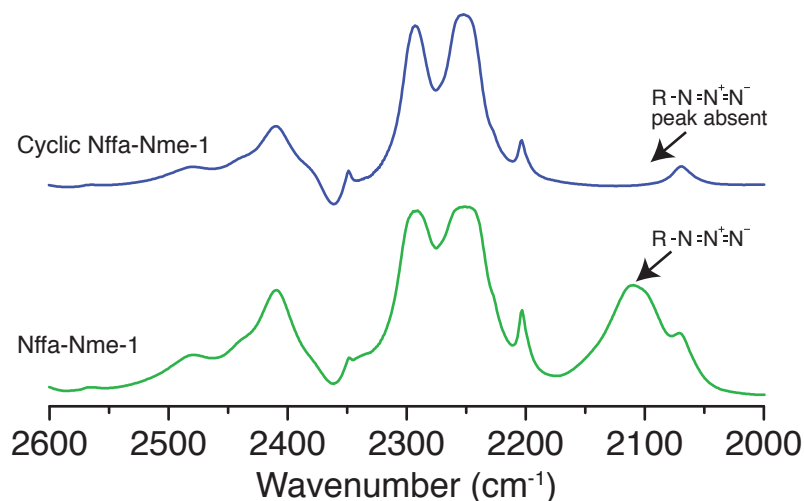
Figure 2.9. FT-IR spectra showing the presence of the of the characteristic azide peak (~2100cm^{-1}) in the acyclic peptoid that does not appear in the cyclic sample

In order to further confirm the formation of cyclic compounds, a large excess of ethylene glycol-based azide small molecule, 1-azido-2-(2-(2-methoxyethoxy)ethoxy)ethane(TEG azide), was added to the macrocycles in the presence of a copper catalyst. As a negative control, the linear peptoids were also treated under the same conditions. Figure 2.10 shows the resulting MALDI-TOF spectrum of each of the acyclic peptoids and cyclized peptoids after incubation with the excess TEG azide. MALDI-TOF was selected for characterization because of the ability to easily suppress lower molecular weight molecules such as the excess amounts of TEG azide. The linear peptoids experienced an increase in observed molecular weight corresponding to the peptoid with a conjugated TEG azide whereas the molecular weights of the macrocycles remained the same. This supports the RP-HPLC and FT-IR results suggesting the formation of the macrocycles showing that in the acyclic peptoids with a free alkyne group the TEG azide was able to undergo CuAAC reaction to form a triazole but the cyclic compounds remained unchanged under the same conditions.
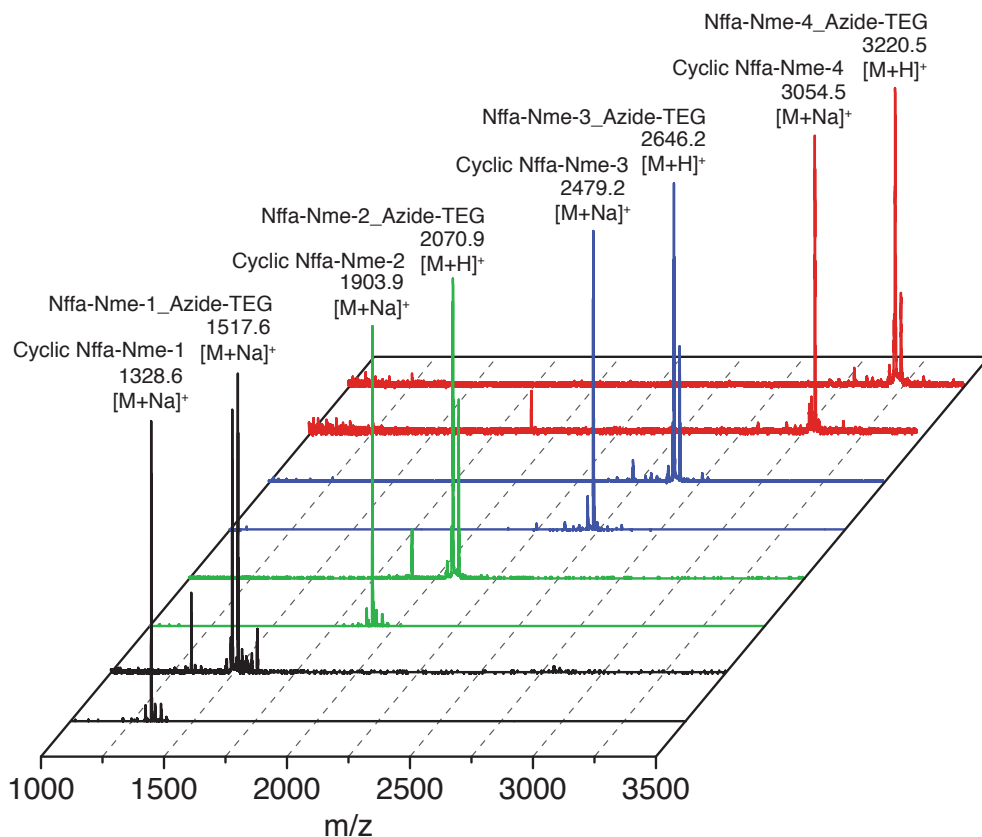
Figure 2.10. MALDI-TOF mass spectra of the crude reaction mixtures of the linear peptoids and macrocycles treated with an excess PEG azide in the presence of a Cu(I) catalyst. Calculated molecular weights for acyclic peptoids conjugated to the PEG azide: [Nffa-Nme-1+Na]$^+$ = 1517.58 g/mol; [Nffa-Nme-2+H]$^+$ = 2070.90 g/mol; [Nffa-Nme-3+H]$^+$ = 2646.22 g/mol; [Nffa-Nme-4+H]$^+$ = 3220.54 g/mol. The calculated molecular weights for the cyclic peptoids: [Nffa-Nme-1+Na]$^+$ = 1328.58 g/mol; [Nffa-Nme-2+Na]$^+$ = 1903.89 g/mol; [Nffa-Nme-3+Na]$^+$ = 2479.21 g/mol; [Nffa-Nme-4+Na]$^+$ = 3054.53 g/mol

The reaction mixtures of varying peptoid lengths were analyzed with RP-HPLC, individual peaks were collected and the corresponding fractions verified using ESI-MS (Figures 8.11-8.15). These spectra highlight the differences in the acyclic and cyclic peptoids. The cyclic peptoids eluted at the same retention time as the excess TEG azide small molecule. The acyclic peptoid had three substantial peaks in the RP-HPLC owing to the excess azide, the peptoid with the affixed azide, and the unreacted acyclic peptoid. The cyclic peptoids were also analyzed with RP-HPLC showing just one sharp peak with a shoulder; the ESI-MS of this peak showed molecular weights corresponding to the TEG azide and the cyclic compound.
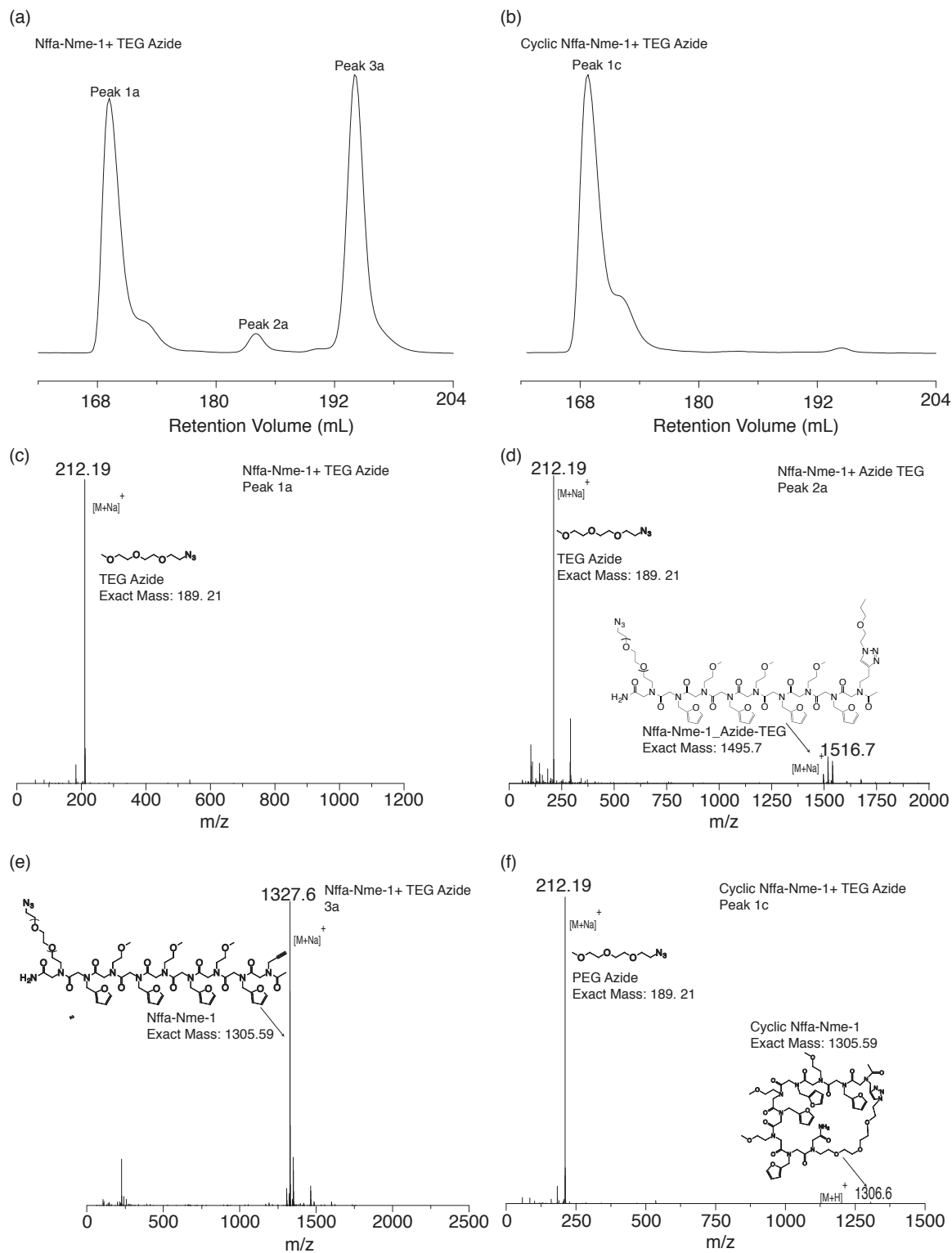
Figure 2.11. Excess TEG azide with Nffa-Nme-p1 (a) RP-HPLC trace of Nffa-Nme-p1 with excess TEG Azide (b) RP-HPLC trace of cyclic Nffa-Nme-p1 with excess TEG Azide (c)

ESI-MS of peak 1a of Nffa-Nme-p1 with excess TEG Azide (d) ESI-MS of peak 1b of Nffa-Nme-p1 with excess TEG Azide (e) ESI-MS of peak 1c of Nffa-Nme-p1 with excess TEG Azide (f) ESI-MS of peak 1c of cyclic Nffa-Nme-p1 with excess TEG Azide
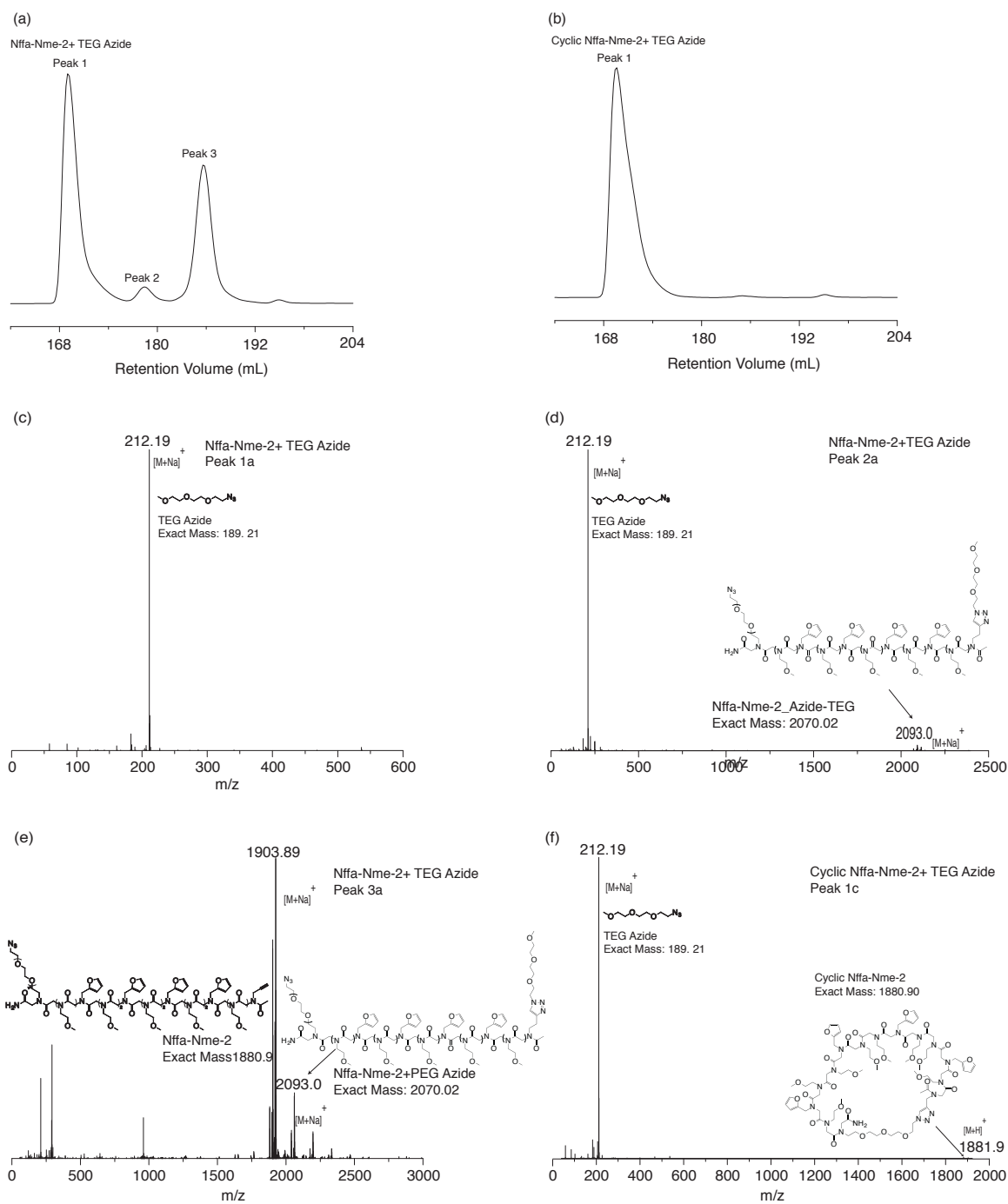
Figure 2.12. Excess TEG azide with Nffa-Nme-p2 (a) RP-HPLC trace of Nffa-Nme-p2 with excess TEG Azide (b) RP-HPLC trace of cyclic Nffa-Nme-p2 with excess TEG Azide (c)

ESI-MS of peak 1a of Nffa-Nme-p2 with excess TEG Azide (d) ESI-MS of peak 1b of Nffa-Nme-p2 with excess TEG Azide (e) ESI-MS of peak 1c of Nffa-Nme-p2 with excess TEG Azide (f) ESI-MS of peak 1c of cyclic Nffa-Nme-p2 with excess TEG Azide
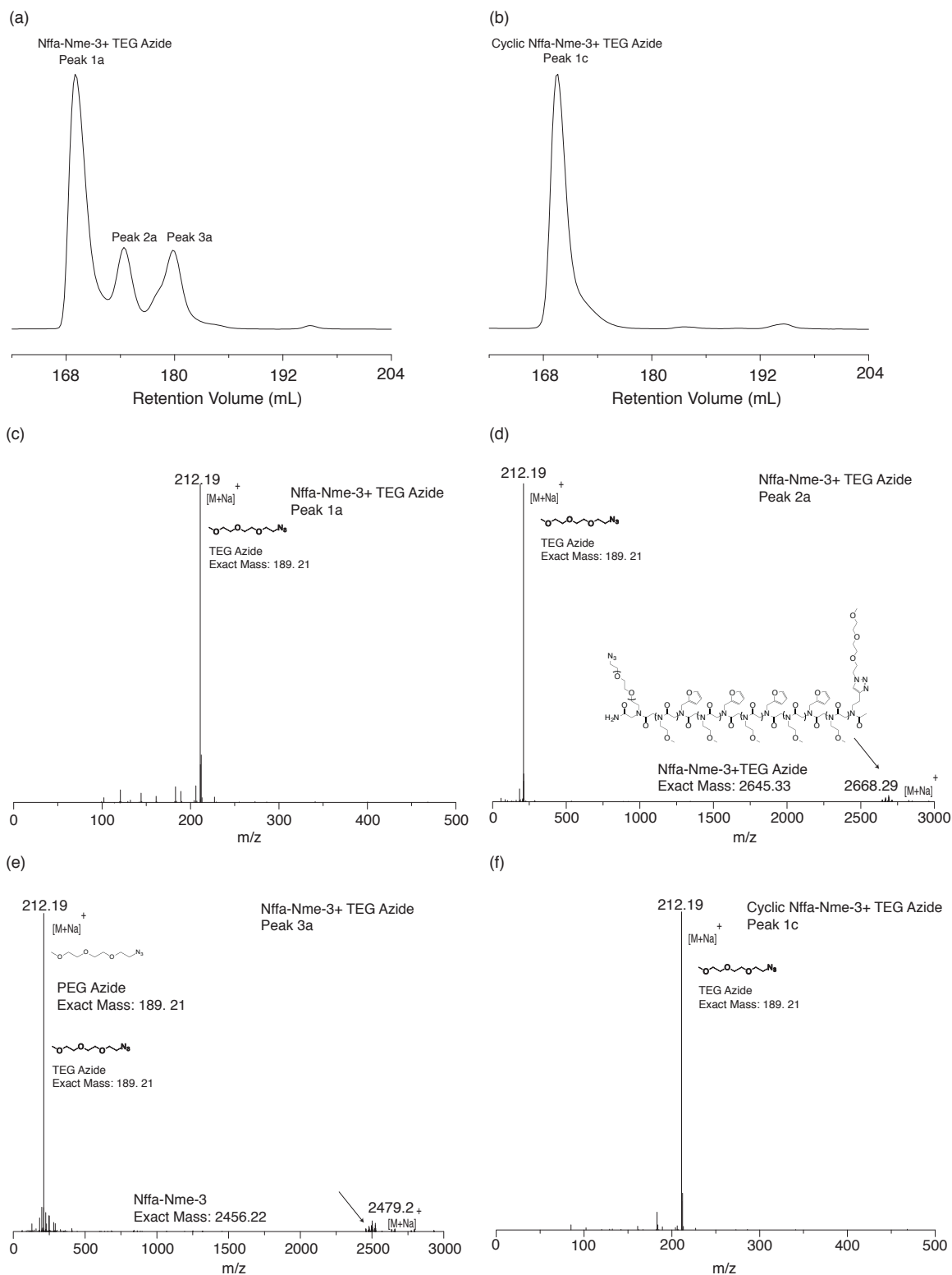
Figure 2.13. Excess Azide with Nffa-Nme-p3 (a) RP-HPLC trace of Nffa-Nme-p3 with excess TEG Azide (b) RP-HPLC trace of cyclic Nffa-Nme-p3 with excess TEG Azide (c) ESI-MS of peak 1a of Nffa-Nme-p3 with excess TEG Azide (d) ESI-MS of peak 1b of Nffa-

Nme-p3 with excess TEG Azide (e) ESI-MS of peak 1c of Nffa-Nme-p3 with excess TEG Azide (f) ESI-MS of peak 1c of cyclic Nffa-Nme-p3 with excess TEG Azide

(a) Nffa-Nme-4+ TEG Azide — Peak 1a, Peak 2a, Peak 3a

(b) Cyclic Nffa-Nme-4+ TEG Azide — Peak 1c

(c) Nffa-Nme-4 + TEG Azide Peak 1a; 212.19 [M+Na]+; TEG Azide Exact Mass: 189. 21

(d) Nffa-Nme-4 + TEG Azide Peak 2a; 212.19 [M+Na]+; TEG Azide Exact Mass: 189. 21; Nffa-Nme-4 Exact Mass: 3031.54; [M+2Na-H]+ 3076.47

(e) Cyclic Nffa-Nme-4 + TEG Azide Peak 3a; 212.19 [M+Na]+; TEG Azide Exact Mass: 189. 21; Nffa-Nme-4 Exact Mass: 3031.54; [M+2Na-H]+ 3076.47

(f) Cyclic Nffa-Nme-4 + TEG Azide Peak 1c; 212.19 [M+Na]+; TEG Azide Exact Mass: 189. 21
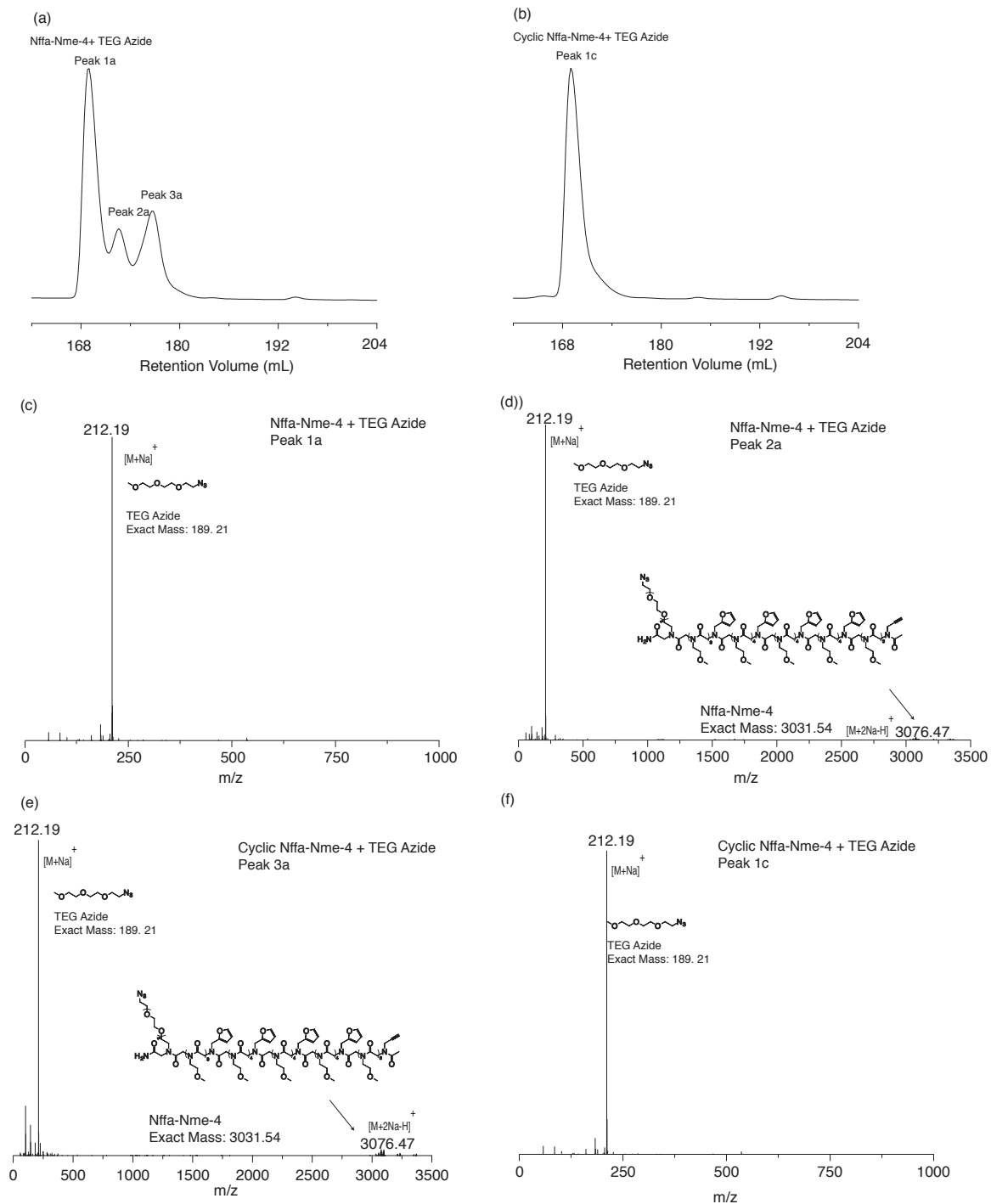
Figure 2.14. TEG azide with Nffa-Nme-p4 (a) RP-HPLC trace of Nffa-Nme-p4 with excess TEG Azide (b) RP-HPLC trace of cyclic Nffa-Nme-p4 with excess TEG Azide (c) ESI-MS of peak 1a of Nffa-Nme-p4 with excess TEG Azide (d) ESI-MS of peak 1b of Nffa-Nme-p4 with excess TEG Azide (e) ESI-MS of peak 1c of Nffa-Nme-p4 with excess TEG Azide (f) ESI-MS of peak 1c of cyclic Nffa-Nme-p4 with excess TEG Azide

2.4.4. Functionalization of Cyclic Peptoids

The post functionalization of the macrocycles was demonstrated by attaching a maleimide amine shown in Figure 2.15. The ESI-MS mass spectrum shows Nffa-Nme-2 and Nffa-Nme-4 functionalized with varying numbers of maleimide groups with complete functionalization being the major product. ESI-MS was used as opposed to MALDI-TOF owing to the shift in the equilibrium of the reaction between the furan and maleimide under MALDI-TOF conditions. We hypothesize that the high temperatures within the MALDI-TOF vacuum chamber owing to the laser power cause the retro-reaction to be more dominant and the functionalized conjugate to not be present.

(a)

Nffa-Nme-2_Maleimide
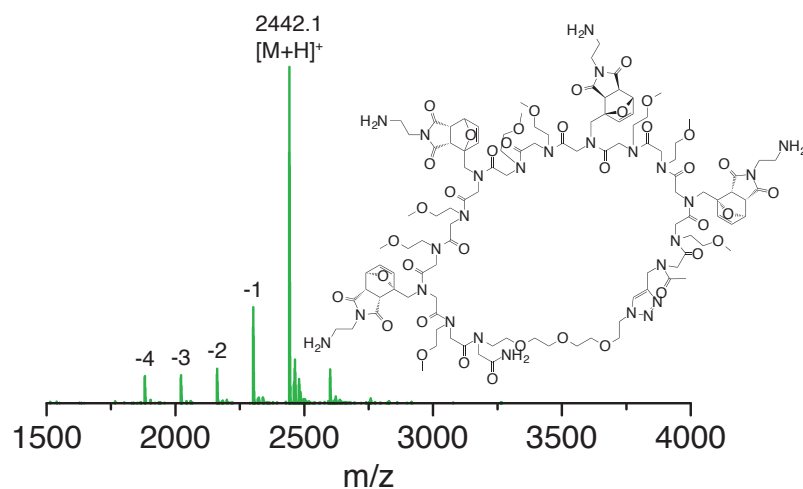
(b)

Nffa-Nme-4_Maleimide
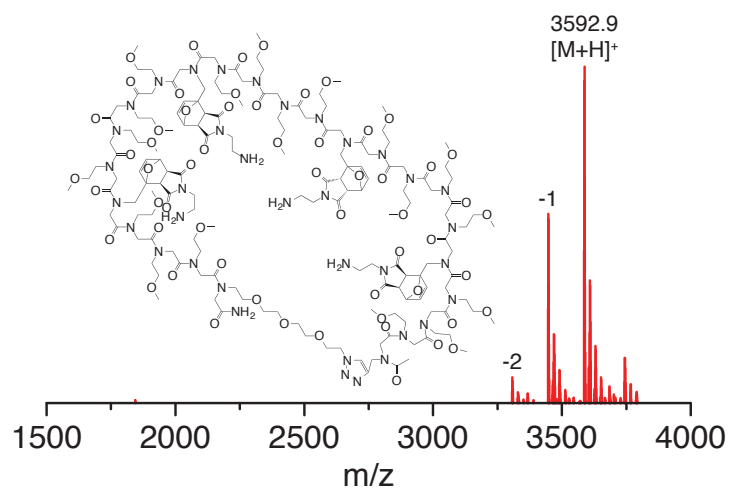
Figure 2.15. ESI-MS mass spectra of the Nffa-Nme-2 and Nffa-Nme-4 cyclic peptoids treated with a maleimide-bearing amine. The calculated molecular weights for the comprehensively functionalized cyclic structures: (a) [Nffa-Nme-2+H]$^{+}$ = 2441.90 g/mol; (b) [Nffa-Nme-4+H]$^{+}$ = 3592.54 g/mol

The macrocycles were challenging to separate from the excess maleimide salt owing to the charged natured of the free amine on the maleimide. This made further purification using RP-HPLC unattainable. The acyclic Nffa-Nme-2 and Nffa-Nme-4 peptoids were treated under the same conditions, and Figure 2.16 shows the ESI-MS mass

spectra of these reactions. The major product for each of the reactions was the fully functionalized peptoid. The order of cyclization then functionalization could have been reversed highlighting the versatility of peptoids in fabricating biological scaffolds.
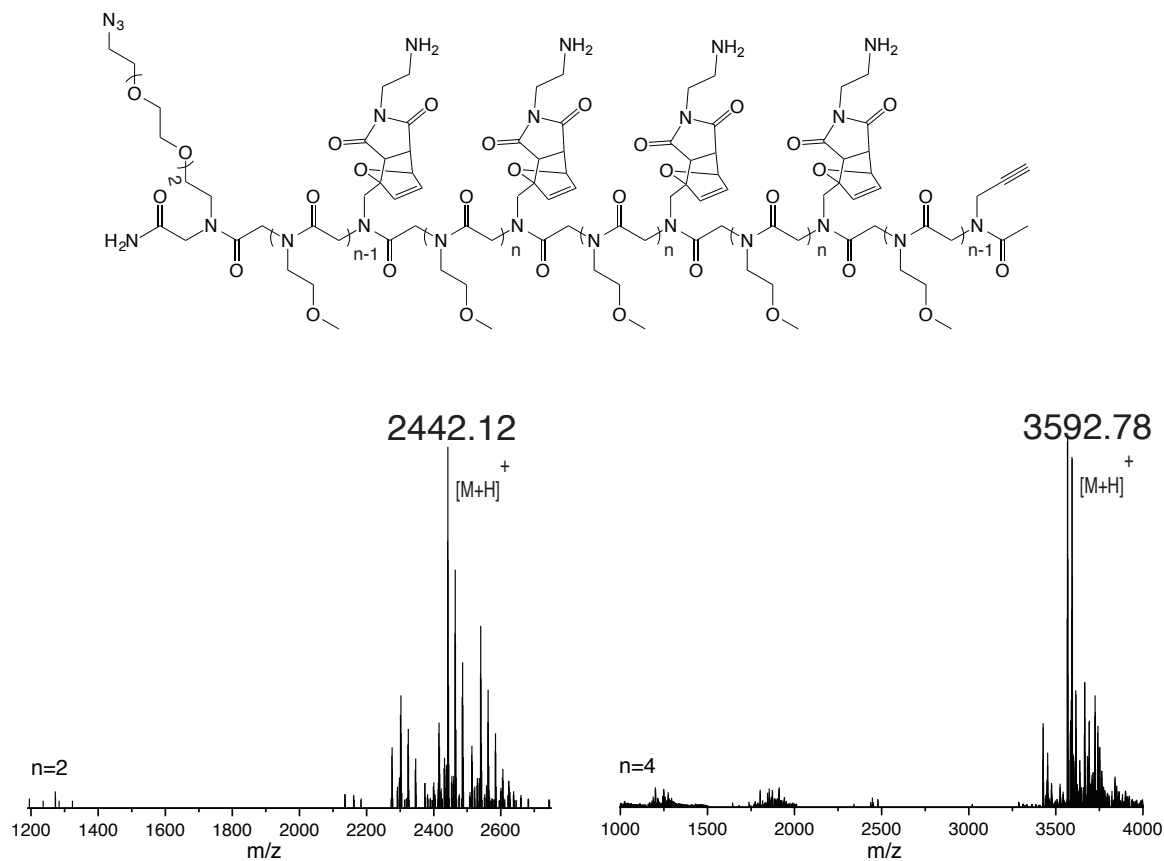
Figure 2.16. ESI-MS spectra of acyclic peptoids functionalized with N-(2-Aminoethyl)maleimide trifluoroacetate salt. The left sample is the peptoid where n=2 for the number of spacers, and the right is the peptoid with n=4.

2.5 Conclusions

We have demonstrated the formation of macrocycles of up to 24 residues that were functionalized with furan groups that allowed for the post synthetic modification through a Diels-Alder cycloaddition reaction with an available maleimide group. We determined that the cyclization efficiency decreased with increasing length, but had no effect on the

ability to functionalize the structure upon cyclization. We were able to observe cyclization through shifts in the retention volume on RP-HPLC, and further confirm the cyclization with FT-IR. Although the furan-maleimide cycloaddition reaction presented characterization strategies, we were able to utilize ESI-MS to confirm site-specific modification of the cyclic structures. This introduces a new synthetic strategy for conjugation of cyclic structures by utilizing two orthogonal chemistries, and serves as a template for building and conjugating structures with biological relevance.

2.6 References

1.   (a) Abdalla, M. A., Medicinal significance of naturally occurring cyclotetrapeptides. *J. Nat. Med.* **2016,** *70* (4), 708-720; (b) Newman, D. J.; Cragg, G. M., Bioactive Macrocycles from Nature. In *Macrocycles in Drug Discovery*, Levin, J. I., Ed. Royal Soc Chemistry: Cambridge, 2015; Vol. 40, pp 1-36.

2.   (a) Spangler, B. D., Structure And Function Of Cholera-Toxin And The Related Escherichia-Coli Heat-Labile Enterotoxin. *Microbiol. Rev.* **1992,** *56* (4), 622-647; (b) Branson, T. R.; McAllister, T. E.; Garcia-Hartjes, J.; Fascione, M. A.; Ross, J. F.; Warriner, S. L.; Wennekes, T.; Zuilhof, H.; Turnbull, W. B., A Protein-Based Pentavalent Inhibitor of the Cholera Toxin B-Subunit. *Angew. Chem.-Int. Edit.* **2014,** *53* (32), 8323-8327.

3.   (a) Ghadiri, M. R.; Granja, J. R.; Buehler, L. K., Artificial Transmembrane Ion Channels From Self-Assembling Peptide Nanotubes. *Nature* **1994,** *369* (6478), 301-304; (b) Montenegro, J.; Ghadiri, M. R.; Granja, J. R., Ion Channel Models Based on Self-Assembling Cyclic Peptide Nanotubes. *Accounts Chem. Res.* **2013,** *46* (12), 2955-2965.

4.   Izadpanah, A.; Gallo, R. L., Antimicrobial peptides. *Journal of the American Academy of Dermatology* **2005,** *52* (3), 381-390.

5.   (a) Fernandez-Lopez, S.; Kim, H. S.; Choi, E. C.; Delgado, M.; Granja, J. R.; Khasanov, A.; Kraehenbuehl, K.; Long, G.; Weinberger, D. A.; Wilcoxen, K. M.; Ghadiri, M. R., Antibacterial agents based on the cyclic D,L-alpha-peptide architecture. *Nature* **2001,** *412* (6845), 452-455; (b) Mallinson, J.; Collins, I., Macrocycles in new drug discovery. *Future Med. Chem.* **2012,** *4* (11), 1409-1438; (c) Collins, S.; Bartlett, S.; Nie, F. L.; Sore, H. F.; Spring, D. R., Diversity-Oriented Synthesis of Macrocycle Libraries for Drug Discovery and Chemical Biology. *Synthesis* **2016,** *48* (10), 1457-1473.

6.   Danial, M.; Tran, C. M. N.; Young, P. G.; Perrier, S.; Jolliffe, K. A., Janus cyclic peptide-polymer nanotubes. *Nature Communications* **2013,** *4*.

7.   Costamagna, J.; Ferraudi, G.; Matsuhiro, B.; Campos-Vallette, M.; Canales, J.; Villagran, M.; Vargas, J.; Aguirre, M. J., Complexes of macrocycles with pendant arms as models for biological molecules. *Coord. Chem. Rev.* **2000,** *196*, 125-164.

8.   Miller, S. M.; Simon, R. J.; Ng, S.; Zuckermann, R. N.; Kerr, J. M.; Moos, W. H., Proteolytic studies of homologous peptide and n-substituted glycine peptoid oligomers. *Bioorg. Med. Chem. Lett.* **1994,** *4* (22), 2657-2662.

9.   Astle, J. M.; Udugamasooriya, D. G.; Smallshaw, J. E.; Kodadek, T., A VEGFR2 Antagonist and Other Peptoids Evade Immune Recognition. *International Journal of Peptide Research and Therapeutics* **2008,** *14* (3), 223-227.

10.   (a) Roy, O.; Faure, S.; Thery, V.; Didierjean, C.; Taillefumier, C., Cyclic beta-peptoids. *Organic Letters* **2008,** *10* (5), 921-924; (b) Lepage, M. L.; Schneider, J. P.; Bodlenner, A.; Meli, A.; De Riccardis, F.; Schmitt, M.; Tarnus, C.; Nguyen-Huynh, N. T.; Francois, Y. N.; Leize-Wagner, E.; Birck, C.; Cousido-Siah, A.; Podjarny, A.; Izzo, I.; Compain, P., Iminosugar-Cyclopeptoid Conjugates Raise Multivalent Effect in Glycosidase Inhibition at Unprecedented High Levels. *Chem.-Eur. J.* **2016,** *22* (15), 5151-5155; (c) Elduque, X.; Pedroso, E.; Grandas, A., Orthogonal Protection of Peptides and Peptoids for Cyclization by the Thiol-Ene Reaction and Conjugation. *J. Org. Chem.* **2014,** *79* (7), 2843-2853.

11.   Webster, A. M.; Cobb, S. L., Recent Advances in the Synthesis of Peptoid Macrocycles. *Chemistry-a European Journal* **2018,** *24* (30), 7560-+.

12.   Rostovtsev, V. V.; Green, L. G.; Fokin, V. V.; Sharpless, K. B., A stepwise Huisgen cycloaddition process: Copper(I)-catalyzed regioselective "ligation" of azides and terminal alkynes. *Angewandte Chemie-International Edition* **2002,** *41* (14), 2596-+.

13.   Pasini, D., The Click Reaction as an Efficient Tool for the Construction of Macrocyclic Structures. *Molecules* **2013,** *18* (8), 9512-9530.

14.   (a) Vieyres, A.; Lam, T.; Gillet, R.; Franc, G.; Castonguay, A.; Kakkar, A., Combined Cu-I-catalysed alkyne-azide cycloaddition and furan-maleimide Diels-Alder "click" chemistry approach to thermoresponsive dendrimers. *Chemical Communications* **2010,** *46* (11), 1875-1877; (b) Gunay, U. S.; Ozsoy, B.; Durmaz, H.; Hizal, G.; Tunca, U., V-Shaped Graft Copolymers via Triple Click Reactions: Diels-Alder, Copper-Catalyzed Azide-Alkyne Cycloaddition, and Nitroxide Radical Coupling. *Journal of Polymer Science Part a-Polymer Chemistry* **2013,** *51* (21), 4667-4674; (c) Gunay, U. S.; Durmaz, H.; Gungor, E.; Dag, A.; Hizal, G.; Tunca, U., 3-miktoarm star terpolymers using triple click reactions: Diels-Alder, copper-catalyzed azide-alkyne cycloaddition, and nitroxide radical coupling reactions. *Journal of Polymer Science Part a-Polymer Chemistry* **2012,** *50* (4), 729-735; (d) Dedeoglu, T.; Durmaz, H.; Hizal, G.; Tunca, U., Synthesis of tadpole polymers via triple click reactions: Copper-catalyzed azide-alkyne cycloaddition, diels-alder, and nitroxide radical coupling reactions. *Journal of Polymer Science Part a-Polymer Chemistry* **2012,** *50* (10), 1917-1925; (e) Cakir, N.; Yavuzarslan, M.; Durmaz, H.; Hizal, G.; Tunca, U., Heterograft Brush Copolymers via Romp and Triple Click Reaction Strategies Involving CuAAC, Diels-Alder, and Nitroxide Radical Coupling Reactions. *Journal of*

Polymer Science Part a-Polymer Chemistry **2013,** *51* (4), 899-907; (f) Candan, O. A.; Kopan, D.; Durmaz, H.; Hizal, G.; Tunca, U., Quadruple click reactions for the synthesis of cysteine-functional heterograft brush copolymer. *European Polymer Journal* **2013,** *49* (7), 1796-1802.

15.   Zuckermann, R. N.; Kerr, J. M.; Kent, S. B. H.; Moos, W. H., Efficient method for the preparation of peptoids oligo(n-substituted glycines) by submonomer solid-phase synthesis. *J. Am. Chem. Soc.* **1992,** *114* (26), 10646-10647.

16.   Lieber, E.; Rao, C. N. R.; Chao, T. S.; Hoffman, C. W. W., Infrared Spectra of Organic Azides. *Analytical Chemistry* **1957,** *29* (6), 916-918.

Chapter 3 Fabrication of Molecular Ladders Utilizing Diels-Alder Chemistry

3.1 Abstract

Nucleic acids (e.g., DNA and RNA), polymers that serve as ubiquitous information-bearing species throughout biology, present the most versatile class of materials for producing diverse, specific nanostructures to date owing to their predictable, information-directed self-assembly. The information borne by nucleic acids is encoded in the sequence of nucleobases affixed to a single (deoxy)ribophosphate strand. Thus, through careful consideration of their residue sequence, nucleic acids can be designed to predictably self-assemble via the hydrogen bond-based hybridization of complementary strands into arbitrary, although thermally and mechanically fragile, structures with nanometer precision. In contrast to hydrogen-bonded Watson-Crick base pairs, we utilized the thermally reversible dynamic covalent base pair, furan/maleimide, to affect oligomer hybridization. Mixtures of oligomers bearing the reversible functional groups were initially subjected to steady raised temperature for deprotection and, as the reaction mixture is allowed to slowly cool and reach equilibrium, the oligomers will would self-assemble via hybridization between strands with complementary sequences. Oligomer sequences were designed and synthesized such that they would self-assemble into molecular ladder structures upon temperature-mediated rearrangement and annealing, they would self-assemble into molecular ladder structures.

3.2 Introduction

Molecular self-assembly is a process in which components of a disordered system aggregate to form organized structures or patterns based on the local interactions between the individual components.[1] These interactions must either be reversible or allow for the aggregates

to adjust their position after formation to provide the most thermodynamically stable product. Most molecular self-assembly processes often rely upon weak intermolecular interactions such as hydrogen bonding, π stacking, or van der Waals interactions[2] resulting in fragile assembled structures.

Nucleic acids are information-bearing self-assembled macromolecules that transport information through a sequence of nucleotides. Specifically, DNA consists of two single stranded sugar-phosphate backbones attached with a sequence of complementary nucleobase residues that self-assemble into a double helix formation *via* hydrogen bonding.[3] The selectivity of the complementary nucleobase led to the utilization of DNA as a construction material.[4] Despite nucleic acid nanotechnology making significant strides in recent years, there are still mechanical and thermal limitations in assembled structures owing in part to the hydrogen bonds holding the DNA strands together.

The limitations of nucleic acids has created a desire to fabricate strucutres with stronger covalent bonds. Most covalent bonds are considered "irreversible" rearing them uneffective in self-assembly mechanisms; however, dynamic covalent chemistry, a class of reactions where products containing covalent bonds can revert back to their initial reactants under a particular set of reaction conditions, can be readily incorporated in self-assembled structures.[5] Several stimuli, such as temperaure,[6] pH,[7] and photochemical triggers,[8] can be employed to reversibly affect the equilibrium of a reaction. This project examines specifically the thermally-mediated Diels-Alder reaction, a cycloaddition reaction between a diene and a substituted alkene. At moderate temperatures, the equilibrium will lie towards the Diels–Alder adduct and at raised temperatures (>100°C) the adduct will revert back to the reactants (see Figure 3.1).[9] This reaction is analogous to the hydrogen bonding between complementary nucleobases, where the double-stranded

structure of nucleic acids is 'melted' at raised temperature and subsequently annealed upon a gradual ramp to moderate temperature. Here, we describe the design and synthesis of peptoid-based Diels-Alder oligomers that were designed to self-assemble into molecular ladders.
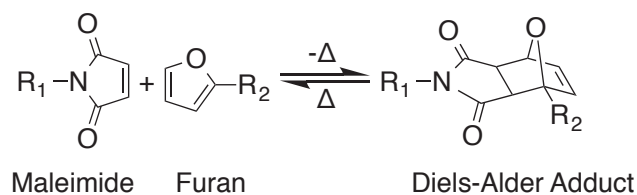
Figure 3.1. Diels-Alder chemistry between furan (diene) and maleimide(dienophile)

3.3 Experimental

3.3.1. General Experimental Procedure

Electrospray ionization mass spectrometry (ESI-MS) mass spectra were collected using an Agilent Q-TOF 1200 series spectrometer in positive ion mode. Matrix-assisted laser desorption/ionization time-of-flight (MALDI-TOF) mass spectra were recorded using a Bruker Autoflex mass spectrometer in reflectron position ion mode using 2-(4-hydroxyphenylazo)benzoic acid (HABA) as the matrix. The MALDI-TOF samples were prepared with a 3:1 ratio of matrix (100mM, 200μL acetonitrile) to sample (crude reaction mixtures). A prominence gel permeation chromatography (GPC, Shimadzu Corporation) system was used in this study. This system is equipped with two Phenogel (Phenomenex) analytical size exclusion columns in series with pore sizes of 100 Å (particle size 5 μm) and and 50 Å (particle size 10 μm), respectively. Additionally, this system is equipped with a single Phenogel preparative size exclusion column with a pore size of 100 Å (particle size 5 μm). Reverse phase high performance liquid chromatography (RP-HPLC) was performed using preparative reversed phase Phenomenex Luna C18 (2) columns with a linear gradient of water and acetonitrile as the eluent at 30°C. The RP-HPLC was equipped with Shimadzu LC-6AD HPLC pump, Shimadzu

FRC 70A fraction collector, and monitored using Shimadzu Prominence detector at 214nm. Samples were lyophilized to a white powder to remove all residual solvents using a Labconco lyophilzer. An EasyMax 102 automatic laboratory reactor (Mettler-Toledo) was utilized for hybridization. Unless otherwise noted all reagents and materials were purchased from commercial sources Sigma Aldrich, AK Scientific, and TCI Chemical.

3.3.2. Oligomer Preparation
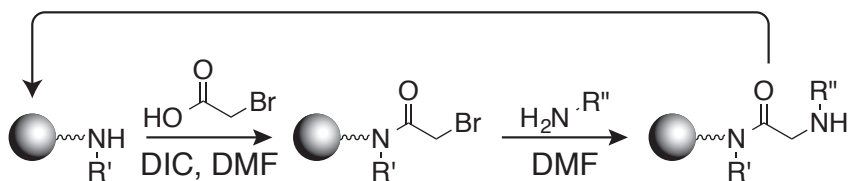
Scheme 3.1. Submonomer solid-phase synthesis scheme utilized for synthesizing peptoids

Peptoids were primarily synthesized by a microwave-assisted Liberty Blue peptide synthesizer (CEM Corporation) on acid-labile Rink amide 4-methylbenz-hydrylamine (MBHA) resin (ChemPep Inc.) using Zuckermann's submonomer protocol shown in Scheme 3.1.[10] Although initial syntheses were performed manually using a 25 mL solid-phase peptide synthesis vessel (CG-1866, Chemglass), they followed the same submonomer protocol. This is a sequential addition reaction whereby a terminal amine from the solid support is acetylated with bromoacetic acid (1 M prepared in dimethylformamide(DMF)) using diisopropylcarbodiimide (1M prepared in DMF) as an activating agent, to afford a terminal bromide which is subsequently displaced *via* nucleophilic substitution with a primary amine (0.5M prepared in N-methyl-2-pyrrolidone or DMF) bearing the pendant group. This two-step process of acetylation and displacement is repeated until the desired chain length is achieved. Typically, a 10 fold excess was calculated from the resin substitution value.

The primary amines (Figure 3.2) used in this study possessed one of two different functions, either to promote solubility or direct the assembly of the oligomers into ladders. The two monomers that directed assembly were commercially-available furfurylamine (Nffa) bearing the furan functional group and N4-(2-amino-ethyl)-10-oxa-4-aza-tricyclo[5.2.1.0^{2,6}]-dec-8-ene-3,5-dione (Nfpm) shown in Scheme 3.2, the maleimide-based primary amine prepared below was adapted from methods outlined by Elduque et al.[11] This maleimide-bearing monomer must be protected with thermally labile furan, as unprotected maleimides are incompatible with basic, nucleophilic reagents and hence susceptible to hydrolysis or addition reactions at the double bond throughout peptoids synthesis. The other set of primary amine monomers used were inert spacers that consisted of both commercially available monomers isobutylamine (Nleu) and 2-methoxyethylamine (Nme) and two polyethylene glycol-like monomers prepared by the method reported by Wei et al.,[12] 2-ethoxyethoxyethylamine (Neee) and 2-(2-(2-methoxyethoxy)ethoxy)ethylamine (Nmee). Complementary sequences were synthesized alternating between the active dynamic covalent monomer and the inert spacer monomers.
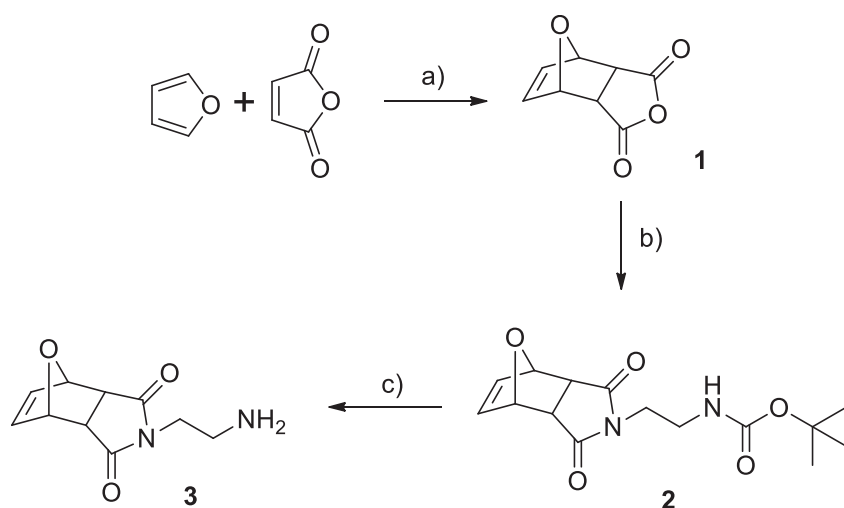
Scheme 3.2. Synthesis of 4-(2-amino-ethyl)-10-oxa-4-aza-tricyclo[5.2.1.0^{2,6}]-dec-8-ene-3,5-dione (3). Reagents and conditions: (a) ethyl acetate, r.t., (b) *tert*-butyl-2-aminoethyl carbamate, reflux, (c) TFA/DCM.

4,10-Dioxatricyclo[5.2.1.0^{2,6}]dec-8-ene-3,5-dione (**1**). A 500 ml round bottom flask was charged with furan (99 ml, 1.36 mol), maleic anhydride (100 g, 1.02 mol), and ethyl acetate (125 ml). This reaction mixture was stirred for 24 hrs at room temperature. A colorless crystal was filtered and dried under vacuum. The product was used without further purification (yield 90 %). Characterization data: ^{1}H NMR (acetone-d_6, δ ppm): 6.63 (2 H, s, -CHC*H*=C*H*CH-), 5.36 (2 H, s, -C*H*CH=CHC*H*-), 3.37 (2 H, s, O=CC*H*).

***tert*-Butyl-(2-(1,3-dioxo-3a,4,7,7a-tetrahydro-1H-4,7-epoxyisoindol-2(3H)-yl)ethyl)-**

carbamate (**2**). Compound **1** (30 g, 0.18 mol) and ethanol (45 ml) were placed in a 250 ml three necked round bottom flask equipped with a reflux condenser and a magnetic stirrer. To this, a solution of *tert*-butyl-2-aminoethyl carbamate (29.8 g, 0.19 mol) and ethanol (10 ml) was added dropwise with continuous stirring. The resulting mixture was refluxed at 85°C for 4 hrs. After the reaction, the solution was allowed to cool to room temperature for overnight and the white solid was filtered off and recrystallized from ethanol. The collected white crystals were dried under vacuum to afford **2** (25 g, 45 %). Characterization data: ^{1}H NMR (acetone-d_6, δ ppm): 6.59 (2 H, s, -CHC*H*=C*H*CH-), 5.91 (1 H, s, -N*H*), 5.14 (2 H, s, -C*H*CH=CHC*H*-), 3.53 (2 H, t, NC*H*$_2$CH$_2$NHC=O), 3.24 (2 H, t, NCH$_2$C*H*$_2$NHC=O), 2.90 (2 H, s, O=CC*H*), 1.40 (9 H, t, -C(C*H*$_3$)$_3$).

4-(2-amino-ethyl)-10-oxa-4-aza-tricyclo[5.2.1.0^{2,6}]-dec-8-ene-3,5-dione (**3**). In a 1 L round bottom flask, the compound **2** (20 g, 65 mmol) was dissolved in 3:7 trifluoroacetic acid (TFA)/dichloromethane (DCM) mixture (400 ml) and stirred for 1 hr at room temperature. Then excess reagent and solvent were removed by evaporation. The resulting oil was added diethyl ether (40 ml) to precipitate. After centrifugation, the supernatant was discarded and diethyl ether

was added again. This step was repeated three times. The white product was collected and dried

under vacuum. The resulting white solid was dissolved minimum amount of water and

neutralized by saturated NaHCO$_3$, extracted with DCM and dried over MgSO$_4$. The solution was

dried under vacuum to yield compound **3** white solid at 70% yield. Characterization data: ^{1}H

NMR (DMSO-*d$_6$*, *δ* ppm): 6.54 (2 H, s, -CHC*H*=C*H*CH-), 5.11 (2 H, s, -C*H*CH=CHC*H*-), 3.34

(2 H, t, NC*H$_2$*CH$_2$NH$_2$), 2.91 (2 H, s, O=CC*H*), 2.59 (2 H, t, NCH$_2$C*H$_2$*NH$_2$).

Dynamic Covalent Monomers   Inert Spacer Monomers
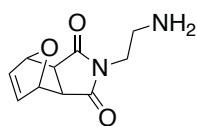
Nfpm = furan-protected maleimide
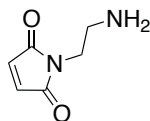
Nmal = malemide
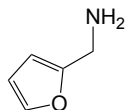
Nffa = furfurylamine

Nleu= isobutylamine
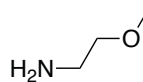
Nme = 2-methoxyethylamine
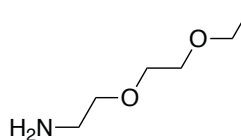
Neee = 2-(2-ethoxyethoxy)ethylamine
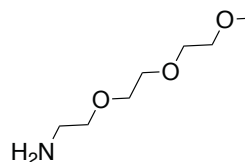
Nmee = 2-(2-(2-methoxyethoxy)ethoxy)ethylamine

Figure 3.2. Primary amine monomers used throughout this chapter

The N-terminal of the oligomers was capped with acetic anhydride (1M prepared in DMF) to

prevent further chain elongation. The peptoids were released from the solid-support resin by

immersion in a mixture of trifluoroacetic acid (TFA):dichloromethane (DCM) (20:80 volume

ratio) for 30 minutes at room temperature. ESI-MS mass spectrometry was used to verify the identity of the crude peptoids.

3.3.3. Peptoid Purification

Initially, GPC was utilized in the purification of oligopeptoids; this chromatographic system is capable of separating tens to hundreds of milligrams of crude peptoid samples based on the molecular weight of the components. Dimethylformamide (DMF) was used as the mobile phase at a flow rate of 1.0 mL/min. The elution fractions were collected at times determined from an analytical run of the crude peptoid sample. The fractions were combined and the molecular weights confirmed using ESI-MS.

Subsequently, peptoids were purified by RP-HPLC, where the crude peptoids were ran through a linear gradient of 10%-acetonitrile-water to 90%-acetonitrile-water over 22 minutes. Fractions corresponding to the major peaks were collected through each subsequent run before the purified peptoid fractions combined and lyophilized to a fine white powder. ESI-MS was likewise employed to confirm the exact mass of the fractions.

3.3.4. Oligomer Deprotection

Peptoids containing the furan-protected maleimide monomers (Nfpm) were deprotected by raising and maintaining the temperature of a solution of the peptoid in anhydrous anisole to 140°C for 30 minutes such that the adduct undergoes the retro-Diels–Alder reaction, where the reaction equilibrium is favored towards the reactants, and the free furan (boiling point ~32°C) volatilizes. EasyMax 102 automatic laboratory reactor (Mettler-Toledo) was used for precise temperature ramps under inert atmospheres. Maleimides are sensitive to hydrolysis[13] it is paramount to maintain dry and inert conditions throughout peptoid deprotection for oligomer stability.

3.3.5. Molecular Ladder Fabrication

Preliminary exploration of the self-assembly (Figure 3.5) of these strands was investigated using the EasyMax 102 reactor. There were two methods for testing the hybridization of complementary peptoid strands. The first method involved repurifying the maleimide-bearing peptoids with RP-HPLC after deprotection before mixing it with stoichiometric ratios of the furan-bearing peptoids in the inert EasyMax 102 reactor. The mixture would be quickly heated to 120°C then cooled a rate of 0.5°C per minute until room temperature. The second method included an in-situ deprotection of the furan group from the maleimide oligomers before a slow and controlled temperature drop. This was to mimic the annealing process of DNA.[14] Here the reaction vessel would be charged with stoichiometric equivalents of the furan- and maleimide-based oligomers with furan protection intact in anhydrous anisole under inter condition, the reaction mixture would then be heat to 140°C for 30 minutes then the mixture would be cooled at a rate of 0.5°C per minute until room temperature. In both methods, the reaction mixture was then analyzed by ESI-MS and MALDI-TOF.
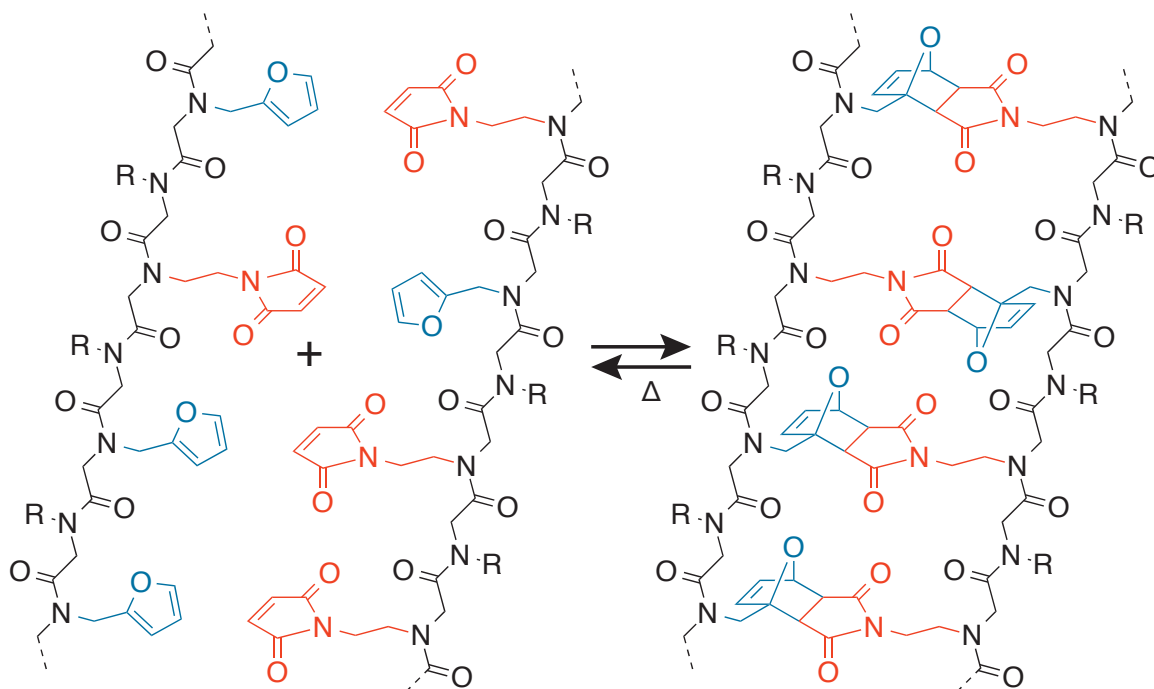
Figure 3.5. Reversible hybridization of dynamic covalent oligomers bearing furan and maleimide functional groups

3.4. Results and Discussion

3.4.1. Nleu Containing Peptoids

Peptoids were prepared by determining the optimal conditions for the synthesis and cleavage of complementary furan- and maleimide-based oligomers using Zuckerman's two-step submonomer synthesis scheme.[10] We explored varied reaction times, reaction temperature, and stoichiometric excess of the reactants. These syntheses were initially performed manually before ultimately utilizing a microwave-assisted automated peptide synthesizer. We first synthesized a furan-based peptoid comprised of four repeat units of alternating Nleu and Nffa structure (NleuNffa)$_4$ shown in Figure 3.6a. This peptoid was synthesized using a Rink amide resin solid support that was initially deprotected with 4-methylpiperidine:DMF (20:80, volume ratio) six times for 10 minutes at room temperature. The acetylation was carried out at 50°C for 15 minutes with bromoacetic acid (20 equivalents) and diisopropylcarbodiimide (DIC) (20 equivalents) in DMF. The submonomers (10 equivalents) Nleu and Nffa used for displacement were prepared in DMF. The displacement was performed at 50°C for 30 minutes. The two-step process of bromoacetylation followed by displacement was continued until the final chain length, in this case four monomeric units long, was achieved. End-group capping was performed to prevent further chain elongation by using acetic anhydride (20 equivalents) and DIC (20 equivalents) in DMF. Between each step the solid-support resin was rinsed five times with DMF at room temperature. Subsequently, the cleavage cocktail and reaction times were varied to determine the most favorable conditions to release the peptoids from the solid-support, ultimately determined to be submersion in a cleavage cocktail comprised of 20% TFA in DCM reacting for 30 minutes.

We were able to use ESI-MS (Figure 3.6a) to confirm the synthesis of the oligomer before preparing the complementary strands. The same reaction conditions were used to synthesize a furan-protected maleimide-bearing peptoid (NleuNfpm)$_4$ shown in Figure 3.6b. Likewise, ESI-MS analysis was done of the complementary peptoid strand confirming the synthesis of both oligomers. These two peptoids were designed to form a dynamic covalent molecular ladder with four Diels-Alder rungs.
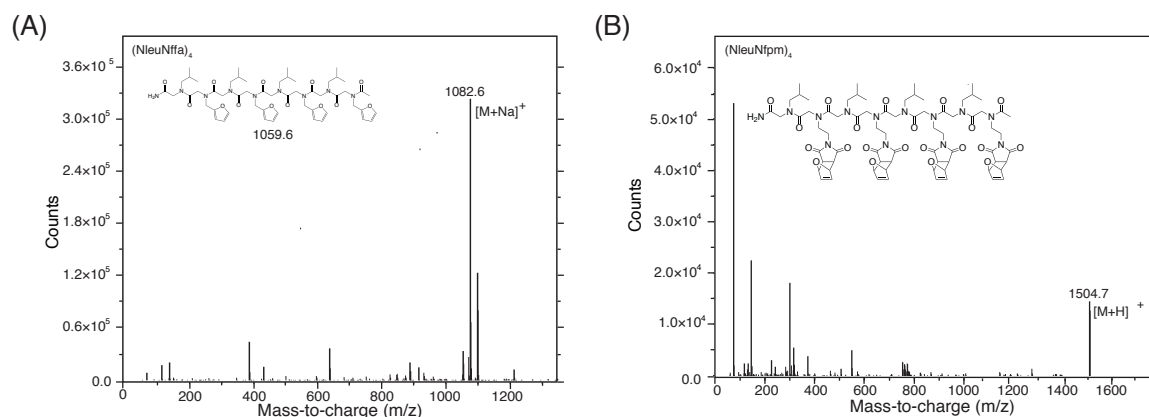
Figure 3.6. ESI-MS mass spectra of Nleu bearing peptoids after cleavage from the solid support resin (a) [(NleuNffa)$_4$+Na]$^+$ =1082.6 g/mol (b) [(NleuNfpm)$_4$+H]$^+$ =1504.7g/mol

Upon successful synthesis of the oligomers, they were purified by the GPC. An analytical trace of each of the peptoids was used to determine the elution time before collecting subsequent fractions. These fractions were combined and ESI-MS confirmed the exact mass of the resulting samples. Figure 3.7 shows GPC traces for both the crude product represented by the black lines and the combined purified peptoid shown by the blue lines for the furan peptoid (Figure 3.7a) and the maleimide oligomer (Figure 3.7 b). The GPC trace after purification suggests that the purification process was successful as evident by the symmetric peaks; however, it was discovered during this step that the furan-based peptoid has a limited solubility in the eluent, DMF, at room temperature. An alternative course of action was taken to modify the peptoid

structures to include spacer amines that improved the solubility ultimately allowing for the peptoids to be purified using RP-HPLC, a more conventional approach to peptoid purification.
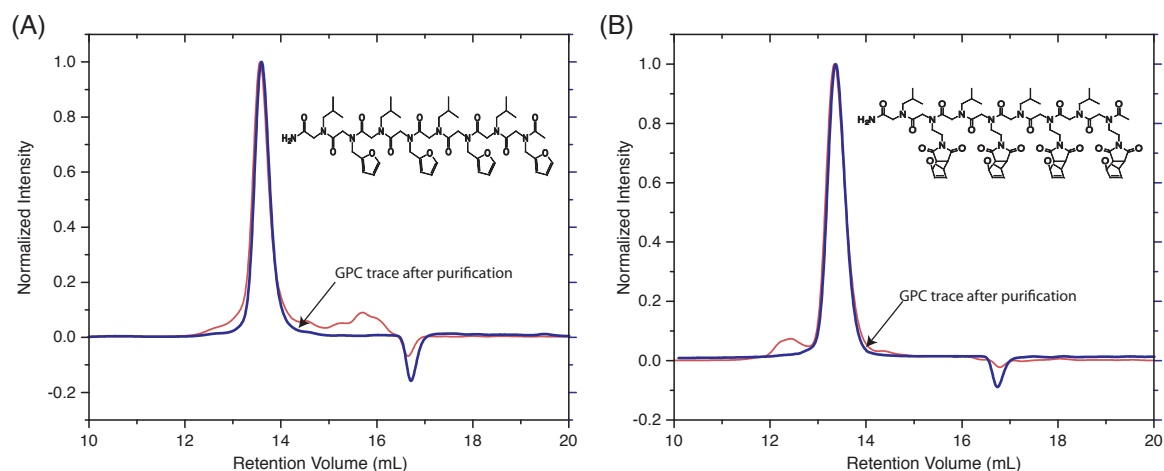
Figure 3.7. GPC traces of Nleu-bearing peptoids before (red) and after (blue) purification (a) (NleuNffa)₄, and (b) (NleuNfpm)₄

3.4.2. Nme-bearing Peptoids

We hypothesized that the limited solubility of the Nleu-bearing peptoids would not only be challenging to purify, but also saddle the resulting hybrids with limited solubility. Indeed, one of the key features that allows for water solubility of nucleic acids is a consequence of the charged, hydrophilic phosphate functional groups incorporated in their backbone. We similarly wanted to influence solubility in our oligomers by synthesizing peptoids that incorporated the more polar inert spacer monomer, Nme, at alternating positions along the peptoid backbone. We first synthesized and characterized (NmeNffa)₄ by ESI-MS as shown in Figure 3.8a. This mass spectrum confirmed that we could successfully synthesize peptoids with this new spacer pendent group. It is worth noting that there was a decrease in cleavage time (down to ~10 minutes) with these peptoids owing to the peptoids experiencing truncation with the acetylated end group.[15] The same conditions were applied to (NmeNfpm)₄, and the ESI-MS spectrum in Figure 3.8b

confirms the exact mass of the peptoid. After the peptoids were synthesized *via* solid-phase synthesis, the increased solubility allowed them to be purified by preparative RP-HPLC. Figure 3.9 shows an analytical trace of each of (A) (NmeNffa)$_4$ and (B) (NmeNffa)$_4$ after purified fraction were collected and combined. This confirms the ability to purify the peptoids (>95%) using RP-HPLC.
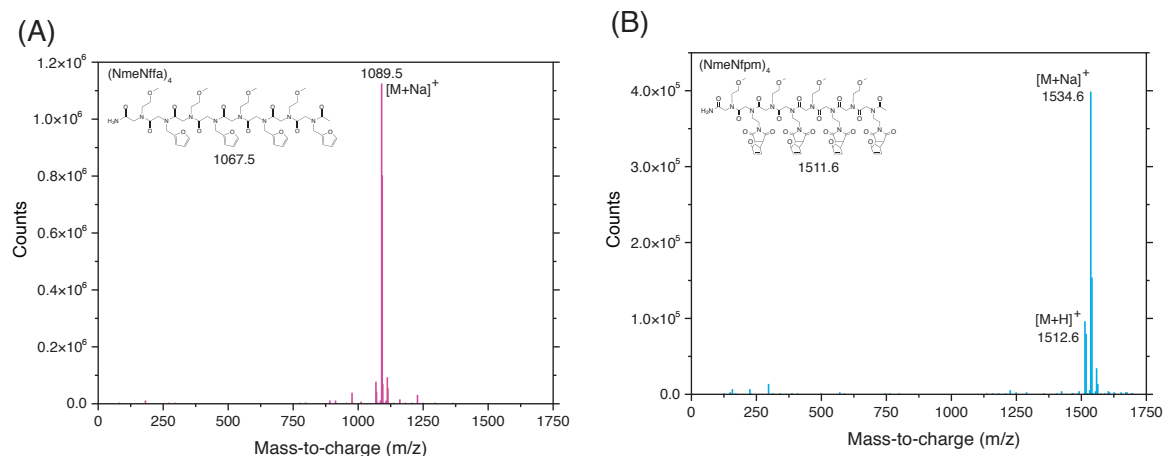
Figure 3.8. ESI-MS mass spectra of Nme-bearing peptoids (a) [(NmeNffa)$_4$+Na]$^+$ = 1089.5 g/mol, and (b) [(NmeNfpm)$_4$+H]$^+$ = 1512.6g/mol and (NmeNfpm)$_4$+Na]$^+$ = 1535.6g/mol
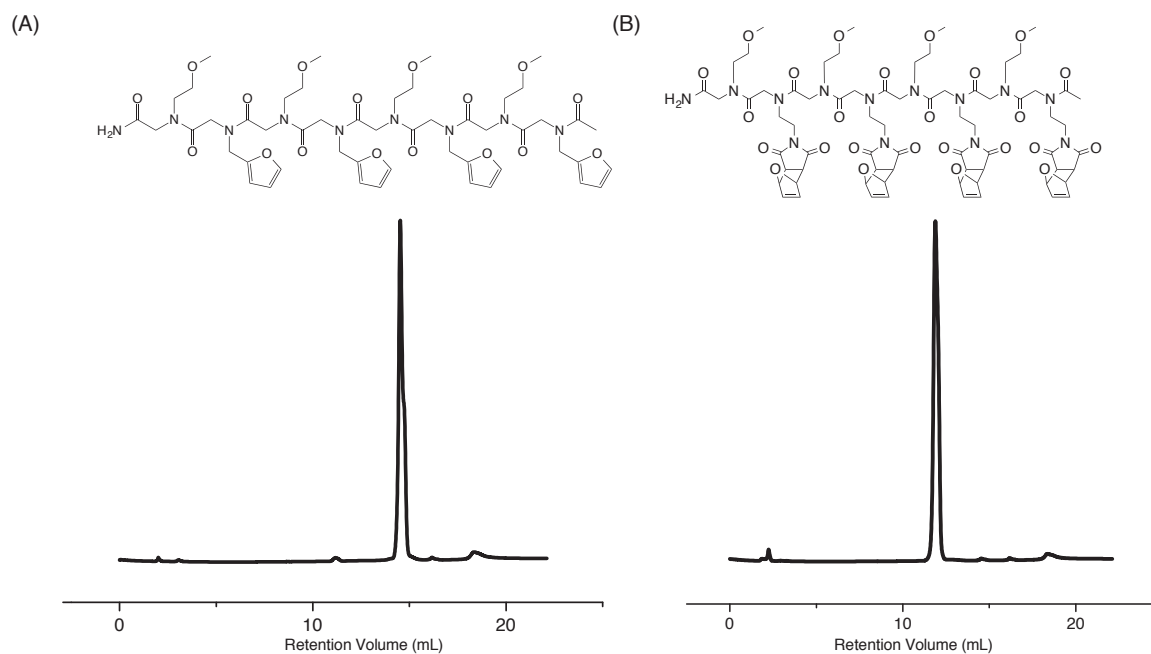
Figure 3.9. Analytical RP-HPLC traces of Nme-bearing peptoids after purification (a) (NmeNffa)₄, and (b) (NmeNfpm)₄

3.4.3. Maleimide Deprotection

(NmeNfpm)₄ was subsequently deprotected of the thermally-labile furan group (boiling point ~32°C) through a brief heating of the Diels-Alder adduct-incorporating oligomer to 140°C in anisole resulting in quantitative deprotection (Figure 3.10). Anhydrous anisole was the optimal choice owing to its relative dry nature and high boiling point. This exposed the maleimide-group necessary to direct the assembly of molecular ladders.
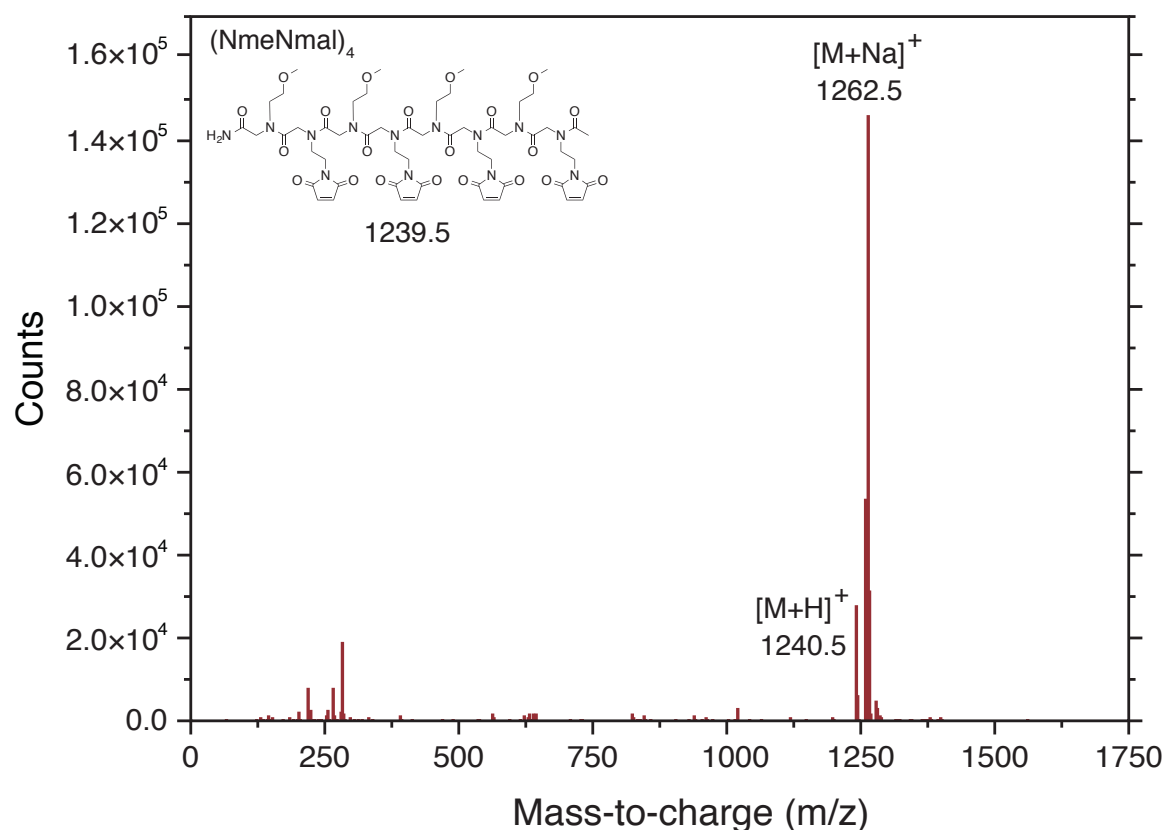
Figure 3.10. ESI spectrum confirming the comprehensive removal of the furan protecting group from the maleimide-bearing peptoid. [(NmeNmal)₄+H]$^+$ = 1240.5 g/mol and (NmeNmal)₄+Na]$^+$ = 1262.5 g/mol

3.4.4. Diels-Alder Hybridization

The reversible nature of the Diels-Alder system was exploited to form molecular ladders similar to the process of melting and annealing in nucleic acids. First $(NmeNffa)_4$ and $(NmeNmal)_4$ were added in stoichiometric ratios and the temperature was raised to 110°C to promote the retro reaction before being slowly cooled. This slow temperature decrease prevented misaligned, out-of-register hybrids from becoming kinetically trapped and ensure minimization of the Gibbs energy through ideal hybridization. Although heating and annealing a mixture of the furan- and maleimide-based tetramers yielded an essentially insoluble precipitate, ESI-MS on the filtered solvent revealed that the tetramer hybrid (Figure 3.11) had been formed. Subsequent hybridization studies employed and in situ thermal deprotection by combining the 30 minutes hold at 140°C followed by slow cooling.
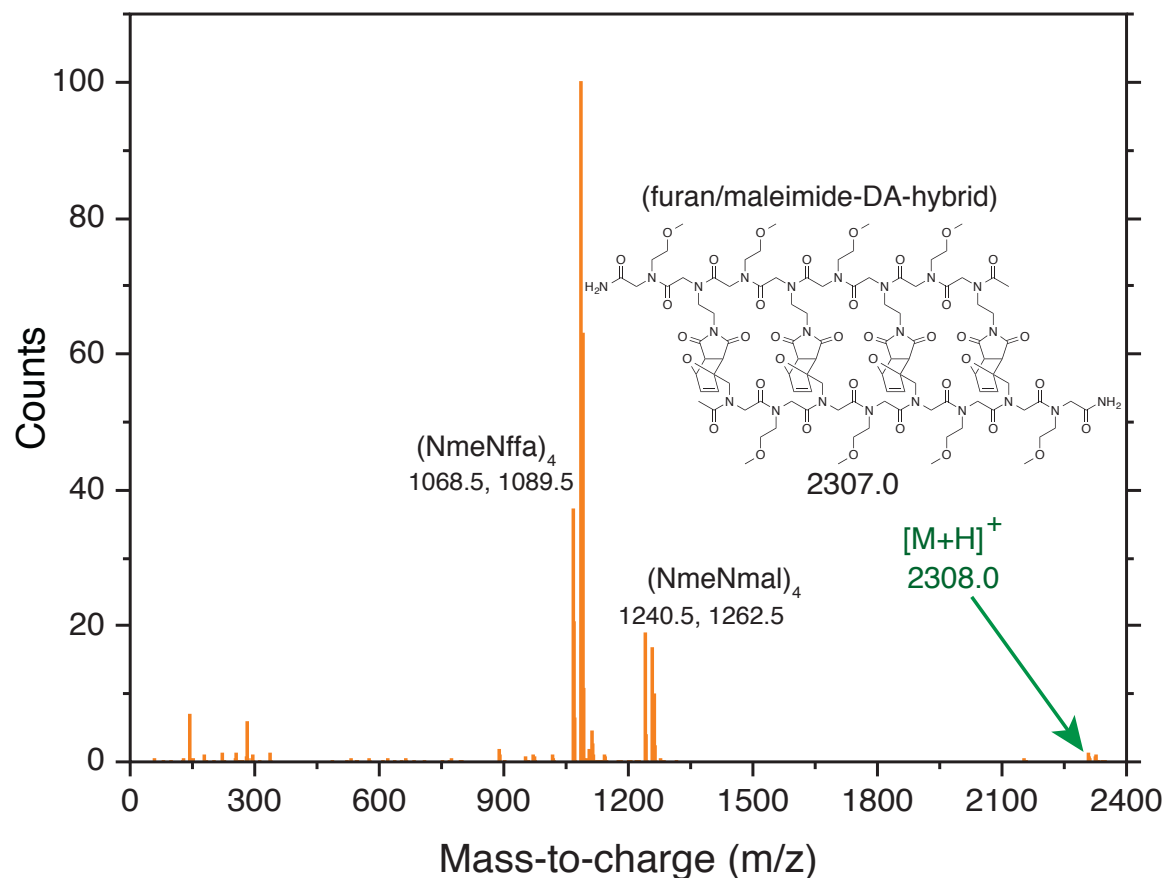
Figure 3.11. ESI-MS spectra confirming the formation of a Diels-Alder hybridized molecular ladder. [Hybrid+H]$^+$ = 2308.0 g/mol

3.4.5. System Limitations

The first major challenge of this system is the limited solubility of the formed molecular ladders. We would routinely observe insoluble precipitant on the sides of the reaction vessel. In order to address this, we began to incorporate different inert spacers into the peptoid backbones, Neee and Nmee, as shown in the furan-bearing peptoids in Figure 3.12. The structures formed with these longer more flexible pendent groups still would result in an insoluble precipitant that was not present in mass spectrum. We also looked into a variety of solvents that had a high boiling point to allow for the slow temperature ramps necessary for the formation of in registry ladders without success.

(NeeeNffa)$_4$

(NmeeNffa)$_4$
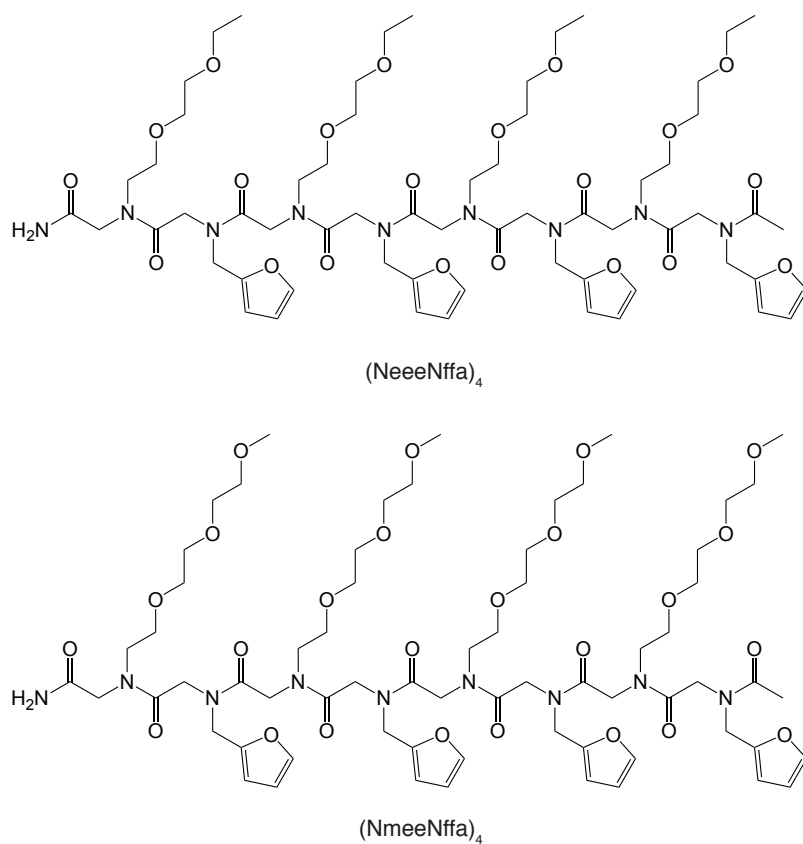
Figure 3.12. Structures of different furan-bearing peptoids that were used to improve solubility of the formed hybridized structures

In addition to solubility concerns, the structures were incompatibility with MALDI-TOF,[16] a common technique used for confirming the exact mass of higher molecular weight structures. MALDI-TOF shifts the equilibrium of the reaction between the furan and maleimide; we hypothesize that the high temperatures within the MALDI-TOF vacuum chamber owing to the laser power cause the dominance of the retro-reaction and the absence of the molecular ladders. In ESI-MS, it is challenging to see the formed hybrids if single stranded oligomers, that tend to more readily ionize, remain in the mixture.

Another challenge facing this system is the ability to discern between fully formed and partially formed molecular ladders using conventional mass spectra. There would be no mass difference between, for example, 3 or 2 rungs being formed in a Diels-Alder molecular ladder whereas with other molecular ladders resulting from other reactions can use this technique to monitor the ladders coming into registry.[12, 17] While other techniques for monitoring the reaction exist mass spectrometry would be the most straightforward approach. An example of another technique is FTIR, the furan/maleimide system could be assessed by monitoring the furan peak area, centered at 1010 cm^{-1}, and the maleimide peak area, centered at 690 cm^{-1},[18] for solutions containing stoichiometric concentrations of the two reactants. The generated olefinic oxanorbornene of the adduct can be subject to radical-mediated thiol–ene reaction with a monothiol (e.g., butyl 3-mercaptopropionate) and the consumption of the vinyl and thiol can be determined using FT-IR spectroscopy by monitoring the peak areas centered at 910 cm^{-1} and 2570 cm^{-1}, respectively.[19] While this option and others exist, the burden of overcoming characterization challenges remained strong.

3.5. Conclusions

Diels-Alder chemistry between a furan and a maleimide shows to be a promising method of preparing molecular ladders that mimic DNA's ability of to melt and anneal into sequence specific structures. We have been able to form oligomers comprised of these functional groups and mediate their assembly into molecular ladders. This work discovered different challenges that ultimately come down to solubility and characterization. While these issues are not insurmountable, they do prove to be difficult to overcome at the current time. This work led to the formation of an analogous molecular ladder system between boronic acid and catechol to be discussed in subsequent chapters.

3.6. References

1.   Whitesides, G. M.; Mathias, J. P.; Seto, C. T., Molecular Self-Assembly and Nanochemistry: A Chemical Strategy for the Synthesis of Nanostructures. *Science* **1991,** *254* (5036), 1312-1319.

2.   Zhang, S. G., Fabrication of novel biomaterials through molecular self-assembly. *Nat. Biotechnol.* **2003,** *21* (10), 1171-1178.

3.   Watson, J. D.; Crick, F. H. C., Molecular Structure of Nucleic Acids: A Structure for Deoxyribose Nucleic Acid. *Nature* **1953,** *171* (4356), 737-738.

4.   (a) Rothemund, P. W. K., Folding DNA to create nanoscale shapes and patterns. *Nature* **2006,** *440* (7082), 297-302; (b) Seeman, N. C., Nucleic Acid Junctions and Lattices. *J. Theor. Biol.* **1982,** *99* (2), 237-247; (c) Chen, J. H.; Seeman, N. C., Synthesis from DNA of a molecule with the connectivity of a cube. *Nature* **1991,** *350* (6319), 631-633.

5.   Rowan, S. J.; Cantrill, S. J.; Cousins, G. R. L.; Sanders, J. K. M.; Stoddart, J. F., Dynamic covalent chemistry. *Angew. Chem.-Int. Edit.* **2002,** *41* (6), 898-952.

6.   Boul, P. J.; Reutenauer, P.; Lehn, J. M., Reversible Diels-Alder reactions for the generation of dynamic combinatorial libraries. *Organic Letters* **2005,** *7* (1), 15-18.

7.   Nishiyabu, R.; Kubo, Y.; James, T. D.; Fossey, J. S., Boronic acid building blocks: tools for self assembly. *Chem. Commun.* **2011,** *47* (4), 1124-1150.

8.   Arumugam, S.; Popik, V. V., Light-Induced Hetero-Diels-Alder Cycloaddition: A Facile and Selective Photoclick Reaction. *J. Am. Chem. Soc.* **2011,** *133* (14), 5573-5579.

9.   Koehler, K. C.; Durackova, A.; Kloxin, C. J.; Bowman, C. N., Kinetic and thermodynamic measurements for the facile property prediction of diels–alder-conjugated material behavior. *AIChE Journal* **2012,** *58* (11), 3545-3552.

10.   Zuckermann, R. N.; Kerr, J. M.; Kent, S. B. H.; Moos, W. H., Efficient Method for the Preparation of Peptoids [Oligo(N-substituted glycines)] by Submonomer Solid-Phase Synthesis. *J. Am. Chem. Soc.* **1992,** *114* (26), 10646-10647.

11.   Elduque, X.; Sanchez, A.; Sharma, K.; Pedroso, E.; Grandas, A., Protected Maleimide Building Blocks for the Decoration of Peptides, Peptoids, and Peptide Nucleic Acids. *Bioconjugate Chem.* **2013,** *24* (5), 832-839.

12.   Wei, T.; Jung, J. H.; Scott, T. F., Dynamic Covalent Assembly of Peptoid-Based Ladder Oligomers by Vernier Templating. *J. Am. Chem. Soc.* **2015,** *137* (51), 16196-16202.

13.   (a) Machida, M.; Machida, M. I.; Kanaoka, Y., Fluorescent Thiol Reagents .14. Hydrolysis Of N-Substituted Maleimides - Stability Of Fluorescence Thiol Reagents In Aqueous-Media. *Chem. Pharm. Bull.* **1977,** *25* (10), 2739-2743; (b) Fontaine, S. D.; Reid, R.; Robinson, L.; Ashley, G. W.; Santi, D. V., Long-Term Stabilization of Maleimide-Thiol Conjugates. *Bioconjugate Chem.* **2015,** *26* (1), 145-152.

14.   Gibson, D. G.; Young, L.; Chuang, R. Y.; Venter, J. C.; Hutchison, C. A.; Smith, H. O., Enzymatic assembly of DNA molecules up to several hundred kilobases. *Nat. Methods* **2009,** *6* (5), 343-351.

15.   Kim, S.; Biswas, G.; Park, S.; Kim, A.; Park, H.; Park, E.; Kim, J.; Kwon, Y. U., Unusual truncation of N-acylated peptoids under acidic conditions. *Organic & Biomolecular Chemistry* **2014,** *12* (28), 5222-5226.

16.   Elduque, X.; Pedroso, E.; Grandas, A., Orthogonal Protection of Peptides and Peptoids for Cyclization by the Thiol-Ene Reaction and Conjugation. *J. Org. Chem.* **2014,** *79* (7), 2843-2853.

17.   Wei, T.; Furgal, J. C.; Jung, J. H.; Scott, T. F., Long, self-assembled molecular ladders by cooperative dynamic covalent reactions. *Polym. Chem.* **2017,** *8* (3), 520-527.

18.   (a) Decker, C.; Bianchi, C.; Jonsson, S., Light-induced crosslinking polymerization of a novel N-substituted bis-maleimide monomer. *Polymer* **2004,** *45* (17), 5803-5811; (b) Tarducci, C.; Badyal, J. P. S.; Brewer, S. A.; Willis, C., Diels-Alder chemistry at furan ring functionalized solid surfaces. *Chem. Commun.* **2005,** (3), 406-408.

19.   (a) Adzima, B. J.; Kloxin, C. J.; DeForest, C. A.; Anseth, K. S.; Bowman, C. N., 3D Photofixation Lithography in Diels-Alder Networks. *Macromolecular Rapid Communications*

2012, *33* (24), 2092-2096; (b) Scott, T. F.; Kloxin, C. J.; Draughon, R. B.; Bowman, C. N., Nonclassical dependence of polymerization rate on initiation rate observed in thiol-ene photopolymerizations. *Macromolecules* **2008,** *41* (9), 2987-2989.

Chapter 4 Boronic Acid-bearing Oligomers

4.1 Abstract

In light of the challenges experienced building Diels-Alder molecular ladders, we began to explore a different set of chemistry to direct the assembly of molecular structures. We hypothesized that by utilizing a pH-mediated condensation between a boronic acid and diol that we could more easily characterize the resulting structures using typical mass spectrometry techniques. A necessary pre-requisite to fabricating more complex structures, we needed to synthesize oligomers comprised of the boronic acid and diol functional groups. The diol can readily be incorporated into an oligopeptoid as a protected catechol as will be discussed in subsequent chapters, but the boronic acid-bearing oligomers presented concerning stability challenges. This chapter will discuss how we overcame these obstacles by exploring different methods of incorporating the boronic acid functionality. We looked into different commercial sources of boronic acid monomers that could be directly added the peptoid backbone, and we developed different methods of post-synthetically modifying existing peptoids containing reactive amine groups to ultimately bear the desired boronic acid functional group. Through these different trials, we were able to determine a method for reliably producing stable boronic acid-based oligomers that served as the foundation for future assembly studies.

4.2 Introduction

Dynamic covalent chemistry is a class of reactions where products containing covalent bonds can be reverted back to their initial reactants under a particular set of reaction conditions. Several stimuli, such as temperaure,[1] pH,[2] and photochemical triggers,[3] can be employed to

reversibly affect the equilibrium of a reaction. The reversibility of these reactions open the possibility to incorporate them in self-assembly proeceses where they can undergo the error correction necessary to achive the most thermodynamically stable product.[4] Diols undergo a pH-reversible condensation reaction with boronic acids to form boronate esters.[2] Our goal is to use this esterificaiton reaction to construct molecular structures through directed assembly of oligomeric stuctures. The diol-bearing structures were prepared from a straightforward route; however, the boronic acid-based oligomers required a more focused study as discussed here.

Peptoids, or poly(N-substituted glycine)s, are structurally similar to peptides; however, the side chains are attached to the amide nitrogen instead of the alpha-carbon. Peptoids have a two-step synthetic scheme of acylation with a carbodiimide-activated bromoacetic acid followed by displacement with a primary amine. This synthetic approach is amendable to the facile fabrication of oligomeric strands with predetermined residue sequences as the purification steps, required after the addition of each monomer residue, are performed by simply rinsing the solid support resin.[5] Peptoids can be readily synthesized from any available primary amine leading to large structural diversity making them ideal for exploring boronic acid fabrication.

To the best of our knowledge, there are three examples of boronic acid-bearing peptoids in the literature. The first is an exploration of a library of boronic acid primary amines that were incorporated into peptoids to later undergo Pd-mediated Suzuki cross coupling.[6] This method utilized direct addition into the peptoid-based backbone from novel primary amines. The other two examples use esterification to add conformational constraint to the peptoid backbone through cyclization.[7] These two methods introduce the functionality into backbone through post-synthetic modification. This chapter highlights our attempts of fabricating boronic acid-bearing

peptoids by both directly adding primary amine monomers and modifying strands after synthesis

to illicit the desired functionality needed for further assembly experiments.

4.3 Experimental

4.3.1. General Experimental Procedure

Electrospray ionization mass spectrometry (ESI-MS) mass spectra were collected using

an Agilent Q-TOF 1200 series spectrometer in positive ion mode. Matrix-assisted laser

desorption/ionization time-of-flight (MALDI-TOF) mass spectra were recorded using a Bruker

Autoflex mass spectrometer in reflectron position ion mode using 2-(4-

hydroxyphenylazo)benzoic acid (HABA) as the matrix. The MALDI-TOF samples were

prepared with a 3:1 ratio of matrix (100mM, 200μL acetonitrile) to sample (crude reaction

mixtures). Reverse phase high performance liquid chromatography (RP-HPLC) was performed

using preparative reversed phase Phenomenex Luna C18 (2) columns with a linear gradient of

water and acetonitrile as the eluent at 30°C. The RP-HPLC was equipped with Shimadzu LC-

6AD HPLC pump, Shimadzu FRC 70A fraction collector, and monitored using Shimadzu

Prominence detector at 214nm. Unless otherwise noted, all materials were purchased from

commercial sources and used as received.

4.3.2. Oligomer Synthesis
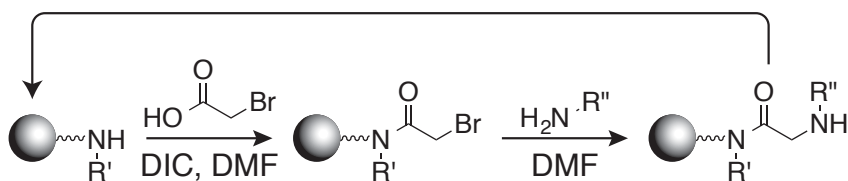
Scheme 4.1. Two-step submonomer synthesis scheme for fabricating peptoids

Peptoids were synthesized using a microwave-assisted Liberty Blue peptide synthesizer (CEM Corporation) using a submonomer protocol (Scheme 4.1).[5] The peptoids were built off of a solid support resin (0.1mmol scale) containing a fluorenylmethyloxycarbonyl (Fmoc)-protected amine that is initially deprotected before synthesis by treatment in 4-methylpiperidine: dimethylformamide (DMF) (20:80, volume ratio). The synthesis then proceeds by a sequential addition reaction whereby the N-terminal amine from the solid support is acetylated with 1 M bromoacetic acid using 1.2 M diisopropylcarbodiimide (DIC) as an activating agent for 5 minutes at 75°C, to afford a terminal bromide which is subsequently displaced *via* nucleophilic substitution with a 0.5 M primary amine bearing the pendant group for 5 minutes at 75°C. The displacement reagents, bromoacetic acid and DIC, were prepared in DMF, and the amines were prepared in *N*-methyl-2-pyrrolidone (NMP). This two-step process of acetylation and displacement is repeated until the desired chain length is achieved. The N-terminal of the complementary oligomers was capped with 1 M acetic anhydride (in DMF) activated with DIC to prevent further chain elongation.

Directly Added Dynamic Covalent Monomers
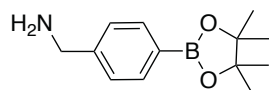
Npbe = 4-aminomethylphenylboronic acid, pinacol ester
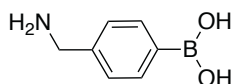
Npba = (4-(aminomethyl)phenyl)boronic acid
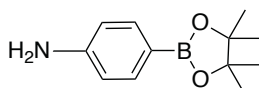
Npbea = 4-aminophenylboronic acid, pinacol ester
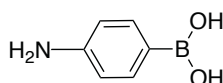
Npbaa = 4-aminophenylboronic acid

Inert Spacer Monomers
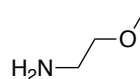
Nme = 2-methoxyethylamine
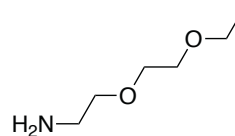
Neee = 2-(2-ethoxyethoxy)ethylamine

Post-synthetic Functionalization Monomers
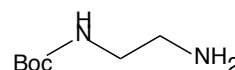
Nbeda = N-boc-ethylenediamine
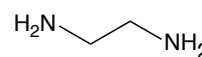
Neda = ethylenediamine

Figure 4.1. Primary amine monomers in both protected and deprotected forms used throughout this chapter split into three categories: directly added dynamic covalent monomers, inert spacer monomers, and post-synthetic functionalization monomers.

There were three different categories of primary amine monomers that were used in throughout this chapter and are shown in Figure 4.1. The first category is the directly added active dynamic covalent boronic acid-bearing amines. In this group, the boronic acid was protected with a pinacol group because the exposed hydroxyl groups could undergo esterification reaction with bromoacetic acid in the presence of DIC resulting in unfavorable side reactions. The two directly added monomers were both commercially available from three sources (Combi-blocks, Frontier Scientific, and Accela ChemBio Inc.). 4-aminomethylphenylboronic acid pinacol ester (Npbe) was initially purchased from Combi-blocks, but it was ultimately replaced owing to inconsistencies between monomer batches. It was first replaced by 4-aminophenylboronic acid pinacol ester (Npbea, Frontier Scientific) to overcome issues with stability, but this monomer's primary amine group was substituted on the phenyl ring made it

challenging to comprehensively add to the peptoid backbone.[8] Ultimately, Npbe was purchased from Accela ChemBio Inc. and used to directly add the boronic acid functionality to the peptoid backbone. The second category of primary amine monomers was inert spacer monomers to help control solubility. Additionally by incorporating the inert spacer amines, the resulting peptoids have six atoms along the backbone between each active dynamic covalent monomer similar to the distance between nucleobases in nucleic acids, a major design inspiration for this project. The first spacer amine used was commercially available 2-methoxyethylamine (Nme). To increase the solubility of the formed hybrids, 2-ethoxyethoxylamine (Neee) was synthesized using methods outlined by Wei et al.[9] The third category of primary amines was the post-synthetic functionalization monomers N-bocethylenediamine (Nbeda), a boc-protected amine group that could be functionalized after the synthesis to incorporate the boronic acid group through different chemistries.

In addition to peptoids, we synthesized peptide-peptoid hybrids using Tentagel (Rapp Polymere) resin with an exposed terminal amine. In contrast to peptoids that must first deprotect the FMOC from the resin, the Tentagel resin's first step is to add an FMOC-protected methionine residue (MET, 0.5 M in DMF) with an equal volume of a coupling cocktail (4g hydroxybenzotriazole (HOBt), 5mL N, N-diisopropylethylamine(DIPEA) final volume of 20mL in DMF). The FMOC is then removed by being treated with 4-methylpiperidine: DMF (20:80, volume ratio) for 5 minutes. The remainder of the synthesis follows the two-step process of acetylation and displacement of general peptoid synthesis.

4.3.3. Removing Protecting Groups

Several different methods were explored for removing the acid-labile pinacol protecting group from the peptoids exposing the boronic acid functionality. The first method was exposure

to an aqueous trifluoroacetic solution (95:5 volume ratio of TFA:water) for 10 minutes with a steady stream of N_2 gas gently mixing the solution in a 25 mL solid-phase peptide synthesis vessel (CG-1866, Chemglass). The second deprotection method involved treating the resin bound peptoid with 10 times excess (in DMF) of phenylboronic acid overnight. This would encourage the pinacol group to leave the peptoid and form an ester with the excess phenylboronic acid in the solution.[10] The next method removed the pinacol using RP-HPLC owing to pinacol's limited on-column stability.[11] The final deprotection method was adapted from a two-step method developed by the Santos group to deprotect alkylpinacolyl boronate esters which involved first undergoing a transesterification reaction with diethanolamine that was followed by hydrolysis.[12] Our method began by treating the pinacol-bearing resin with diethanolamine (1M in ether or DMF) for 40 minutes at room temperature with a N_2 stream gently mixing the solution in a peptide synthesis vessel then hydrolysis with an aqueous cleavage cocktail.

In addition to the pinacol being removed from the boronic acids, the boc-protected (Nbeda) monomer for post-synthetic modification was deprotected to expose an aliphatic amine group (Neda) by exposure to a 95:5 volume ratio of TFA: Water for 10 minutes with a steady stream of N_2 gas gently mixing the solution in a 25 mL solid-phase peptide synthesis vessel.

4.3.4. Peptoid Cleavage

Three different resins were used throughout this study that each had a unique cleavage method. The first was the acid-labile Rink amide 4-methylbenz-hydrylamine (MBHA) resin (ChemPep Inc.). This resin was cleaved by treating the resin with 4 mL of a cleavage mixture containing a 95:5 volume ratio of TFA: Water for 10 minutes with a steady stream of N_2 gas gently mixing the solution in a 25 mL solid-phase peptide synthesis vessel.

The second resin was Fmoc-Photolabile Resin SS (100-200 mesh, 1% DVB, Advanced ChemTech). This resin was cleaved by immersion in 10 mL DMF in a 20 mL glass vial before purging with nitrogen for approximately 30 seconds. The vial was then capped and the suspension gently stirred while under irradiation at ~25 mWcm^{-2} with 405 nm for 1 hour. The cleavage solution was collected by filtering the suspension through a 0.45 mm PTFE syringe filter and the resin was rinsed twice with 1 mL DMF. The filtrate and subsequent washes were combined and evaporated to dryness under vacuum to yield crude peptoids.

The final resin was Tentagel resin for the peptide-peptoid hybrids. The resin was divided into two and placed in 20 mL glass vial. The vials were then treated with an 8 mL total volume of a 2mg/mL Cyanogen Bromide in 50:50 0.25N hydrochloric acid /acetonitrile overnight while being stirred with a magnetic stir bar. The cleavage mixture was then evaporated to dryness under vacuum to yield a mixture of resin and crude peptoids. The solids were then added to a 50:50 acetonitrile: water solution before being filtered with a 0.45 mm PTFE syringe filter.

4.3.5 Peptoid Functionalization
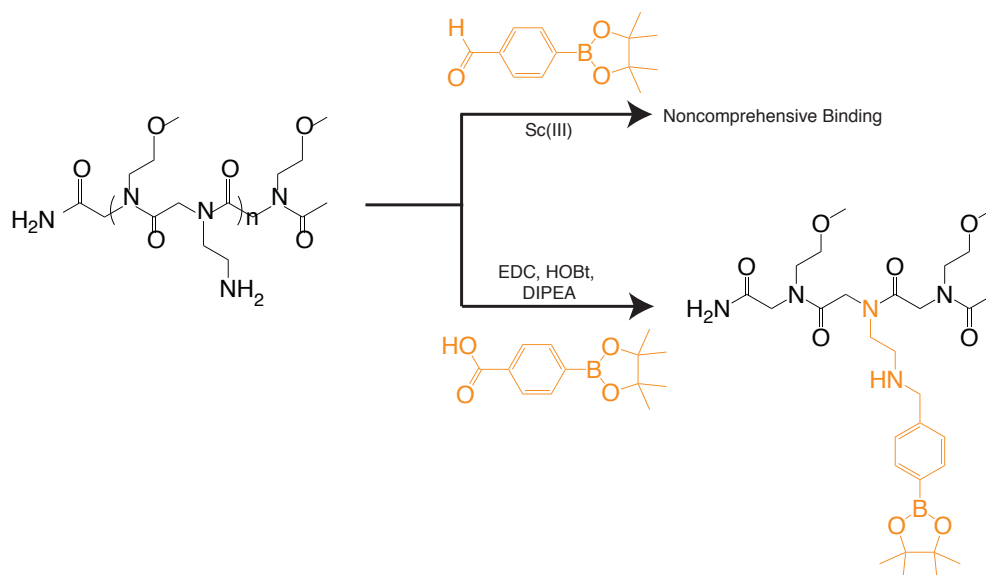
Scheme 4.2. Different pathways for post-synthetic boronic acid functionalization of aliphatic amine peptoids using a dynamic covalent reaction between amine and aldehyde with a scandium (III) catalyst (top) and using an amine and standard peptide coupling reagents (bottom)

Peptoids that were prepared with the Nbeda (aliphatic amine) monomer were treated with different boronic acid-bearing molecules to add functionality to the peptoid strand. They were first cleaved and deprotected to expose the amine group on unbound peptoids before two different approaches were followed to incorporate functionality as shown in Scheme 4.2. The first was to add 10 times excess of 4-formylphenylboronic acid and 0.02 equivalents of a 10mM aqueous solution of scandium (III) triflate with the unbound peptoid overnight in DMF. The second method was to incubate the peptoid with 5 times excess of 1-ethyl-3-(3-dimethylaminopropyl)carbodiimide (EDC), HOBt, DIPEA, and 4-carboxyphenylboronic acid pinacol ester in DMF overnight. These are common coupling conditions used in peptide chemistry. In each case, the solvent was removed with vacuum to yield the functionalized peptoid and excess coupling reagents.
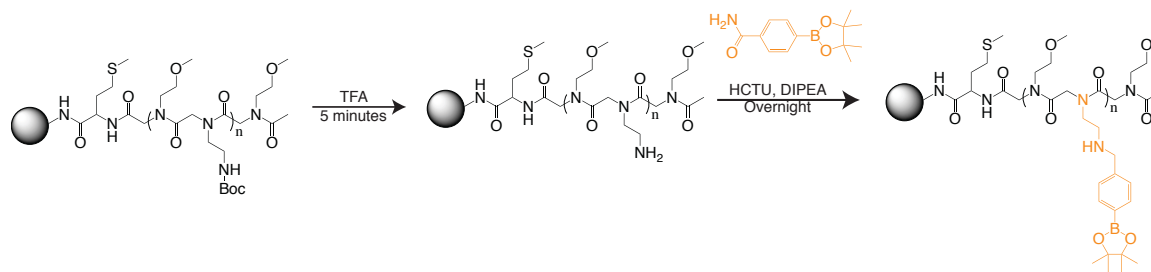
Scheme 4.3. Two-step process used for preparing boronic acid-bearing peptoids. The first step is removal of the boc-protecting group from the aliphatic amine peptoid monomer. The second step is coupling with 4-carboxyphenylboronic acid pinacol ester, HCTU, and DIPEA overnight.

Another approach to adding functionality to the peptoids was to do the post-synthetic functionalization on resin to remove any excess reagents from the peptoids prior to purifications as shown in Scheme 4.3. The on-bead functionalization employed peptide coupling reagents and a boronic acid-bearing carboxylic acid. Moreover, the resin was incubated with 5 fold excess of

2-(6-chloro-1-H-benzotriazole-1-yl)-1,1,3,3-tetramethylaminium hexafluorophosphate (HCTU), DIPEA, and 4-carboxyphenylboronic acid pinacol ester in DMF overnight.

4.3.6. Peptoid Purification and Characterization

The peptoids were purified with an RP-HPLC system equipped with a C-18 column. There was a linear gradient from 10%-acetonitrile-water to 90%-acetonitrile-water over 22 minutes. This chromatographic system is capable of separating tens to hundreds of milligrams of crude peptoid samples based on the hydrophobicity of the components. The elution fractions were collected and combined before lyophilizing to a white powder. The exact mass of the oligomers after purification was verified by using either ESI-MS or MALDI-TOF mass spectrometry.

4.4. Results and Discussion

4.4.1. Directly Added Boronic Acid Monomers

The first attempt at making the boronic acid-based oligomer was to incorporate the commercially available monomer Npbe (4-aminomethylphenylboronic acid pinacol ester) directly into the peptoid backbone. This ultimately proved to be a more challenging task that anticipated, but the different attempts brought to light many characteristics of the boronic acid functional group that were essential to the success of the overarching project. The first goal was to determine harmonious conditions for the peptoid cleavage and deprotection by preparing peptoids using standard peptoid chemistry and testing different methods. The first method was to simultaneously cleave and deprotect the peptoid ((NeeeNpba)₃Neee) by immersion in an aqueous TFA cocktail for 10 minutes. The results are shown in Figure 4.2, and the highlight that the TFA alone was not enough to comprehensively deprotect the peptoid of the pinacol group. There is a

major peak attributed to the correct peptoid, but it is in the presence of many unfavorable byproducts. In addition to peaks attributed to pinacol groups remaining, there was a peptoid truncation product that typically is a result of prolonged exposure to acid.[13] This suggested that lengthening the cleavage time which might result in further removal of pinacol groups would most likely lead to further peptoid degradation. This peptoid, (NeeeNpba)₃Neee, included the synthesized solubility enhancing monomer Neee, but in order to preserve materials the subsequent methods utilized the commercially available monomer Nme.
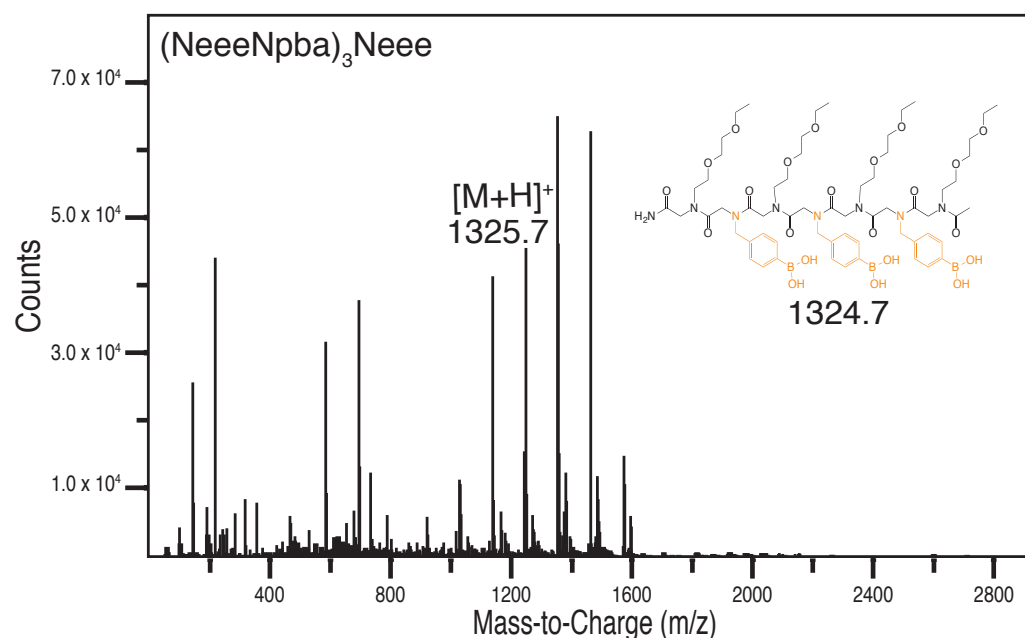
Figure 4.2. ESI-MS spectrum of boronic acid-bearing peptoid prepared by simultaneous deprotection and cleavage in a TFA cocktail. [(NeeeNpba)₃Neee+H]$^+$ = 1325.7 g/mol

The next method began with synthesizing the peptoid on photolabile resin; in contrast to the first method that used acid-labile rink amide resin, in this method the photolabile resin only require light to liberate the peptoids from the solid-support. The peptoid was then incubated with an excess amount of phenyboronic acid to remove to pinacol by a transesterification reaction between the peptoid boronic acid and the free boronic acids in solution. The peptoid was then cleaved from the solid support resin for 1 hour and ESI-MS was performed to confirm the exact

mass of the peptoid (Figure 4.3). These results showed that the correct peptoid was made and deprotected using this method, but the relative yield of this method was low. We anticipate this is a result of a short cleavage time for the photolabile resin compared to other analogous experiments that would cleave the peptoids for greater than 24 hours.[9, 14] This shorter cleavage time was necessary to observe the correct product. As the cleavage time increased, the product would degrade resulting in nonfunctional structures. These results highlighted the sensitivity of the boronic acid-bearing peptoids to UV-light.
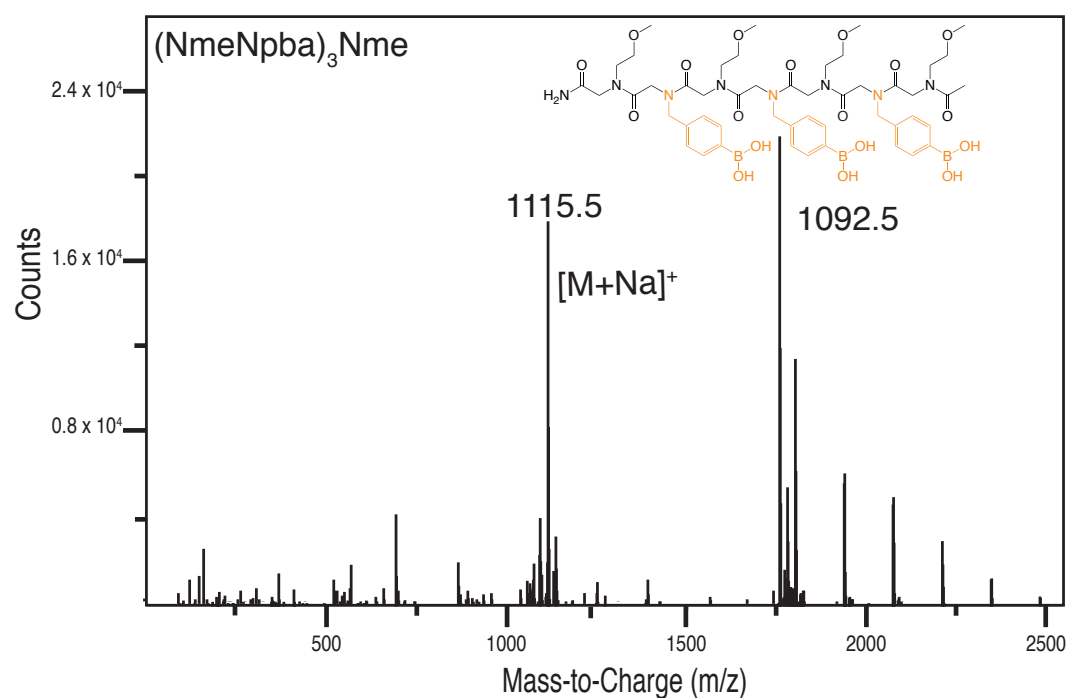
Figure 4.3. ESI-MS mass spectrum of boronic acid-bearing peptoid prepared on photolabile resin and deprotected with excess phenylboronic acid. [(NmeNpba)₃Nme+Na]⁺ = 1115.5 g/mol

The final method utilizing the Npbe monomer involved synthesizing the peptoid on acid–labile resin followed by an on-bead transesterification reaction with diethanolamine,[15] efficiently replacing the pinacol group, followed by hydrolysis and simultaneous cleavage of the peptoid from the solid support with aqueous TFA to afford free peptoids bearing exposed

boronic acid residues. The ESI-MS mass spectrum highlights the comprehensive deprotection of the boronic acid-based peptoid by this method shown in Figure 4.4. This suggested that this method of deprotection and cleavage would be promising in preparing boronic acid-based oligomers.
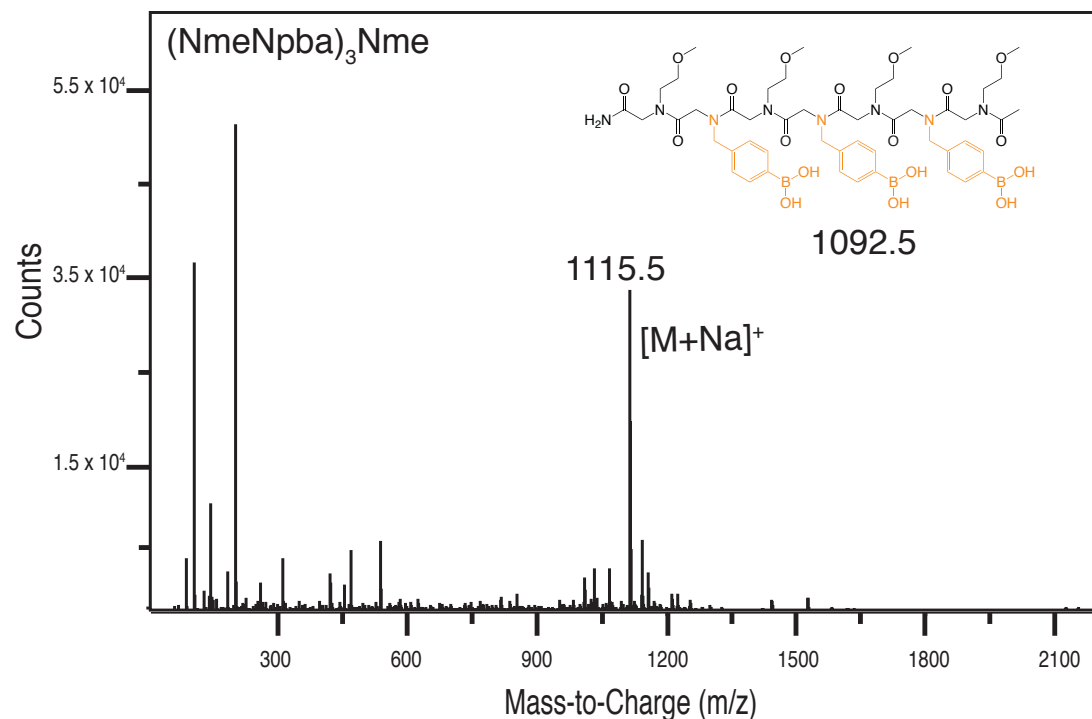
Figure 4.4. ESI-MS mass spectrum of boronic acid-bearing peptoid prepared by first an on-resin transesterification reaction to replace the pinacol and a hydrolysis reaction in aqueous TFA to expose the boronic acid functional groups and cleave the peptoid. [(NmeNpba)₃Nme+Na]$^+$ = 1115.5 g/mol

The boronic acid-based peptoids were purified to remove any unfavorable byproducts or initial reactants utilizing RP-HPLC a standard peptoid purification method. Here we observed an issue with the stability of the boronic acids on the peptoid chains. It appeared that the boronic acid would oxidize to an alcohol regardless of the deprotection method used. Boronic acids are known to readily oxidize under multiple reaction conditions[16]; however, they are primarily shown to oxidize in the presence of peroxides.[17] Figure 4.5a shows an RP-HPLC spectrum where

the major peak is attributed to the oxidized peptoid; this is verified by ESI-MS shown in Figure 4.5b. The peak to the left of the major product in Figure 4.5a corresponds to a peptoid where all but one of the boronic acid groups was oxidized. We were unable to isolate the correct product or determine the exact conditions that led to the instability in our structures. We then began to explore alternative strategies to form these oligomers.
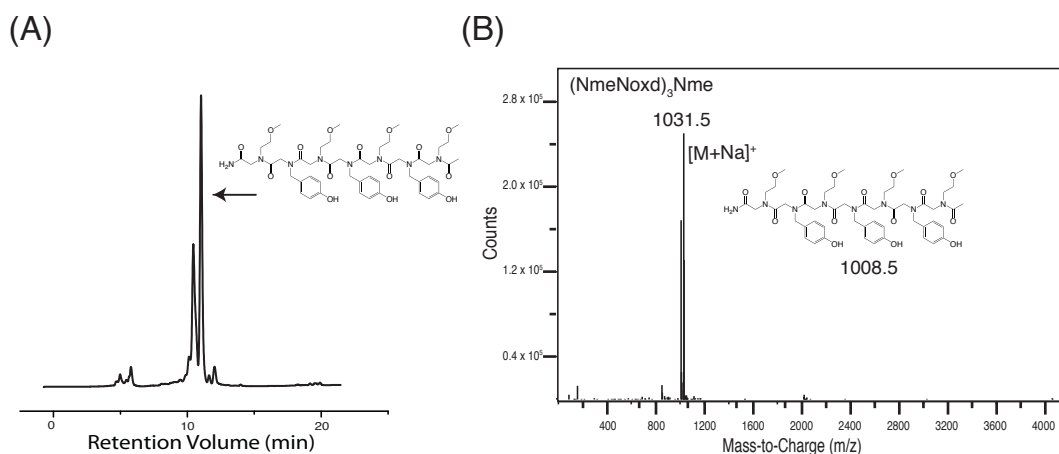
Figure 4.5. Results of RP-HPLC purification of boronic acid-bearing peptoid(a) RP-HPLC spectrum of the crude peptoid mixture and the structure of the corresponding peak(b) ESI-MS spectrum confirming the oxidation of the peptoid [(NmeNoxd)₃Nme+Na]⁺ = 1031.5 g/mol

Owing to the instability of the boronic acids, a new boronic acid-based monomer was used in peptoid synthesis, Npbea (4-aminophenylboronic acid pinacol ester). This is similarly a pinacol-protected boronic acid, but the primary amine is attached directly to the phenyl ring. The peptoid was prepared on acid-labile resin and deprotected using the two-step transesterification and hydrolysis method before being purified using RP-HPLC. One of the major HPLC peaks for this peptoid (Figure 4.6a) was attributed to the anticipated peptoid, confirmed by ESI-MS in Figure 4.6b. The other substantial peaks shown in the RP-HPLC spectrum are attributed to the oxidized and partially oxidized peptoids. While this monomer did not completely eliminate the unfavorable oxidation, it did minimize the oxidation products allowing for the correct peptoid to

be isolated. The peptoid seemed to remain stable after purification suggesting the possibility of the presence of some sort of impurity in the crude reaction mixture leading to the oxidation in RP-HPLC. This monomer was relatively expensive, and it did not completely solve the stability issues, so we continued to explore alternative methods for preparing the oligomers.
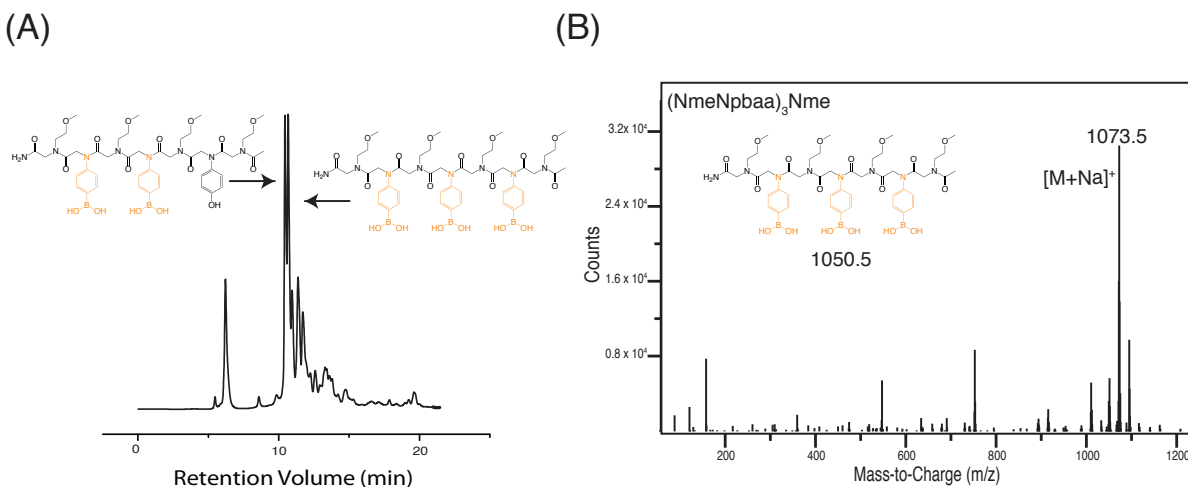
Figure 4.6. Results of RP-HPLC purification of boronic acid-bearing peptoid containing the new Npbea monomers (a) RP-HPLC spectrum of the crude peptoid mixture and the structures of the two largest peaks (b) ESI –MS spectrum confirming the isolation of the correct peptoid [(NmeNpbaa)$_3$Nme+Na]$^+$ = 1073.5 g/mol

4.4.2. Post-synthetic Boronic Acid Functionalization

The stability and expense of both of the directly added methods led us to brainstorm new fabrication strategies. We started by incorporating a reactive aliphatic amine monomer (Neda) in the peptoid backbone that could be reacted with a boronic acid-bearing species to elicit the desired functionality. We first prepared peptoids with Nbeda using the standard two-step submonomer synthesis protocol then simultaneously deprotected the boc group and released the peptoid from the resin beads. Once the peptoids with the exposed aliphatic amine functional group were prepared, we first employed an orthogonal dynamic covalent chemistry where amines and aldehydes are co-reacting to form Schiff base imines. This is an attractive dynamic covalent reactant pair owing to their ability to be incoporated into oligomeric peptoid strands and

106

the imine can be reduced upon condensation to the corresponding secondary amine, halting the reversibility.[18] We reacted the exposed amine groups, Neda, with 4-formylphenylboronic acid and a catalytic amount of scandium (III) triflate. This resulted in incomprehensive addition of the boronic acid groups to multi-substituted amine-bearing peptoids even at large percent excess.
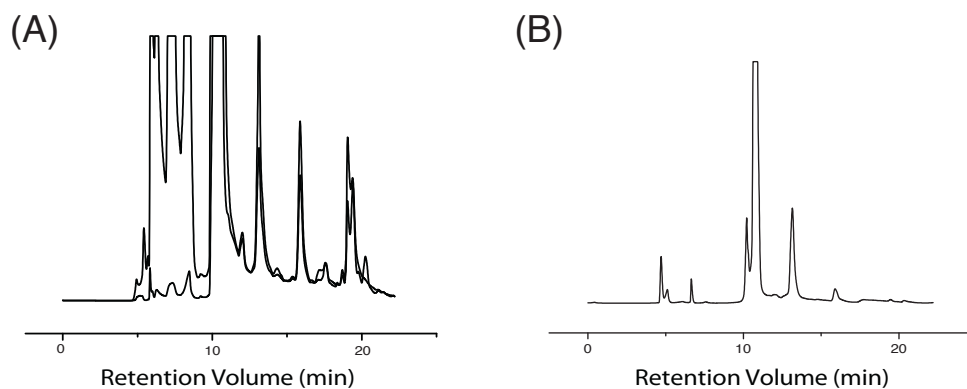
Figure 4.7. RP-HPLC purification of boronic acid-bearing peptoid prepared by post-synthetic functionalization (a) first purification to remove the excess coupling reagents (b) additional purification to isolate the peptoid

We then began to incorporate the boronic acid moiety through peptide chemistry, the coupling of a carboxylic acid to a primary amine to form an amide bond.[19] We explored different combinations of coupling reagents before determining a set with the optimal efficiency. We would allow EDC, HOBt, DIPEA, and 4-carboxyphenylboronic acid pinacol ester to react overnight with the aliphatic amine-bearing peptoids to affix the boronic acid functional groups with a protecting pinacol group. We used a 5 times excess of the coupling reagents in this reaction which then needed to be removed as well as any unreacted peptoid. First the solvent was removed under vacuum and the mixture was dissolved in a 50:50 mixture of acetonitrile and water before filtering off any insoluble particles. The mixture was then purified through RP-HPLC, which simultaneously deprotected the pinacol group from the boronic acid. The first RP-HPLC run was a rather messy spectra of many peaks as shown in Figure 4.6a, but a second pass

through the column (Figure 4.6b) would ultimately result in a relatively pure peptoid as confirmed through ESI-MS in Figure 4.7. The mass spectrum confirmed that the desired peptoid was indeed fabricated through the two-step process of synthesizing an aliphatic amine peptoid and then coupling a boronic acid functional group to the backbone through peptide chemistry. While the purification was challenging, it was not impossible, and we were able to purify the desired structure. We took extra care to store the peptoids under inert conditions and had no substantial issues with stability utilizing this approach, but the multiple purifications had a negative effect on yields making the process rather labor intensive to get substantial product.
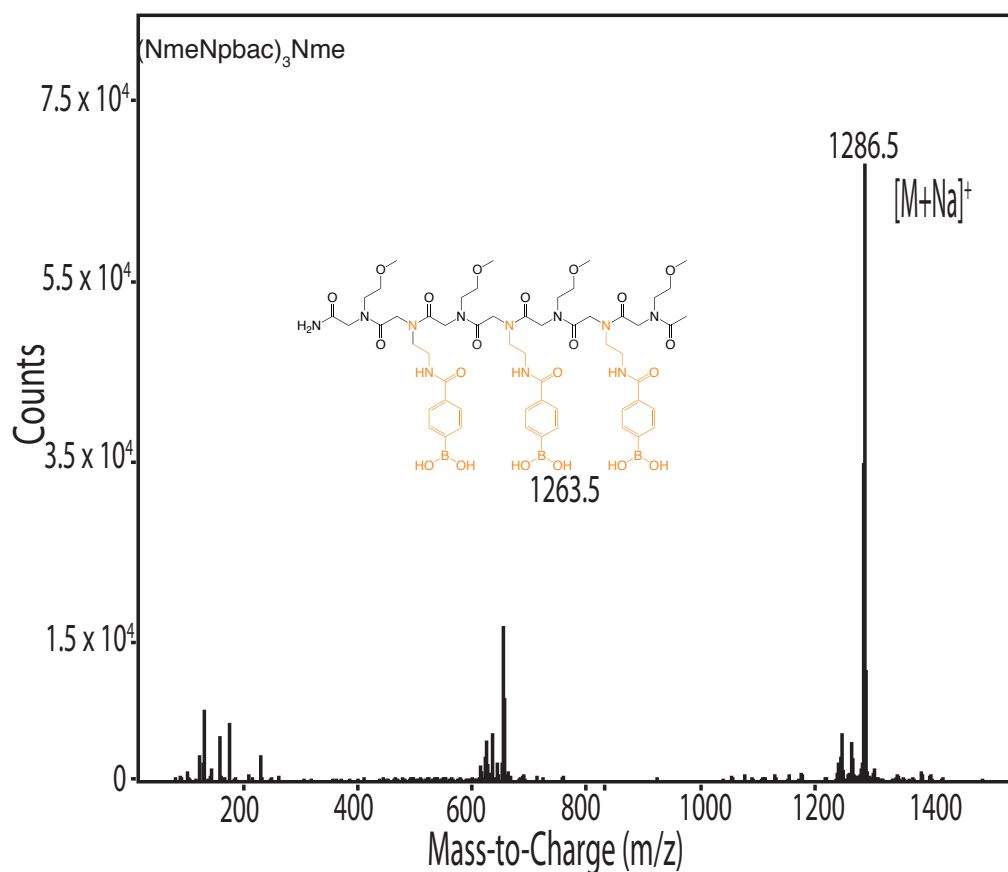
Figure 4.8. ESI-MS spectrum of boronic acid-bearing peptoid prepared by post-synthetic functionalization of an aliphatic amine peptoid with a boronic acid group. [(NmeNpbac)$_3$Nme+Na]$^+$ = 1286.5 g/mol

4.4.3. Coupling on Resin

In addition to complex purification, the solution-based functionalization was challenging to adapt for different peptoid sequences for example, longer oligomers with more boronic acid groups. We then looked into the possibility of coupling on bead to allow for the resin to be washed removing any excess coupling reagent prior to cleavage. We were not able to use acid-labile resin because it was necessary to remove the similarly acid-labile boc-protecting group on the amine monomer before coupling. We had considered utilizing a photolabile strategy, but as previous described the photocleavage time had to be significantly reduced impacting the yield of the structure to maintain boronic acid stability.
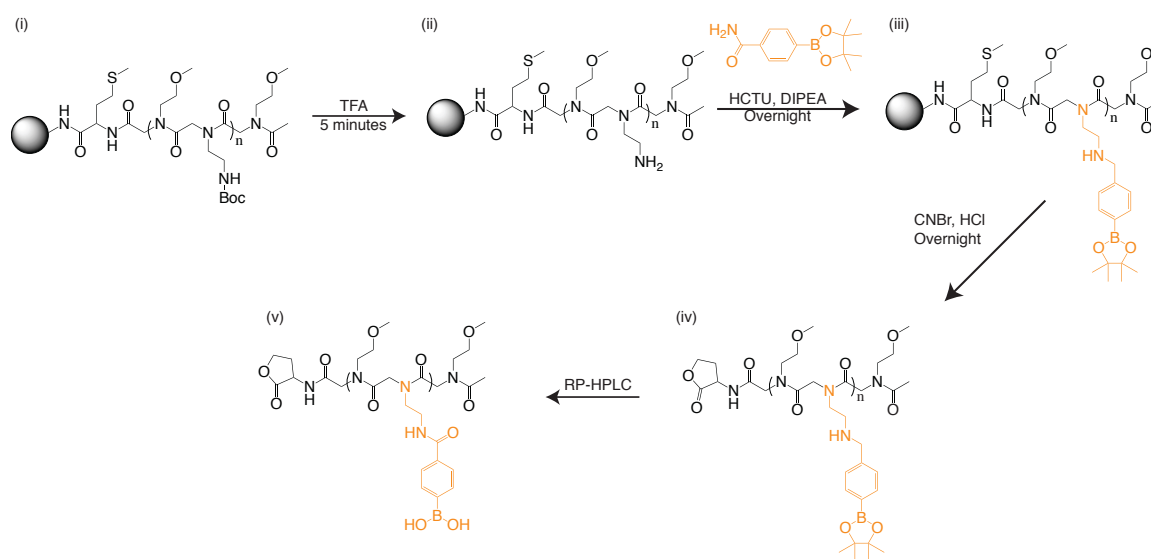
Scheme 4.4. Coupling of the boronic acid functionality to an aliphatic amine group on-bead (i) synthesis of amine peptoid with Nbeda monomer (ii) removal of the boc-protecting group to give Neda monomer (iii) coupling to incorporate boronic acid functionality (iv) cleavage with CNBr to release the peptoid from the resin (v) deprotection and final purification with RP-HPLC

We were ultimately introduced to the method of synthesizing peptide-peptoid hybrids with a methionine residue that cleaves under exposure to cyanogen bromide.[20] This method outlined in scheme 4.4 begins by synthesizing an oligomer that first incorporates an fmoc-protected methionine residue using standard peptide chemistry then builds the rest of the

oligomer using the two-step submonomer method for synthesizing peptoids. We then remove the boc protecting group from the Nbeda monomers by immersion of the resin in a TFA solution. We then evaluated a library of coupling conditions before selecting HCTU and DIPEA to be used to couple 4-carboxyphenylboronic acid pinacol ester to the peptoid. The resin was then washed to remove any additional coupling reagents before cleavage with a CNBr containing solution. The final step was to use RP-HPLC to deprotect the pinacol group from the boronic acid ultimately yielding a peptoid with the desired functionaility. Figure 4.8 shows the MALDI-TOF spectrum of the peptoid after purification confirming the successful synthesis of the peptoid ((NmeNpba)$_3$Nme-MET). This method increased the efficiency of making the boronic acid-bearing peptoid when compared to coupling in solution while maintaining stability.
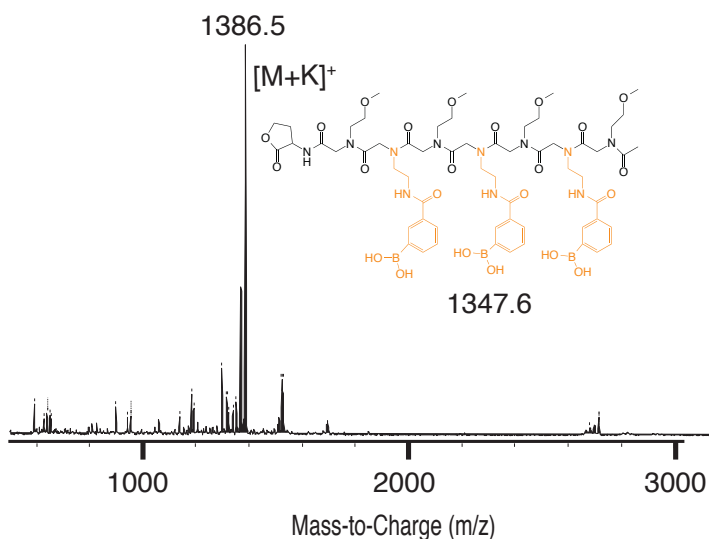
Figure 4.8. Boronic acid-bearing peptoid prepared by post-synthetic functionalization of an aliphatic amine peptoid with a boronic acid group on-bead. [(NmeNpba)$_3$Nme-MET+K]$^+$ = 1347.6 g/mol

4.4.4. Revisiting Monomer Sources
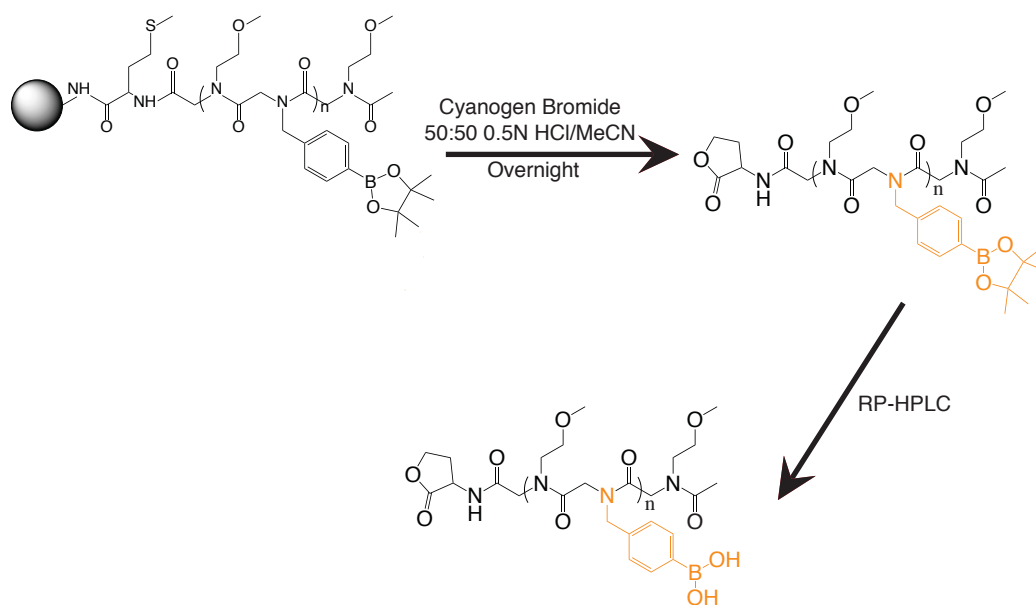
Scheme 4.5. Method for utilizing peptide-peptoid hybrids and commercially available Npbe monomer to directly synthesize boronic acid-bearing amines

With the success of the on-bead coupling we began to ask the question: could the cleavage conditions have been the source of the initial stability issues with the directly added monomer? We then circled back to our initial strategies of directly adding the boronic acid monomer (Npbe) to the peptoid backbone but utilizing the peptide-peptoid strategy of incorporating a CNBr cleavable methionine residue at the N-terminus as shown in Scheme 4.5. We first purchased the monomer from Combi Blocks Inc. and noticed that the boronic acid would not be oxidized during the purification, but it did not comprehensively add to the peptoid backbone resulting in deletion sequences with less than intended number of boronic acid groups as shown in Figure 4.9. This ESI-MS mass spectrum was taken after RP-HPLC highlighting how challenging these two sequences were to separate from one another.

111
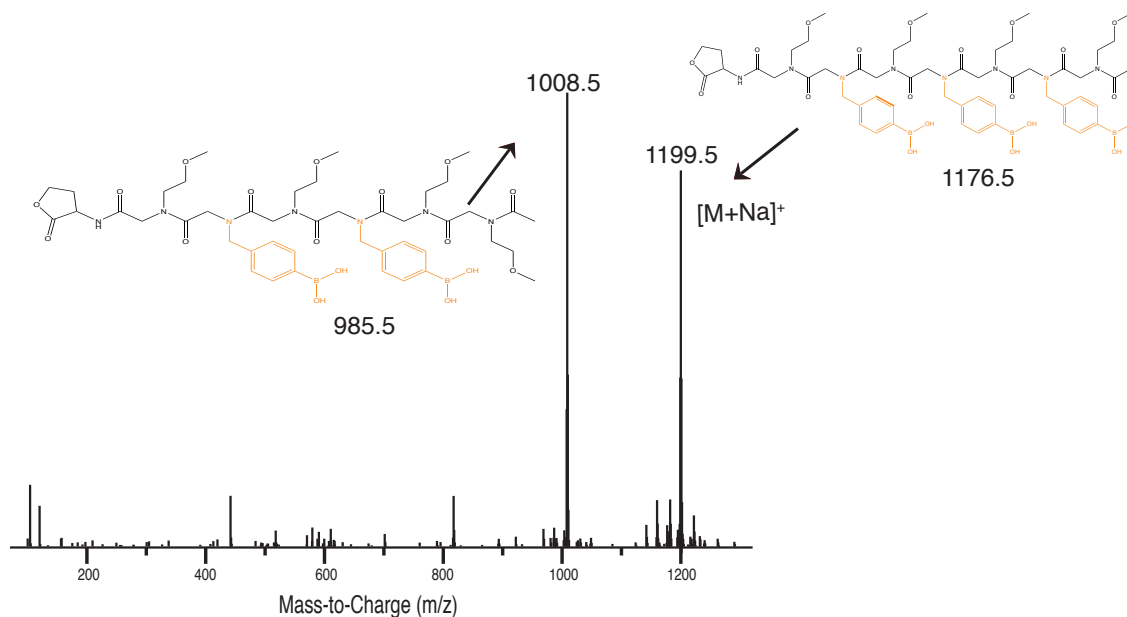
Figure 4.9. Boronic acid-bearing peptoid prepared by direct addition Npbe purchased from CombiBlocks, Inc with products corresponding to the correct peptoid and a peptoid with only 2 Npba groups affixed to the peptoid backbone characterized by MALDI-TOF. [(NmeNpba)₃Nme+Na]⁺ = 1199.5 g/mol

We then were able to find a new commercial source for the Npbe monomer (Accela ChemBio Inc.). This monomer was efficiently and comprehensively added to the peptoid backbone while maintaining stability of the boronic acid functional group. While the ^{1}H-NMR of both of the commercially available monomers appeared to contain the intended monomer, the new source seemed to be stable and more soluble in peptoid synthesis reagents. The ease of incorporating the new monomer suggested that our initial issues could have been a result of an impurity in the initial monomer sources. We then began to synthesize the peptoid on the acid-labile Rink amide resin. Fortunately, this method was successful with the new monomer allowing for us to synthesize and purify the peptoid without any stability issues. This eliminated the need for multiple steps in the fabrication and limited our exposure to the dangerous cleavage conditions of the peptide-peptoid structures.

(A)

(B)
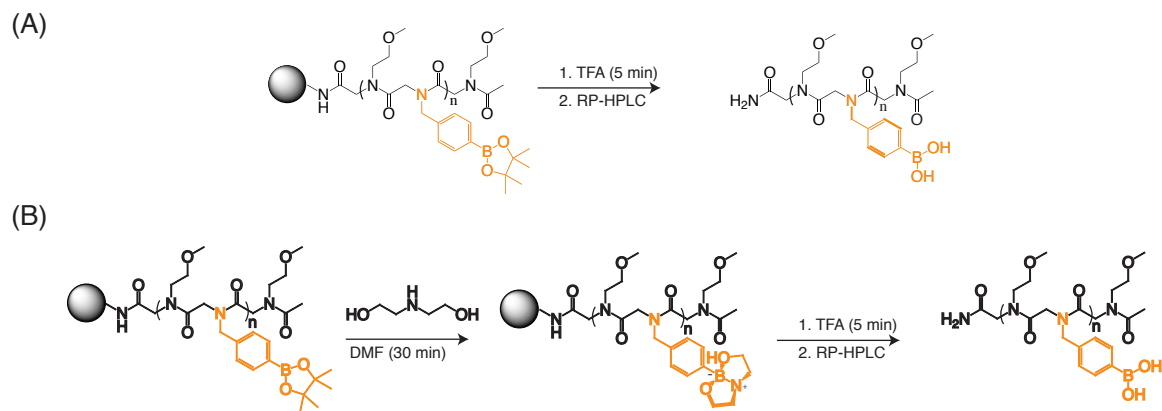
Scheme 4.6. Deprotection strategies of the boronic acid-bearing peptoids (a) Simultaneous cleavage and partial deprotection with TFA followed by deprotection with RP-HPLC (b) Esterification reaction with diethanolamine to remove the pinacol followed by hydrolysis and cleavage with aqueous TFA

From this point we circle back to the initial challenge of determining a harmonious method of incorporating a monomer that is stable for synthesis, deprotection, and purification. We explored two different deprotection methods as shown in Scheme 4.6. The first method relied on a combination of partial deprotection with TFA and partial deprotection by RP-HPLC to ultimately produce the desired peptoid as shown in Figure 10a. The major peak in the RP-HPLC corresponds to the ESI-MS spectrum confirming the peptoid was correctly made. The other substantial peaks in the RP-HPLC correspond to the partially protected oligomer. The second method followed the method developed by the Santos group[15] that first uses a transesterfication reaction to remove the pinacol group on resin with diethanolamine before hydrolysis during cleavage to yield the peptoid with the exposed boronic acid functionality as shown in Figure 10b. Likewise, the major peak corresponds to the fully deprotected peptoid as confirmed by the adjoining ESI-MS spectrum. There are no major peaks corresponding to partially protected peptoids using this method suggesting that this is a more efficient method of fabricating the desired product.
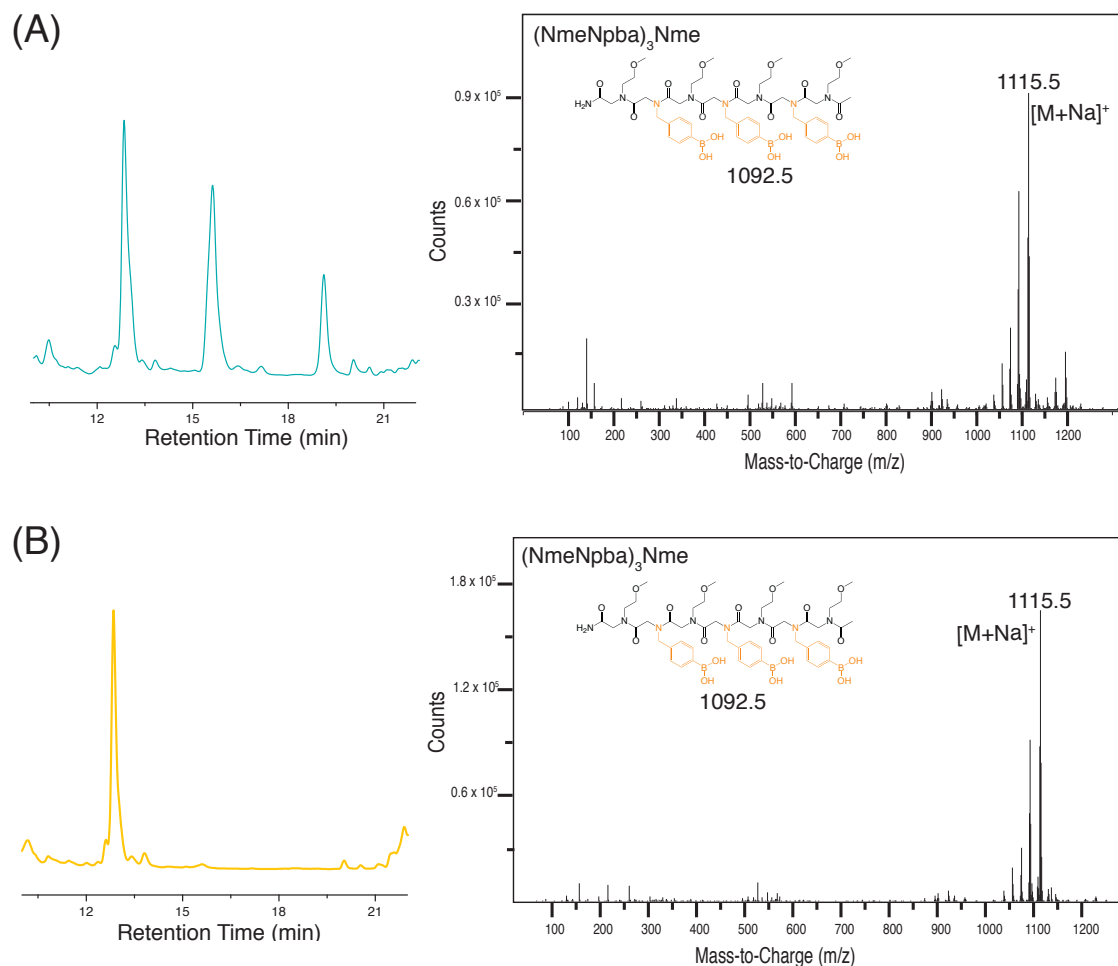
Figure 4.10. Boronic acid-bearing peptoid deprotected using two methods and the corresponding ESI-MS of major peak. (a) Utilizing RP-HPLC to deprotect the pinacol group and ESI of the major product [(NmeNpba)₃Nme+Na]⁺ = 1115.5 g/mol (b) Deprotection by transesterfication and hydrolysis and ESI-MS of the major product [(NmeNpba)₃Nme+Na]⁺ = 1115.5 g/mol

4.5 Conclusions

We looked at different methods of preparing boronic acid-bearing oligomers by both directly adding them to the peptoid backbone and incorporating the functionality through post-synthetic modification of an aliphatic amine peptoid. This process was plagued with stability issues leading to boronic acid oxidation to the hydroxyl group in a variety of reaction conditions. We were able to overcome these issues and develop different methods for reliably synthesizing these oligomers. Ultimately, this process led to a synthetic strategy for synthesizing and

114

deprotecting oligopeptoids-bearing the desired boronic acid functional group. There was admittedly a circle of strategies explored here, but they each provided invaluable observations about the boronic acid functional group that helped to afford the reaction conditions necessary for future experiments. This is an essential foundational step in overall goal of building complex molecular structures direct by a boronate ester forming reaction between a diol and a boronic acid.

4.6. References

1.	Koehler, K. C.; Durackova, A.; Kloxin, C. J.; Bowman, C. N., Kinetic and thermodynamic measurements for the facile property prediction of diels–alder-conjugated material behavior. *AIChE Journal* **2012,** *58* (11), 3545-3552.

2.	Nishiyabu, R.; Kubo, Y.; James, T. D.; Fossey, J. S., Boronic acid building blocks: tools for self assembly. *Chem. Commun.* **2011,** *47* (4), 1124-1150.

3.	Arumugam, S.; Popik, V. V., Light-Induced Hetero-Diels-Alder Cycloaddition: A Facile and Selective Photoclick Reaction. *J. Am. Chem. Soc.* **2011,** *133* (14), 5573-5579.

4.	Whitesides, G. M.; Mathias, J. P.; Seto, C. T., Molecular Self-Assembly and Nanochemistry: A Chemical Strategy for the Synthesis of Nanostructures. *Science* **1991,** *254* (5036), 1312-1319.

5.	Zuckermann, R. N.; Kerr, J. M.; Kent, S. B. H.; Moos, W. H., Efficient Method for the Preparation of Peptoids [Oligo(N-substituted glycines)] by Submonomer Solid-Phase Synthesis. *J. Am. Chem. Soc.* **1992,** *114* (26), 10646-10647.

6.	Chung, S. H.; Lin, T. J.; Hu, Q. Y.; Tsai, C. H.; Pan, P. S., Synthesis of Boron-Containing Primary Amines. *Molecules* **2013,** *18* (10), 12346-12367.

7.	(a) Chirayil, S.; Luebke, K. J., Cyclization of peptoids by formation of boronate esters. *Tetrahedron Lett.* **2012,** *53* (7), 726-729; (b) Webster, A. M.; Cobb, S. L., Synthesis of biaryl-linked cyclic peptoids. *Tetrahedron Lett.* **2017,** *58* (10), 1010-1014.

8.	Culf, A. S.; Ouellette, R. J., Solid-Phase Synthesis of N-Substituted Glycine Oligomers (alpha-Peptoids) and Derivatives. *Molecules* **2010,** *15* (8), 5282-5335.

9.	Wei, T.; Jung, J. H.; Scott, T. F., Dynamic Covalent Assembly of Peptoid-Based Ladder Oligomers by Vernier Templating. *J. Am. Chem. Soc.* **2015,** *137* (51), 16196-16202.

10.   B. Crumpton, J.; Zhang, W.; L. Santos, W., Facile Analysis and Sequencing of Linear and Branched Peptide Boronic Acids by MALDI Mass Spectrometry. *Analytical Chemistry* **2011,** *83* (9), 3548-3554.

11.   Xu, J.; Duran, D.; Mao, B., On-Column Hydrolysis Kinetics Determination of Boronic Pinacol Ester Intermediates for Use in Optimization of Fast HPLC Methods. *Journal of Liquid Chromatography & Related Technologies* **2006,** *29* (19), 2795-2806.

12.   Sun, J.; Perfetti, M. T.; Santos, W. L., A Method for the Deprotection of Alkylpinacolyl Boronate Esters. *The Journal of Organic Chemistry* **2011,** *76* (9), 3571-3575.

13.   Kim, S.; Biswas, G.; Park, S.; Kim, A.; Park, H.; Park, E.; Kim, J.; Kwon, Y. U., Unusual truncation of N-acylated peptoids under acidic conditions. *Organic & Biomolecular Chemistry* **2014,** *12* (28), 5222-5226.

14.   Wei, T.; Furgal, J. C.; Jung, J. H.; Scott, T. F., Long, self-assembled molecular ladders by cooperative dynamic covalent reactions. *Polym. Chem.* **2017,** *8* (3), 520-527.

15.   Sun, J.; Perfetti, M. T.; Santos, W. L., A Method for the Deprotection of Alkylpinacolyl Boronate Esters. *J. Org. Chem.* **2011,** *76* (9), 3571-3575.

16.   (a) Wu, S.; Waugh, W.; Stella, V. J., Degradation pathways of a peptide boronic acid derivative, 2-Pyz-(CO)-Phe-Leu-B(OH)2. *Journal of Pharmaceutical Sciences* **2000,** *89* (6), 758-765; (b) Webb, K. S.; Levy, D., A facile oxidation of boronic acids and boronic esters. *Tetrahedron Lett.* **1995,** *36* (29), 5117-5118; (c) Iwasawa, N.; Takahagi, H., Boronic Esters as a System for Crystallization-Induced Dynamic Self-Assembly Equipped with an "On−Off" Switch for Equilibration. *J. Am. Chem. Soc.* **2007,** *129* (25), 7754-7755.

17.   Ainley, A. D.; Challenger, F., CCLXXX.-Studies of the boron-carbon linkage. Part I. The oxidation and nitration of phenylboric acid. *Journal of the Chemical Society (Resumed)* **1930,** (0), 2171-2180.

18.   AbdelMagid, A. F.; Carson, K. G.; Harris, B. D.; Maryanoff, C. A.; Shah, R. D., Reductive amination of aldehydes and ketones with sodium triacetoxyborohydride. Studies on direct and indirect reductive amination procedures. *J. Org. Chem.* **1996,** *61* (11), 3849-3862.

19.   Merrifield, R. B., Solid Phase Peptide Synthesis .1. Synthesis Of A Tetrapeptide. *J. Am. Chem. Soc.* **1963,** *85* (14), 2149-&.

20.   Thakkar, A.; Cohen, A. S.; Connolly, M. D.; Zuckermann, R. N.; Pei, D., High-Throughput Sequencing of Peptoids and Peptide-Peptoid Hybrids by Partial Edman Degradation and Mass Spectrometry. *Journal of Combinatorial Chemistry* **2009,** *11* (2), 294-302.

Chapter 5 Aqueous Self-Assembly Of Molecular Ladders Bearing Boronate Ester Rungs

5.1 Original Publication Information

The content of this chapter is submitted for publication in the following paper with modifications to adapt to the proper format.

5.2 Abstract

Mimicking the self-assembly of nucleic acid sequences into double-stranded molecular ladders that incorporate hydrogen bond-based rungs, dynamic covalent chemistry enables the fabrication of molecular ladder and grid structures with covalent bond-based rungs. Here, we describe the synthesis of boronic acid- and catechol-bearing peptoid oligomers and utilize the dynamic, reversible condensation reaction between these reactive pendant groups to mediate the dynamic covalent assembly in aqueous solution of complementary oligomers, affording both molecular ladders and grids linked by covalent, boronate ester-based rungs. The generation of in-registry molecular ladders with up to six rungs and triplex molecular grids was confirmed by matrix-assisted laser desorption/ionization time-of-flight (MALDI-TOF) mass spectrometry, and the dynamic nature of the condensation reaction was demonstrated by strand displacement with pre-assembled molecular ladders. Additionally, through the use of a competitive binding assay with alizarin red S (ARS), the boronic acid/catechol binding constant for the formation of molecular ladders was determined.

5.3 Introduction

Important examples of self-assembly, such as the formation of lipid bilayers,[1] polypeptide folding,[2] and nucleic acid hybridization,[3] can be found ubiquitously in biological systems. These molecular self-assembly processes often rely upon weak, kinetically-labile intermolecular interactions, such as hydrogen bonding, π stacking, or van der Waals interactions,[4] to afford a mechanism for rearrangement and error correction. Consequently, the assembled structures can be fragile and susceptible to thermal and mechanical degradation. Several synthetic approaches have been employed to stabilize self-assembled structures *via* post-assembly covalent cross-linking.[5] Alternatively, the assembly process itself can be mediated by dynamic covalent bond-forming reactions, where the covalent bond connectivity can be reversed or rearranged under specific reaction conditions to effect a mechanism for error correction, thereby directly affording covalently cross-linked assemblies.[6]

A dynamic covalent interaction of particular interest is the reversible, pH-sensitive condensation reaction between boronic acids and diols to yield boronate esters (see Scheme 5.1). This reaction has been employed extensively in applications ranging from the assembly of macrocycles,[7] cages,[8] and covalent organic frameworks[9] to pH-dependent healable gels[10] and targeted drug delivery vehicles.[11] Moreover, there has been considerable work into the use of boronic acids for saccharides detection.[12] Wang et al. have investigated the binding between aryl boronic acids and a library of different diols including many common sugars.[13] They were able to develop a method using alizarin red S (ARS), a fluorescent diol, to calculate boronic acid/diol binding constants and examine the influence of pH on conjugation. This method has been adapted to demonstrate oligomer cyclization[14] and determine the binding affinity of functionalized polymers strands for a library of diols.[15]

The use of asymmetric dynamic covalent reactions for paired interactions between complementary oligomeric strands to form molecular ladder structures was first described by the Moore group, who employed Sc(III)-catalyzed imine rearrangement for to mediate the self-assembly of complementary *m*-phenylene ethynylene oligomers into *n*-rung molecular ladders, where $n \leq 5$.[16] We recently described the self-assembly of molecular ladders with up to 16 imine-based rungs in organic solvents *via* Sc(III)-catalyzed imine rearrangement;[17] nevertheless, the reversible boronic acid/catechol condensation as a dynamic reaction pair to mediate molecular ladder fabrication may lend itself as an orthogonal dynamic covalent interaction[18] for oligomer hybridization and enable the assembly itself to proceed in aqueous conditions.[19]

Here, we employ the dynamic covalent boronic acid/diol interaction to mediate the self-assembly of boronic acid- and catechol-bearing oligomers into molecular ladders incorporating covalent boronate ester rungs. Additionally, we describe the fabrication of triplex, 'grid' structures from the co-assembly of three peptoid oligomers, where two strands flank a central core. We also demonstrate the dynamic nature of the system by characterizing the strand rearrangement that proceeds upon addition of a mass-labeled, catechol-bearing peptoid to an already formed molecular ladder. Finally, we examine the binding affinity of the system through competitive binding with alizarin red S (ARS) as a fluorescent diol both quantitatively with peptoid strands that each have one dynamic covalent functional group, and qualitatively for a longer hybridized structure bearing four reactive pendant groups.
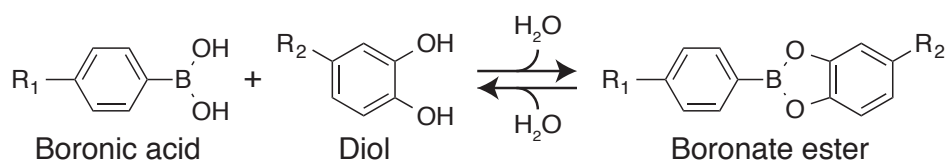
Scheme 5.1. Reversible condensation reaction between a boronic acid and a diol to afford a boronate ester.

119

5.4 Experimental

5.4.1. General Experimental Procedures

^{1}H NMR spectra of the acetonide-protected dopamine were collected using a Varian VNMRS 500 spectrometer. Electrospray ionization mass spectrometry (ESI-MS) mass spectra were recorded using an Agilent Q-TOF 1200 series spectrometer in positive ion mode. Matrix-assisted laser desorption/ionization (MALDI-TOF) time-of-flight mass spectra were collected by utilizing a Bruker Autoflex mass spectrometer used in reflectron mode with both positive and negative ionizations as indicated. Reverse phase high performance liquid chromatography (RP-HPLC) was performed using both a preparative reversed phase Phenomenex Luna C18(2) columns with a linear gradient of water and acetonitrile as the eluent at 30°C as well as an analytical scale column. The RP-HPLC system was equipped with dual Shimadzu LC-6AD HPLC pump, Shimadzu FRC 70A fraction collector, and monitored using Shimadzu Prominence detector at 214nm. Fluorescent and ultraviolet-visible (UV-vis) spectroscopy readings were collected on a BioTek Synergy H1 multi-mode microplate reader. Unless otherwise noted all reagents and materials were purchased from commercial sources including Sigma Aldrich, AK Scientific, Oakwood Chemical, and TCI Chemical.

5.4.2. Monommer Preparation
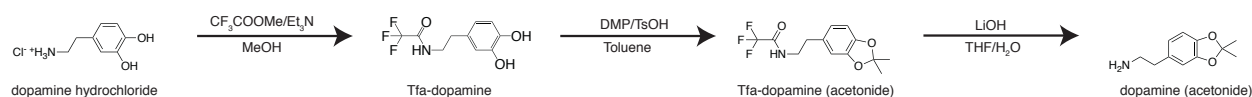
Scheme 5.2. Synthetic scheme for preparation of acetonide-protected dopamine

The acetonide-protected dopamine monomer for peptoid synthesis was synthesized *via* a three-step process (Scheme 5.2) adapted from a published protocol from Messersmith et al.[20] The synthesis of the Tfa-dopamine proceeded by treatment of dopamine hydrochloride (21.3 g) with methyl trifluoroacetate (23 mL) in 250 mL of methanol in the presence of triethylamine (64 mL) overnight at room temperature. The solvent was removed by rotary evaporation, and the pH of the resulting solid was adjusted to ~1 with 1 N HCl solution. A liquid extraction was then performed with ethyl acetate followed by water washes. The product was dried with sodium sulfate and rotary evaporation was used to remove the solvent. ^{1}H-NMR of the Tfa-dopamine measured in δ (ppm) relative to residual solvent (C_2D_6OS = 2.50) is shown in Figure 5.1. Subsequently, Tfa-dopamine (5 g) was refluxed with 2,2-dimethoxypropane (10 mL) and a catalytic amount of *p*-toluenesulfonic acid (172 mg) in toluene. The reaction was outfitted with a Soxhlet extractor filled with granular anhydrous $CaCl_2$. The reaction was refluxed for 2 hours and then allowed to cool to room temperature before being filtered with a short silica gel column washed with dichloromethane (DCM). The solvent was then removed from the product by rotary evaporation before recrystallization in hexanes to afford Tfa-dopamine (acetonide) as confirmed by ^{1}H-NMR in δ (ppm) relative to residual solvent ($CDCl_3$ = 7.24), shown in Figure 5.2. The acetonide-protected dopamine was obtained by hydrolysis of Tfa-dopamine (acetonide) in THF and an aqueous lithium hydroxide solution (2 equivalents), followed by a liquid-liquid extraction with ethyl acetate. The ethyl acetate was removed by rotary evaporation before the monomer was dried under high vacuum. The ^{1}H-NMR of dopamine(acetonide) in δ (ppm) relative to residual solvent ($CDCl_3$ = 7.24) is shown in Figure 5.3.
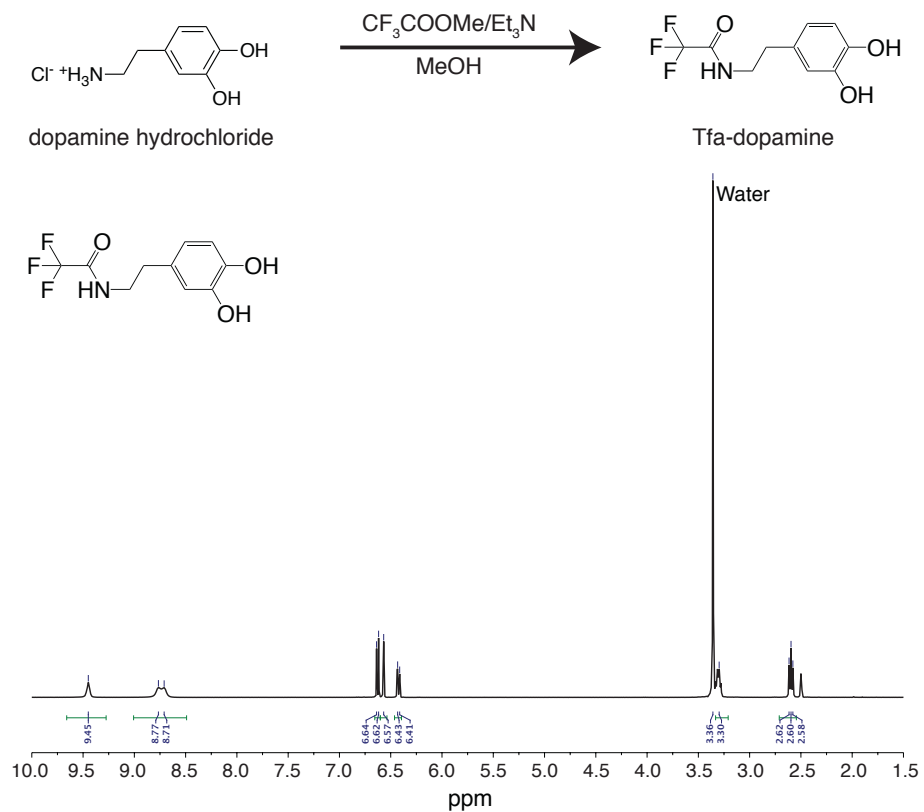
Figure 5.1. ^{1}H-NMR confirming the synthesis of Tfa-dopamine
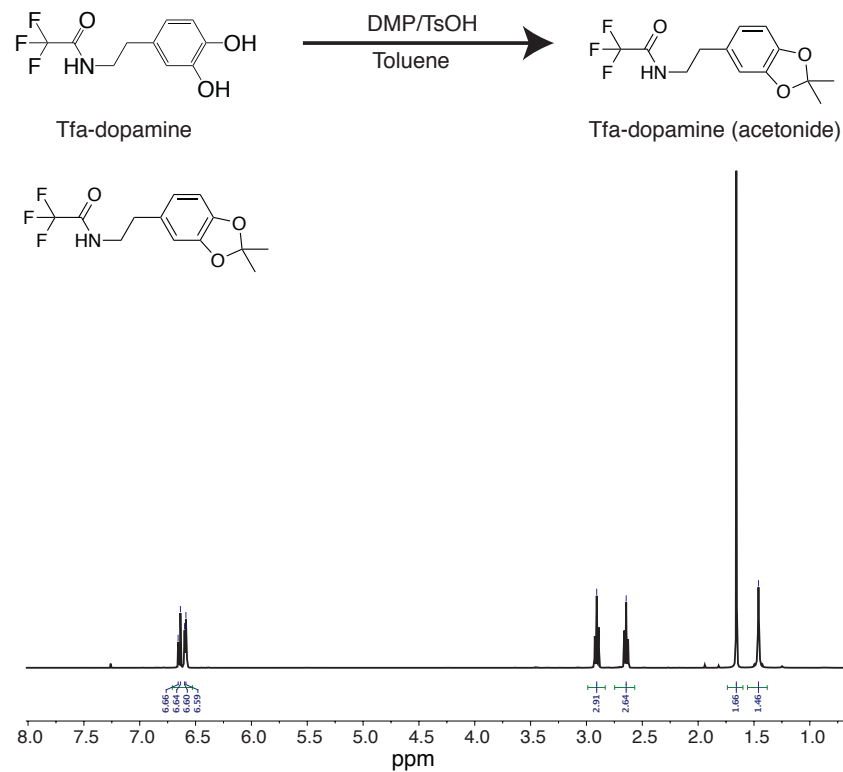
Figure 5.2. ¹H NMR confirming the synthesis of Tfa-dopamine(acetonide)

Tfa-dopamine (acetonide)   dopamine (acetonide)
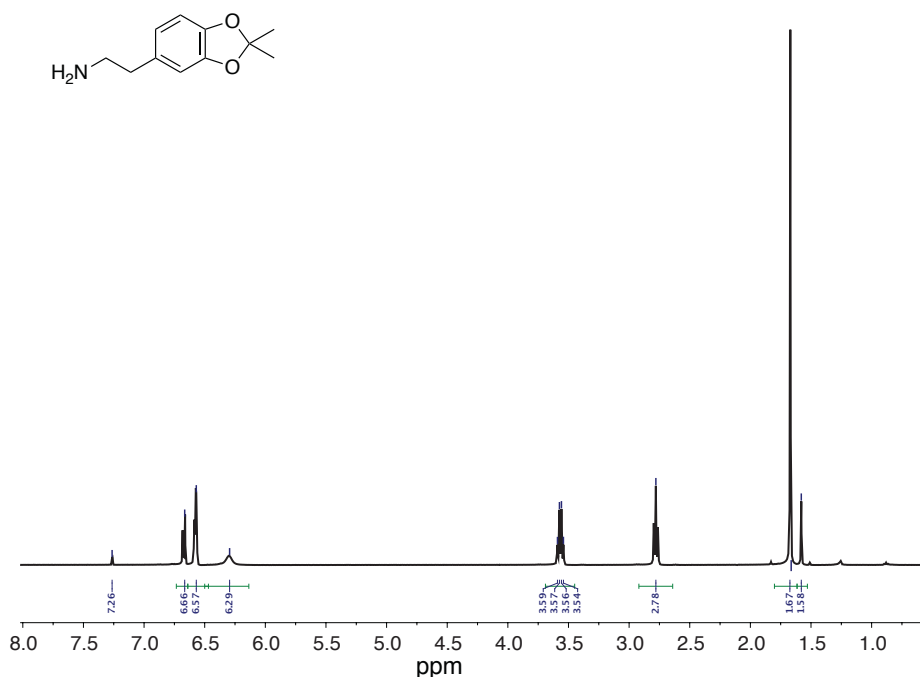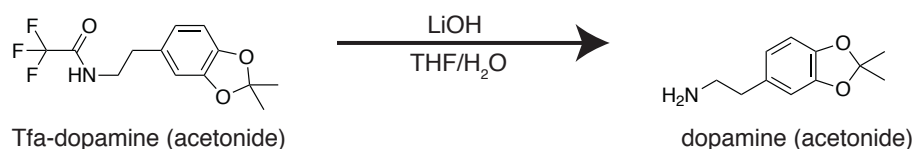
Figure 5.3. ¹H-NMR confirming the synthesis of acetonide-protected dopamine

5.4.3. Preparation of Oligopeptoids

The majority of the peptoid-based oligomers were prepared using a microwave-assisted Liberty Blue peptide synthesizer (CEM Corporation) on Rink amide 4-methylbenzhydrylamine (MBHA) resin (ChemPep Inc.) using a submonomer solid phase synthesis scheme.[21] Four of the catechol functionalized peptoids ((NmeNdop)$_n$Ndop where n = 3-6) were synthesized on Rink amide MBHA resin using an AAPPTec Apex 396 Peptide Synthesizer at the Molecular Foundry at Lawrence Berkley National Laboratory following the same protocol. The resin contains a fluorenylmethyloxycarbonyl (Fmoc)-protected amine that is initially deprotected before synthesis by treatment in 4-methylpiperidine: dimethylformamide (DMF) (20:80, volume ratio).

The synthesis then proceeds by a sequential addition reaction whereby the *N*-terminal amine from the solid support is acetylated with 1 M bromoacetic acid using 1.2 M diisopropylcarbodiimide (DIC) as an activating agent for 5 minutes at 75°C, to afford a terminal bromide which is subsequently displaced via nucleophilic substitution with a 0.5 M primary amine bearing the pendant group for 5 minutes at 75°C. This two-step process of acetylation and displacement is repeated until the desired chain length is achieved. The *N*-terminal of the complementary oligomers was capped with 1 M acetic anhydride activated with DIC to prevent further chain elongation. The primary amines bearing the pendant groups used are shown in Figure 5.4. The primary amines fall into two categories, dynamic covalent functional groups and inert spacer monomers. The dynamic covalent functional group consisted of the prepared acetonide-protected dopamine (Nace) and commercially available 4-aminomethylphenylboronic acid, pinacol ester (Npbe) purchased from AccelaChem. The inert spacer monomers were commercially-available 2-methoxyethylamine (Nme) and 2-ethoxyethoxyethylamine (Neee) prepared according to the protocol established in Wei et al.[17a] All of the reagents were prepared in DMF with the exception of the Neee monomer that was prepared in N-methyl-2-pyrrolidone (NMP).

Dynamic Covalent Monomers
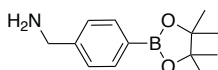
Npbe = 4-aminomethylphenylboronic acid, pinacol ester
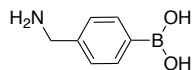
Npba = (4-(aminomethyl)phenyl)boronic acid
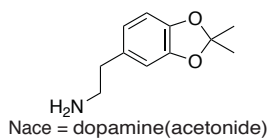
Nace = dopamine(acetonide)
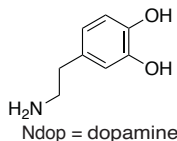
Ndop = dopamine

Inert Spacer Monomers
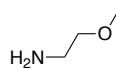
Nme = 2-methoxyethylamine
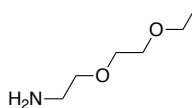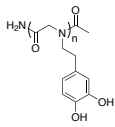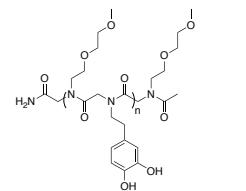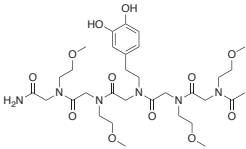
Neee = 2-(2-ethoxyethoxy)ethylamine

Figure 5.4. Primary amine monomers used in this study divided into two categories: dynamic covalent monomers and inert spacer monomers

Table 5.1. Exact mass and nomenclature of the oligopeptoids used throughout this chapter

	n	exact mass (g/mol)
$(NmeNpba)_n Nme$	3	1092.5
	4	1398.7
	5	1704.8
	6	2010.9

	exact mass (g/mol)
$Nme_2 NpbaNme_2$	710.4

	n	exact mass (g/mol)
$(NmeNdop)_n Nme$	3	1098.5
	4	1406.6
	5	1714.8
	6	2022.9

	n	exact mass (g/mol)
Ndop$_n$	6	1217.5
	8	1603.6
(NeeeNdop)$_3$Neee	exact mass (g/mol)	
	1217.5	
Nme$_2$NdopNme$_2$	exact mass (g/mol)	
	712.4	

The solid support resin of the pinacol-protected boronic acid-functionalized peptoids((NmeNpbe)$_n$Nme) underwent a two-step process to rapidly and efficiently prepare a peptoid with exposed boronic acid functionality. The first step is an esterification with a 1 M solution diethanolamine prepared in DMF (5mL) for 30 minutes with the resin being mixed by a steady nitrogen stream. The second step is hydrolysis by immersion in a mixture of trifluoroacetic acid (TFA) and water (95:5 volume ratio) at room temperature for 5 minutes leaving an unbound and deprotected peptoid ((NmeNpba)$_n$Nme) with a C-terminal primary amide. The catechol-functionalized peptoids ((NmeNace)$_n$Nme) were cleaved from the resin by a TFA/water mixture (95:5 volume ratio) at room temperature for 25 minutes. In addition to the peptoid being cleaved from the resin, the acid-labile acetonide protecting group is removed leaving the exposed catechol peptoids ((NmeNdop)$_n$Nme). The deprotected peptoids were then

purified by preparative RP-HPLC at a linear gradient of 10%-acetonitrile-water to 90%-acetonitrile-water over 22 minutes. The molecular weight of the major peak was confirmed using ESI-MS in positive mode. The purified fractions were combined and lyophilized to afford a fine white powder. The peptoids sequences and characterization can be found below. Figure 5.5 shows the ESI-MS and analytical RP-HPLC traces with corresponding relative purity for the boronic acid peptoids used in this study while Figure 5.6 shows the catechol functionalized peptoids.

(A) (NmeNpba)$_3$Nme
C$_{49}$H$_{71}$B$_3$N$_8$O$_{18}$
Exact Mass: 1092.5

1110.5
[M+NH$_4$]$^+$

(B) (NmeNpba)$_4$Nme
C$_{63}$H$_{90}$B$_4$N$_{10}$O$_{23}$
Exact Mass: 1398.6

1421.6
[M+Na]$^+$
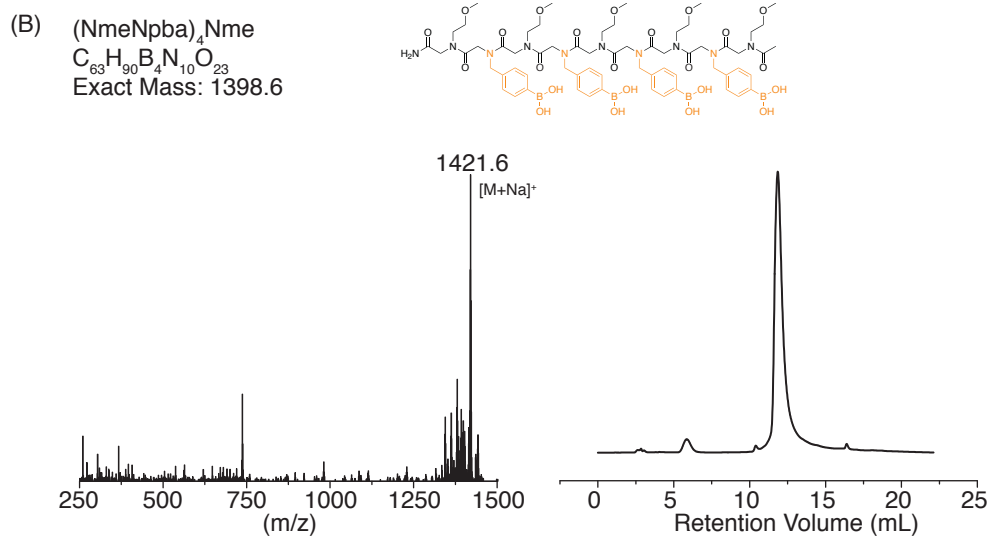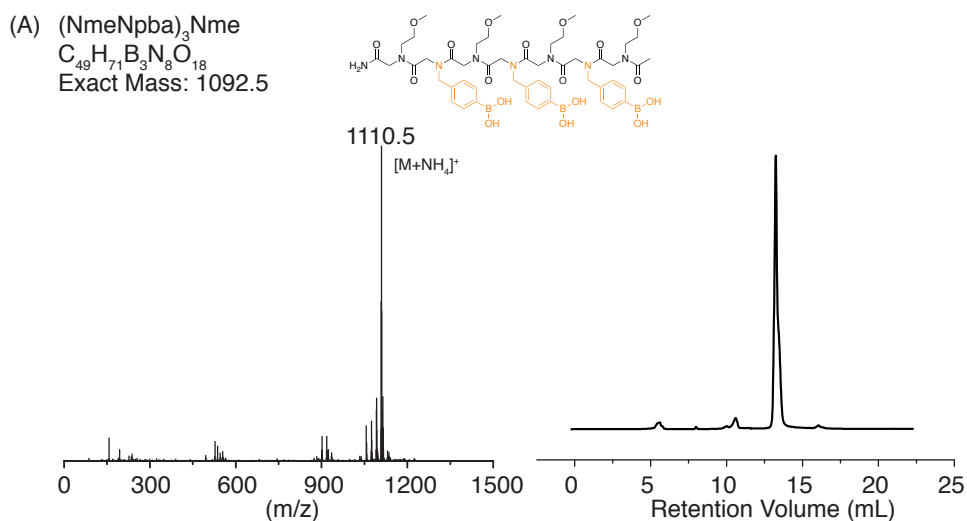
(C) (NmeNpba)₅Nme
$C_{77}H_{109}B_5N_{12}O_{28}$
Exact Mass: 1704.8
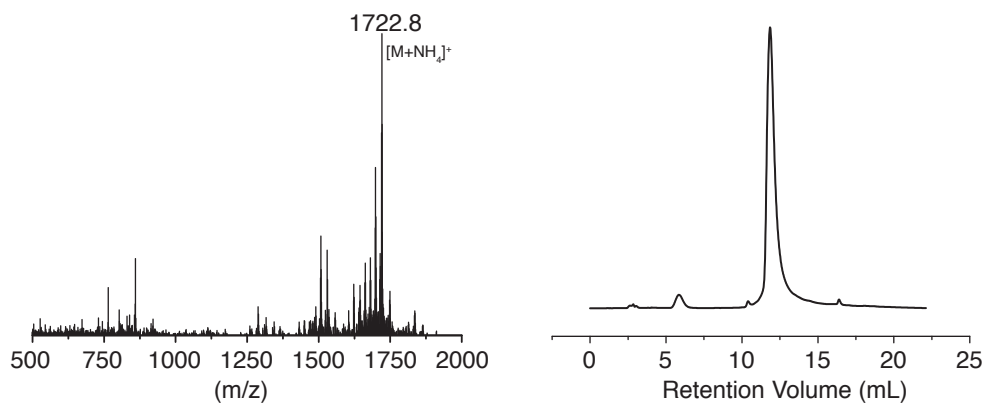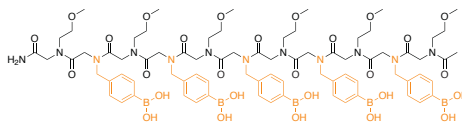
(D) (NmeNpba)₆Nme
$C_{91}H_{128}B_6N_{14}O_{33}$
Exact Mass: 2010.9
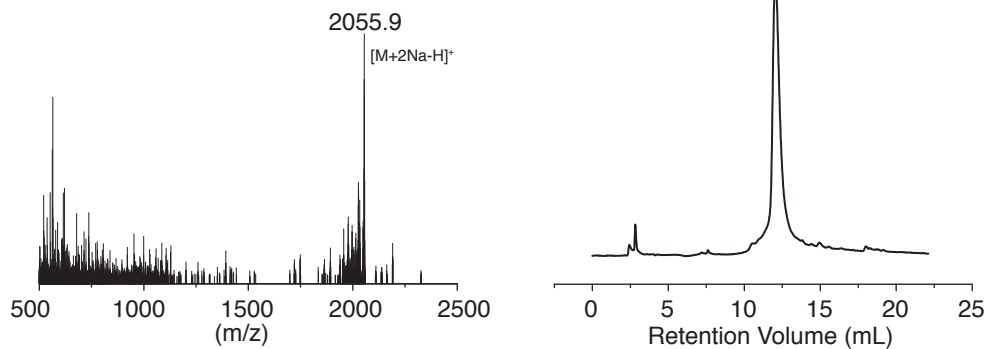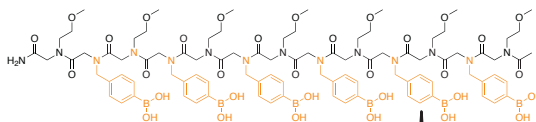
(E) Nme₂NpbaNme₂
$C_{31}H_{51}BN_6O_{12}$
Exact Mass: 710.4

128
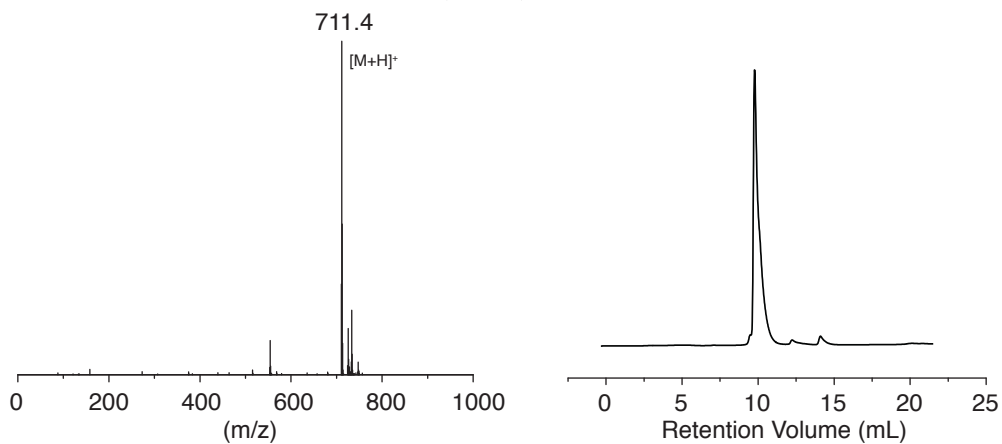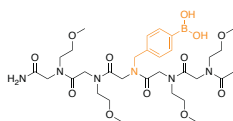
Figure 5.5. ESI-MS mass spectra of boronic acid functionalized oligopeptoids analyzed after cleavage from the solid-support and HPLC purification and analytical HPLC traces of the corresponding peptoids: (A) [(Nme-Npba)$_3$Nme + NH$_4$]$^+$ = 1110.5 g/mol and 97.2% purity; (B) [(Nme-Npba)$_4$Nme + Na]$^+$ = 1421.6 g/mol and 98.1% purity; (C) [(Nme-Npba)$_5$Nme + NH$_4$]$^+$ = 1722.8 g/mol and 96.5% purity; (D) [(Nme-Npba)$_6$Nme + 2Na-H]$^+$ = 2055.9 g/mol and 96.5% purity; and (E) [Nme$_2$NdpbaNme$_2$ + H]$^+$ = 711.4 g/mol and 95.5% purity.

(A) (NmeNdop)$_3$Nme
C$_{52}$H$_{74}$N$_8$O$_{18}$
Exact Mass: 1098.5

1121.5
[M+Na]$^+$

(B) (NmeNdop)$_4$Nme
C$_{67}$H$_{94}$N$_{10}$O$_{23}$
Exact Mass: 1406.7

1429.6
[M+Na]$^+$
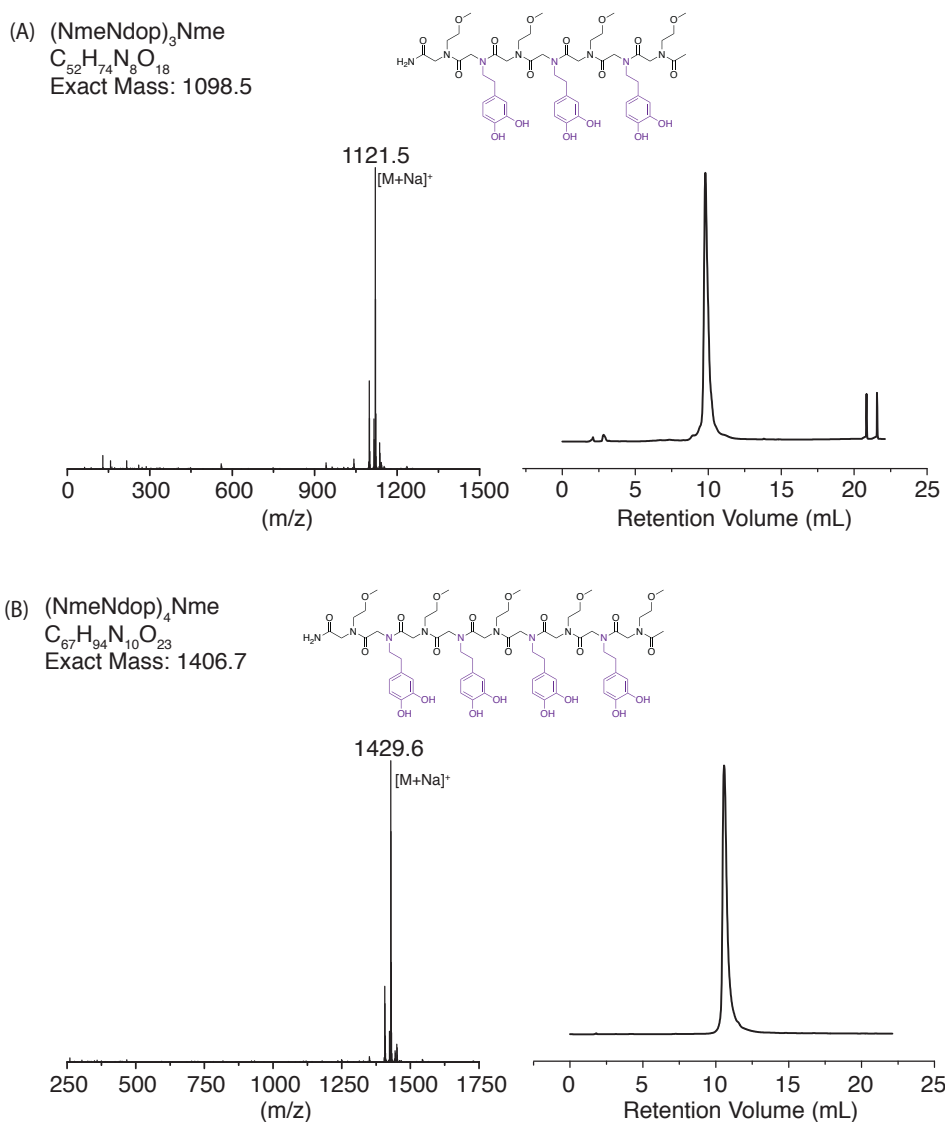
(C) (NmeNdop)₅Nme
$C_{82}H_{114}N_{12}O_{28}$
Exact Mass: 1714.8

1715.8

[M+H]⁺

(m/z)

Retention Volume (mL)
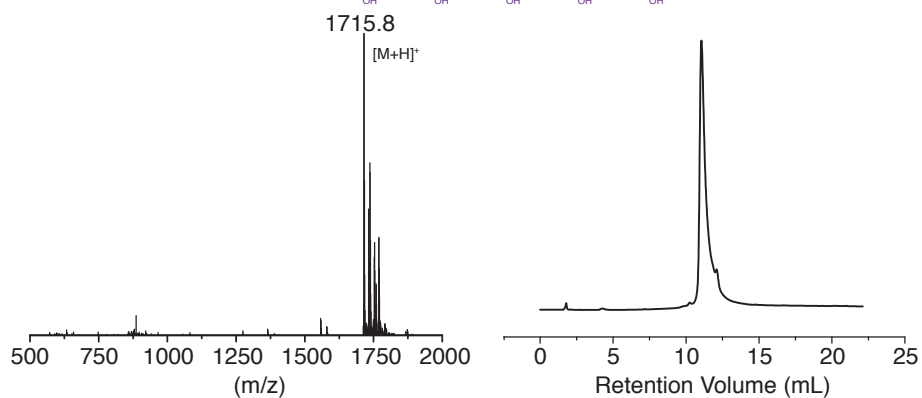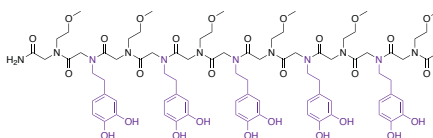
(D) (NmeNdop)₆Nme
$C_{97}H_{134}N_{14}O_{33}$
Exact Mass: 2022.9

2023.9

[M+H]⁺

(m/z)

Retention Volume (mL)

130
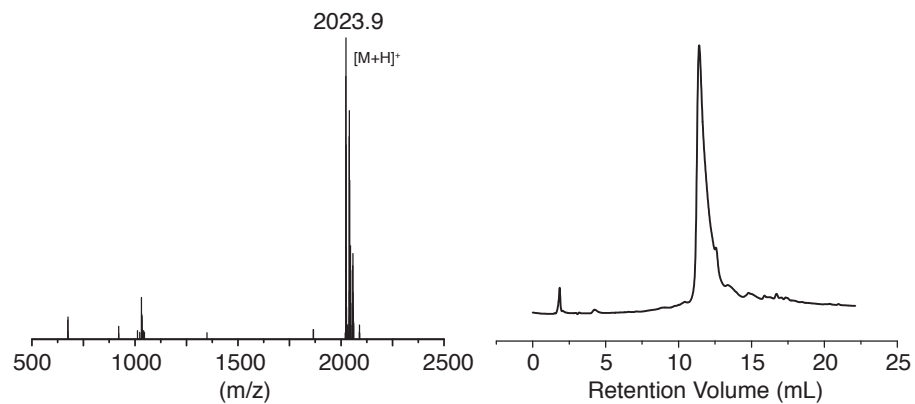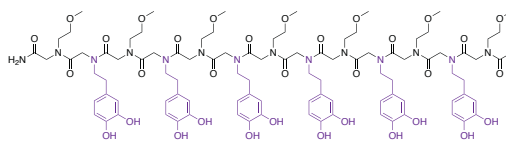
(E) Ndop$_6$
C$_{62}$H$_{71}$N$_7$O$_{19}$
Exact Mass: 1217.5

1218.5

[M+H]$^+$

250   500   750   1000   1250   1500
(m/z)

0   5   10   15   20   25
Retention Volume (mL)
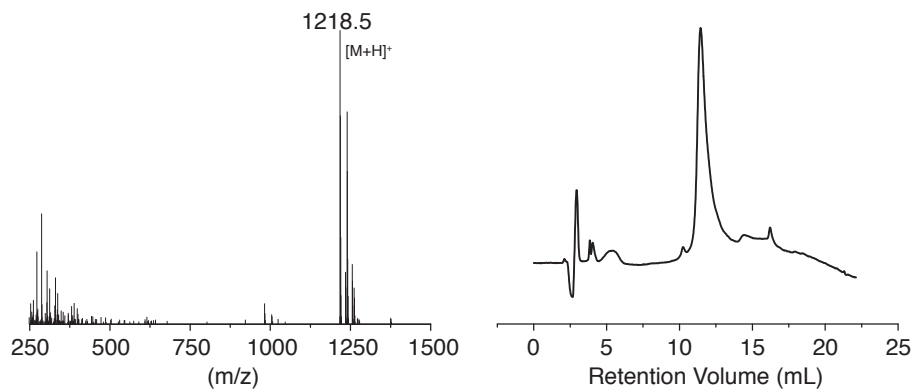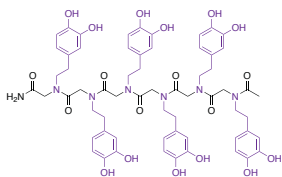
(F) Ndop$_8$
C$_{82}$H$_{93}$N$_9$O$_{25}$
Exact Mass: 1603.6

1604.6

[M+H]$^+$

250   500   750   1000 1250 1500 1750
(m/z)

0   5   10   15   20   25
Retention Volume (mL)

(G) (NeeeNdop)₃Neee
C₆₄H₉₈N₈O₂₂
Exact Mass: 1330.7

1353.7
[M+Na]⁺

(H) Nme₂NdopNme₂
C₃₂H₅₂N₆O₁₂
Exact Mass: 712.4

713.4
[M+H]⁺
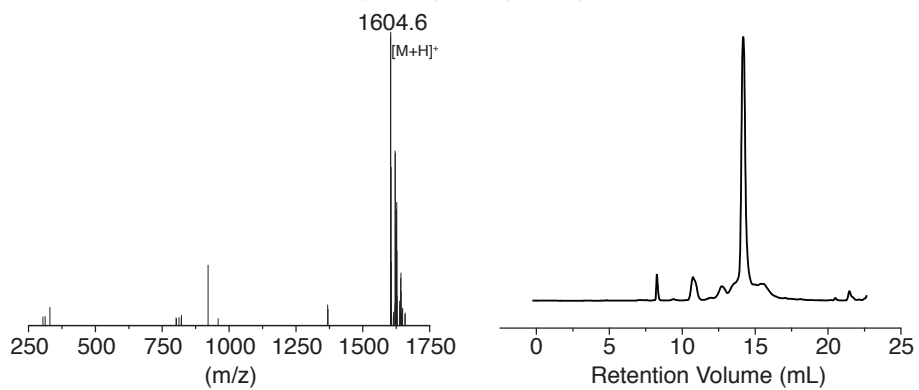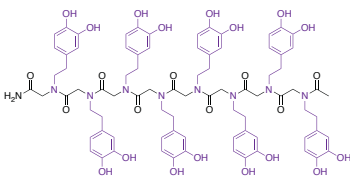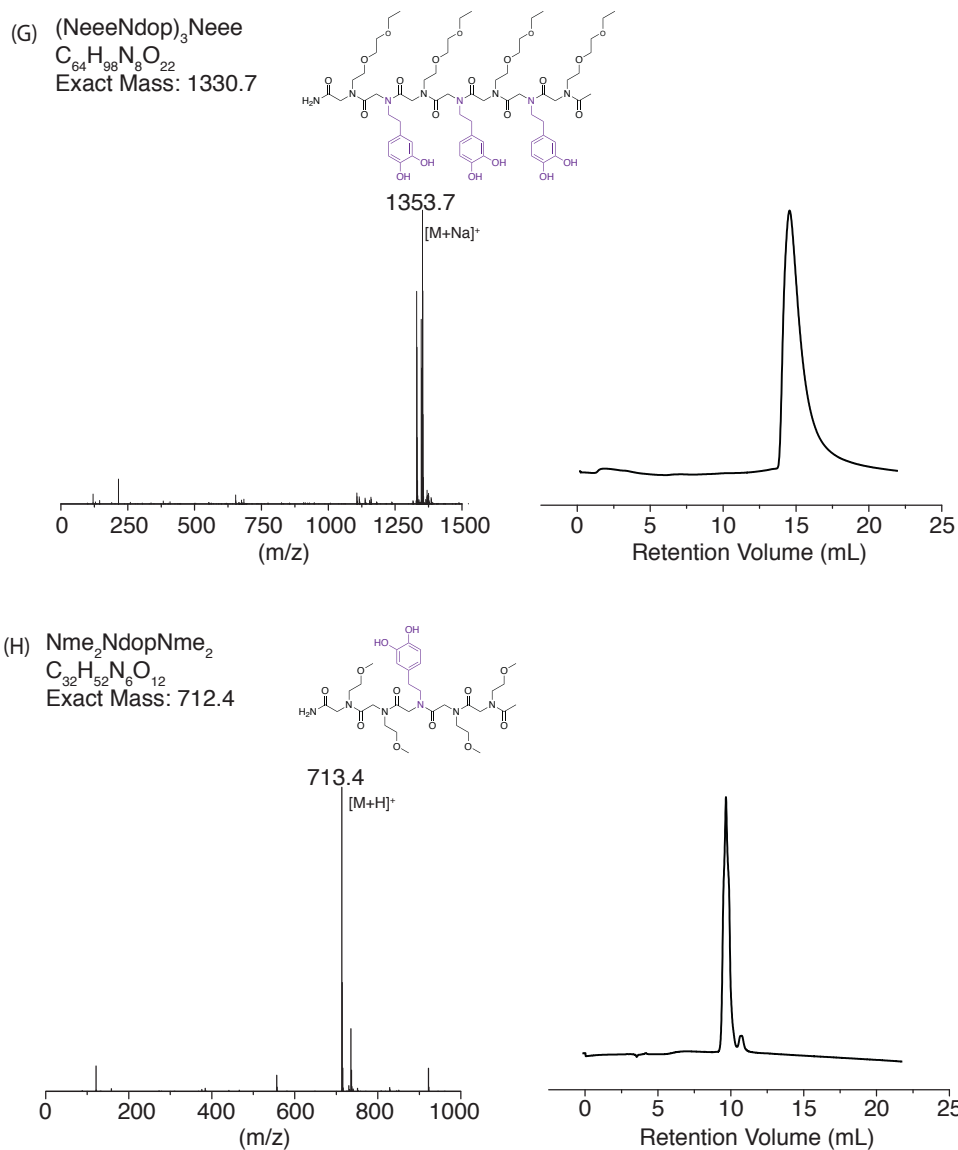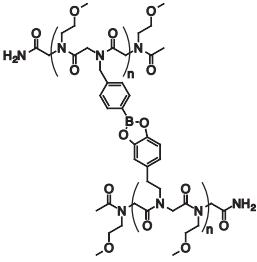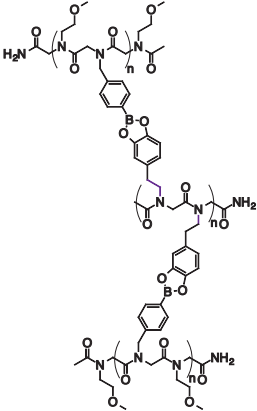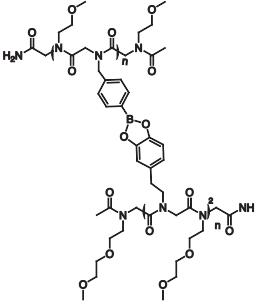
Figure 5.6. ESI-MS mass spectra of catechol functionalized oligopeptoids analyzed after cleavage from the solid-support and HPLC purification and analytical HPLC traces of the corresponding peptoids: (A) [(NmeNdop)₃Nme + Na]⁺ = 1121.5 g/mol and 95.2% purity; (B) [(NmeNdop)₄Nme + Na]⁺ = 1429.6 g/mol and 99.2% purity; (C) [(NmeNdop)₅Nme + H]⁺ =1715.8 g/mol and 86.4% purity; (D) [(NmeNdop)₆Nme + H]+ =2023.9 g/mol and 97.5% purity; (E) [Ndop₆ + H]⁺ = 1218.5 g/mol and 80.3% purity; (F) [Ndop₈ + H]⁺ = 1604.6 g/mol and 89.4% purity; (G) [(NeeeNdop)₃Neee + Na]⁺ = 1353.7 g/mol and 97.5% purity; and (H) [Nme₂NdopNme₂ + H]⁺ = 713.4 g/mol and 99.4% purity.

5.4.4 Hybridization of Oligopeptoids into Molecular Ladders

All hybridization experiments were performed in an anaerobic chamber to minimize the risk of oxidation of the individual strands. Stock solutions of the peptoids were prepare at a 10 mM concentration in water with the exception of the Ndop$_6$ and Ndop$_8$ peptoids which were prepared in 50:50 MeCN:water mixture due to a decrease in polarity with these strands. For the single molecular ladders, 160 µL of a sodium hydroxide solution adjusted to a pH of 9 was added to a vial with a magnetic stir bar. 20 µL (10 mM stock solution) of each of the complementary strands were added to the vial. For the double rung molecular ladders, 140 µL of the same alkaline aqueous solution was added to a vial with a magnetic stir bar. 20 µL (10 mM stock solution) of the catechol-functionalized peptoids and 40 µL of the corresponding boronic acid-functionalized peptoids were added to the vial. The solutions were stirred overnight before preparing a MALDI-TOF sample in α-cyano-4-hydroxycinnamic acid (CHCA). The MALDI-TOF samples were ran in negative reflectron mode. The molecular structures and the expected exact mass are shown in Table 5.2.

Table 5.2. Nomenclature and exact masses of hybridized structures

	n	exact mass (g/mol)
Hybrid-n	3	2083.0
	4	2661.2
	5	3239.5
	6	3817.7
Triplex-n	n	exact mass (g/mol)
	6	3186.4
	8	4112.8
Hybrid-E3	exact mass (g/mol)	
	2313.2	

5.4.5. Dynamic Strand Rearrangement

A sample of the duplex hybrid-3 solution was prepared as described above. The solution was monitored in positive reflectron mode MALDI-TOF with 2-(4-hydroxyphenylazo)benzoic acid (HABA) as the matrix after being allowed to stir overnight. 20 μL of the ((NeeeNdop)$_3$Neee) peptoid (10 mM stock solution) was added to the already-formed solution of hybrid-3. The solution was stirred overnight before taking a MALDI-TOF spot using HABA matrix and positive reflectron mode.

5.4.6. Determination of the Boronic Acid/Diol Binding Constant

In anaerobic conditions, 0.25 mM alizarin red S (ARS) was prepared in an aqueous NaOH solution (pH = 9), and 30 μL of the solution was added to each of the wells in a clear 96-well plate. Using the peptoid, Nme$_2$NpbaNme$_2$, bearing a single boronic acid pendant group, samples were made ranging from 1 to 100 equivalents of the peptoid. 30 μL of the different boronic acid samples were added to the wells containing the ARS to give a stoichiometric equivalence per each of the functional groups on the peptoid. The solution was mixed with a micropipette. An absorbance scan in 400-800 nm wavelength region was performed as well as a fluorescent scan at excitation 485 nm and emission 620 nm. This data was fitted to a Benesi-Hildebrand equation to determine the equilibrium binding constant.

A solution 50% ARS (0.25 mM) and 50% Nme$_2$NpbaNme$_2$ (0.25 mM) in an aqueous NaOH solution (pH = 9) was prepared and 60 μL was added to each well. Nme$_2$NdopNme$_2$, a short peptoid with one catchol functional group was used to make samples ranging from 0.5 to 100 equivalents of the diol pendent group; 30 μL of each of these samples were added to the corresponding well. An absorbance scan in 400-800 nm wavelength region was performed as well as a fluorescent scan at excitation 485 nm and emission 620 nm. This data was used to calculate the binding constant between two different peptoid strands.

5.4.7. Qualitative demonstration of the competitive binding of tetramer peptoids

ARS (0.25 mM) was prepared in an aqueous NaOH solution (pH = 9), and 60 μL of the solution was added to each of the wells. Using the (NmeNpba)$_4$Nme as a model peptoid, samples were made ranging from 1 to 100 equivalents of the boronic acid functional group. 15 μL of the different boronic acid samples were added to the wells to give a stoichiometric equivalence per each of the functional groups on the peptoid. An absorbance scan in 400-800 nm wavelength region was performed as well as a fluorescent scan at excitation 485 nm and emission 620 nm. Similarly, 60 μL of ARS (0.25 mM) and 15 μL of (NmeNpba)$_4$Nme (0.25 mM) was added to each well. (NmeNdop)$_4$Nme was used to make catechol samples ranging from 0.5 to 100 equivalents; 15 μL of each of these samples were added to the corresponding well. An absorbance scan in 400-800 nm wavelength region was performed as well as a fluorescent scan at excitation 485 nm and emission 620 nm.

5.5 Results and Discussion

5.5.1. Dynamic Covalent Assembly of Molecular Ladder and Grid Structures

Peptoids (i.e., poly(N-substituted glycine)s) were employed here as the oligomeric precursor strands for dynamic covalent assembly owing to their ready synthetic accessibility *via* the 'submonomer' solid phase synthetic scheme,[21] enabling the facile incorporation of a variety of pendant functionalities, including reactive boronic acid- and catechol-based functional groups and inert 'spacer' moieties, through the use of primary amine monomers.[22] For the pair of dynamic covalent-reactive monomers, the pendant boronic acid and catechol functionalities were protected with acid-labile groups to ensure that they did not participate in deleterious side

reactions during the oligomer syntheses. The catechol pendant functionality was incorporated on the peptoid chain *via* acetonide-protected dopamine (Nace), whereas the boronic acid functionality was incorporated through the use of 4-aminomethylphenyl boronic acid pinacol ester (Npbe). Additionally, the inert spacer monomers 2-methoxyethylamine (Nme) and 2-(2-ethoxyethoxyethylamine) (Neee) were incorporated between each of the dynamic covalent-reactive pendant groups to improve the solubility of both the initial oligomers and the resulting hybridized structure. The dynamic covalent reactants incorporated on the synthesized peptoid strands were either exclusively boronic acid or catechol functional groups to ensure an absence of premature inter-strand reaction that would impede oligomer purification. All of the peptoid oligomers used in this study were generated by solid phase synthesis using an automated peptide synthesizer and were purified by preparative RP-HPLC.

Boronic acid-bearing peptoid oligomers were initially synthesized as sequences of alternating inert Nme spacer and dynamic covalent Npbe residues, where the number of Npbe residues was varied from 3 to 6. Whereas pinacol ester is widely used as an acid-labile boronic acid protecting group,[23] attempts at direct deprotection by treatment with trifluoroacetic acid (TFA) proved inconsistent and often resulted in significant amounts of boronic acid oxidation to the corresponding phenol, adversely affecting yield upon purification. Consequently, we employed a two-step process to effect its removal whereby the boronate ester was initially subject to an on-bead transesterification reaction with diethanolamine,[24] efficiently replacing the pinacol group, followed by hydrolysis and simultaneous cleavage of the peptoid from the solid support with TFA and water to afford free peptoids bearing exposed boronic acid residues (i.e., Npba) that were denoted as $(NmeNpba)_n Nme$, where $n = 3\text{-}6$. In contrast to the single-step TFA treatment of the pinacol-protected boronic acid during peptoid cleavage, this two-step process

avoided oxidation and yielded a more comprehensive cleavage of the pinacol group from the boronate ester. For the complementary, catechol-bearing oligomers, peptoids were synthesized with alternating Nme and Nace monomers, as well as two peptoids that exclusively incorporated Nace residues. The acetonide protecting group were removed by extended treatment with TFA during peptoid cleavage to afford free peptoids bearing the desired catechol functionality, denoted by Ndop.
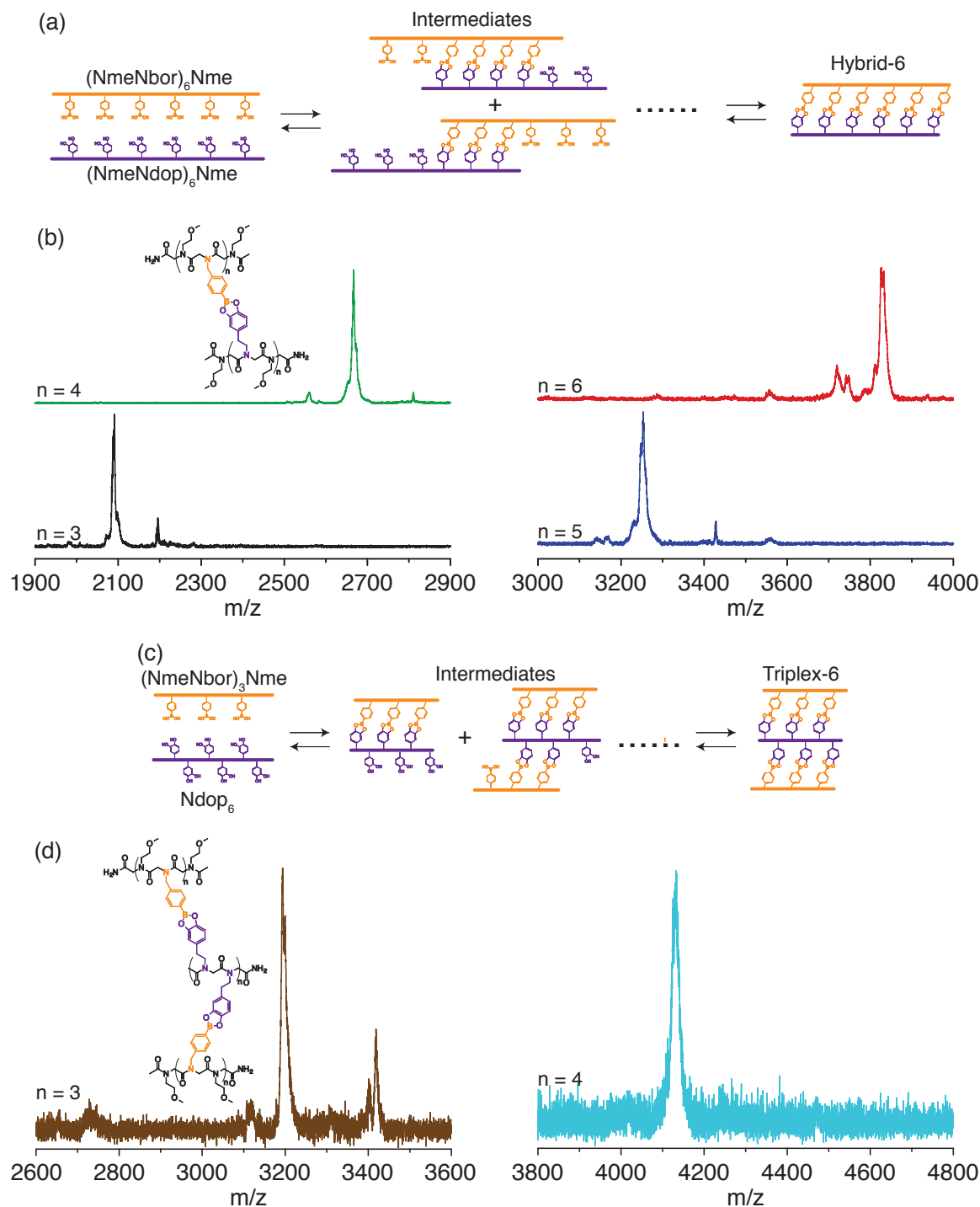
Figure 5.7. Dynamic covalent assembly of boronate ester-based molecular ladders and grids. a) Schematic diagram showing the dimerization of complementary, boronic acid- and catechol-bearing oligomers to afford in-registry molecular ladders. b) Negative mode MALDI-TOF mass spectra confirming the formation of peptoid-based molecular ladders bearing from 3 to 6 boronate ester rungs (molecular structures as shown). c) Schematic diagram showing the hybridization of two boronic acid-bearing oligomers with a catechol-

bearing core oligomer to afford a triplex grid. d) Negative mode MALDI-TOF mass spectra of assembled 3 × 3 and 3 × 4 grid structures (molecular structures as shown).

To illustrate the oligomer hybridization process employed here, a schematic diagram showing the self-assembly of a molecular ladder with six rungs is presented in Figure 5.7a. Here, co-reaction of complementary precursor oligomers, each incorporating six reactive pendant groups, initially affords a mixture of intermediate ladder species with varying numbers of rungs, species which are annealed out of the mixture as the reaction proceeds owing to the dynamic rearrangement of the generated boronate ester linkages to ultimately form the fully in-registry, six-rung molecular ladder (i.e., Hybrid-6). This hybridization process was experimentally executed by mixing complementary, boronic acid- and catechol-bearing oligomers bearing equal numbers of reactive pendant groups (i.e., (NmeNpba)$_n$Nme and (NmeNdop)$_n$Nme) at a 1:1 stoichiometric ratio in an aqueous solution, the pH of which was adjusted to 9 by addition of a dilute sodium hydroxide solution to maximize the boronic acid/catechol binding constant.[13a] Importantly, these hybridization experiments were performed in an anaerobic environment owing to the susceptibility of the pendant catechol groups to oxygen under alkaline conditions;[10,25] indeed, the reaction mixture would progressively turn a pale pink color upon exposure to air, providing a visual indication of catechol oxidation to the corresponding *o*-quinone.[26] As the forward condensation reaction between a boronic acid and a catechol yields a boronate ester and two water molecules such that the mass of any molecular ladder formed decreases by 36 for each rung generated, MALDI-TOF mass spectrometry was performed in negative mode on aliquots of the crude reaction mixtures after reaction overnight (see Figure 5.7b) to determine the identity of the products. Hybridization experiments were performed using precursor oligomers bearing from three to six reactive pendant groups, and the major peak in each of the MALDI-TOF spectra was assigned as the desired, fully in-registry molecular ladder for the respective reaction mixtures.

Notably, positive mode MALDI-TOF mass spectra were also collected on the reaction mixture aliquots (Figure 5.8, 5.9, and 5.10); however, this method was limited to characterizing molecular ladders with five rungs owing to poor signal strength for higher molecular weight, boronate ester-bearing species. Nevertheless, the major peak in the spectra for each of the mixtures of oligomers with three to five reactive pendant groups was again identified as the target, in-registry molecular ladder product, supporting the identification as determined by negative mode mass spectrometry.

Recent work on peptoid-based, two-dimensional 'nanosheets', assembled from amphiphilic sequences of ionic and hydrophobic residues revealed that their constituent peptoid chains adopt a 'Σ-strand' conformation, where adjacent pendant groups are presented on opposite sides of the peptoid backbone.[27] Moreover, the chemical and mechanical stability of these structures was effected by the post-assembly covalent cross-linking of their hydrophobic core. Inspired by this work and having successfully realized the hybridization of complementary oligomers to afford dimeric, molecular ladder structures, we employed dynamic covalent assembly to afford finite molecular grids from the interaction of multiple precursor peptoid oligomers in a preliminary effort towards the fabrication of inherently cross-linked nanosheets. To ensure their facile characterization by mass spectrometry, the assembly of these grids was designed to proceed between two boronic acid-bearing oligomers flanking a catechol-bearing core to afford designed well-defined, three-stranded structures, denoted here as 3 × 3 and 3 × 4 grids to represent the 3 strands with either 3 or 4 dynamic covalent interactions per oligomer pair. Whereas the sequences of the flanking strands maintain the use of alternating dynamic covalent-reactive and inert spacer residues, the triplex cores were composed exclusively of residues bearing reactive pendant groups1`. Thus, triplex grids were assembled by adding 2

equivalents of a boronic acid-bearing peptoid ((NmeNpba)$_n$Nme) to a catechol-bearing hexafunctional peptoid (Ndop$_{2n}$), as shown in Figure 5.7c. MALDI-TOF mass spectrometry was again employed to confirm the formation of the target 3 × 3 and 3 × 4 grid structures (Figure 5.7d). Our previous work on Vernier-templated dynamic covalent assembly examined the concurrent interaction of greater than two oligomeric precursor strands to afford long, linear molecular ladders;[17a] nevertheless, the multi-oligomer molecular grids described here demonstrate an approach to achieve assembly perpendicular to the precursor oligomer axes to yield wide, non-linear structures, suggesting the potential for the fabrication of covalently-bonded, raft-like nanosheets composed of many linear oligomers.
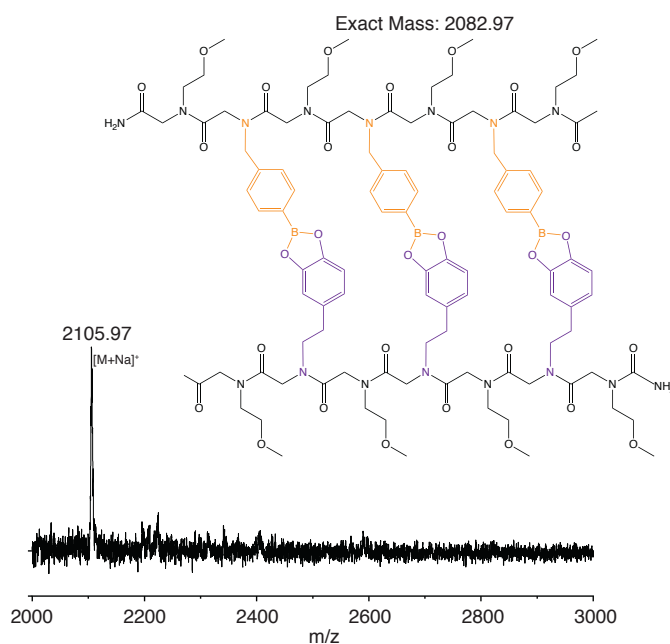
Figure 5.8. Positive ion mode MALDI-TOF spectra confirming the formation of hybrid 3 [hybrid-3 + Na]$^+$ = 2105.95 g/mol.

Exact Mass: 2661.2

2683.7

[M+Na]⁺
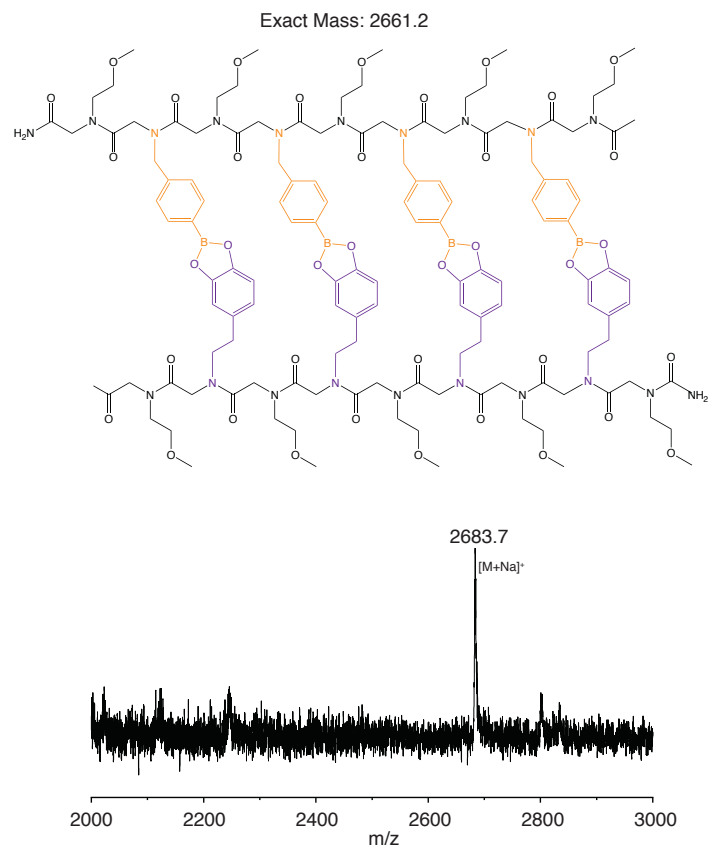
Figure 5.9. Positive ion mode MALDI-TOF spectra confirming the formation of hybrid 4 [hybrid-4 + Na]⁺ = 2684.2 g/mol.

143
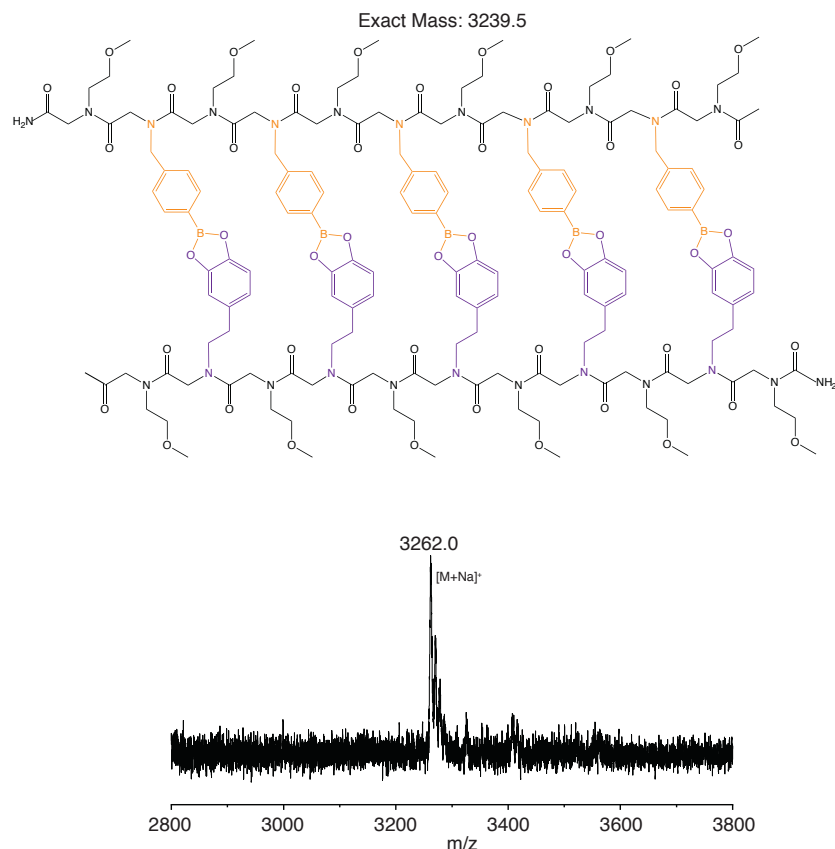
Figure 5.10. Positive ion mode MALDI-TOF spectra confirming the formation of hybrid 5 [hybrid-5 + Na]$^+$ = 3262.5 g/mol.

5.5.2. Molecular Ladder Scrambling by Strand Displacement

In order to determine the dynamic nature of the boronate ester-based molecular ladders and grids assembled from boronic acid- and catechol-bearing precursors, a mass-labeled, catechol-functionalized peptoid strand was added to an existing dimeric hybrid and the strand rearrangement and displacement by transesterification monitored (see Figure 5.11a). Whereas the initial hybrid (hybrid-3) incorporated the Nme spacer for both boronic acid- and catechol-bearing precursor oligomers (i.e., (NmeNpba)$_3$Nme and (NmeNdop)$_3$Nme, respectively), the catechol-bearing peptoid added to the hybrid solution was mass-labeled by employing Neee as the spacer residue owing to its a higher molecular weight than Nme. Thus, exchange of the catechol-bearing (NmeNdop)$_3$Nme strand in the parent molecular ladder for (NeeeNdop)$_3$Neee yields a daughter

144

ladder with a higher molecular weight than its parent and readily differentiated by mass spectrometry. The MALDI-TOF spectrum of the initial reaction mixture of (NmeNdop)$_3$Nme and (NmeNpba)$_3$Nme (Figure 5.11b, bottom) shows a single peak at 2105.97, attributable to the Na$^+$ ionization of the initial hybridized molecular ladder structure generated by the interaction of the two peptoid strands; however, upon addition of the (NeeeNdop)$_3$Neee strand, two distinct product peaks in the MALDI-TOF spectrum of the reaction mixture are observed (Figure 2b, top), one at 2105.97 corresponding to the initial, parent hybrid, and a second pair at 2336.1 and 2346.3, corresponding to the Na$^+$ and CH$_3$OH+H$^+$ ionizations, respectively, of a daughter molecular ladder composed of (NmeNpba)$_3$Nme and (NeeeNdop)$_3$Neee peptoid strands. The mass spectrum showing both the parent and daughter hybrids (i.e., Figure 2b, top) was collected after overnight incubation; however, a peak attributable to the daughter ladder was observable in mass spectra collected within minutes after adding the (NeeeNdop)$_3$Neee strand, suggesting that, in contrast to earlier work in our lab with imine-forming tetramers,[17a] this dynamic rearrangement proceeded rapidly. Whereas progress of the generation and scrambling reactions for the imine-bearing molecular ladders could be readily monitored by employing MALDI-TOF on reaction mixture aliquots, this time-resolved method proved ill-suited for quantitatively following either the initial assembly or rearrangement of boronate ester-based molecular ladders owing to their rapid reaction rates.
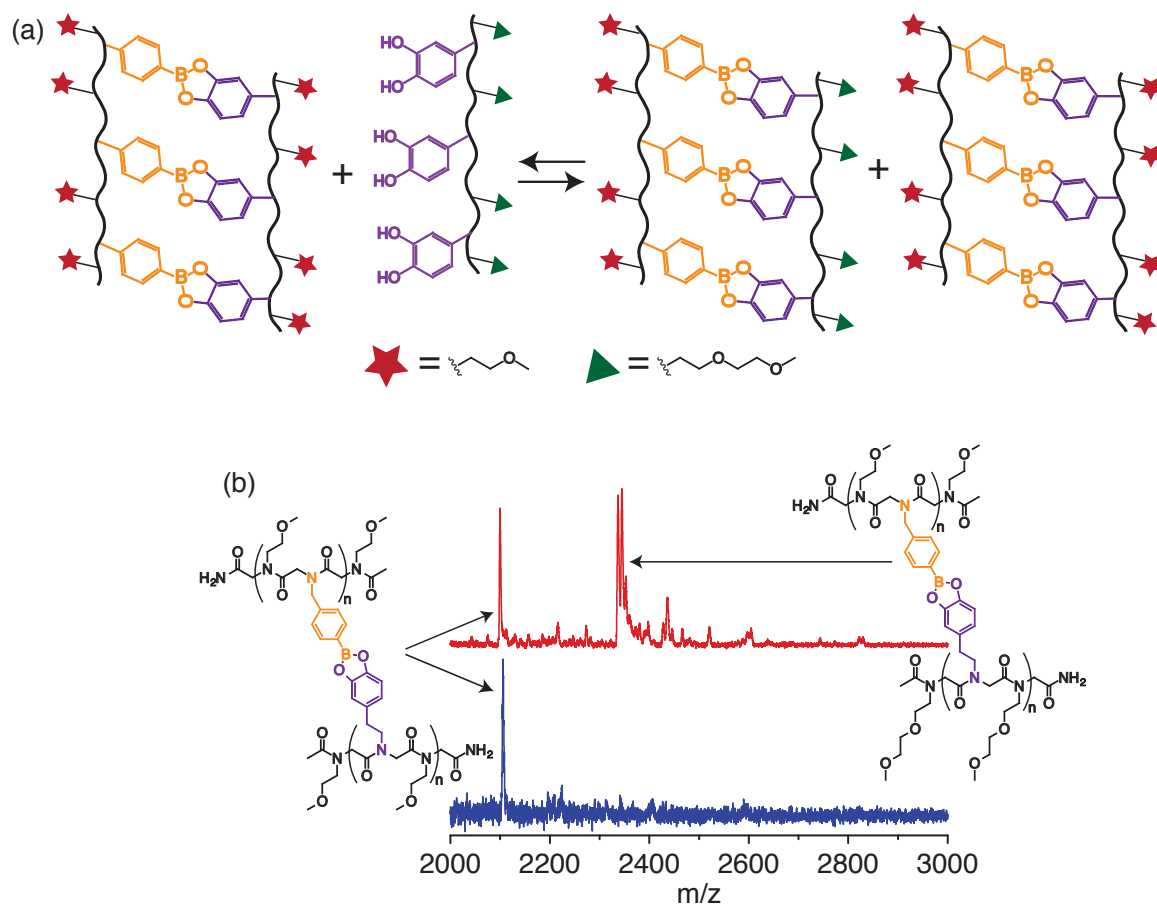
Figure 5.11. Molecular ladder strand displacement. a) Schematic diagram of strand rearrangement where the fully-formed hybrid-3, assembled from oligomers incorporating the inert Nme spacer residue (denoted by a star), is reacted with (NeeeNdop)₃Neee, a peptoid oligomer bearing the Neee spacer residue (denoted by a triangle). Upon displacement of the original, Nme-bearing (NmeNdop)₃Nme by the introduced, Neee-bearing oligomer, the mixture achieves a new equilibrium state that includes the original hybrid-3, the newly-hybridized structure, hybrid-E3, and both catechol-bearing peptoids as free oligomers. b) Positive mode MALDI-TOF spectra of (bottom) the initial reaction mixture incorporating the hybrid-3 structure ([M+Na]$^+$ = 2105.97), and (top) the reaction mixture after the addition of (NeeeNdop)₃Neee, incorporating both the initially-formed hybrid-3 ([M+Na]$^+$ = 2105.97 g/mol) and the newly-formed hybrid-E3 ([M+Na]$^+$ = 2336.19 g/mol).

146

5.5.3. Monitoring Transesterification Rate and Binding Constant
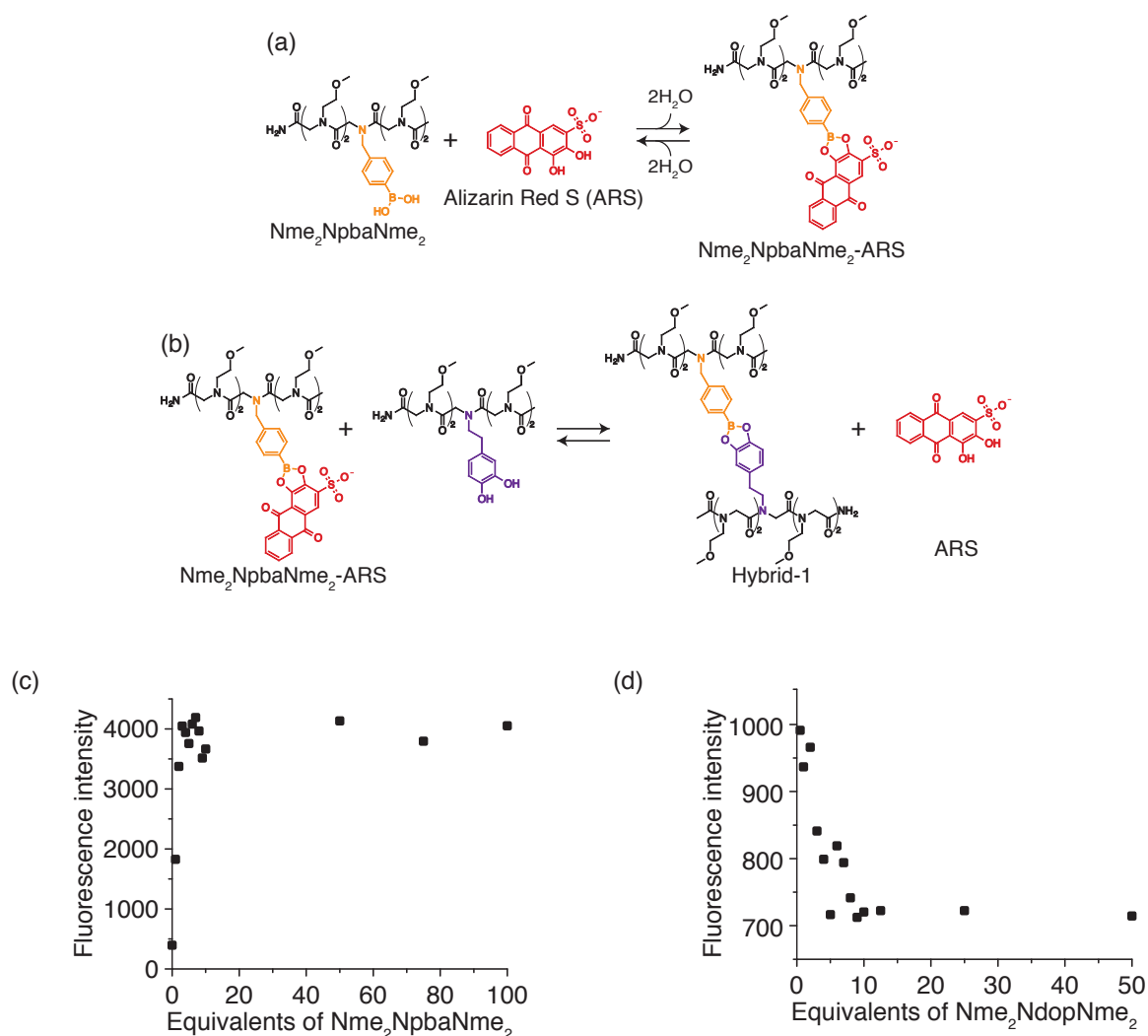
Figure 5.12. Competitive binding between boronic acid- and catechol-bearing peptoids and the diol fluorophore, ARS. Schematic diagrams showing a) the binding between Nme$_2$NpbaNme$_2$ and ARS, and b) the displacement of ARS bound to Nme$_2$NpbaNme$_2$ when Nme$_2$NdopNme$_2$ is introduced to the system. c) Increase in fluorescent intensity as increasing equivalents of Nme$_2$NpbaNme$_2$ bind with ARS. d) Changes in fluorescent intensity as Nme$_2$NdopNme$_2$ displaces ARS, bound to Nme$_2$NpbaNme$_2$, and is released into solution.

Given the influence of reaction rates on suppressing kinetically-trapped species and thereby ensuring self-assembly success, we further explored strategies to ascertain molecular ladder transesterification rates. Thus, a competitive binding assay was performed by using ARS, a diol that affords an observably lower fluorescence signal in free solution than when bound to a

boronic acid (Figure 3a). A plate reader was used to obtain a kinetic scan (Figure S12) that compared the change in fluorescent intensity (λ_{exc} = 485±20 nm and λ_{em} = 620±20 nm) between a control sample that contained only (NmeNpba)$_4$Nme bound to ARS and a sample where 10 equivalents of (NmeNdop)$_4$Nme was added to the ARS bound (NmeNpba)$_4$Nme. The kinetic scan began immediately after (NmeNdop)$_4$Nme was added to the sample, and it is noted that the samples had already plateaued before the first time point was completed. This suggests that the samples were at equilibrium before the readings were taken, and that the kinetic rate could not be determined by this approach. Nevertheless, the rapid rate of this exchange reaction enabled the binding constant between peptoids bearing boronic acid and catechol pendant groups to be readily evaluated. Here, the binding constant between Nme$_2$-Ndop-Nme$_2$ and Nme$_2$-Ndpba-Nme$_2$ was determined to serve as a proxy for the relationship between each of the complementary peptoid structures. Briefly, varying equivalents of boronic acid peptoid was incubated with stoichiometric ratios of ARS to first establish an equilibrium-binding constant, K_{eq}. This relationship followed a logarithmic curve (Figure 5.12c) that plateaued at approximately 10 equivalents of the boronic acid peptoid. In contrast, increasing equivalents of the catechol oligomer were added to the boronic acid oligomer bound to ARS that yielded an exponential decay of fluorescence intensity (Figure 5.12d). This trend can be attributed to the release of ARS back into solution as the catechol oligomer starts to displace the bound ARS and dimerize with the boronic acid peptoid. The exchange reaction between the ARS and catechol oligomer further demonstrates the dynamic nature of this system through the reversible formation of boronate esters. The same experiments were repeated with complementary tetramer peptoids, (NmeNdop)$_4$Nme and (NmeNpba)$_4$Nme (Figure 5.14). This was a qualitative test to

demonstrate that the longer peptoid ladders follow a similar trend to the one functional group peptoids.
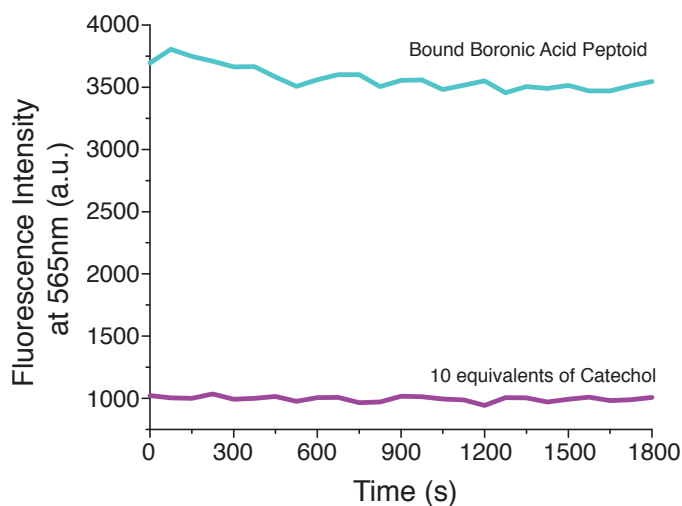
Figure 5.13. Kinetic study of the interaction between (NmeNpba)₄Nme bound to ARS and (NmeNdop)₄Nme. Two samples were prepared with a stoichiometric ratio of ARS and (NmeNpba)₄Nme, where one sample was used as a control (blue line) with only water added and the other was treated with 10 equivalents of (NmeNdop)₄Nme (purple) immediately before monitoring the sample with the plate reader. A kinetic scan monitored the fluorescent intensity of each of the samples for 30 minutes readings were taken every 75 seconds.
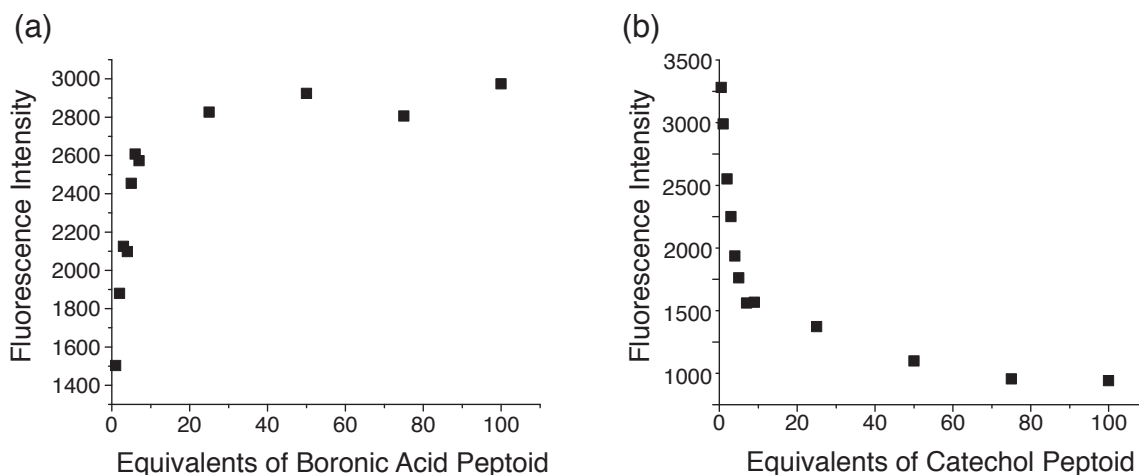
Figure 5.14. Competitive binding between (NmeNpba)₄Nme and (NmeNdop)₄Nme using ARS as a model diol. (A) The increase in fluorescent intensity experienced by adding

increasing equivalents of boronic acid peptoid (NmeNpba)₄Nme to ARS. The increase in intensity is a result of the ARS binding to the boronic acid peptoid. (B) The decrease in fluorescent intensity caused by increasing equivalents of catechol peptoid (NmeNdop)₄Nme to (NmeNpba)₄Nme bound to ARS. The decrease in intensity is a result of the catechol interaction with the boronic acid peptoid releasing the ARS into the system.

A mathematical method for determining equilibrium constants of non-bonding interaction, Benesi-Hildebrand method,[28] was adapted for use with fluorescence data and used to determine the equilibrium constant, K_{BA}, of the boronic acid and ARS complex. The analysis followed a method outlined by Gennari et al.[15] where the inverse of the change in fluorescent intensity (ΔI_f) was plotted against the inverse of the boronic acid concentration (C_{BA}), and K_{BA} was determined by fitting the line and dividing the intercept by the slope following equation (1). In the equation Δkp_0 is a constant that is dependent on the laser power and the intrinsic fluorescence, and CARS is the concentration of ARS. This yielded a K_{BA} value of 2664 M⁻¹.

$$\frac{1}{\Delta I_f} = (\Delta kp_0 C_{ARS} K_{BA})^{-1} \frac{1}{C_{BA}} + (\Delta kp_0 C_{ARS})^{-1} \quad (1)$$

The equilibrium constant between the boronic acid and catechol peptoids can be expressed by the equilibrium reaction shown in equation 2 where A is the ARS, B is the boronic acid oligomer, and C is the catechol oligomer. The equilibrium of this reaction, K, (equation 3) can be shown as the ratio of the equilibriums between the two boronate esters (AB and CB). This equation can be further expanded to be represented in terms of the concentration of free ARS, [A] (equation 4).

$$AB + C \leftrightarrow CB + A \quad (2)$$
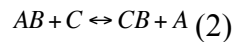
$$K = \frac{[A][CB]}{[AB][C]} = \frac{K_{CAT}}{K_{BA}} \quad (3)$$

$$K = \frac{[A](C_{BA} - [AB])}{(C_{ARS} - [A])[C]} \quad (4)$$

$$K = \frac{[A](C_{BA} - C_{ARS} + [A])}{(C_{ARS} - [A])(C_{CAT} - C_{BA} + (C_{ARS} - [A]))} \quad (5)$$

The concentration of free ARS ([A]) for each of the different catechol equivalents was calculated by determining the percentage of free ARS by the change in fluorescent intensity and multiplying that by the initial concentration, C_{ARS}. Once K (Equation 5) is determined it can be multiplied by K_{BA} to determined K_{cat}. The K_{cat} values for the various concentrations of catechols was averaged to find a binding constant of 276 M^{-1}. Although the Benesi-Hildebrand method is effective for determining binding constants for 1:1 interactions, quantitatively characterizing a sample that has multiple possible interactions, such as the tetramer peptoids where there are four boronic acid functional groups that can bind with ARS each interaction eliciting a change in the fluorescent intensity, is more challenging. Indeed, the multivalent binding between the peptoid strands likely contribute to a stronger affinity than single interaction when considering the effective local functional group concentration, a phenomena prevalent in biological systems.[29] The different sites could follow this so-called "cluster effect" owing to the proximity of the interactions along the peptoid backbone where the binding of one group will lead to increased localized concentration of the unreacted functional groups resulting in strong binding affinity in the remaining groups.

5.6 Conclusions

We have demonstrated the successful dynamic covalent assembly of molecular ladders and grids incorporating boronate ester rungs in aqueous solution through the hybridization of complementary, peptoid-based precursor oligomers bearing boronic acid and catechol pendant groups. Ladders with up to 6 rungs were assembled in alkaline aqueous solution and identified by mass spectrometry, as were 3 × 3 and 3 × 4 molecular grid structures composed of catechol-functionalized peptoid cores flanked by boronic acid-bearing strands. Strand rearrangement by

transesterification between a fully formed, hybridized structure and a competing, mass-labeled single-stranded oligomer demonstrated the rapid dynamic nature of the esterification. Although a competitive binding assay between boronic acid- and catechol-bearing peptoids and the diol fluorophore, ARS, was ineffective in monitoring the rapid transesterification reaction, it provided sufficient data to determine a binding constant for this system of 276 M^{-1} using the changes in fluorescent intensity of solutions containing ARS and dynamic covalent oligomers. The detailed knowledge of the affinity between our peptoid-based oligomers informs reaction conditions necessary to ultimately build more complex molecular architectures. This work establishes a route towards the self-assembly of complex and robust biomimetic nanostructures.

5.7. References

1. Schnur, J. M., Lipid Tubules: A Paradigm for Molecularly Engineered Structures. *Science* **1993,** *262* (5140), 1669-1676.

2. Gething, M. J.; Sambrook, J., Protein folding in the cell. *Nature* **1992,** *355* (6355), 33-45.

3. Zuker, M., Mfold web server for nucleic acid folding and hybridization prediction. *Nucleic Acids Res.* **2003,** *31* (13), 3406-3415.

4. Zhang, S. G., Fabrication of novel biomaterials through molecular self-assembly. *Nat. Biotechnol.* **2003,** *21* (10), 1171-1178.

5. (a) Rajendran, A.; Endo, M.; Katsuda, Y.; Hidaka, K.; Sugiyama, H., Photo-Cross-Linking-Assisted Thermal Stability of DNA Origami Structures and Its Application for Higher-Temperature Self-Assembly. *J. Am. Chem. Soc.* **2011,** *133* (37), 14488-14491; (b) Abdallah, H. O.; Ohayon, Y. P.; Chandrasekaran, A. R.; Sha, R. J.; Fox, K. R.; Brown, T.; Rusling, D. A.; Mao, C.; Seeman, N. C., Stabilisation of self-assembled DNA crystals by triplex-directed photo-cross-linking. *Chem. Commun.* **2016,** *52* (51), 8014-8017; (c) Maeda, K.; Hong, L.; Nishihara, T.; Nakanishi, Y.; Miyauchi, Y.; Kitaura, R.; Ousaka, N.; Yashima, E.; Ito, H.; Itami, K., Construction of Covalent Organic Nanotubes by Light-Induced Cross-Linking of Diacetylene-Based Helical Polymers. *J. Am. Chem. Soc.* **2016,** *138* (34), 11001-11008.

6. Rowan, S. J.; Cantrill, S. J.; Cousins, G. R. L.; Sanders, J. K. M.; Stoddart, J. F., Dynamic covalent chemistry. *Angew. Chem.-Int. Edit.* **2002,** *41* (6), 898-952.

7.   Christinat, N.; Scopelliti, R.; Severin, K., Multicomponent assembly of boron-based dendritic nanostructures. *J. Org. Chem.* **2007,** *72* (6), 2192-2200.

8.   Christinat, N.; Scopelliti, R.; Severin, K., Multicomponent assembly of boronic acid based macrocycles and cages. *Angew. Chem.-Int. Edit.* **2008,** *47* (10), 1848-1852.

9.   Cote, A. P.; Benin, A. I.; Ockwig, N. W.; O'Keeffe, M.; Matzger, A. J.; Yaghi, O. M., Porous, crystalline, covalent organic frameworks. *Science* **2005,** *310* (5751), 1166-1170.

10.   He, L. H.; Fullenkamp, D. E.; Rivera, J. G.; Messersmith, P. B., pH responsive self-healing hydrogels formed by boronate-catechol complexation. *Chem. Commun.* **2011,** *47* (26), 7497-7499.

11.   Li, Y. P.; Xiao, W. W.; Xiao, K.; Berti, L.; Luo, J. T.; Tseng, H. P.; Fung, G.; Lam, K. S., Well-Defined, Reversible Boronate Crosslinked Nanocarriers for Targeted Drug Delivery in Response to Acidic pH Values and cis-Diols. *Angew. Chem.-Int. Edit.* **2012,** *51* (12), 2864-2869.

12.   Zhang, X. T.; Liu, G. J.; Ning, Z. W.; Xing, G. W., Boronic acid-based chemical sensors for saccharides. *Carbohydr. Res.* **2017,** *452*, 129-148.

13.   (a) Yan, J.; Springsteen, G.; Deeter, S.; Wang, B. H., The relationship among pKa, pH, and binding constants in the interactions between boronic acids and diols - it is not as simple as it appears. *Tetrahedron* **2004,** *60* (49), 11205-11209; (b) Springsteen, G.; Wang, B. H., A detailed examination of boronic acid-diol complexation. *Tetrahedron* **2002,** *58* (26), 5291-5300.

14.   Chirayil, S.; Luebke, K. J., Cyclization of peptoids by formation of boronate esters. *Tetrahedron Lett.* **2012,** *53* (7), 726-729.

15.   Gennari, A.; Gujral, C.; Hohn, E.; Lallana, E.; Cellesi, F.; Tirelli, N., Revisiting Boronate/Diol Complexation as a Double Stimulus-Responsive Bioconjugation. *Bioconjugate Chem.* **2017,** *28* (5), 1391-1402.

16.   (a) Hartley, C. S.; Elliott, E. L.; Moore, J. S., Covalent assembly of molecular ladders. *J. Am. Chem. Soc.* **2007,** *129* (15), 4512-4513; (b) Elliott, E. L.; Hartley, C. S.; Moore, J. S., Covalent ladder formation becomes kinetically trapped beyond four rungs. *Chem. Commun.* **2011,** *47* (17), 5028-5030.

17.   (a) Wei, T.; Jung, J. H.; Scott, T. F., Dynamic Covalent Assembly of Peptoid-Based Ladder Oligomers by Vernier Templating. *J. Am. Chem. Soc.* **2015,** *137* (51), 16196-16202; (b) Wei, T.; Furgal, J. C.; Jung, J. H.; Scott, T. F., Long, self-assembled molecular ladders by cooperative dynamic covalent reactions. *Polym. Chem.* **2017,** *8* (3), 520-527.

18.   Zhang, D.-W.; Li, Z.-T., Orthogonal Dynamic Covalent and Non-covalent Reactions. In *Dynamic Covalent Chemistry*, 2017.

19.   Furikado, Y.; Nagahata, T.; Okamoto, T.; Sugaya, T.; Iwatsuki, S.; Inamo, M.; Takagi, H. D.; Odani, A.; Ishihara, K., Universal Reaction Mechanism of Boronic Acids with Diols in Aqueous Solution: Kinetics and the Basic Concept of a Conditional Formation Constant. *Chemistry-a European Journal* **2014,** *20* (41), 13194-13202.

20.   Liu, Z. Q.; Hu, B. H.; Messersmith, P. B., Acetonide protection of dopamine for the synthesis of highly pure N-docosahexaenoyldopamine. *Tetrahedron Lett.* **2010,** *51* (18), 2403-2405.

21.   Zuckermann, R. N.; Kerr, J. M.; Kent, S. B. H.; Moos, W. H., Efficient Method For The Preparation Of Peptoids Oligo(N-Substituted Glycines) By Submonomer Solid-Phase Synthesis. *J. Am. Chem. Soc.* **1992,** *114* (26), 10646-10647.

22.   Kirshenbaum, K.; Barron, A. E.; Goldsmith, R. A.; Armand, P.; Bradley, E. K.; Truong, K. T.; Dill, K. A.; Cohen, F. E.; Zuckermann, R. N., Sequence-specific polypeptoids: a diverse family of heteropolymers with stable secondary structure. *Proc Natl Acad Sci U S A* **1998,** *95* (8), 4303-8.

23.   Churches, Q. I.; Hutton, C. A., Introduction, Interconversion and Removal of Boron Protecting Groups. In *Boron Reagents in Synthesis*, Coca, A., Ed. Amer Chemical Soc: Washington, 2016; Vol. 1236, pp 357-377.

24.   Sun, J.; Perfetti, M. T.; Santos, W. L., A Method for the Deprotection of Alkylpinacolyl Boronate Esters. *J. Org. Chem.* **2011,** *76* (9), 3571-3575.

25.   Wu, S.; Waugh, W.; Stella, V. J., Degradation pathways of a peptide boronic acid derivative, 2-Pyz-(CO)-Phe-Leu-B(OH)2. *Journal of Pharmaceutical Sciences* **2000,** *89* (6), 758-765.

26.   (a) Jackson, H.; Kendal, L. P., The Oxidation Of Catechol And Homocatechol By Tyrosinase In The Presence Of Amino-Acids. *Biochem. J.* **1949,** *44* (4), 477-487; (b) Yang, J.; Saggiomo, V.; Velders, A. H.; Stuart, M. A. C.; Kamperman, M., Reaction Pathways in Catechol/Primary Amine Mixtures: A Window on Crosslinking Chemistry. *PLoS One* **2016,** *11* (12), 17.

27.   Robertson, E. J.; Battigelli, A.; Proulx, C.; Mannige, R. V.; Haxton, T. K.; Yun, L. S.; Whitelam, S.; Zuckermann, R. N., Design, Synthesis, Assembly, and Engineering of Peptoid Nanosheets. *Accounts Chem. Res.* **2016,** *49* (3), 379-389.

28.   Benesi, H. A.; Hildebrand, J. H., A Spectrophotometric Investigation Of The Interaction Of Iodine With Aromatic Hydrocarbons. *J. Am. Chem. Soc.* **1949,** *71* (8), 2703-2707.

29.   Badjic, J. D.; Nelson, A.; Cantrill, S. J.; Turnbull, W. B.; Stoddart, J. F., Multivalency and cooperativity in supramolecular chemistry. *Accounts Chem. Res.* **2005,** *38* (9), 723-732

Chapter 6 Information-directed Assembly of Base-4 Molecular Ladders and Grids

6.1 Abstract

Dynamic covalent chemistry has been introduced as a method of assembling molecular architectures that are both tough and precise when compared to structures built from classic molecular self-assembly mechanisms. This chapter combines two of these chemistries, the boronate ester and Schiff base imines from amine and aldehyde groups, to ultimately direct the assembly of base-4 molecular ladders and grids. We developed analogous pH-mediation conditions between the two systems to control their hybridization. We then began to explore the orthogonality between to the two reactions through a detailed cross-examination of monomers that suggested the systems were compatible. Fabricating a 3 x 3 molecular grid that was comprised of a catechol and aldehyde functionalized core strand and two complementary boronic acid and amine side strands further demonstrated their orthogonality. The four functional groups were then incorporated into the same strands to build a base-4 molecular ladder and another 3 x 3 molecular grid. This approach highlights the potential of utilizing these two chemistries to fabricate structures with an increased information density.

6.2 Introduction

Nucleic acids (DNA and RNA) are information-bearing molecular ladders that transport information through a sequence of nucleotides. Specifically, DNA consists of two single stranded sugar-phosphate backbones attached with a sequence of complementary nucleobase residues that self-assembly into a base-4 molecular ladder *via* hydrogen bonding.[1] The select

hybridization of DNA led to the genesis of the field of nucleic acid nanotechnology.[2] The idea of utilizing DNA as a construction material was further developed by techniques such as DNA origami[3], a fabrication technique, that involves the synthesis of pre-determined two-dimensional shapes by raster-filling with a long, viral single-stranded DNA of a known sequence held in places with several shorter oligomeric 'staple strands.' Other methods were developed that exclusively utilize shorter nucleic acid strands which can be synthetically fabricated for increased chemical diversity; these so-called 'DNA tiles' and 'DNA bricks' are able to assemble into complex 2D and 3D structures in a single annealing reaction.[4] The process of DNA melting and annealing is central to DNA's ability to form sequence-specific structures without mismatched pairs. The sensitivity of nucleic acid hybridization has resulted in widespread use of techniques such as PCR[5] and DNA microarrays.[6]

Despite nucleic acid nanotechnology making significant strides in recent years, there are still mechanical and thermal limitations in assembled structures owing to the hydrogen bonds between nucleobases. Throughout several biological processes, it is essential that DNA be able to undergo force-induced melting;[7] in fact, double stranded DNA mechanically unzips under a force of ~15 pN.[8] This is unfavorable for producing durable nanostructures. In previous work, we have shown the fabrication of double stranded structures that incorporate stronger covalent bonds through reversible dynamic covalent bonds. [9] Dynamic covalent chemistry, a class of chemical reactions that are reversible under a particular set of reaction conditions, is essential for the bonds to rearrange to form the most thermodynamically stable product while maintaining the strength of covalent bonds. We have explored this idea first through a condensation reaction that of amines and aldehydes co-reacting to form Schiff base imines, and more recently with a likewise condensation reaction between boronic acid and catechol to form a boronate ester.

Orthogonality has been used to describe many chemical processes throughout time, but here it refers to the ability of the two reactions to proceed efficiently in the presence of the other functional groups. Some of the early examples of chemical orthogonality between dynamic covalent reactions were reported between the boronate ester and imine reactions.[10] Indeed, the Severin group used these two reactions to assemble macrocycles molecular cages, and dendritic nanostructures.[11] This work highlights the combination of two dynamic covalent chemistries in the synthesis of a base-4 information system that has been designed to form double stranded molecular ladders and molecular grids. Herein we describe the conditions necessary to form specific molecular architectures comprised of imine and boronate ester linkages by first exploring reaction conditions for the individual systems and then combining them to form base-4 information directed assemblies.
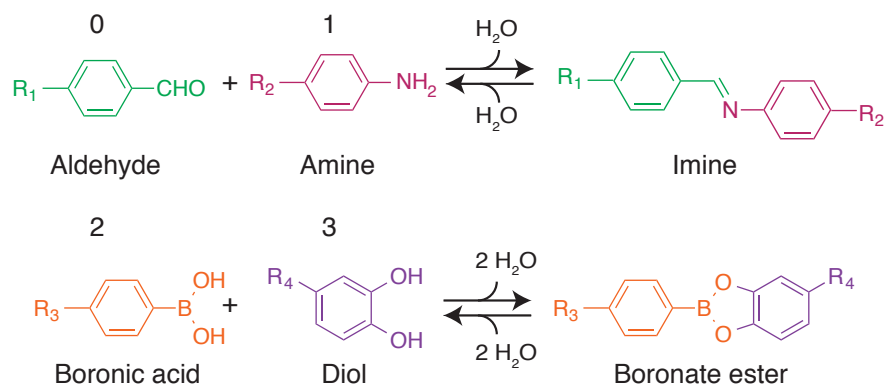
Scheme 6.1. Dynamic Covalent Chemistries a) Schiff base imine system: where the amine functional group will be referred to as "1" and the aldehyde as "0" b) boronate ester system: where the boronic acid functional group will be referred to as "2" and the catechol as "3"

6.3 Experimental

6.3.1. General Methods

^{1}H NMR and ^{11}B NMR spectra of the monomers were collected using a Varian MR400 spectrometer. Chemical shifts were measured in δ (ppm) relative to residual solvent (CD$_3$CN = 1.94). Electrospray ionization mass spectrometry (ESI-MS) mass spectra were recorded using an Agilent Q-TOF 1200 series spectrometer in positive ion mode. Matrix-assisted laser desorption/ionization (MALDI-TOF) time-of-flight mass spectra were collected by utilizing a Bruker Autoflex mass spectrometer used in reflectron mode with both positive and negative ionizations as indicated. Reverse phase high performance liquid chromatography (RP-HPLC) was performed using both a preparative reversed phase Phenomenex Luna C18(2) columns with a linear gradient of water and acetonitrile as the eluent at 30°C as well as an analytical scale column. The RP-HPLC system was equipped with dual Shimadzu LC-6AD HPLC pump, Shimadzu FRC 70A fraction collector, and monitored using Shimadzu Prominence detector at 214nm. Unless otherwise noted all reagents and materials were purchased from commercial sources including Sigma Aldrich, AK Scientific, Oakwood Chemical, and TCI Chemical.

6.3.2. Oligomer Synthesis

Oligopeptoid Synthesis

Peptoid Backbone
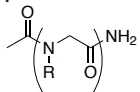
Inert Spacer Monomers
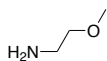
Nme = 2-methoxyethylamine
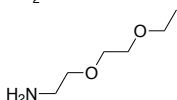
Neee = 2-(2-ethoxyethoxy)ethylamine

Dynamic Covalent Monomers
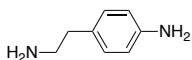
Nam = 4-(2-aminoethyl)aniline
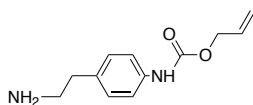
Npam = 4-(2-aminoethyl)-N-(allylcarbonyloxy)phenylamine
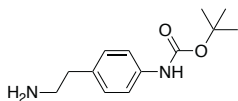
Nbam = tert-butyl (4-(2-aminoethyl)phenyl)carbamate
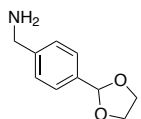
Nal = 4-(aminomethyl)benzaldehyde
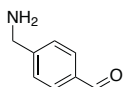
Npal = 4-(1,3-dioxacyclopent-2-yl)benzylamine
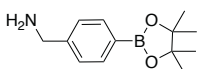
Npbe = 4-aminomethylphenylboronic acid, pinacol ester
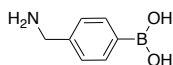
Npba = (4-(aminomethyl)phenyl)boronic acid

Nace = dopamine(acetonide)

Ndop = dopamine

159
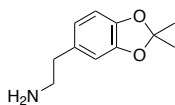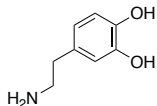
Figure 6.1. Primary amine monomers used throughout this study. The "R" on the oligopeptoid backbone can be any primary amine. We used two categories of primary amine to incorporate functionality into our oligomers: inert spacer monomers and dynamic covalent monomers. The inert spacers are used to control solubility and spatial resolution and the dynamic covalent monomers are used to direct the assembly of the oligomers.

The peptoid-based oligomers were prepared using a microwave-assisted Liberty Blue peptide synthesizer (CEM Corporation) that had been modified to synthesize peptoids. The peptoids of the imine only system were synthesized on a photolabile solid support resin to maintain the acid-labile acetal and alloc protecting groups. The remaining peptoids were synthesized on acid labile rink amide resin. Both of the resins contain a fluorenylmethyloxycarbonyl (Fmoc)-protected amine that is initially deprotected prior to synthesis by treatment in 4-methylpiperidine: dimethylformamide (DMF) (20:80, volume ratio) to yield a terminal amine on the solid support. The synthesis then proceeds by a sequential addition reaction whereby that amine is acetylated with 1 M bromoacetic acid using 1.2 M diisopropylcarbodiimide (DIC) as an activator for 5 minutes at 75°C, to afford a terminal bromide which is subsequently displaced via nucleophilic substitution with a 0.5 M primary amine for 5 minutes at 75°C. This two-step process is followed to synthesize the different predefined sequences. The N-terminal of the complementary oligomers was capped with 1 M acetic anhydride activated with DIC to prevent further chain elongation. The primary amines fall into two categories, dynamic covalent functional groups and inert spacer monomers (Figure S1). The dynamic covalent functional group consisted of the prepared dopamine (acetonide) (Nace), 4-(2-aminoethyl)-*N*-(*tert*-butoxycarbonyl)phenylamine (Nbam)[9a], 4-(2-aminoethyl)-N-(allylcarbonyloxy)phenylamine (Npam)[12] , (Npal)[9a], and commercially available 4-Aminomethylphenylboronic acid, pinacol ester (Npbe) purchased from AccelaChem. The inert spacer monomers were commercially available 2-methoxyethylamine (Nme) and 2-

ethoxyethoxyethylamine (Neee) prepared from the established protocol of Wei et al.[9a] All of the

reagents were prepared in dimethylformamide (DMF) with the exception of the monomers used

in the imine only system that were prepared in N-Methyl-2-pyrrolidone (NMP) for increased

solubility. A table of the peptoid strands and their expected masses can be found in

supplementary information Table S1.

Table 6.1. Shorthand nomenclature of peptoids used in Chapter 6, and the associated sequence and exact mass

peptoid	sequence	exact mass (g/mol)
imine system		
11000	$(NeeeNam)_2(NeeeNpal)_3$	1934.0
00111	$Nme(NeeeNpal)_2(NeeeNam)_3Nme$	2121.1
01010	$(NpalNeeeNamNee)_2Npal$	1760.9
10101	$(NamNeeeNpalNee)_2NamNme$	1832.9
boronate ester system		
222333	$(NmeNdop)_2(NmeNpba)_2$	2016.9
223233	NmeNdopNmeNdopNmeNpbaNmeNdopNmeNpbaNpba	1901.9
single interaction		
0	$Nme_2NalNme_2$	694.4
1	$Nme_2NamNme_2$	695.4
2	$Nme_2NpbaNme_2$	710.4
3	$Nme_2NdopNme_2$	712.4
orthogonal grid		
303030	$(NdopNal)_3$	1163.5
222	$(NmeNpba)_3Nme$	1092.5
111	$(NeeeNam)_3$	1106.6
base-4 system		
211312	$NmeNpba(NmeNam)_2NmeNdopNmeNamNmeNpbaNme$	1968.0
300203	NmeNdopNmeNalNmeNalNmeNpbaNmeNalNmeNdop	1851.8
base-4 grid		
230	NmeNpbaNmeNdopNmeNal	963.4
123231	$Nam(NpbaNdop)_2Nam$	1179.5

6.3.3. Imine System Deprotection and Cleavage

Peptoids bearing alloc-protected amines (imine only system) were deprotected via an adaptation of a previously reported approach.[12] On-resin peptoids were suspended in dry DCM and treated with 0.1 equivalents tetrakis(triphenylphosphine)palladium(0) and 25 equivalents of phenylsilane per alloc group for one hour. After filtration, deprotection was repeated and the photo-labile resin was subsequently cleaved in DMF for 36 hours under irradiation at approximately 25 mW/cm^2 with 405 nm. The cleavage solution was filtered and evaporated to dryness under vacuum.

6.3.4. Additional Peptoids Deprotection and Cleavage

The remaining peptoids (boronate ester and base-4 systems) were cleaved from the acid-labile solid support resin by a 5 minute incubation with a cleavage cocktail containing 95% trifluoroacetic acid (TFA) and 5% water in a glass fritted reaction vessel. The resin was then rinsed with methylene dichloride (DCM) to remove any residual peptoid on the resin. The solvents (DCM and trace water) and TFA were removed by blowing with a N$_2$ stream. The acid-labile protecting groups acetonide, acetal, and boc were removed by TFA during the cleavage. The pinacol protecting group is not compressively removed during the cleavage step, but the remaining pinacol can be removed during purification with reverse phase high performance chromatography (RP-HPLC).[13] Once only the peptoid residue remained, the peptoids were put into a 50:50 solution of 0.1%TFA acetonitrile and 0.1%TFA water (approximate pH=3) this was to influence the equilibrium of the dynamic covalent reactions towards the initial functional groups.

6.3.5. Peptoid Purification

The oligopeptoids were purified by preparative scale RP-HPLC using a linear gradient of acetonitrile and water. Major peaks were collected and fractions were combined before utilizing ESI-MS to confirm the identity of each strand. ESI-MS and analytical RP-HPLC traces of the purified peptoids can be found in supplementary information Figures 6.2-6.7. Fractions of the peptoids were combined and lyophilized to a white powder.
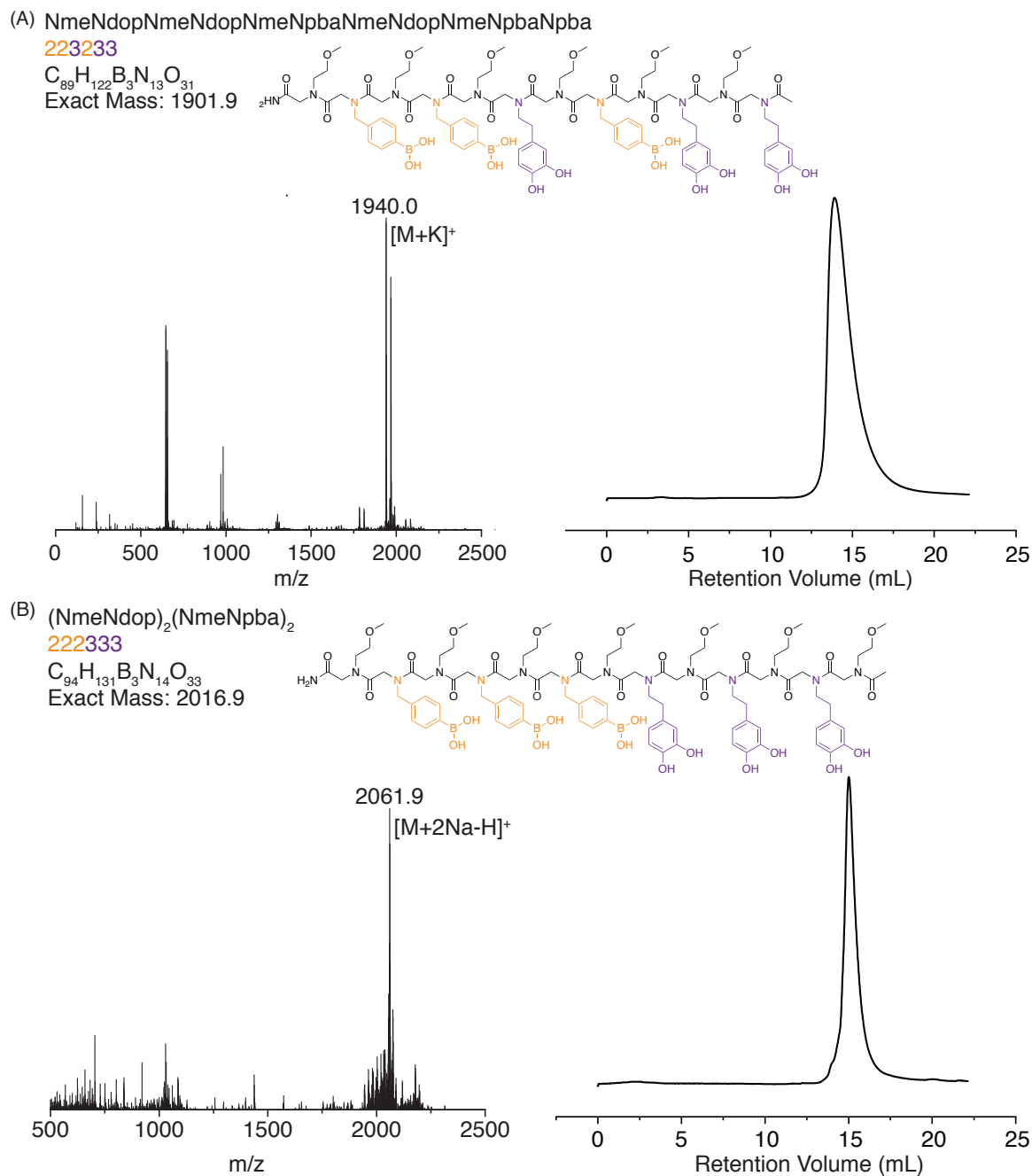
Figure 6.2. ESI-MS mass spectra and corresponding analytical HPLC traces for the self-hybridizing boronate ester peptoids (a) [223233+K]$^+$ = 1940.0g/mol, 99.5% purity (b) [222333+2Na-H]$^+$ = 2061.9 g/mol, 99.1% purity

(A) (NeeeNam)₂(NeeeNpal)₃
11000
C₉₈H₁₄₃N₁₃O₂₇
Exact Mass: 1934.0
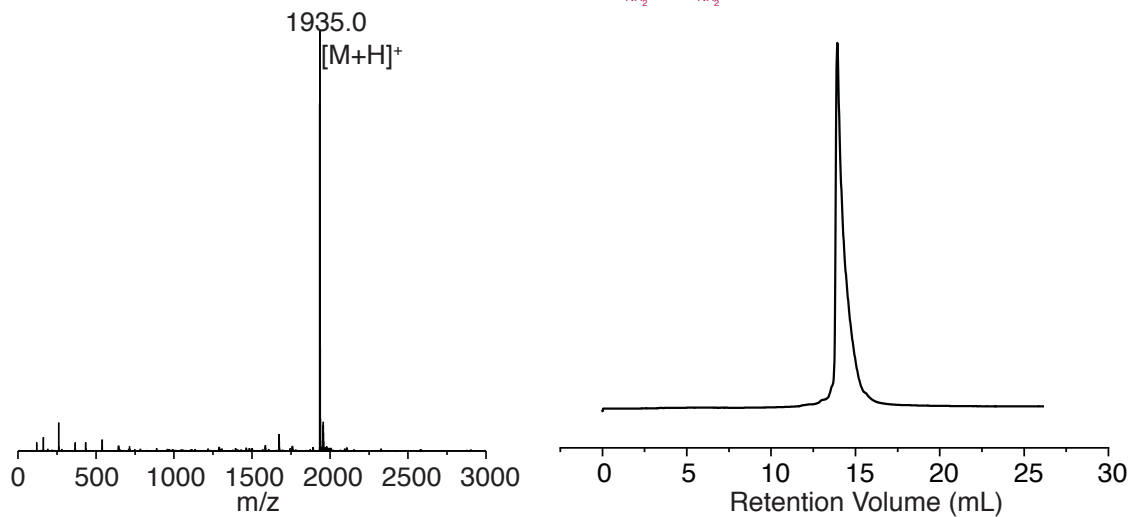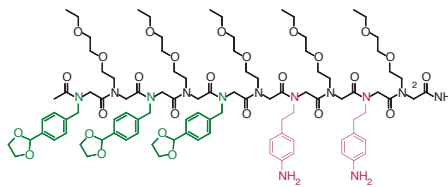
1935.0
[M+H]⁺

(B) Nme(NeeeNpal)₂(NeeeNam)₃Nme
00111
C₁₀₆H₁₆₀N₁₆O₂₉
Exact Mass: 2121.1

2122.1
[M+H]⁺

707.4
[M+3H]³⁺

(C) (NamNeeeNpalNee)$_2$NamNme
01010
$C_{90}H_{128}N_{12}O_{24}$
Exact Mass: 1760.9

1761.9

[M+H]$^+$

m/z

Retention Volume (mL)

(D) (NamNeeeNpalNee)$_2$NamNme
10101
$C_{93}H_{136}N_{14}O_{24}$
Exact Mass: 1832.9

1833.9

[M+H]$^+$

611.3
[M+3H]$^{3+}$

m/z

Retention Volume (mL)
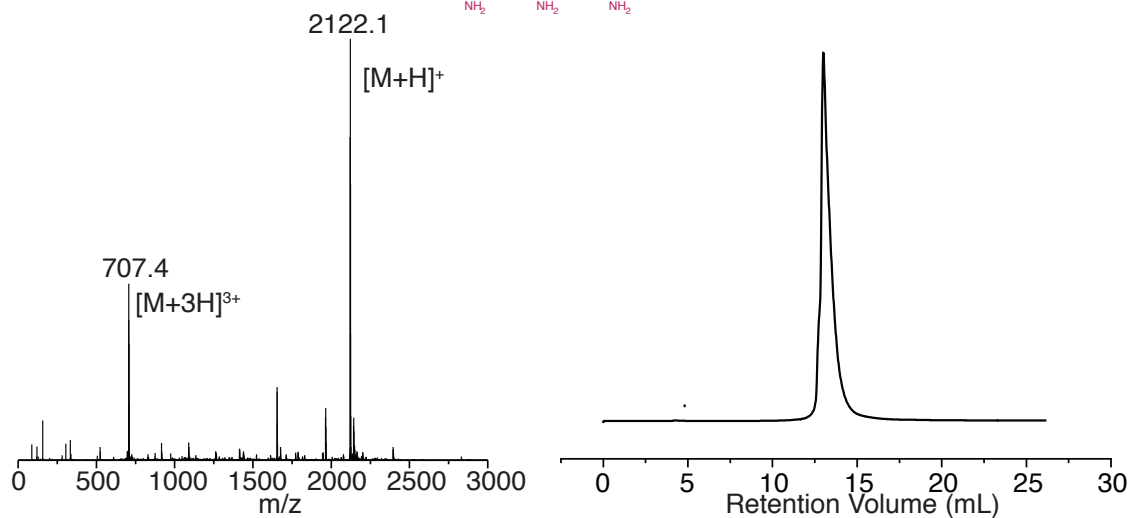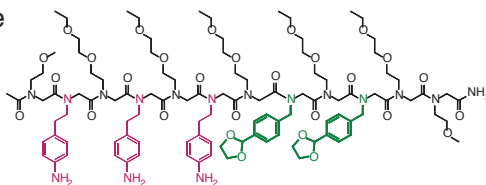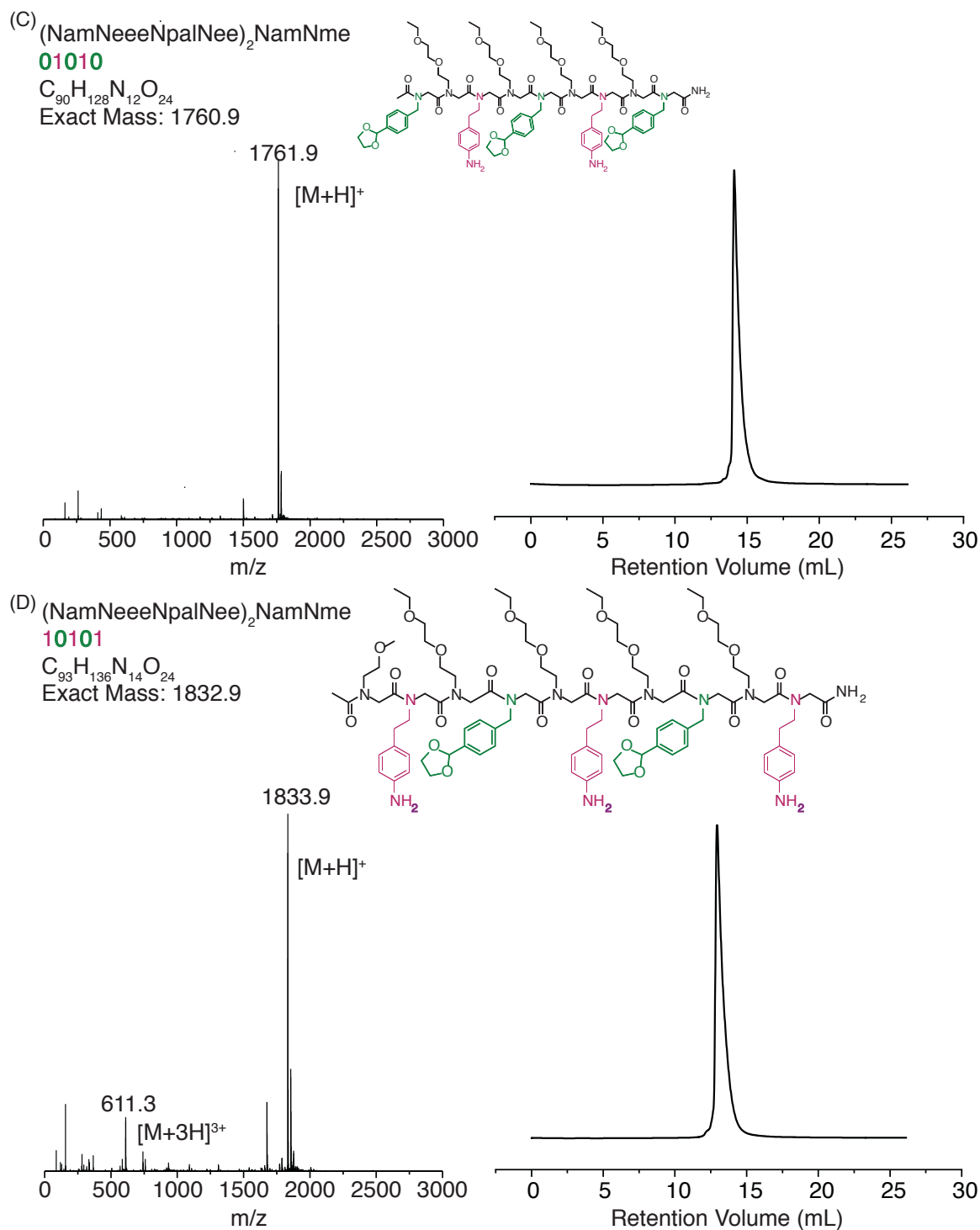
Figure 6.3. ESI-MS mass spectra and corresponding analytical HPLC traces for the peptoids that formed the imine only molecular ladders (a) [11000+H]$^+$ = 1935.0g/mol, 98,7% purity (b) [00111+H]$^+$ = 2122.1 g/mol, 99.6% purity c) [01010+H]$^+$ = 1761.9 g/mol, 99.2% purity; and (d) [10101+H]$^+$ = 1833.9 g/mol, 99.6% purity

167

(A)
Nme$_2$NalNme$_2$
0
C$_{32}$H$_{50}$N$_6$O$_{11}$
Exact Mass: 694.4

717.4

[M+Na]$^+$

[M+H]$^+$

0   200   400   600   800   1000
(m/z)

0   5   10   15   20   25
Retention Volume (mL)
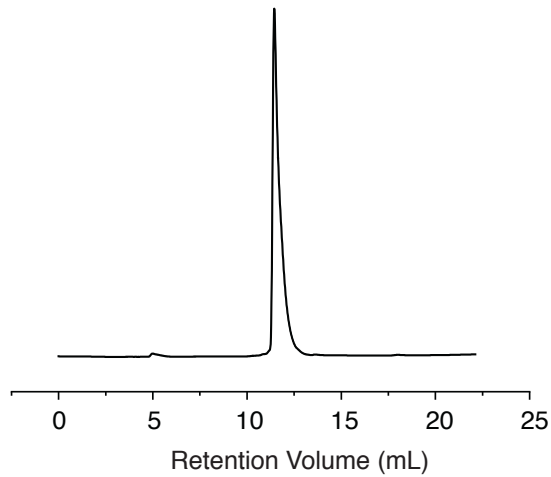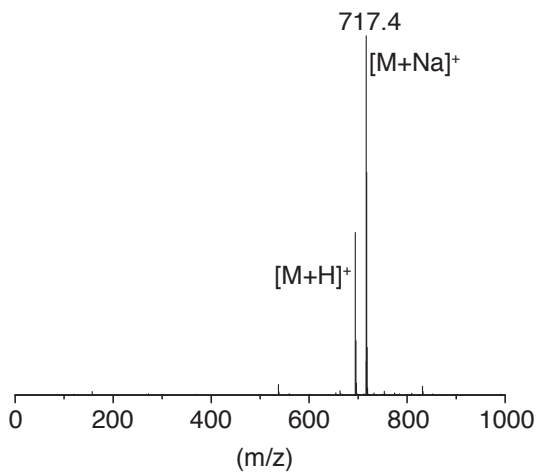
(B)
Nme$_2$NamNme$_2$
1
C$_{32}$H$_{53}$N$_7$O$_{10}$
Exact Mass: 695.4

718.4

[M+Na]$^+$

[M+H]$^+$

0   200   400   600   800   1000
m/z

0   5   10   15   20   25
Retention Volume (mL)

168

(C) Nme₂NpbaNme₂
2
$C_{31}H_{51}BN_6O_{12}$
Exact Mass: 710.4

711.4
[M+H]⁺

(D) Nme₂NdopNme₂
3
$C_{32}H_{52}N_6O_{12}$
Exact Mass: 712.4

713.4
[M+H]⁺
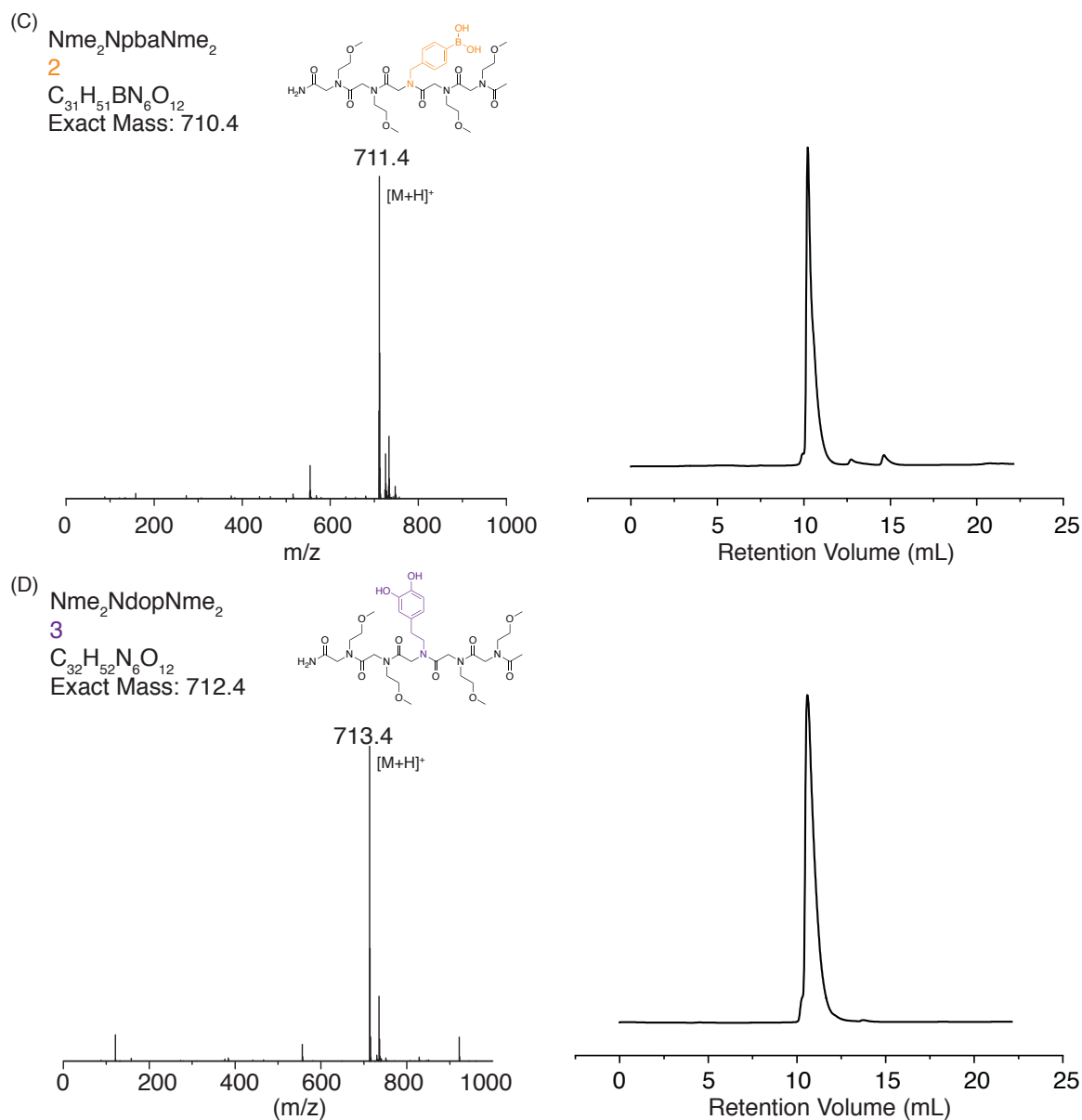
Figure 6.4. ESI-MS mass spectra and corresponding analytical HPLC traces for the single interaction peptoids used for NMR analysis. (a) $[0+Na]^+$ = 717.4 g/mol, 98.4% purity (b) $[1+Na]^+$ = 718.4 g/mol, 97.9% purity (c) $[2+H]^+$ = 711.4 g/mol, 93.5% purity; and (d) $[2+H]^+$ = 711.4 g/mol, 99.3% purity

(A)
(NdopNal)₃
303030
$C_{62}H_{65}N_7O_{16}$
Exact Mass: 1163.5

1186.4

$[M+Na]^+$

(m/z)

Retention Volume (mL)
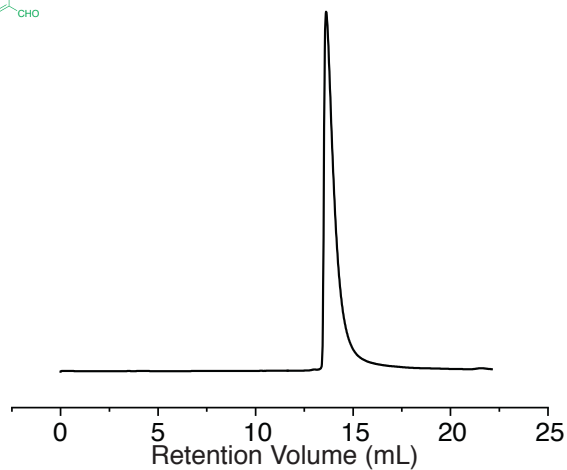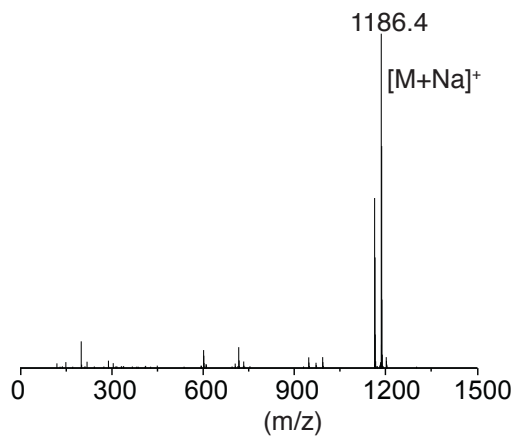
(B) (NmeNpba)₃Nme
222
$C_{49}H_{71}B_3N_8O_{18}$
Exact Mass: 1092.5

1110.5

$[M+NH_4]^+$

(m/z)

Retention Volume (mL)

170

(C) (NeeeNam)$_3$
111
$C_{56}H_{86}N_{10}O_{13}$
Exact Mass: 1106.6

1107.6

[M+H]$^+$

m/z

Retention Volume (mL)
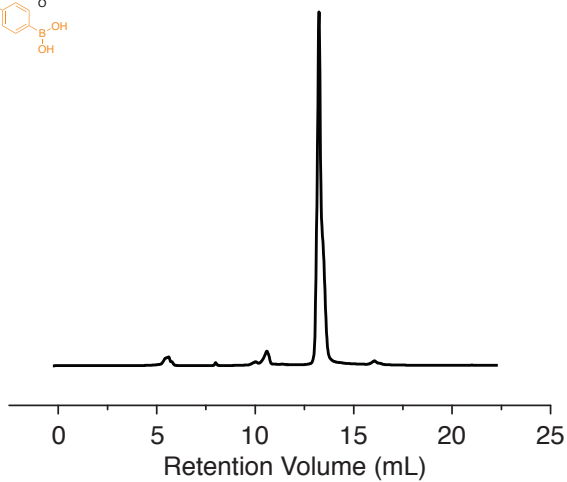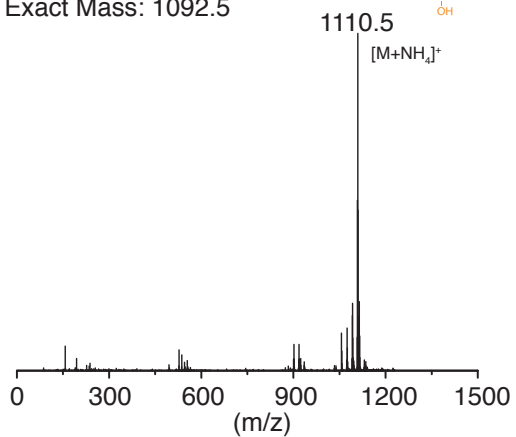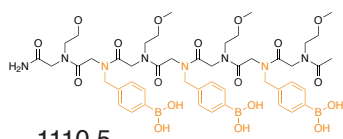
Figure 6.5. ESI-MS mass spectra and corresponding analytical RP-HPLC traces for the peptoids that assembled into the 3 x 3 molecula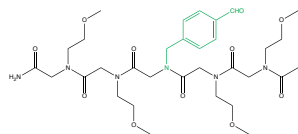r grid from a core peptoid comprised of catechol and aldehyde functional groups. (a) [303030+Na]$^+$ = 1186.4 g/mol, 99.4% purity (b) [222+NH$_4$]$^+$ = 1110.5 g/mol, 95.5% purity; and (c) [111+H]$^+$ = 1761.9 g/mol, 97.7% purity

(A)
NmeNpba(NmeNam)₂NmeNdopNmeNamNmeNpbaNme
211312
$C_{95}H_{135}B_2N_{17}O_{27}$
Exact Mass: 1968.0

1969.0
[M+H]⁺

m/z

Retention Volume (mL)

(B)
NmeNdopNmeNalNmeNalNmeNpbaNmeNalNmeNdop
300203
$C_{96}H_{118}BN_{13}O_{28}$
Exact Mass: 1851.8
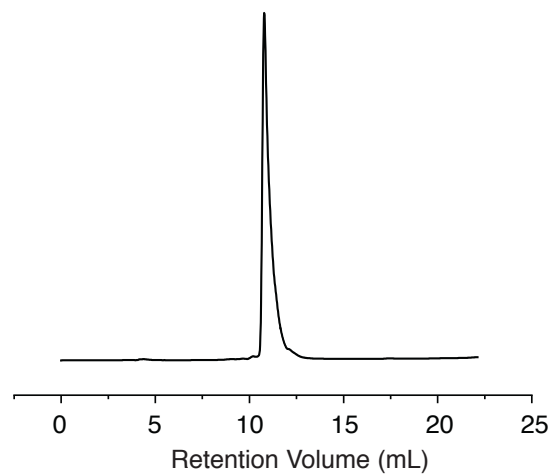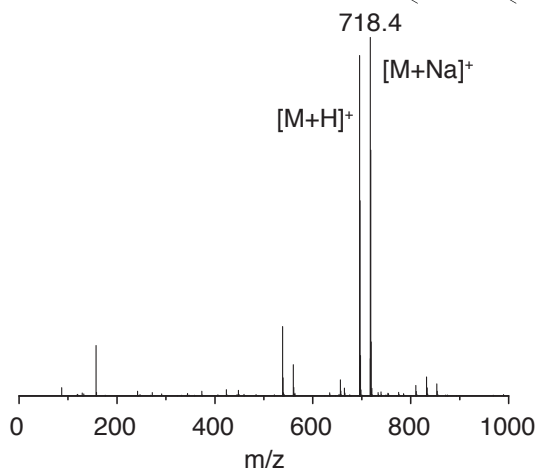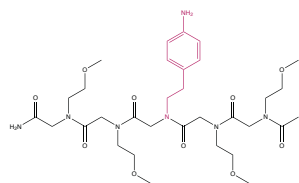
1874.8
[M+Na]⁺

[M+3H]³⁺

m/z

Retention Volume (mL)
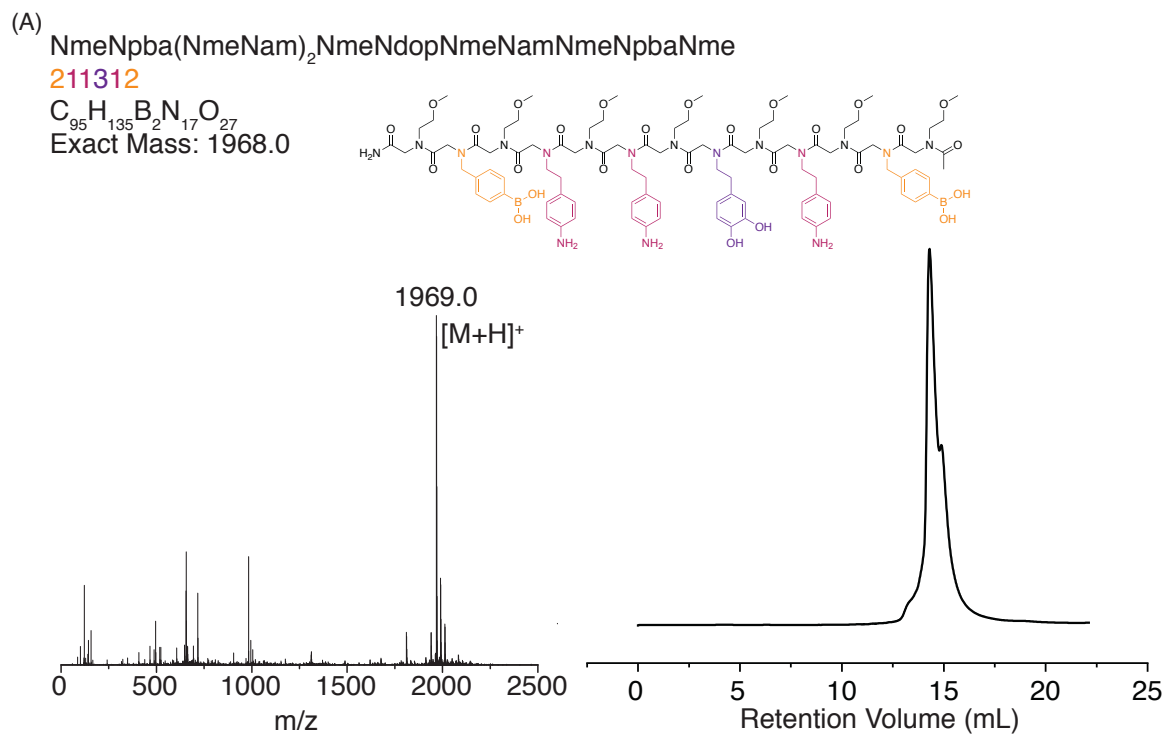
Figure 6.6. ESI-MS mass spectra and corresponding analytical RP-HPLC traces for the peptoids that assembled into base-4 molecular ladder (a) [211312+H]⁺ = 1969.0 g/mol, 65.0% purity (b) [300203+Na]⁺ = 1874.8 g/mol, 96.9% purity

172

(A)
NmeNpbaNmeNdopNmeNal
230
$C_{46}H_{62}BN_7O_{15}$
Exact Mass: 963.4

986.4

[M+Na]$^+$

(m/z)

Retention Volume (mL)

(B)
Nam(NpbaNdop)$_2$Nam
123231
$C_{60}H_{71}B_2N_9O_{15}$
Exact Mass: 1179.5

1180.5

[M+H]$^+$

(m/z)

Retention Volume (mL)
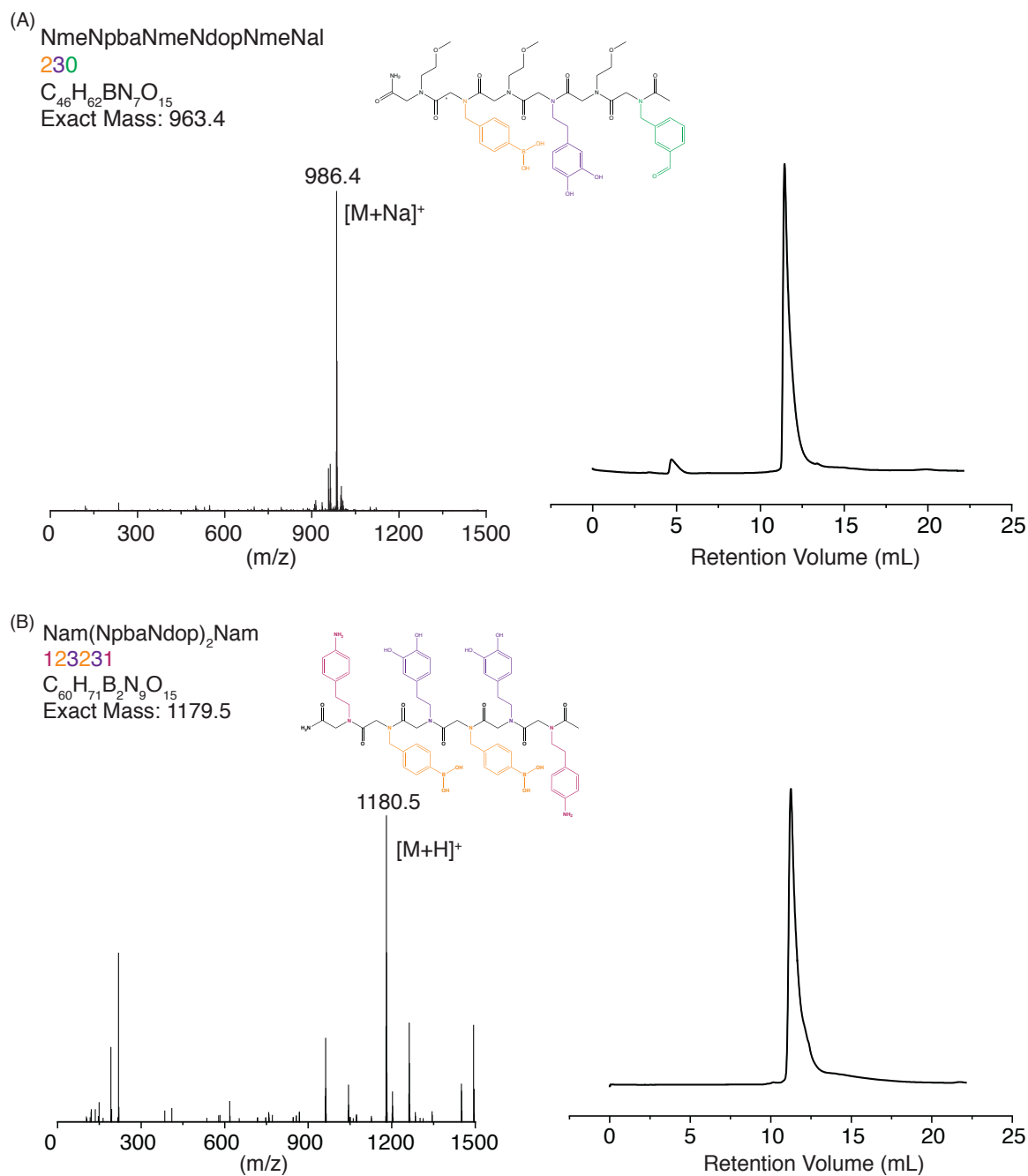
Figure 6.7. ESI-MS mass spectra and corresponding analytical RP-HPLC traces for the peptoids that assembled into base-4 molecular grid (a) [230+Na]$^+$ = 986.4 g/mol, 95.4% purity (b) [123231+H]$^+$ = 1180.5 g/mol, 99.3% purity

173

6.3.6. Boronate Ester Molecular Ladders (Hybrid-BE-1 and Hybrid-BE-2)

10 mM stock solutions of the self-hybridizing boronic acid and catechol-bearing peptoids were prepared in a 50:50 mixture 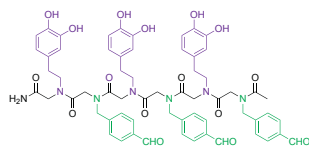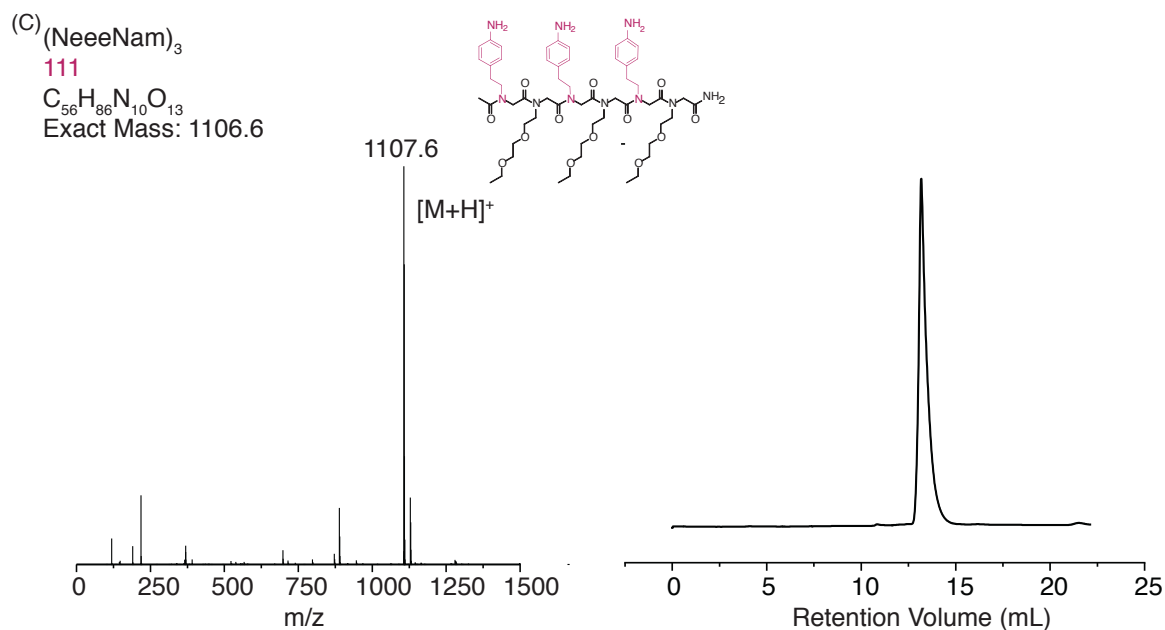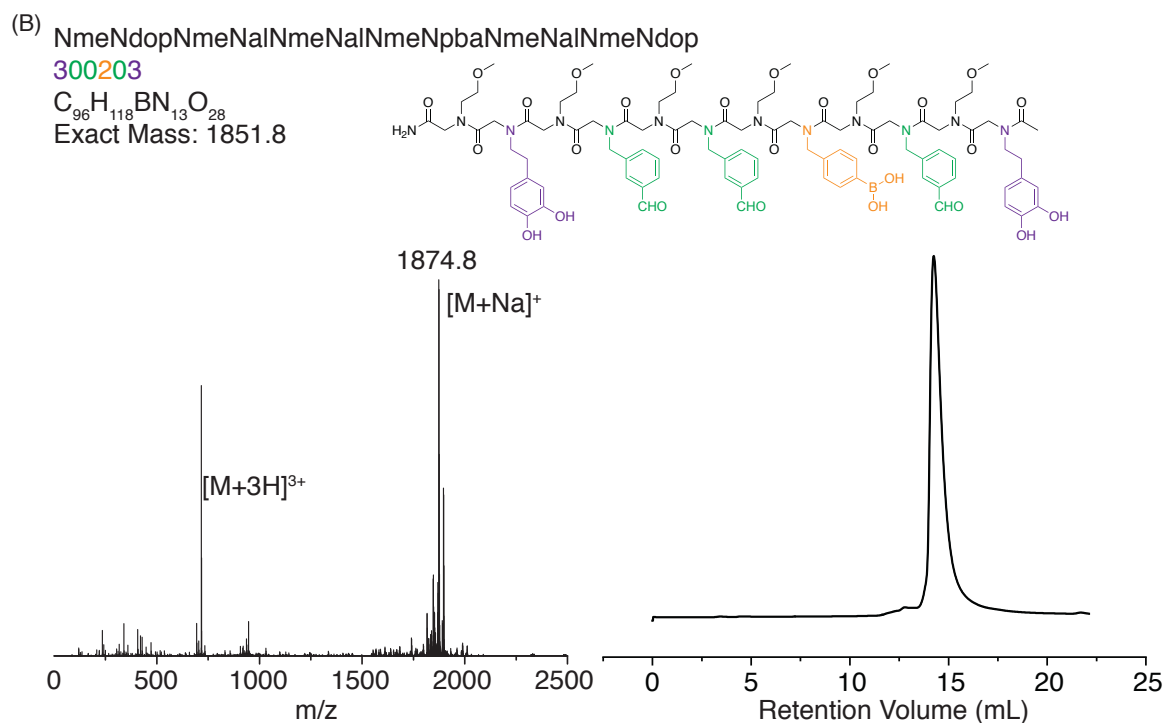of acetonitrile and water. 20 μL of the boronate ester peptoids were put in a vial of 180 μL basic aqueous solution where the pH of the solution was previously adjusted to be approximately 9 with sodium hydroxide. The vial was stirred overnight and MALDI-TOF mass spectrometry in negative ion mode was used to confirm the formation of a molecular ladder in the anti-parallel configuration. The negative mode MALDI-TOF samples were prepared by mixing 4 μL of matrix (5 mg of α-Cyano-4-hydroxycinnamic acid in 1mL of 50:50 MeCN:Water) with 2 μL of the reaction mixture. Table 6.2 shows the nomenclature of all assembled structures and their corresponding exact mass.

Table 6.2. Nomenclature and corresponding exact mass for assembled structures used in this study.

Molecular Ladder	Exact Mass (g/mol)	Initial Peptoids
Hybrid-BE-1	3817.9	$(222333)^2$
Hybrid-BE-2	3587.7	$(223233)^2$
Hybrid-I-1	3745.0	00111 x 11000
Hybrid-I-2	3283.7	10101 x 01010
Triplex-1	3200.5	303030 x 111 x 222
Hybrid-O1	3657.7	211312 x 300203
Triplex-2	2926.4	123321 x $(230)^2$

6.3.7. Imine Molecular Ladders (Hybrid-I-1 and Hybrid-I-2)

A vial was charged with 20 μL of 10 mM imine-bearing peptoids and 100 μL of trifluoroacetic acid. The mixture was gently stirred for 20 minutes. 400 μL of chloroform were added before adjusting the pH to 14 with 1 M NaOH. The solution was allowed to stand until a clean phase separation was observed. The organic layer was removed using a pipette. Residual NaOH was removed via subsequent extractions with brine and water. The mixture was stirred overnight and characterized by positive mode MALDI-TOF mass spectrometry using

hydroxyazobenzene-2-carboxylic acid (HABA) as the matrix. HABA samples were prepared by mixing 3:1 ratio of a saturated HABA solution in acetonitrile to the reaction mixture.

6.3.8. Orthogonal Molecular Grid (Triplex-1)

Triplex-1 was formed by adding 20μL from 10mM stock solutions of both the boronic acid bearing peptoid (NmeNpba)$_3$Nme and the peptoid with both aldehyde and catechol functional groups (NdopNald)$_3$ along with 5 μL of 10mM solution of the amine functionalized peptoid (NeeeNam-p3), and lastly, 2 μL of a 10mM solution of scandium (III) triflate into an aqueous solution. We looked at 3 different pH solutions ~5, 7, and 9 that brought the final volume of the reaction mixture to 200 μL. The solution was allowed to stir overnight before being analyzed by both positive and negative mode MALDI-TOF. There were also observable amounts of duplex structures formed by the core peptoid ((NdopNald)$_3$) and two complementary side strands ((NmeNpba)$_3$Nme and (NeeeNam)$_3$). The imine-bearing duplex structure tended to have a higher relative intensity in MALDI-TOF spectra ultimately leading to the decrease in the initial concentration of (NeeeNam)$_3$. This allowed for the triplex structure to have a higher intensity in mass spectra. We also varied the order of adding each of the reactants by adding the core strand (NdopNald)$_3$ and just one of the side strands and allowing that reaction to proceed overnight before adding the third peptoid strand.

6.3.10. Cross Reactivity

100mM stock solutions of commercially purchased aniline, benzaldehyde, phenylboronic acid, and catechol were prepared in CD$_3$CN. Six different sample pairs were prepared by adding equal volumes (300 μL) of each monomer to a vial. These samples were such that each functional group was reacted with each of the other three functional groups. The reaction was allowed to stir for 3 hours before ^{1}H NMR and ^{11}B NMR spectra were collected. The ^{11}B NMR

spectra were collected in a quartz NMR tube. 50 mM stock solutions of the single interaction peptoids (Nme$_2$NpbaNme$_2$, Nme$_2$NdopNme$_2$, Nme$_2$NamNme$_2$, and Nme$_2$NpbaNme$_2$) in CD$_3$CN, the peptoids were then mixed with their complementary strand and allowed to react overnight before collecting ^{1}H NMR spectra.

6.3.11. Base-4 Molecular Ladder (Hybrid-O1) and Grid (Triplex-2)

10 mM stock solutions of the base-4 molecular ladder and molecular grid peptoids were prepared in a 50:50 mixture of acetonitrile and water. The base-4 molecular ladder (Hybrid-O1) was prepared by adding 20µL of each of the two complementary peptoids (211312 x 300203) with 2 µL of a 10mM solution(water) of scandium (III) triflate were put in a vial of 158 µL basic aqueous solution where the pH of the solution was previously adjusted to be approximately 9 with sodium hydroxide. The vial was stirred overnight in anaerobic conditions and MALDI-TOF mass spectrometry in negative ion mode was used to confirm the formation of a molecular ladder in the anti-parallel configuration. The negative mode MALDI-TOF samples were prepared by mixing 4 µL of matrix (5 mg of α-cyano-4-hydroxycinnamic acid in 1mL of 50:50 MeCN:Water) with 2 µL of the reaction mixture. Likewise, the base-4 molecular grid (Triplex-2) was prepared by adding 10 µL of the core strand (123321) with 20 µL of the side strand (230) and 2 µL of the same 10mM solution (water) of scandium (III) triflate into a basic aqueous water solution final volume 200 µL. The reaction was allowed to stir overnight in anaerobic conditions before a negative mode MALDI-TOF sample was prepared as described for the base-4 molecular ladder.

6.4.12. Base-4 Selectivity

4 µL of a 10mM solution of a self-hybridizing boronate ester peptoid (223233) was added to a solution with the two complementary peptoids (211312 x 300203) with 2 µL of scandium (III) triflate (10mM) in a basic aqueous solution to a final volume of 200 µL. The mixture

176

reacted overnight in anaerobic conditions before a negative mode MALDI-TOF spectrum was collected.

6.4 Results and Discussion

6.4.1. Boronate Ester Molecular Ladders

In contrast to DNA, which undergoes a melting and annealing process to form precise double stranded structures, we employed an analogous pH-mediated based system for controlling the reaction equilibrium and ultimately the hybridization of duplex structures. The equilibrium of our dynamic covalent reactions will favor the initial single stranded oligomers at an acidic pH and the assembled structure as the pH increases. First, we examined the two different dynamic covalent systems individually to determine their ability to form structures from binary strands before combining the systems. We did this by designing and synthesizing oligomeric peptoid structures that serve as the sides of our molecular ladders. Peptoids, poly-n-substituted glycine, can be readily synthesized to incorporate the different functionalities necessary to direct the assembly of the oligomers into molecular ladders. We used five different protected monomers bearing dynamic covalent functional groups and two inert spacer monomers throughout this study that can be found in the supporting information. The oligopeptoids were synthesized with protecting groups on the different monomers to minimize potential side reactions during synthesis.

The boronate ester formation is highly dependent on the pH of the solution; has been reported that the binding constants between phenyboronic acids and catechols to be 150 M^{-1} at pH of 6.5; the binding constant dramatically increases to 3300 M^{-1} at a pH of 8.5.[14] This allowed us to use pH to control the hybridization of the oligomers. This was done with peptoids bearing catechol, denoted by "3," and boronic acid, denoted by "2," functional groups that were designed

177

to self-hybridize in an anti-parallel configuration as shown in Figure 1a. The oligopeptoids were synthesized with acid-labile protecting groups on the boronic acid and catechol groups. The oligomers were cleaved from the likewise acid-labile solid support resin and deprotected of the protecting groups to yield the desired peptoids with exposed dynamic covalent functionality after incubation with a cleavage cocktail including trifluoroacetic acid (TFA). The peptoid residue was then put into a mixture of 50:50 acetonitrile: water containing 0.1% TFA. Owing to the pH of the solution (~3) and the water solubility of the oligomers, we were able to use high performance liquid chromatography to purify unhybridized strands with the desired functionality. The purified peptoids were then hybridized in a basic aqueous solution where the pH had been adjusted to 9 with sodium hydroxide to form the desired molecular ladder as shown in the negative mode MALDI-TOF spectra in Figure 6.8. The condensation reaction forming each boronate ester resulted in the loss of two water molecules making out of registry or unreacted functional groups observable through mass spectrometry.
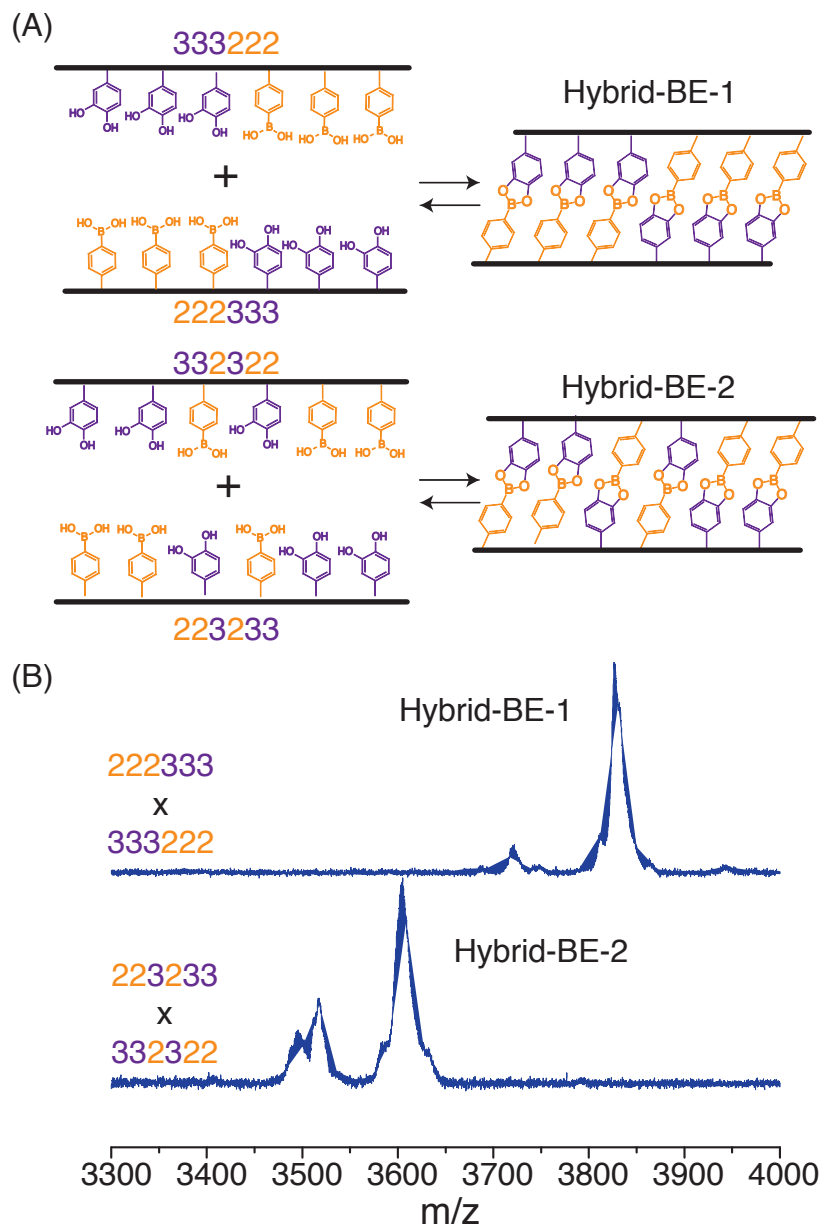
Figure 6.8. Information-directed assembly of boronate ester molecular ladder (a) schematic showing the formation of molecular ladders from self-hybridizing oliogpeptoid strands (b) negative mode MALDI-TOF confirming the formation of the molecular ladders

179

6.4.2. Imine Molecular Ladders

Previous work with imine linked-peptoid ladders[9] concentrated on block encoded oligomers, as scrambled sequences gave rise to incomplete hybridizations stemming from kinetic trapping. By annealing hybridization solutions through a pH increase, similar to that of the boronate ester system, we hope to overcome the previously experienced kinetic trapping. As single strands comprising a significant composition of free-aldehyde functionalities were largely insoluble in aqueous solutions, posing difficulties for RP-HPLC purification, amine-aldehyde oligomers were synthesized in a manner that enabled the protection of aldehyde (acetal-protecting group) throughout purification. To do so required the use of an alloc protecting group for the amine and an in situ deprotection of the aldehyde. To precisely control the deprotection and solubility of the dynamic covalent monomers, the peptoids were synthesized on photolabile solid support resin. Alloc-groups were removed prior to cleavage with UV light, allowing for free strands to bear free amine, denoted by "1," and acetal-protected aldehyde groups – preventing imine formation in stock solutions. Unhybridized peptoid strands designed to form molecular ladders based on imine linkages can be seen in Figure 6.9. Hybridizations began in trifluoracetic acid to simultaneously deprotect the acetal-aldehyde and drive the equilibrium to favor free strands. As the aldehyde groups denoted by "0" reduce solubility of the oligomers in aqueous solutions, chloroform is added to the trifluoracetic acid along with enough sodium hydroxide to reach a pH of 14. Upon collecting the organic layer after a thorough mixing and ensuing phase separation, the hybridization is allowed to proceed resulting in the positive mode MALDI-TOF spectra in Figure 6.9. As imine formation is an equilibrium condensation reaction, molecular ladders with m/z values of +18 are observed in the MALDI-TOF spectra corresponding to a snapshot image of out-of-registry ladders.
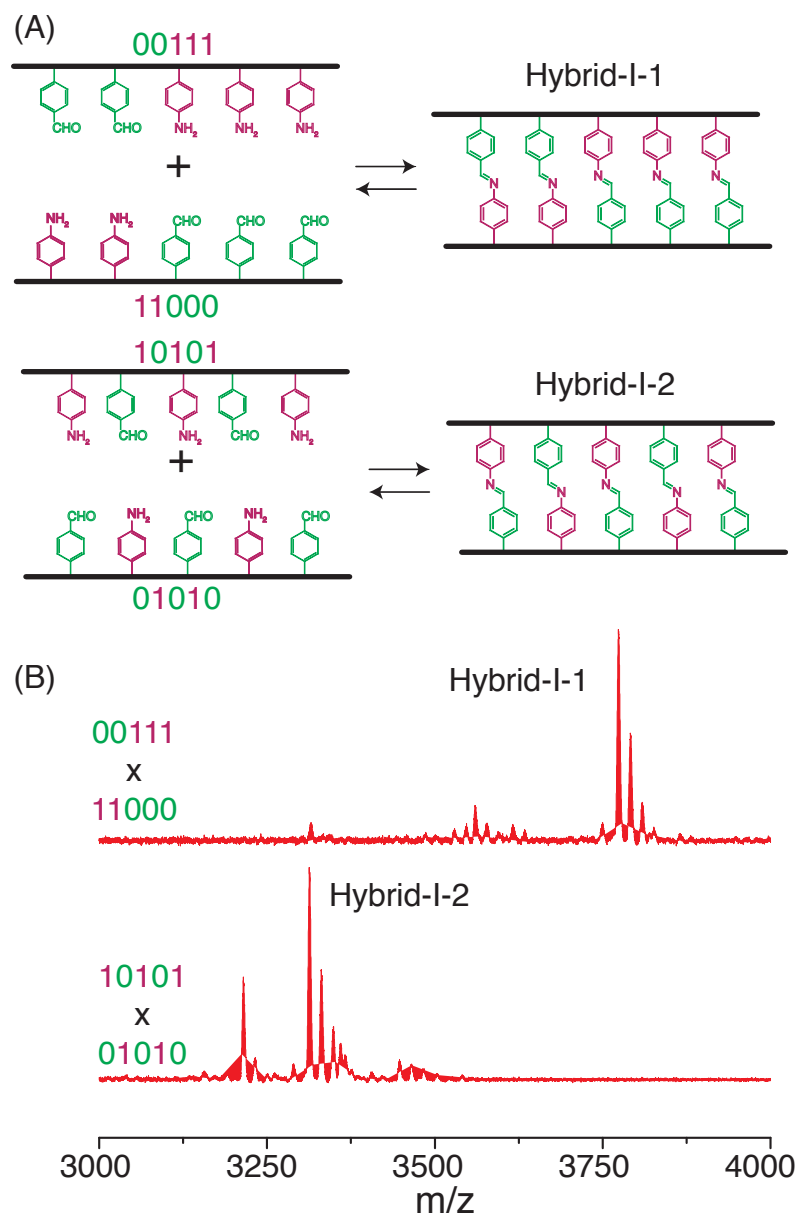
Figure 6.9. **Formation of information-directed molecular ladders with imine rungs (a) schematic showing the formation of molecular ladders with imine rungs (b) positive mode MALDI-TOF spectra of molecular ladders with imine linkages**

181

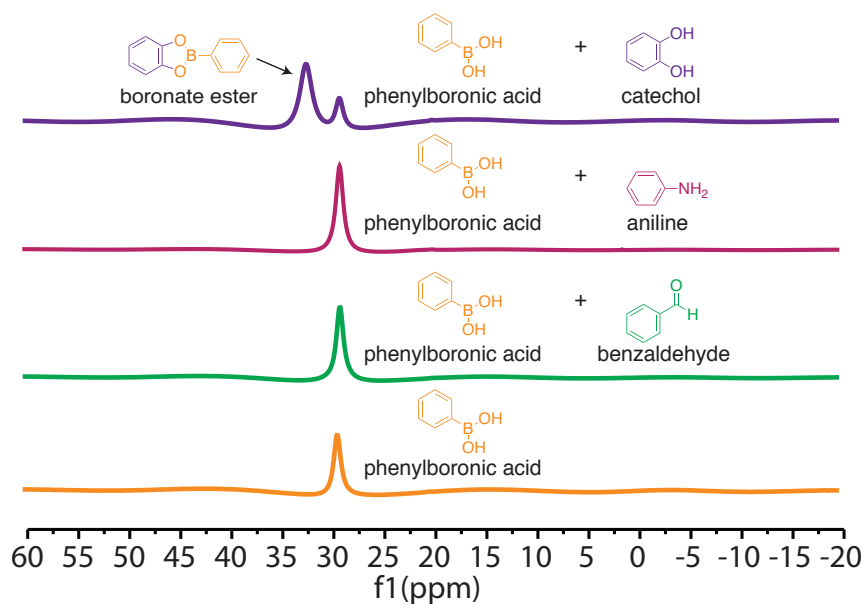### 6.4.3. Orthogonal Dynamic Covalent Chemistries

Figure 6.10. ^{11}B-NMR spectra highlighting orthogonality in the two dynamic covalent systems. The orange line is the boronic acid alone, and the purple line corresponds to the shift associated with the formation of the boronate ester. Aniline (pink) and benzaldehyde (green) show no change to the boronic acid.

In order to increase information density in our strands, we wanted to combine the boronate ester and imine systems to form a base-4 system analogous to the four nucleobases of DNA. The key to being able to do this lies in the orthogonality of the systems. We first looked at the ability of these systems to coexist by looking at monomers used in our individual systems, catechol, phenylboronic acid, aniline, and benzaldehyde. Here we added stoichiometric ratios of the different monomers together and characterized them using ^{11}B NMR (Figure 6.10) and ^{1}H NMR (Figure 6.11-6.16). In particular, we would like to highlight the ^{11}B NMR results, which clearly demonstrate a peak shift in the catechol and phenylboronic acid solution and no change in the aniline and benzaldehyde solutions demonstrating that the intended complexation between the catechol and phenylboronic acid is the only interaction affecting change upon the boron.

182

Imine Proton

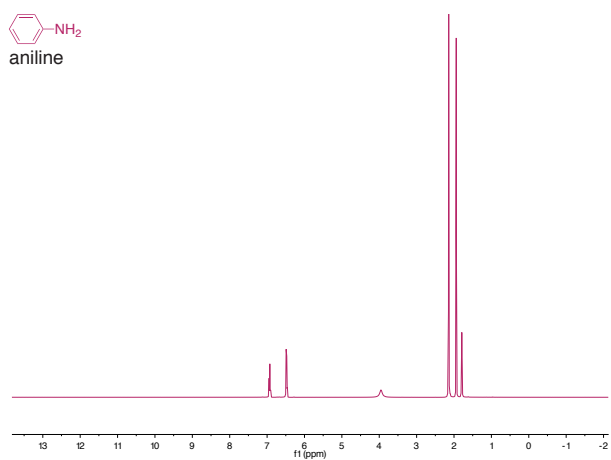benzaldehyde + aniline ⇌ Imine

benzaldehyde

aniline

Figure 6.11. ^{1}H-NMR spectra comparing the differences between a mixture of aniline and benzaldehyde (top, black) with their initial reactants. Aniline is the bottom spectrum shown in pink. Benzaldehyde is the middle spectrum shown in green.

Boronate Ester Proton

phenylboronic acid   catechol   boronate ester

phenylboronic acid

catechol

Figure 6.12. ^{1}H-NMR spectra comparing the differences between a mixture of phenylboronic acid and catechol (top, black) with their initial reactants. Catechol is the bottom spectrum shown in purple. Phenylboronic acid is the middle spectrum shown in orange.
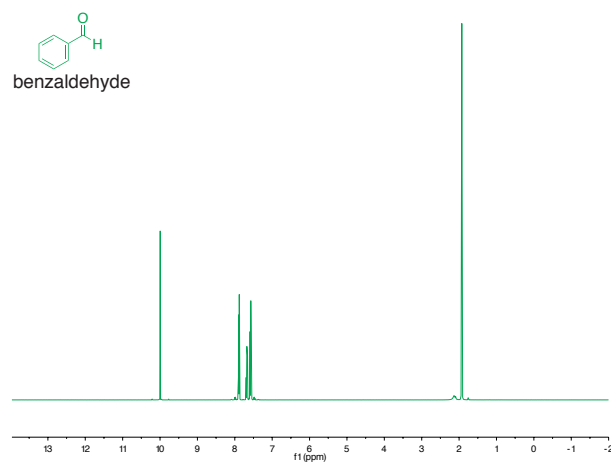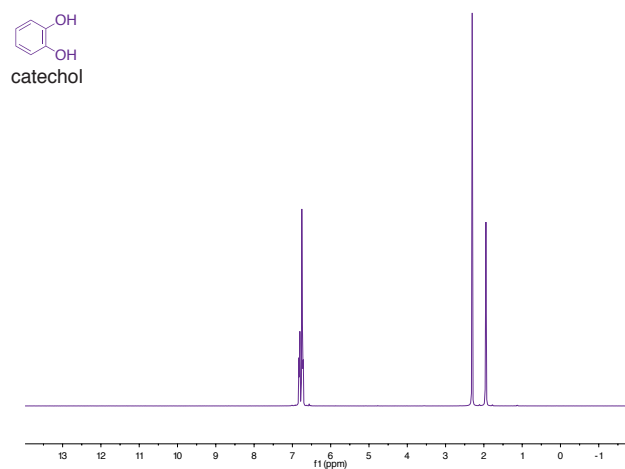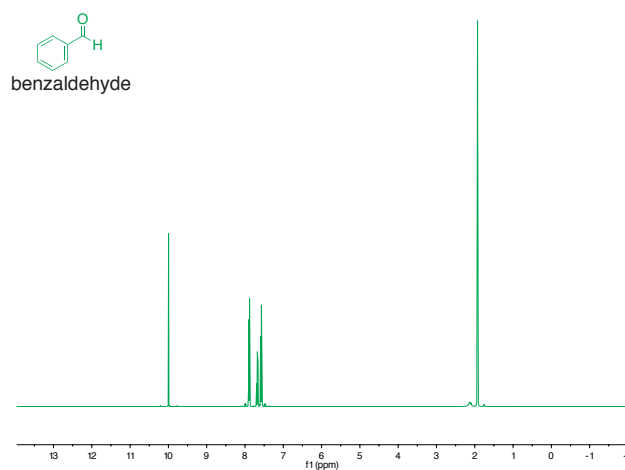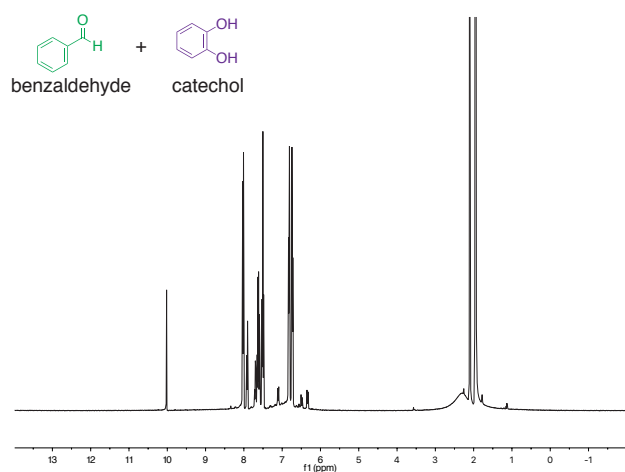
Figure 6.13. ^{1}H-NMR spectra comparing the differences between a mixture of benzaldehyde and catechol (top, black) with their initial reactants. Catechol is the bottom spectrum shown in purple. Benzaldehyde is the middle spectrum shown in green.

Catechol and Amine

catechol + aniline
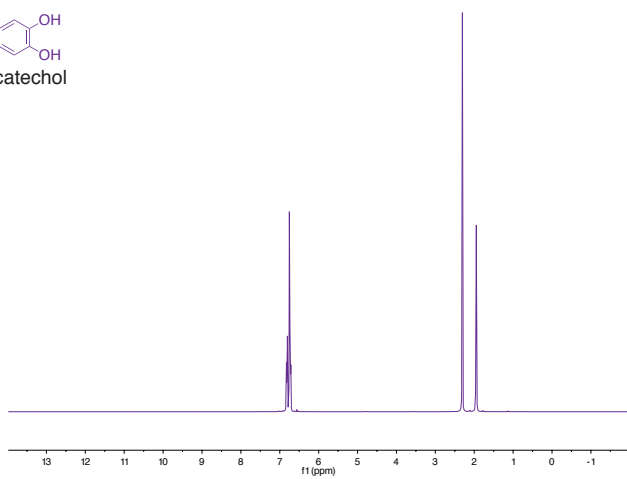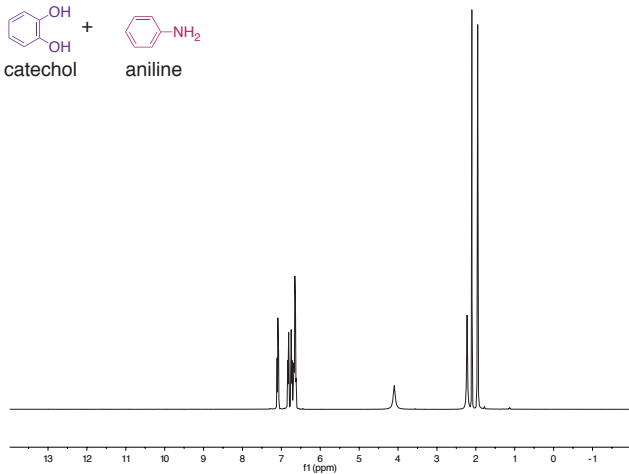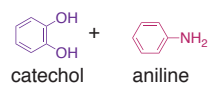
catechol

aniline

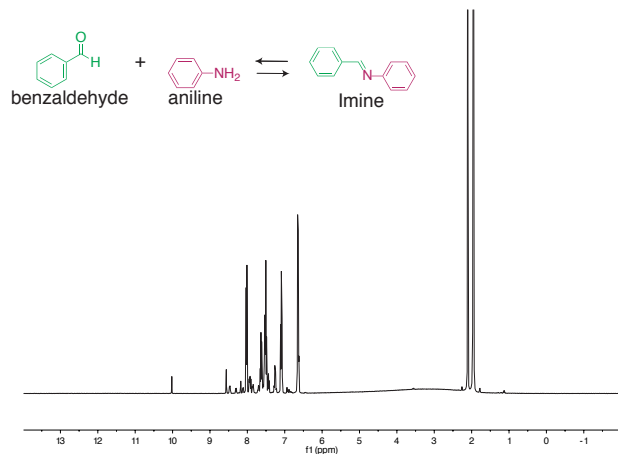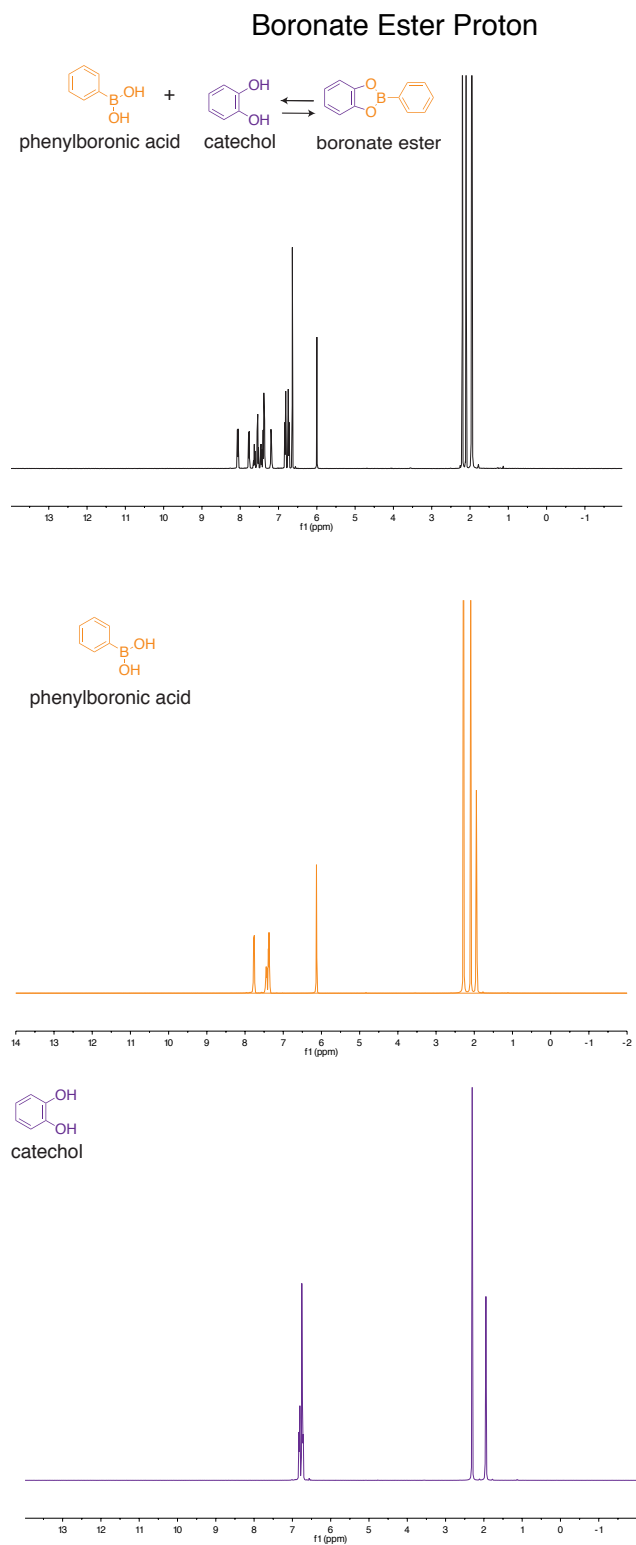**Figure 6.14.** ^{1}H-NMR spectra comparing the differences between a mixture of aniline and catechol (top, black) with their initial reactants. Catechol is the middle spectrum shown in purple. Aniline is the bottom spectrum shown in pink.
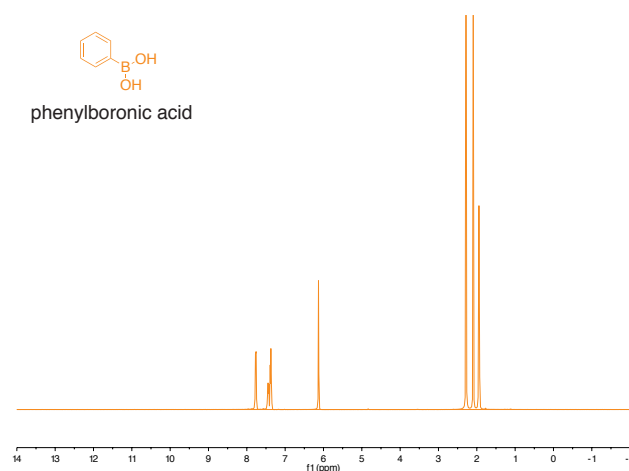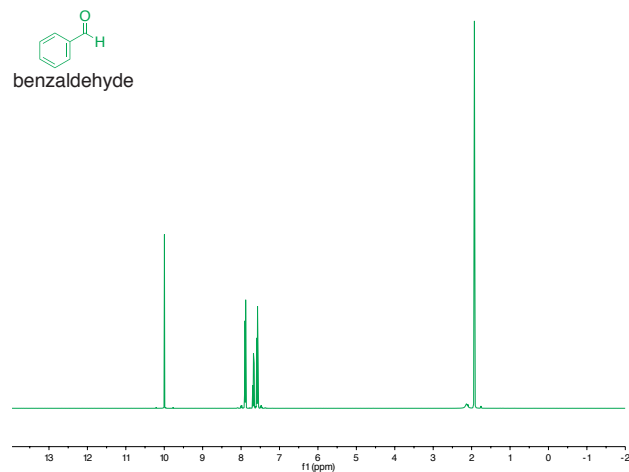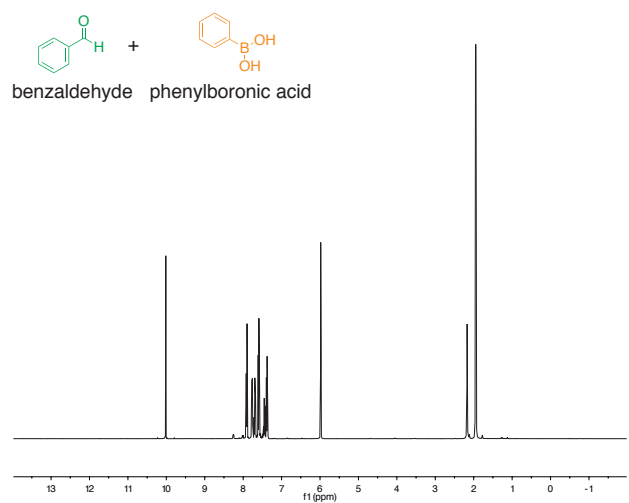
Figure 6.15. ^{1}H-NMR spectra comparing the differences between a mixture of phenylboronic acid and benzaldehyde (top, black) with their initial reactants.

benzaldehyde is the middle spectrum shown in green. Phenylboronic acid is the bottom spectrum shown in orange.
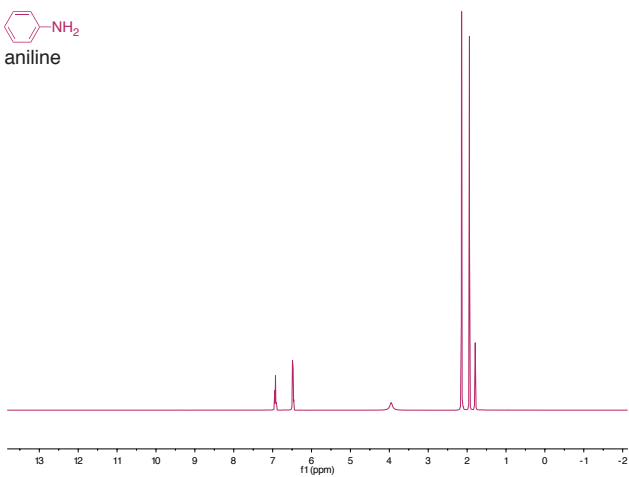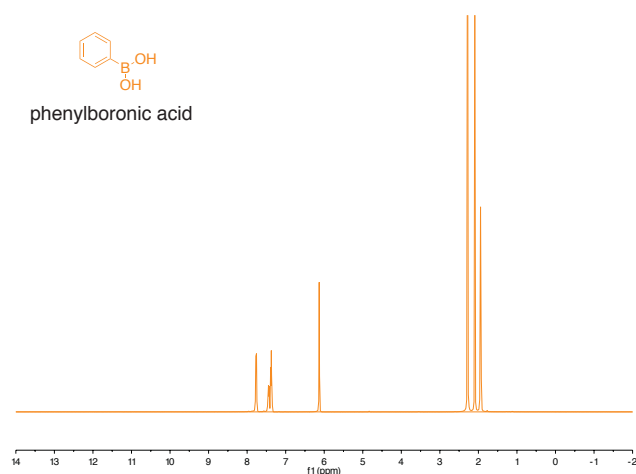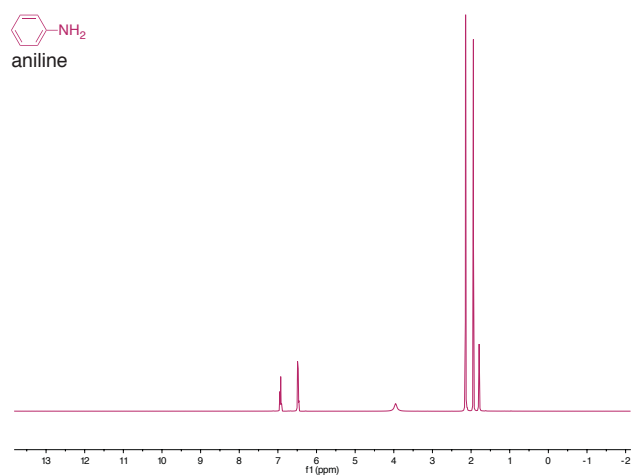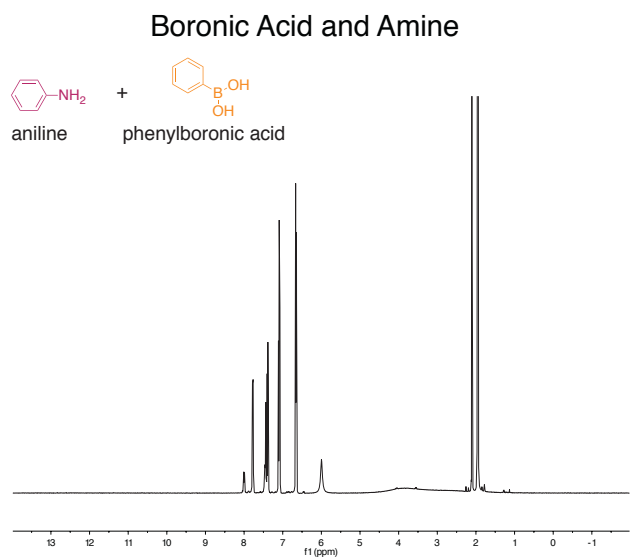
Figure 6.16. ^{1}H-NMR spectra comparing the differences between a mixture of phenylboronic acid and aniline (top, black) with their initial reactants. Aniline is the

middle spectrum shown in pink. Phenylboronic acid is the bottom spectrum shown in orange.

We also showed ^{1}H-NMR of peptoids that were designed with one functional group that would assemble into a molecular ladder with its complementary group to confirm the formation of the imine and boronate ester in an oligomeric system (Figure 6.17 and 6.18, respectively). In the imine forming sample, we observed a peak corresponding to the characteristic imine peak at ~8.5 which suggests that the reaction did indeed occur; however, there was still a peak corresponding to the aldehyde at ~10 suggesting that the reaction did not go to completion. The boronate ester forming mixture does not have a characteristic peak that is easily monitored, but it does have a similar aromatic region to the analysis done with monomers. The other peaks in both spectra can be attributed to the peptoid backbone.
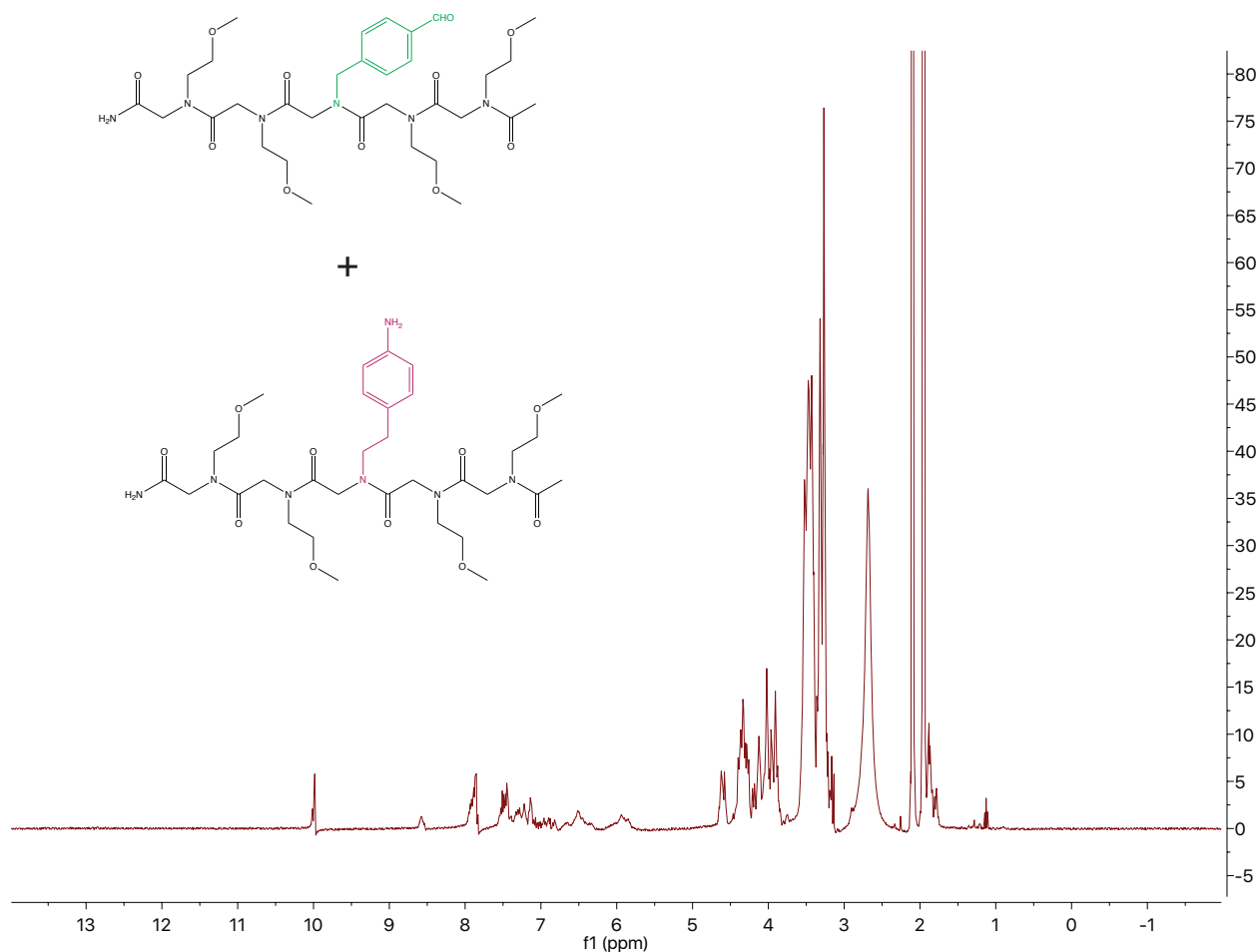
Figure 6.17. ¹H-NMR spectra of an imine molecular ladder with one rung formed from two peptoids (0 and 1) that each have one functional group.
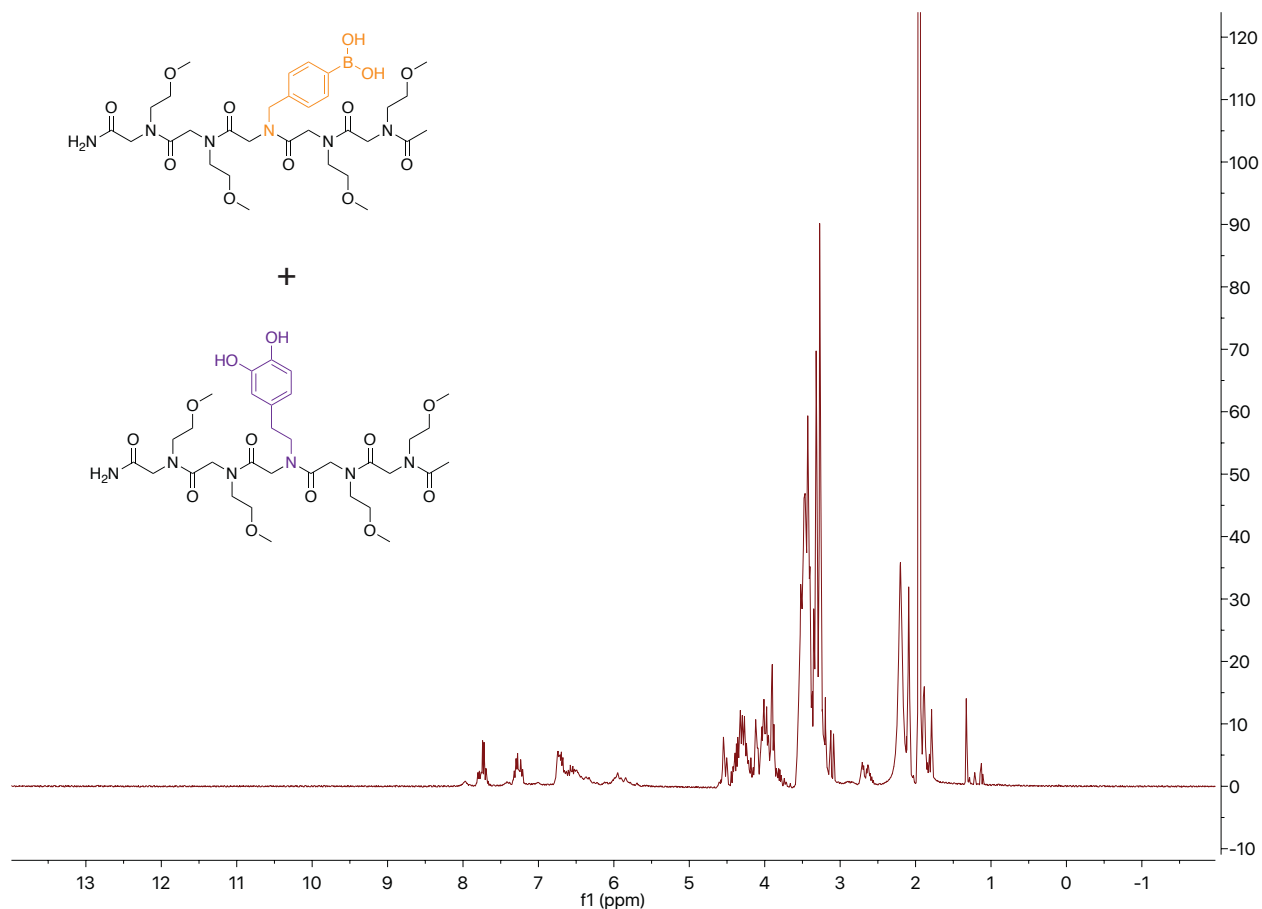
Figure 6.18. ¹H-NMR spectra of a boronate ester molecular ladder with one rung formed from two peptoids (2 and 3) that each have one functional group.

6.4.4. Orthogonal Assembly

The first test of chemical orthogonality in a more complex assembled structure was to build a 3x3 molecular grid from the combined systems. This grid is comprised of core peptoid with alternating catechol and aldehyde functionality, and two side strands each bearing one of the complementary functional groups as shown in Figure 6.19 (left). We were able to form the desired grid structure by employing a scandium (III) triflate catalyst that shifts the equilibrium allowing for rearrangement of the imine bonds in a basic aqueous solution (pH=9) as confirmed

in Figure 6.10 (right). Here we are observing an ionization that is attributed to the scandium ion that was present in the reaction solution. We initially obtained these results by adding the initial oligomers to the reaction solution simultaneously, but we were curious as to whether the order the oligomers were added to the affected the resulting structure. We also characterized the system in positive mode MALDI-TOF (Figure 6.20). Negative mode MALDI-TOF was preferable in characterization of samples that contained the boronate ester owing to its anion being present in aqueous solution whereas the imine only ladders were not observable by themselves.
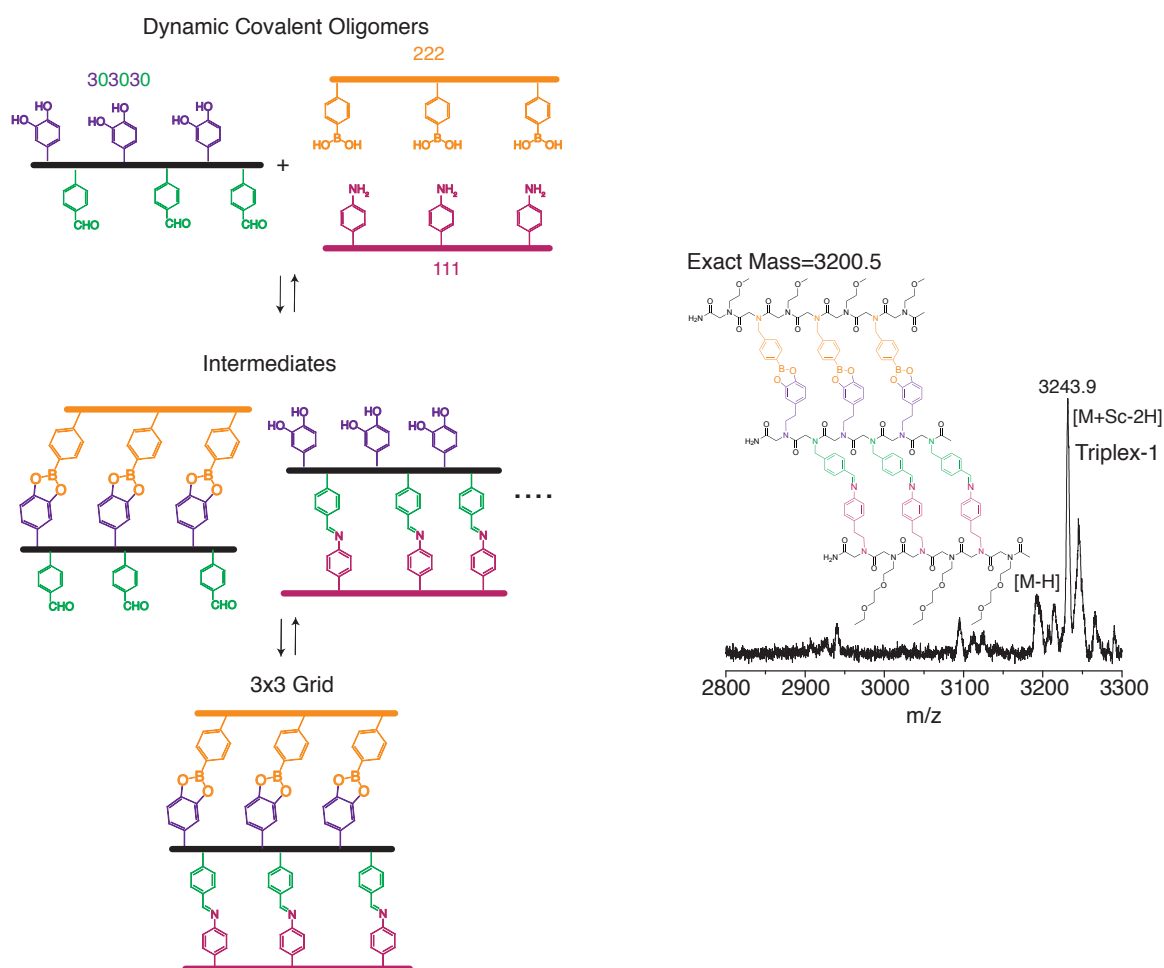
Figure 6.19. Confirmation of orthogonality between imine and boronate ester systems. The left shows a schematic of 3 x 3 grid formed from a core peptoid with aldehyde and catechol functionality and complementary amine and boronic acid side strands. The right is a

negative mode MALDI-TOF confirming the formation of the grid structure with [M+Sc-2H] as the ionization
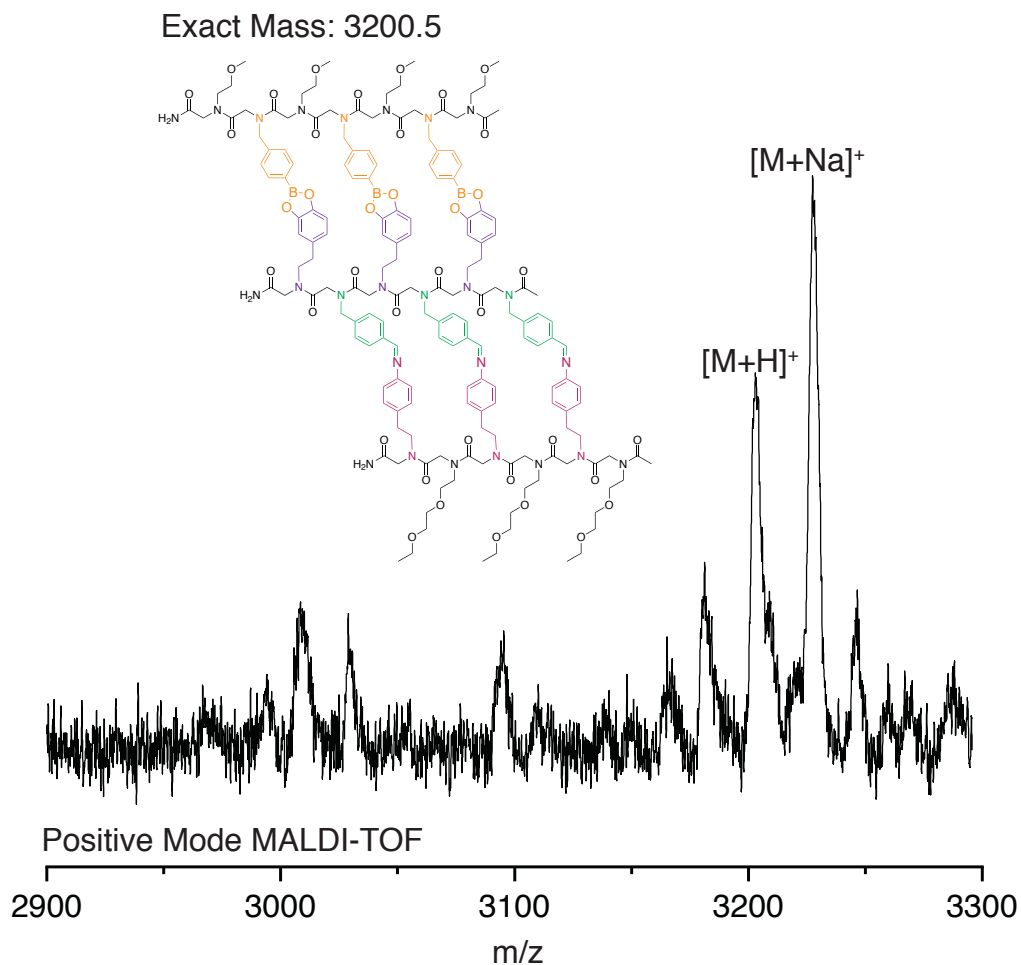
Figure 6.21. Positive mode MALDI-TOF spectrum showing the formation of the 3 x 3 molecular grid, Triplex-1

Two different sample solutions containing the core strand and either the amine- or the boronic acid-bearing peptoids were allowed to react overnight before running a MALDI-TOF analysis (Figure 6.21). Each of the desired duplex structures was confirmed with MALDI-TOF, but there was a noticeable difference in the solubility of the structures in the reaction mixture. Upon adding the core peptoid strand to the aqueous solution, the mixture would become cloudy. The cloudiness would persist in the duplex that included the amine-bearing side strand; however, the duplex mixture with the boronic acid-based peptoid would return to clear. Each of the

195

remaining complementary strands were added to the duplex structures and allowed to react overnight before confirming the formation of the molecular grid with MALDI-TOF (Figure 6.22). Once each of the reaction mixtures was allowed to equilibrate the solution became clear and the desired molecular grid was observed in MALDI-TOF. We also briefly explored the effects of pH on the system by adjusting the reaction solution to both neutral (Figure 6.23a) and slightly acidic (pH=5 using HCl, Figure 6.23b). The pH didn't appear to have any observable changes to the triplex formation. The formation of the molecular grid in a variety of different reaction conditions corroborates the potential of these two dynamic covalent chemistries to proceed without interruption by the additional functionalities.
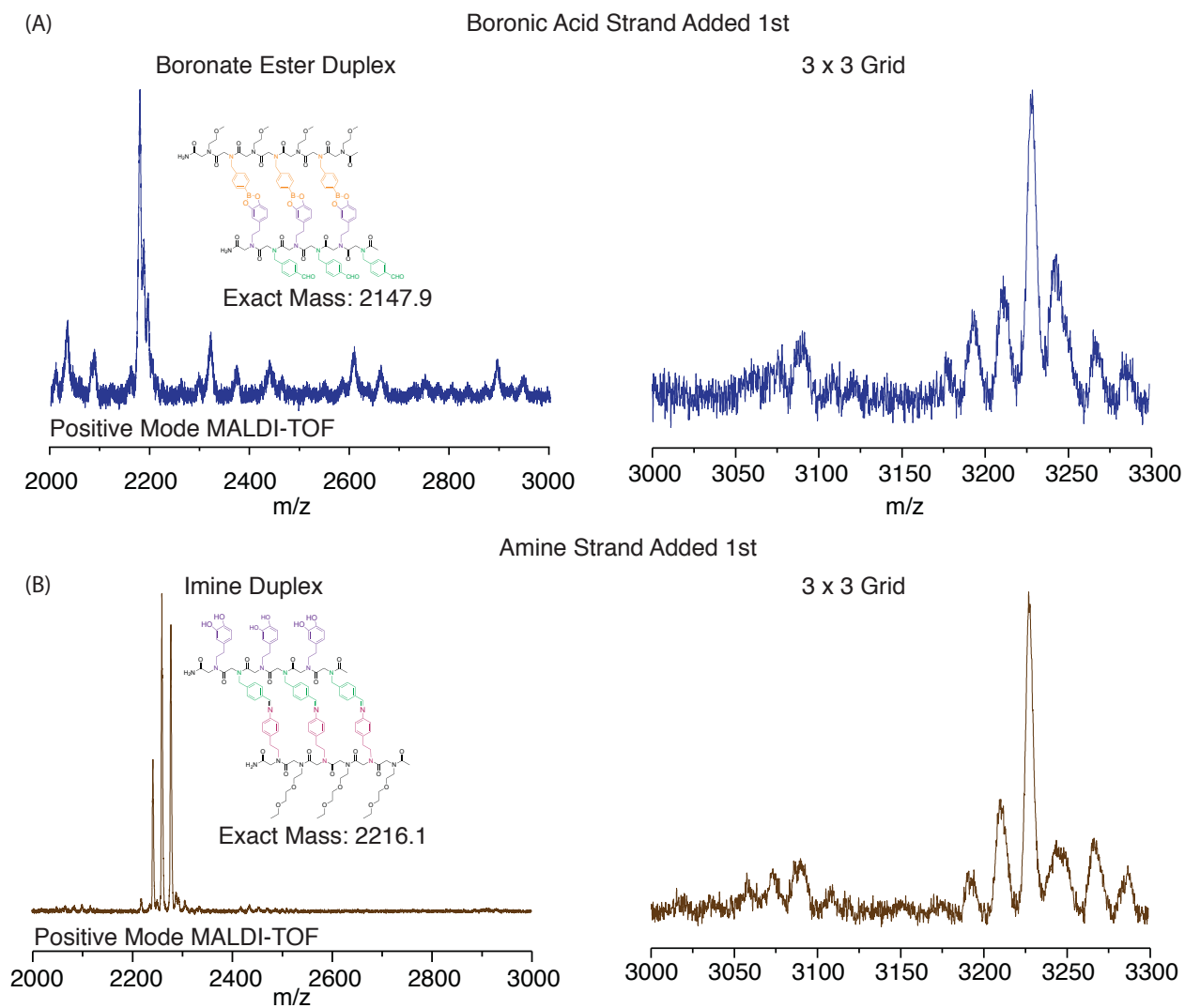
Figure 6.21. Ordered of addition study in the formation of Triplex-1 (a) Positive mode MALDI-TOF confirming the formation of duplex structure from adding the boronic acid strand to the catechol and aldehyde functionalized core (303030) and the resulting grid from adding the amine functionalized strand (b) Positive mode MALDI-TOF confirming the formation of duplex structure from adding the amine strand to the catechol and aldehyde functionalized core (303030) and the resulting grid from adding the boronic acid functionalized strand
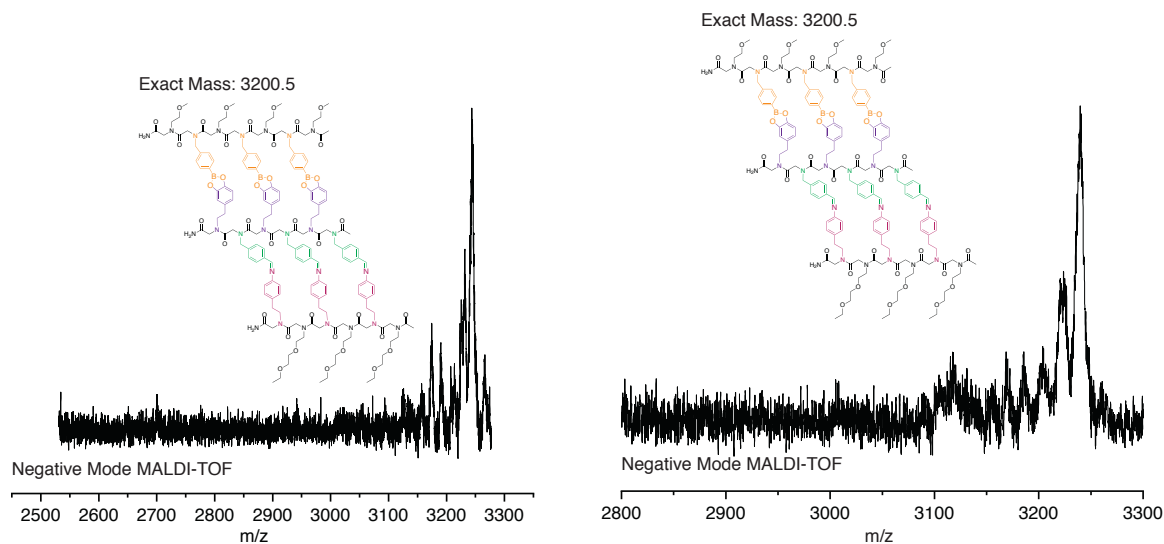
Figure 6.22. pH-dependence in the formation of Triplex-1 (a) Negative mode MALDI-TOF confirming the formation of Triplex-1 in neutral water (b) Negative mode MALDI-TOF spectrum confirming the formation of Triplex-1 in acidic conditions (pH= ~5)

6.4.4. Base-4 Information System

The success of combining the two dynamic covalent chemistries with block segments of each of the functional groups highlighted the potential to incorporate the chemistries in scrambled sequences as shown in Figure 6.23. Here we have two oligomeric strands with complementary sequences designed to form a hybridized molecular ladder with the aid of a scandium(III) triflate catalyst. Here we rely upon pH annealing to form the intended structure similar to the individual systems. The sequences were mass labled synthesized with a different number of inert spacers that illicit a change in exact mass of 116.16 between the two strands to further confirm that the peptoids were interacting with their complementary strand and not forming ladders through self-hybridization. The fully deprotected peptoids maintained water solubility making it possible to follow a similar assembly strategy to the boronate ester system. The oligomers were cleaved and deprotected from the acid-labile resin using TFA then purified using HPLC all while maintaining an acidic pH where the equilibrium will favor the initial functional groups. The oliogmers were then put into a basic aqueous solution to promote

dimerization and the structures were confirmed using MALDI-TOF (Figure 6.23). The major

product is attributed to the ideal ladder with scandium ionization owing to the scandium catalyst.
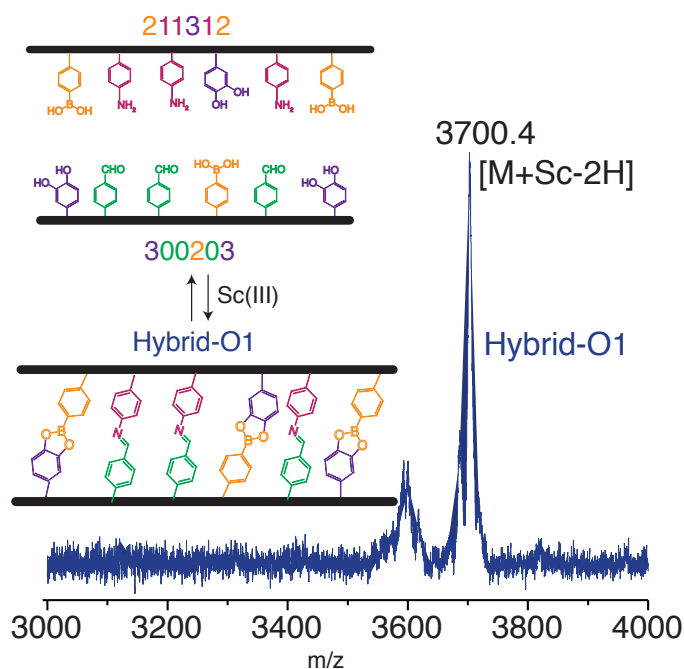
Figure 6.23. Negative mode MALDI-TOF spectrum confirming the formation of hybrid-O1 from two complementary peptoids (211312 and 300203)

We wanted to test the selectivity of forming the base-4 information directed double

stranded structure even in the presence of peptoid strands bearing the same functional groups.

We added the same two complementary sequences forming the ladder in Figure 6.24i (Hybrid-

O1). to a reaction mixture with one of the self-hybridizing boronate ester strands from the

exploration of the individual systems (223233,Figure 6.24ii). We then allowed the reaction to

equilibrate before analyzing the solution with MALDI-TOF mass spectra shown in Figure

2.24iii. Here we see two peaks corresponding to the two different molecular ladders Hybrid-O1

and Hybrid-BE-2. The oligomers are again mass labeled to confirm the correct structures are

forming, and no cross-reaction are occurring between the 3 different strands as they would be

evident through a unique peak in the MALDI-TOF spectra. This suggests that even in the presence of competing functional groups this system will selective form the intended structure.
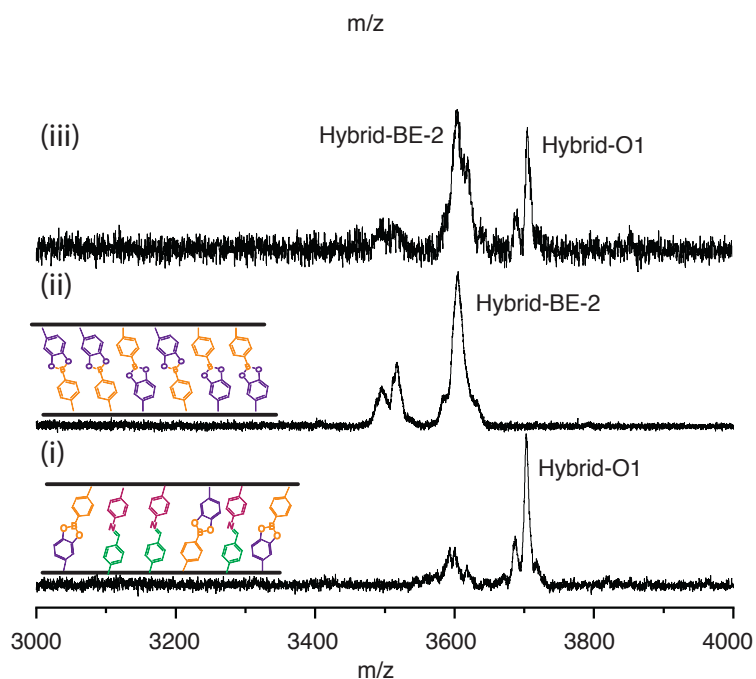
Figure 6.24. Negative mode MALDI-TOF spectra showing the selectivity of mixing self-hybridizing Hybrid-BE-2 with the oligomeric strands that form Hybrid-O1 i: MALDI-TOF of self-hybridizing ladder-b alone ii: MALDI-TOF of Hybrid-O1 iii: MALDI-TOF showing two peaks corresponding to the desired molecular ladders, Hybrid-BE-2 and Hybrid-O1

We then hoped to add more dimensionality to the base-4 system through forming a molecular grid with information-encoded sequences. The grid was formed from a core peptoid that was designed to react with the same side strand in different directionalities, one in the parallel and the other in anti-parallel configuration as shown in Figure 6.25a. The assembly methods here followed the pH-control of the base-4 duplex system, and resulted in the desired structure as confirmed by MALDI-TOF in Figure 6.25b. This highlights the potential of our base-4 system to form more complex structures by relying upon the information encoded in the sequences and pH-mediation.
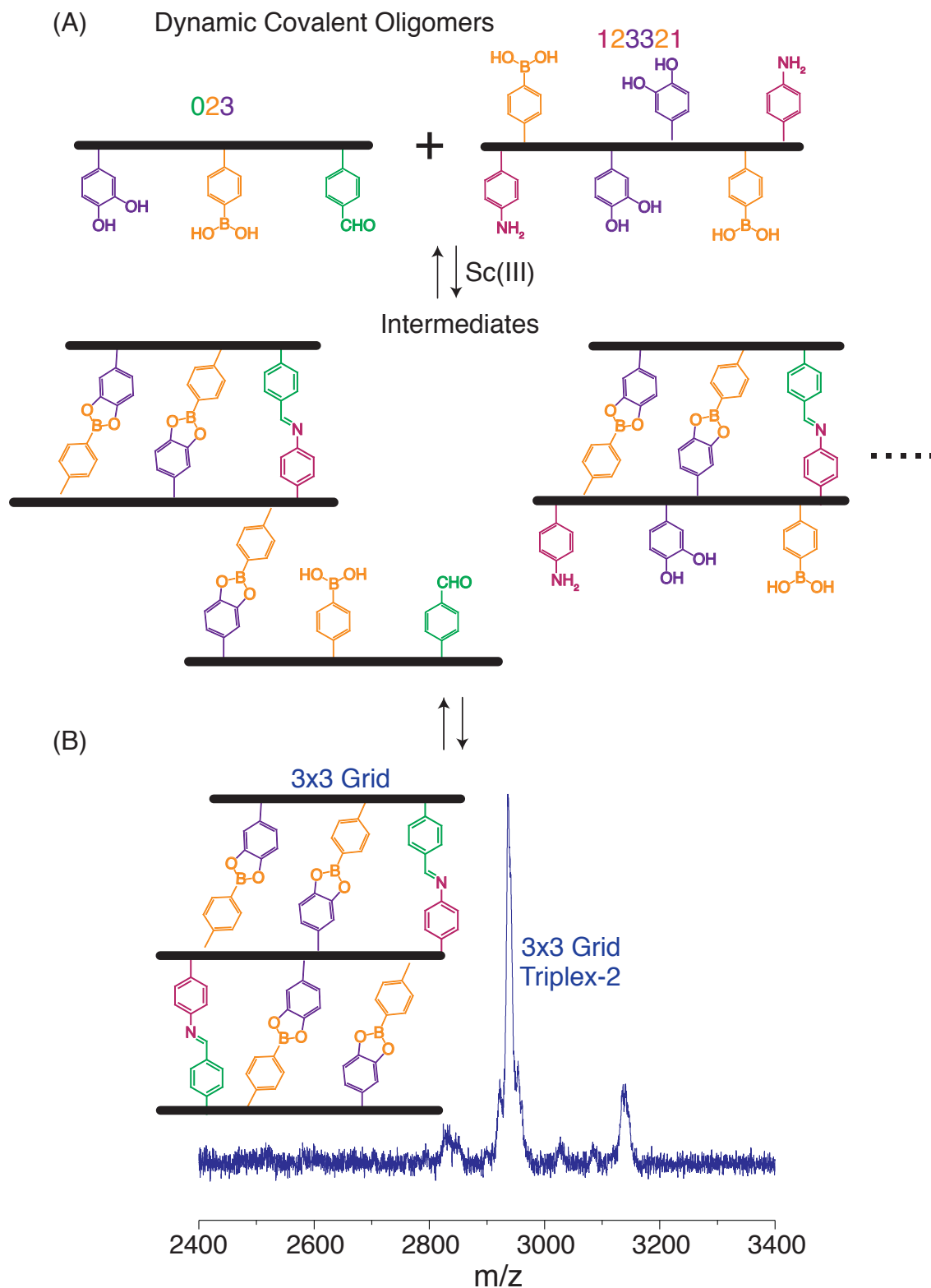
Figure 6.25. Molecular grid formed through incorporating both imine and boronate ester linkages a) schematic showing the two peptoids designed to form a molecular grid from a

core strand containing boronic acid, catechol, and amine functionalities and a side strand that contains boronic acid, catechol, and aldehyde functionalities b) negative mode MALDI-TOF confirming the formation of the 3x3 grid, Triplex-2

6.5 Conclusions

The rise of nucleic acids being used as a construction material has developed a need for stronger and more robust, stable information-driven assemblies. This chapter explored the combination of boronate ester and imine forming dynamic covalent chemistries in the assembly of molecular ladders and grids. We first developed a method for the assembly of binary molecular ladders of each system while utilizing the pH reversibility of each of the chemistries to mediate the hybridization of sequence-specific oligomers. Upon successful ^{11}B- and ^{1}H-NMR cross-reactivity studies, we assembled a simple 3 x 3 molecular grid that was comprised of a catechol and aldehyde functionalized core strand and two complementary boronic acid and amine side strands. This allowed us to test a wide range of orthogonal reaction conditions before ultimately incorporating the functional groups into the same strands to build a base-4 molecular ladder and a more complex 3 x 3 molecular grid. This approach highlights the potential of utilizing these two strong covalent chemistries to fabricate structures with an increased information density.

6.6 References

1.   Watson, J. D.; Crick, F. H. C., Molecular Structure of Nucleic Acids: A Structure for Deoxyribose Nucleic Acid. *Nature* **1953,** *171* (4356), 737-738.

2.   Seeman, N. C., Nucleic Acid Junctions and Lattices. *J. Theor. Biol.* **1982,** *99* (2), 237-247.

3.   Rothemund, P. W. K., Folding DNA to create nanoscale shapes and patterns. *Nature* **2006,** *440* (7082), 297-302.

4.   (a) Wei, B.; Dai, M. J.; Yin, P., Complex shapes self-assembled from single-stranded DNA tiles. *Nature* **2012,** *485* (7400), 623-626; (b) Ke, Y.; Ong, L. L.; Shih, W. M.; Yin, P.,

Three-Dimensional Structures Self-Assembled from DNA Bricks. *Science* **2012,** *338* (6111), 1177-1183.

5.   Heid, C. A.; Stevens, J.; Livak, K. J.; Williams, P. M., Real time quantitative PCR. *Genome Res.* **1996,** *6* (10), 986-994.

6.   Schena, M.; Shalon, D.; Davis, R. W.; Brown, P. O., Quantitative Monitoring of Gene Expression Patterns with a Complementary DNA Microarray. *Science* **1995,** *270* (5235), 467-470.

7.   Santosh, M.; Maiti, P. K., Force induced DNA melting. *J. Phys.-Condes. Matter* **2009,** *21* (3).

8.   (a) Bockelmann, U.; EssevazRoulet, B.; Heslot, F., Molecular stick-slip motion revealed by opening DNA with piconewton forces. *Phys. Rev. Lett.* **1997,** *79* (22), 4489-4492; (b) Bockelmann, U.; Thomen, P.; Essevaz-Roulet, B.; Viasnoff, V.; Heslot, F., Unzipping DNA with optical tweezers: high sequence sensitivity and force flips. *Biophys. J.* **2002,** *82* (3), 1537-1553.

9.   (a) Wei, T.; Jung, J. H.; Scott, T. F., Dynamic Covalent Assembly of Peptoid-Based Ladder Oligomers by Vernier Templating. *J. Am. Chem. Soc.* **2015,** *137* (51), 16196-16202; (b) Wei, T.; Furgal, J. C.; Jung, J. H.; Scott, T. F., Long, self-assembled molecular ladders by cooperative dynamic covalent reactions. *Polym. Chem.* **2017,** *8* (3), 520-527.

10.   Hutin, M.; Bernardinelli, G.; Nitschke, J. R., An iminoboronate construction set for subcomponent self-assembly. *Chemistry-a European Journal* **2008,** *14* (15), 4585-4593.

11.   (a) Christinat, N.; Scopelliti, R.; Severin, K., Multicomponent assembly of boron-based dendritic nanostructures. *J. Org. Chem.* **2007,** *72* (6), 2192-2200; (b) Christinat, N.; Scopelliti, R.; Severin, K., Multicomponent assembly of boronic acid based macrocycles and cages. *Angew. Chem.-Int. Edit.* **2008,** *47* (10), 1848-1852.

12.   Furgal, J. C.; Dunn, M.; Wei, T.; Scott, T. F., Emerging Applications of Dynamic Covalent Chemistry from Macro- to Nanoscopic Length Scales. In *Dynamic Covalent Chemistry*, John Wiley & Sons, Ltd: 2017; pp 389-434.

13.   Xu, J.; Duran, D.; Mao, B., On-Column Hydrolysis Kinetics Determination of Boronic Pinacol Ester Intermediates for Use in Optimization of Fast HPLC Methods. *Journal of Liquid Chromatography & Related Technologies* **2006,** *29* (19), 2795-2806.

14.   AbdelMagid, A. F.; Carson, K. G.; Harris, B. D.; Maryanoff, C. A.; Shah, R. D., Reductive amination of aldehydes and ketones with sodium triacetoxyborohydride. Studies on direct and indirect reductive amination procedures. *J. Org. Chem.* **1996,** *61* (11), 3849-3862.

Chapter 7 Future Directions

7.1. Summary of Research

This dissertation explores the concept of orthogonality and how it relates to building and functionalizing molecular structures. This understanding is key to expanding the complexity of self-assembled structures.

In the second chapter, we discussed the design of cyclic peptoid structures that were first formed from oligopeptoids of different lengths that were cyclized by a copper (I) catalyzed alkyne-azide cycloaddition reaction between terminal alkyne/azide(CuAAC) residues. We were able to monitor cyclization by collecting peaks corresponding to shifts in the retention volume of RP-HPLC traces and confirming their respective masses using MALDI-TOF analysis. The cyclization was further confirmed by monitoring the characteristic azide peak in FT-IR; this showed the presence of the peak prior to cyclization and no observable peak after the CuAAC reaction. The cyclic assemblies were synthesized to include furan functional groups suitable for post-synthetic conjugation to a maleimide-bearing amine through a Diels-Alder reaction. As the length of the oligomer increased, there was a decrease in the cyclization efficiency, but we determined that had no observable effect on subsequent conjugation. This was a proof of concept study that shows the utility of using peptoid-based oligomers to fabricate scaffolds. It also highlights the orthogonality between the Diels-Alder and CuAAC click chemistries.

The third chapter continues work with the furan/maleimide Diels-Alder reaction to form more complex double stranded molecular ladders by exploiting the reversibility dynamic covalent reaction between a furan (diene) and a maleimide (dienophile) to affect oligomer hybridization. This chapter detailed the reaction conditions necessary to form initial oligomers

205

bearing the reversible functional groups, which included the use of a thermally labile protecting group on the maleimide group. We determined the conditions for removing that protecting group and subsequently hybridizing the dynamic covalent oligomers into molecular ladders. It also discussed some of the challenges currently hindering this system chiefly their ability to be characterized by common mass spectrometry techniques. While the issues were not insurmountable, we decided it was best to explore other chemistries in molecular ladder fabrications.

In the fourth chapter, we began to develop the oligomers for a molecular ladder that was formed from a boronate esterification reaction between a boronic acid and catechol to allow for facile characterization. This chapter details the process that ultimately led to an efficient method of preparing oligomers-bearing boronic acid functional groups. We discussed different methods of synthesis that included directly adding the boronic acid group to the oligopeptoid backbone as well as post-synthetic modification of existing peptoids to include the functional group. We also explored different methods of removing a pinacol protecting group from the boronic acid enabling the esterification reaction. This process alerted us to the sensitivities of the boronic acid group to degradation and oxidation under common reaction conditions. These different trials led to a method of reliably and consistently forming stable boronic acid-bearing peptoids.

The fifth chapter further explored the formation of molecular ladders with boronate ester rungs. Utilizing the technique for preparing boronic acid-bearing peptoids for the previous chapter and analogous method for preparing a catechol-based peptoid, we were able to direct the assembly of molecular ladder with up to 6 rungs. We also introduce three stranded structures described as molecular grids. These were formed from 3 different peptoid strands: one core peptoid functionalized with only catechol groups and 2 side strands bearing boronic acid

206

functional groups. We also demonstrated the dynamic nature of this system through adding a new strand to affect the equilibrium of a solution with a fully formed hybrid. By using mass labeling and checking the mass spectra before and after the new strand was added we were able to see the rearrangement of the molecular ladders. We will also demonstrate the rapid and dynamic nature of the reaction through strand rearrangement with pre-assembled molecular ladders. We were able to characterize how strongly our dynamic covalent oligomers bind together through the use of a competition assay with alazarin red S (ARS), a model fluorescent diol. The chapter lays the foundational work for understanding the reaction conditions necessary to build more complex molecular structures.

Finally, the sixth chapter builds upon the boronate ester molecular ladders to include a new dynamic covalent chemistry between an amine and aldehyde that form Schiff base imines to ultimately direct the assembly of base-4 molecular ladders and grids. We first explore analogous reactions for each of the systems before combining them together to form a base-4 information system that was able to fabricate double stranded molecular ladders and molecular grids. This chapter tests the orthogonality between the two dynamic covalent chemistries utilizing NMR before fabricating an orthogonal molecular grid from a core strand comprised of catechol and aldehyde functional groups and two complementary side strands. We explored a range of pH conditions and tested the order of adding the initial oligomers to determine the optimal reaction conditions necessary for each of the reactions to proceed efficiently. These conditions led to the successful formation of a molecular ladder and grid comprised of the two chemistries. This effectively doubled the information density of our system, which in turn highlights the potential of our system in forming complex highly controlled sequence-specific assemblies.

7.2. Future Directions

7.2.1. Expanded Base-4 Assembly

The sixth chapter explored the uses of the two dynamic covalent chemistries incorporated orthogonally into single stranded oligomers. This work showcased structures that incorporated all four dynamic covalent functional groups (aldehyde, amine, boronic acid, and catechol) into a singular molecular ladder. However, we were not looking at incorporating all four groups into each of the oligomeric strands. This would add another level of complexity into the assembly system. We briefly began to explore this through the synthesis of oligopeptoids (Figures 7.1 and 7.2) that were confirmed utilizing ESI-MS. These two strands were designed with all four functional groups to self-assemble into a molecular ladder.
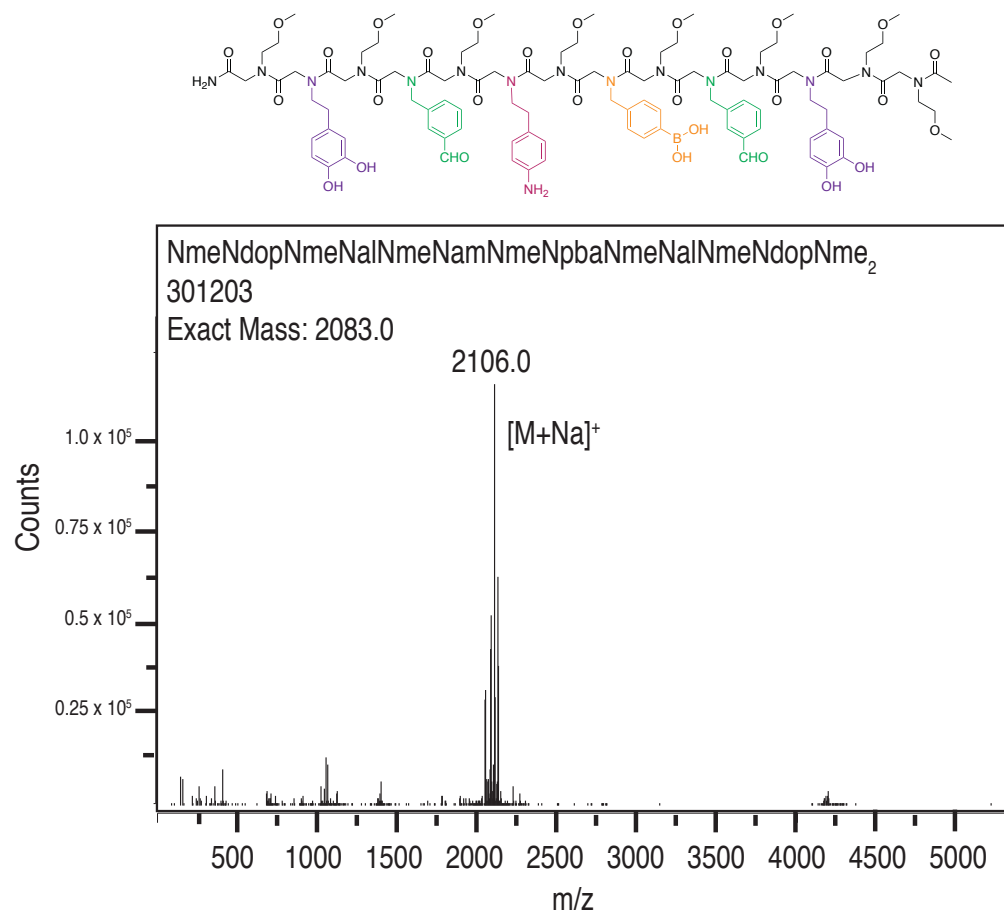
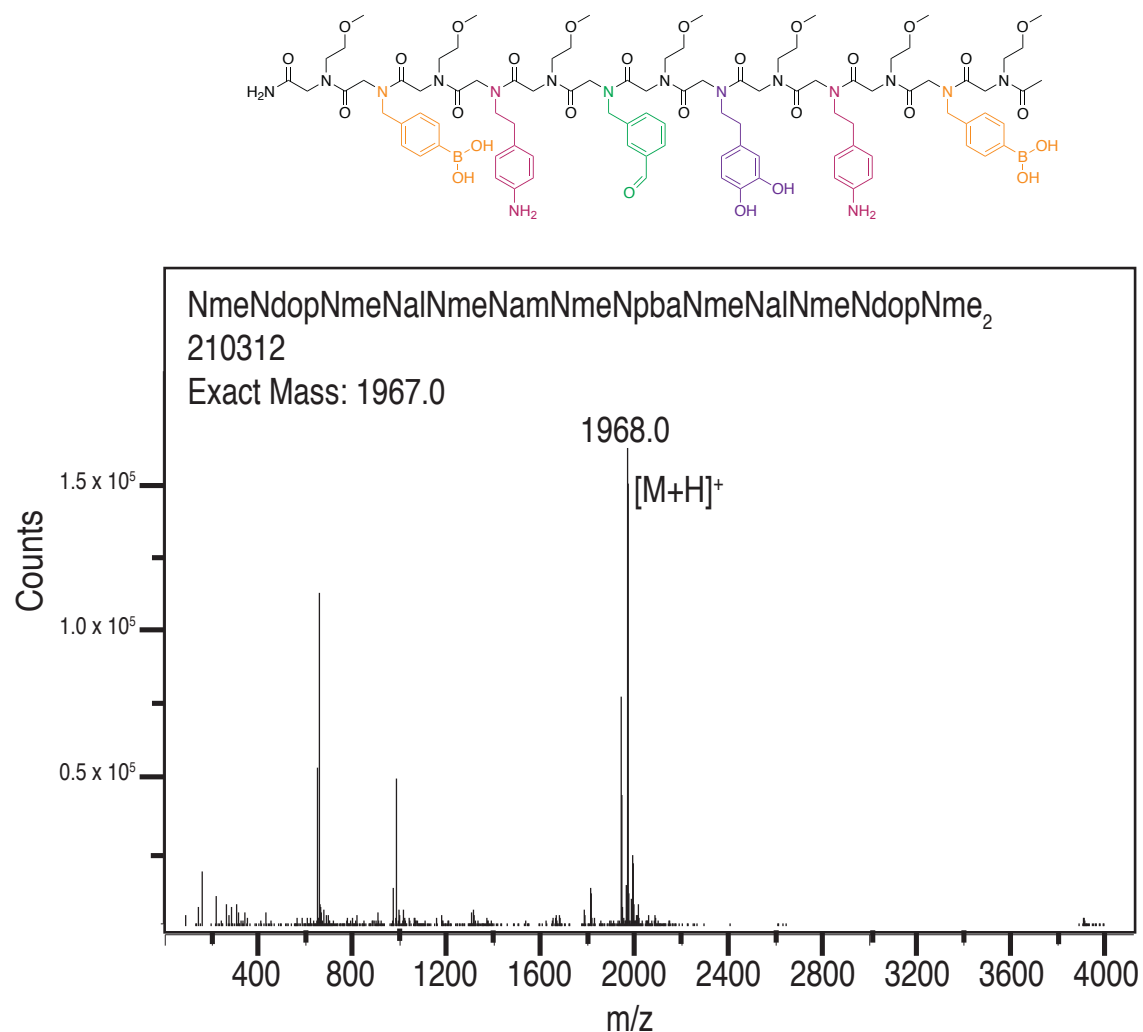**Figure 7.1. ESI-MS spectrum confirming the synthesis of 301203**

Figure 7.2. ESI-MS spectrum confirming the synthesis of 210312

Each of the oligomers was mass labeled to confirm that strands were cross-reacting and not forming dimerized structure with same sequences peptoids. The complementary peptoids were mixed in a stoichiometric ratio with a catalytic amount of scandium (III) triflate and allowed to react overnight. MALDI-TOF mass spectrum was taken to confirm the formation of the molecular ladder (Figure 7.3). This shows that the right ladder was formed, but it also showed a major peak in the higher molecular weight region. This peak was not attributed to non-

selective dimerizing of the initial strands, but it could potentially be out-of-registry assembled structures. This was on the same time scale of the strands from Chapter 6, but the signal-to-noise and side products were far greater. This topic could be further explored in future works with different sequences to develop a better understanding of the reaction conditions necessary to building Base-4 structures.
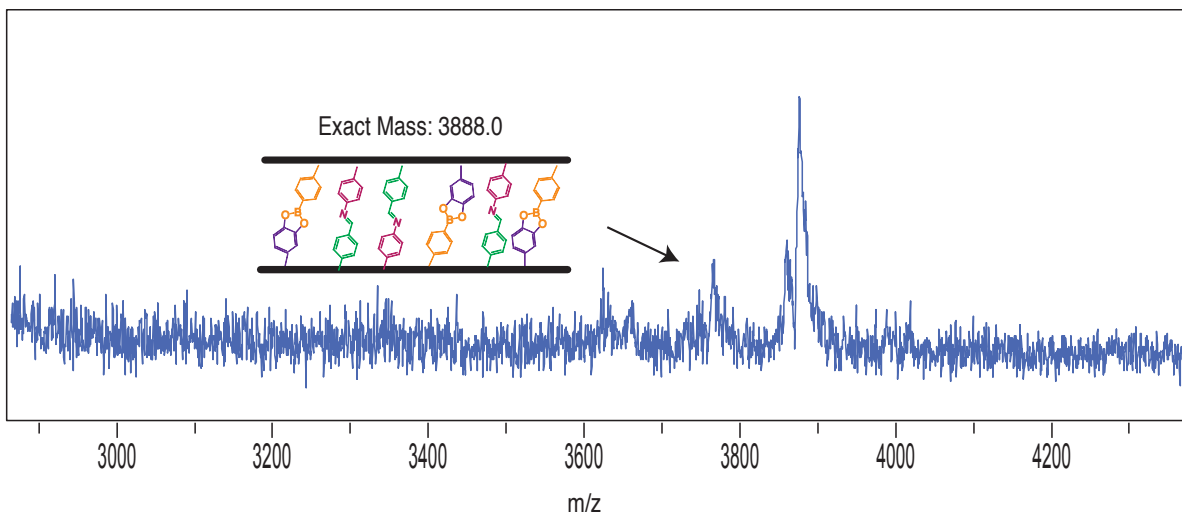

Figure 7.3. MALDI-TOF spectrum showing the Base-4 molecular ladder

7.2.2. Non-linear Branched Structures

The success of dynamic covalent interactions mediating the self-assembly of oligomers, based on the information encoded in the oligomeric sequences, into specific and predictable molecular ladder and grids spurred the goal of creating more complex non-linear branched junctions from dynamic covalent oligomers. Early attempts at fabricating simple junction structures formed from three oligomeric peptoid strands of both boronate ester (Schematic in Figure 7.4) and base-4 systems were unsuccessful. We designed three strands where each strand will react with two other strands with complementary functional groups to form one final structure with the three strands comprehensively reacting. These experiments were generally performed under the analogous conditions to the molecular ladders and grids. I was not able to

determine the issues preventing the junction from being formed. I believe that a comprehensive understanding of the reaction mechanism necessary for the formation of boronic acid-bearing ladders and grids would help better inform these conditions in the future.
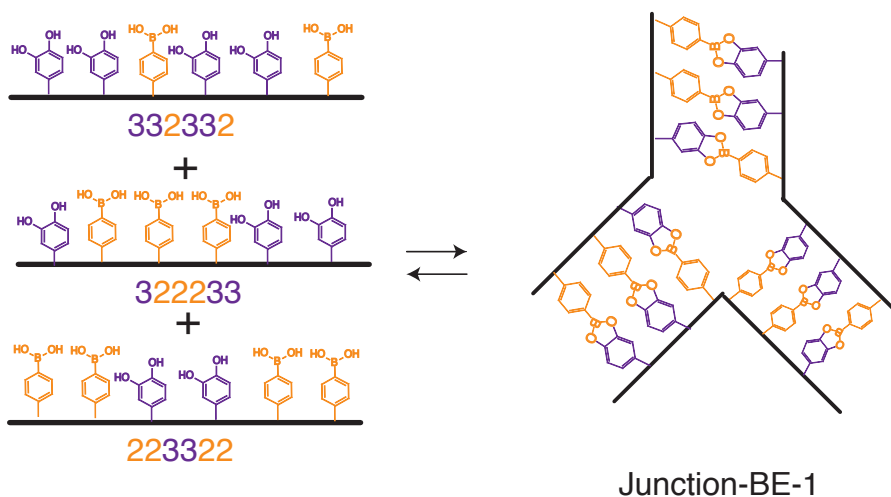

Figure 7.4. Schematic showing the formation of a junction structure from three oligomeric peptoid structures containing boronate ester forming functional groups

For example, early work with nucleic acids capitalized on the hybridization selectivity of DNA in order to assemble non-linear structures marking the emergence of the field of nucleic acid nanotechnology.[1] By annealing oligonucleotide sequences that lack the complementary symmetric sequences typically found in their biological counterparts, junctions from which multiple double stranded structures originate can be fabricated. These junctions can be linked together directly or with linear DNA fragments by utilizing "sticky end" unhybridized nucleotide overhangs. Seeman leveraged this technology to fabricate a cubic molecule composed exclusively of DNA,[2] highlighting the capacity of nucleic acids to form complex nanostructures. These early examples were key in developing a set of guidelines for later fabrication techniques.[3] There remains a need to develop a similar set of reaction parameters for our dynamic covalent

system. I believe a thorough investigation of the thermodynamic and kinetic parameters through

a mixture of computational and experimental analysis is the key to future success of this project.

7.3. References

1.   Seeman, N. C., Nucleic Acid Junctions and Lattices. *J. Theor. Biol.* **1982,** *99* (2), 237-247.

2.   Chen, J. H.; Seeman, N. C., Synthesis from DNA of a molecule with the connectivity of a cube. *Nature* **1991,** *350* (6319), 631-633.

3.   (a) Rothemund, P. W. K., Folding DNA to create nanoscale shapes and patterns. *Nature* **2006,** *440* (7082), 297-302; (b) Ke, Y.; Ong, L. L.; Shih, W. M.; Yin, P., Three-Dimensional Structures Self-Assembled from DNA Bricks. *Science* **2012,** *338* (6111), 1177-1183.